FACULTEIT
BIO-INGENIEURSWETENSCHAPPEN

Academiejaar 2004-2005

MODELLING AND MONITORING THE ANAEROBIC DIGESTION PROCESS IN VIEW OF OPTIMISATION AND SMOOTH OPERATION OF WWTP's

MODELBOUW EN OPVOLGING VAN HET ANAËROBE VERGISTINGSPROCES VOOR DE OPTIMALISATIE EN VLOTTE WERKING VAN RWZI's

door

ir. Usama El-Sayed Zaher, M.Sc., M.Eng.

Thesis submitted in fulfillment of the requirements for the degree of Doctor (Ph.D.) in Applied Biological Sciences: Environmental Technology

Proefschrift voorgedragen tot het bekomen van de graad van Doctor in de Toegepaste Biologische Wetenschappen: Milieutechnologie

op gezag van

Rector: **Prof. Dr. A. De Leenheer**

Decaan:
Prof. Dr. ir. H. VAN LANGENHOVE

Promotor:
Prof. Dr. ir. P. VANROLLEGHEM

To my parents, wife and children

MODELLING AND MONITORING THE ANAEROBIC DIGESTION PROCESS IN VIEW OF OPTIMISATION AND SMOOTH OPERATION OF WWTP's

by

ir. **Usama El-Sayed Zaher**, M.Sc., M.Eng.

PhD Review Committee:

Dr. ir. E. Ayesa	(CEIT, Spain)
Dr. ir. H. Spanjers	(LeAF, The Netherlands)
Dr. ir. J.-P. Steyer	(INRA, France)
Prof. Dr. ir. P. A. Vanrolleghem	(Ghent University, promoter)
Prof. Dr. ir. M. Verloo	(Ghent University)

Other Jury Members:

Prof. Dr. ir. G. Hofman	(Ghent University, Chair)
Prof. Dr. ir. P. Van Der Meeren	(Ghent University, Secretary)
Prof. Dr. ir. W. Verstraete	(Ghent University)

ISBN 90-5989-070-1

Please refer to this work in the following manner:
Zaher U. (2005) Modelling and monitoring the anaerobic digestion process in view of optimisation and smooth operation of WWTP's, PhD thesis, Ghent University, Ghent, Belgium, pp. 346.

Gent, June 2005

De promotor: De auteur:

Prof. Dr. ir. P. A. Vanrolleghem ir. U. Zaher

Acknowledgement

These are the ***last words*** I write for my PhD. I wish they would also be the ***best words,*** to acknowledge all who helped and supported me during this PhD study.

First of all, I would like to deeply thank my supervisor Prof. Peter A. Vanrolleghem. Indeed, in the first place, his recognition of my experience and his positive reply to my request in 2001 to join his highly professional and academic team was highly appreciated. Later on, working with him was amazing. He is so efficient, professional, cooperative, supportive, helpful and friendly. He usually brings in joyful spirits and advanced merits to his work team and students. Indeed, I have to say that I have been lucky to work with him and have him as my PhD supervisor friend☺. It is indeed good luck for any place he has been working in and so it is good luck for any future place! , ….I wish him all the best.

The BIOMATH department and PVR@BIOMATH are a perfect place and group. I have to thank all colleagues for their cooperative attitude and friendship. Many seminars, meetings, discussions, collaborations were fruitful in a wide range of scientific and practical topics. Many sportive and social events were enjoyable and helpful to release work pressure and renew work energy. Special thanks to the BIOMATH secretaries for being always ready for administrative help. Also, special thanks to Griet for helping with my lab responsibilities during the last stage of the dissertation writing.

I appreciate the collaborative work with the large and highly qualified group of the EU TELEMAC project IST-2000-28156. Indeed, all the project meetings were rich in scientific and high-tech subjects that inspired my research. Intensive project work and highly active correspondence were bringing in innovative ideas and leading to interesting results. Many thanks to all project partners and representatives for their cooperation. Special thanks should go to Dr. Jean-Philippe Steyer for his continuous support during the project. Many thanks to Dr. Olivier Bernard, Gonzalo Ruiz, Jorge Rodríguez, Kristof De Neve and Kristof Lievens for the nice and close collaborations.

I also appreciate the support I had from the EU project COST-624 action; special thanks should go to Dr. Eduardo Ayesa, Dr. Christian Rosen and Prof. Ulf Jeppsson. Also, many thanks to Monica de Gracia and Paloma Grau for the close and nice collaboration we had in connection with this project.

Many thanks are should go to all colleagues in the Cairo Wastewater Organisation (CWO) who helped during my job leave and supported my wife in finalising all the administrative decrees and papers I needed.

Many thanks and appreciation to all my friends, brothers and sisters, who helped, supported and motivated me a lot.

From the depth of my heart, many thanks to my mother and father for encouraging to me all the way; I wish them long live to enjoying good health. Many thanks for my wife (Abeer) and children (Ahmed, Salma and Karim) for their love and inspiration that helped me to achieve this work and reach this degree.

Ghent, May 2005

Usama El-Sayed Zaher

Abbreviations:

AAFF: *Attached Anaerobic Fixed Film*

AAFFEB: *Anaerobic Attached Fixed Film Expanded Bed*

ABR: *Anaerobic Baffled Reactor*

ADM: *Anaerobic Digestion Model*

ADM1: *IWA Anaerobic Digestion Model no. 1*

AF: *Anaerobic filter*

AFB: *Anaerobic Fluidized Bed*

AFF: *Attached Anaerobic Fixed Film*

AM2: *TELEMAC Anaerobic Model no. 2*

AnaSense®: *On-line titrimetric analyser*

ASB: *Anaerobic Sludge Bed*

ASBR : *Anaerobic Sequencing Batch Reactor*

ASM1: *IWA Activated Sludge Model no.1*

ASMs: *IWA Activated Sludge Models*

BC: *Buffer Capacity curve*

BCS: *Buffer Capacity Software*

BOMB: *Buffer Capacity Optimal Model Builder*

CBIM : *Continuity-Based Interfacing Method*

COD : *Chemical Oxygen Demand*

CODs: *Chemical Oxygen Demand of soluble compounds*

CODt: *Total Chemical Oxygen Demand*

CSTR: *Continuously Stirred Tank Reactor*

CSUM: *Cumulative SUM control charts*

DSFF: *Down-flow Stationary Fixed Film*

EGSB: *Expanded Granular Sludge Bed*

EWMA: *Exponentially Weighted Moving Average*

FBR: *Fixed Bed Reactor*

FIM: *Fisher Information Matrix*

GC: *Gas Chromatography*

GSL: *Gas/Sludge/Liquid separation system*

GTPs:	*Guiding Transformation Principles*
HRT:	*Hydraulic Retention Time*
ICA:	*Instrumentation, Control and Automation*
IST:	*European Information Society Technologies*
IWA:	*International Water Association*
LCFA:	*Long Chain Fatty Acids*
LCL:	*Lower Control Limit in SPC charts*
MCN:	*An interfacing methodology for ASM1 and ADM1*
MET:	*Monotonic Equivalence-point Titration*
MLVSS:	*Mixed Liquor Volatile Suspended Solids*
MRE:	*Maximum Relative Error*
MSL:	*Model Specification Language*
NaN :	*Not a Number*
OED:	*Optimal Experimental Design*
PA:	*Partial Alkalinity*
PE:	*Parameter Estimation*
q-q:	*quantile-quantile plot*
SPC :	*Statistical Process Control*
SPRTs:	*Sequential Probability Ratio Tests*
SRT:	*Solids Retention Time*
SSAR:	*Staged Sludge Anaerobic Reactor*
SSE:	*Sum of Squared Errors*
TA, Z, Alk_{total}:	*Total Alkalinity*
TAN:	*Total Ammonia Nitrogen*
TAS:	*Titrimetric Analyser Simulator in WEST*
TELEMAC:	*TELEMonitoring and Advanced teleControl of high yield wastewater treatment (TELEMAC project no.: IST-2000-28156)*
ThOD:	*Theoretical Oxygen Demand*
TKN:	*Total Kjeldahl Nitrogen*
TNO_2:	*Total Nitrite Nitrogen*
TOC:	*Total Organic Carbon*
TS:	*Titrimetric Sensor*

TSS: *Total Suspended Solids*

UAF: *Upflow Anaerobic Filter*

UASB: *Upflow Anaerobic Sludge Bed*

UASB-AF: *combined Upflow Anaerobic Sludge Bed – Anaerobic filter UASB-AF*

UCL: *Upper Control Limit in SPC charts*

VFA: *Volatile Fatty Acids*

VSS: *Volatile Suspended Solids*

$\bar{X}$ *-chart :* *Shewhart chart for averages*

Greek symbols:

ε *:* *Error*

μ *:* *Global mean*

θ *:* *Model parameters vector*

σ *:* *standard deviation*

σ^2*:* *Variance*

β*:* *Buffering capacity*

α*:* *Fraction of particulates leaving with effluent*

δ*:* *Net equivalent concentration*

ΔG*:* *free energy*

$\nu_{i,j}$*:* *Rate coefficients for component i on process j(stoichiometry)*

μ_i*:* *Growth rate of biomass component i*

ρ_j*:* *Rate of reaction j*

μ_{max}*:* *Maximum specific growth rate*

Roman symbols:

A_{i_T} *:* *Weak acid concentration*

B: *Buffering component*

$C(\theta)$*:* *Parameter estimation covariance matrix*

C_2*:* *VFA with two carbon atoms (i.e. acetate)*

C_3*:* *VFA with three carbon atoms (i.e. propionate)*

C_4:	*VFA with four carbon atoms (i.e. butyrate)*
C_5:	*VFA with five carbon atoms (i.e. valerate)*
C_a:	*Strong acid concentration*
Cat_{net}:	*Net cation concentration*
C_b:	*Strong base concentration*
C_i:	*Carbon content of component i*
D:	*Dilution rate*
$f_{i,j}$:	*Fraction parameter of component i to component j*
F_{xout}:	*Fraction of particulates leaving the reactor*
H_{gas}:	*Gas law constant*
I_i:	*Inhibition rate of component i*
$J(\theta)$:	*Least squares objective function*
K_a:	*Acidity equilibrium constant*
K_b:	*Base equilibrium constant*
k_{dec}:	*First order decay rate*
K_{dis}:	*First order disintegration rate*
K_H:	*Henry's law coefficient*
K_{hyd}:	*First order hydrolysis rate of component*
K_I:	*50% inhibitory concentration*
k_La:	*gas-liquid transfer coefficient*
k_m:	*Maximum specific uptake rate*
K_S:	*Half saturation constant*
N_a:	*Acid Normality*
N_i:	*Nitrogen content of component i*
p:	*Number of model parameters*
P:	*Total gas pressure*
Pi:	*Partial pressure of gas component i*
$pK_{a,i}$:	$-\log_{10}[K_{a,i}]$
Q:	*Liquid flow*
q_{gas}:	*Total gas flow rate*
Q_i:	*A matrix of user-supplied weighting coefficients to the measurements during PE*

q_i:	*gas flow of a gas component i*
R:	*Universal gas constant*
RATIO:	*Ratio between sensitivities*
r:	*Pearson product moment correlation coefficient*
rbCOD:	*readily biodegradable COD*
$S_\theta(\theta)$:	*Vector of output sensitivity functions*
SAE:	*Sum of absolute errors*
S_i:	*Soluble concentration of a component i*
T:	*Temperature*
t:	*time*
$t_{res,X}$:	*Extended retention of solids*
V_a:	*Titrated acid volume*
V_b:	*Volume of a titrated base*
V_{gas}:	*Volume of a gas compartment*
V_{liquid}:	*Liquid volume of a reactor*
V_s:	*Volume of a titrated sample*
$\bar{X}$:	*Average on a moving window*
X_i:	*Concentration of particulate component i*
y:	*A state variable of a model*
Y:	*Yield of biomass on substrate*
Z, $S_{cat\text{-}net}$:	*Cation concentration*
z_i:	*Ion charge*

TABLE OF CONTENTS

Introduction and review

Part I Modelling

Appendices

Introduction and review

Chapter 1

Introduction and problem statement

CHAPTER 1

1.1 General perspective

1.2 Problem statement

1.3 Research goal

1.4 Research objectives

1.5 Dissertation outline

1.1 General perspective

An increase and an optimisation of anaerobic digestion applications is required to enhance wastewater treatment sustainability. Indeed, the anaerobic digestion process can be applied for the treatment of various types of wastewaters in a more sustainable way than alternative processes. Applications include the treatment of municipal, industrial, agricultural and farming wastewaters. Furthermore, anaerobic digestion is applied for stabilisation, quantity reduction, hygienisation and reuse of sludge that originates from conventional wastewater treatment systems, e.g. activated sludge.

On one hand, the anaerobic digestion process has general advantages such as:

- The production of biogas that can be used as a green source of energy, e.g. for power generation.
- It can accommodate high COD loads.
- It can be applied for low strength wastewaters provided that the proper reactor configuration is chosen.
- It adapts to remove and/or work in the presence of various toxicant components provided that adaptation time is allowed for the anaerobic biomass.
- …

On the other hand, the incorrect design of an anaerobic plant for certain applications and/or the inefficient operation of the plant will cause the following disadvantages to become more evident:

- Anaerobic biomass growth is slow and the optimum growth is achieved at high temperatures.
- The optimum pH for the process lies in a narrow range near neutrality and the process intermediates make the pH drop below the optimum range.
- The process is sensitive to COD overloads and toxicant shock loads.
- The process effluent is high in COD and nutrients compared to consents stated by legislation.
- The process is complex and difficult to operate compared to other conventional processes.
- …

For certain applications, optimisation aims at maximising the anaerobic process advantages and to minimise or eliminate its disadvantages. This can be achieved by understanding the

anaerobic process dynamics and accordingly consider the proper approach for each specific application. The solution can be to take certain actions to upgrade the design and to improve the operation of the anaerobic plant. Also, the solution can be to integrate the anaerobic process with other processes. To understand the process, tools are needed to observe and analyse while certain tools are also needed to study the integration.

1.2 Problem statement

"Advanced tools are needed to optimise anaerobic digestion applications"

There are different anaerobic reactor types and configurations. Each configuration may be optimal for a certain application but not suitable for another. The type of wastewater and the desired operation strategy will influence the choice of the reactor type and design. Therefore, advanced modelling tools are needed to check and optimise this design before investing in the plant construction and installation.

Anaerobic reactors are closed systems and their operation can't only depend on direct operator observations. The process is complex. Many variables need to be monitored frequently to follow up the plant operation and avoid process upsets. It is not feasible to rely only on sampling and off-line analysis since it will be labour and expertise demanding. Also, the plant can be located in a remote place. An enterprise may own more than one plant at different sites and can't afford lab-facilities and technicians at each site. Transfer of samples to one central place may cause a change in their characteristics. Therefore, advanced tools need to be implemented to on-line collect the required data and make data transfer feasible by communication technology. Consequently, advanced tools are needed to analyse operational data, support operation decisions, plan control strategies and take control actions.

In mega-cities, anaerobic digestion can be separately implemented for each district of different community sectors, e.g. industrial, commercial, residential …etc. Also, it can be implemented for sludge treatment at conventional treatment plants. Here too, advanced tools are needed to plan a global wastewater treatment strategy, operate the whole scheme in an integrated manner and optimally operate the plants from a remote control centre.

1.3 Research goal

"Develop, implement and apply anaerobic digestion modelling and monitoring tools"

The modelling and monitoring tools investigated in this PhD research are modularly implemented to fit schemes for the optimisation of anaerobic digestion and wastewater

treatment applications. This research work is conducted in the framework of two major research projects sponsored by the European commission: TELEMAC project no. IST-2000-28156 and COST action no. 624. The TELEMAC project is designing a modular and reliable system to support remote telemonitoring and telecontrol of wastewater treatment units with no local expertise available to them. The project is more specifically focusing on anaerobic wastewater treatment processes (Bernard et al., 2005). The COST-624 action is concerned with optimal management of wastewater systems. For the optimal operation of wastewater treatment plants, an important project task is concerned with instrumentation, control and modelling of anaerobic treatment.

1.4 Research objectives

This research has the following three objectives:

First objective: ***Implementation and validation of anaerobic digestion models.***

Several tasks are done to fulfil this objective. Anaerobic digestion modelling is applied on different levels of complexity. The highest level of complexity is considering the disintegration and hydrolysis steps, the main process pathways of protein, carbohydrate and fat degradation and different forms of inhibition and toxicity. This is applied by implementing the IWA ADM1 model (Batstone et. al, 2002). The lowest level of modelling complexity is only considering the two main steps of anaerobic digestion: acidogenesis and methanogenesis. This is achieved by implementing the model AM2, an upgraded version of the model by Bernard et al. (2001). An intermediate level of complexity is achieved by applying the Siegrist model (Siegrist et al., 1991; 1993; 1995). A general procedure is developed and programmed for pH-simulation in anaerobic models, other process models or titration experiments. The developed models are validated throughout the research. ADM1 is extended and used to evaluate cyanide toxicity and degradation. ADM1 and AM2 are applied in an Optimal Experimental Design procedure (OED) to design and setup anaerobic digestion monitoring systems. ADM1 and the Siegrist models are applied to simulate sludge digestion in the context of plant-wide modelling that is part of the next objective.

Second objective: ***Implementation of anaerobic digestion models in plant-wide models.***

The tasks to fulfil this objective are mainly concerned with interfacing anaerobic digestion models to pre- and post-treatment process models. The concept of using transformers to interface anaerobic digestion models is introduced by its application to the Siegrist and ADM1 models. Different transformer building methodologies (Copp et al., 2003; Vanrolleghem et al., 2005) are compared.

Third objective: ***On-line titrimetric monitoring of anaerobic digestion.***

Titrimetric methods, their applications and the available instrumentation are reviewed and compared. An advanced titrimetric measurement method that uses buffer capacity modelling is further developed and upgraded by an automatic initialisation module. The automatic initialisation is implemented to increase robust on-line monitoring of buffer components. The upgraded method is validated and tested for anaerobic digestion monitoring with different levels of complexities.

1.5 Dissertation outline

The PhD dissertation is organised as follows:

Chapter 2 reviews the main anaerobic reactor types and wastewater characteristics to guide data collection for better definition of anaerobic digestion models. Data validation and Optimal Experimental Design, OED, procedures are introduced since they improve the quality and maximise the information content of measurements for the implementation in next chapters.

Part I: Modelling

Chapter 3 discusses key points for the successful implementation of the IWA anaerobic digestion model No.1, ADM1. It illustrates possible simplification of the gas-liquid transfer and pH modelling by presenting other simpler models.

Chapter 4 illustrates a general pH modelling and simulation procedure. It shows the applicability of the procedure to simulate pH in any process model, dynamically calculate the cations' concentration in samples with known pH (e.g. the influent) and simulate titration experiments.

Chapter 5 develops a conceptual approach for ADM1 application. The approach describes steps to evaluate the influent characteristics along the ADM1 state vector using a concise set of measurements. It implements a simple procedure to model solids transport in anaerobic reactors that is useful to approximate washout and/or retention of biomass in high rate reactors. A very dynamic experiment is performed to validate the IWA ADM1 model. The experiment is one of the first contributions to validate ADM1 dynamically. Simulation was done on three different simulation platforms.

Chapter 6 extends the IWA ADM1 model for modelling anaerobic digestion in presence of irreversible toxicity. Cyanide toxicity and anaerobic degradation are modelled according the process pathways found in literature. The adaptation of the anaerobic process to cyanide was explained by modelling a population shift in aceticlastic methanogens. The model is validated by experimentation on three lab-scale UASB reactors. The general pH procedure developed in chapter 4 is used to estimate the influent cations and simulate the pH in the reactors.

Chapter 7 validates the AM2 control model implementation. Then, a protocol is designed to setup the monitoring system at an anaerobic digestion plant by applying an iterative OED procedure. The protocol is tested by a virtual case study. A virtual plant is designed using ADM1 and is subsequently used for the generation of virtual data. These virtual data were then used to run the iterative OED procedure to improve the confidence in the AM2 model parameters. For the improvement of the parameters' estimates, an optimal selection of on-line measurements, measuring intervals and experimental conditions are designed.

Part II: Plant-wide modelling

Chapter 8 introduces the use of transformers to integrate anaerobic digestion models in plant-wide models. It provides an example of using transformers to interface the input and output terminals of the Siegrist model to the IWA Activated Sludge Model no. 1, ASM1 (Henze et al., 2000). This chapter highlights the importance of modelling anaerobic sludge digesters and evaluates its impacts on the other treatment systems.

Chapter 9 compares two transformation approaches to interface ADM1 with ASM1. It illustrates the step-wise application of a general approach to interface any two models, maintaining the continuity of COD, elemental mass and charge. It applies the example of the previous chapter to compare the general methodology with another methodology that is designed to interface ASM1 and ADM1 only. The latter is conceptually similar to the methodology introduced in the previous chapter 8.

Part III: Monitoring

Chapter 10 starts with a review of the commercial availability of monitoring equipment for anaerobic digestion applications and points out that titrimetric analysers are not commercially available till recently. Then it focuses on the description of reported titrimetric analysers and the methods that are applied, further developed and compared in this part of the PhD dissertation.

Chapter 11 develops and implements an automatic initialisation module to the software sensor Buffer capacity Optimal Model Builder (BOMB). The resulting Buffer Capacity Software, BCS, increases the robustness of the sensor for on-line implementation to determine different buffer combinations. BCS is validated in this chapter using the Titrimetric Analyser Simulator (TAS) that is described in chapter 4. Also, the BCS is validated with lab experiments titrating standard solutions and with the on-line implementation of an industrial titrimetric analyser.

Chapter 12 classifies different detailed and approximate calculation methods that are applied for titrimetric monitoring. The BCS is tested on lab-, pilot and industrial scales and is compared with other, approximate methods. Tests comprise three case studies of titrimetric monitoring. The first case study is the monitoring of anaerobic digestion overloads by measuring bicarbonate, VFA and lactate. The second is for monitoring a complicated digester effluent by measuring combinations of bicarbonate, VFA, lactate and ammonia in the presence of precipitation. The third case study is an application to anaerobic digestion post treatment processes (SHARON and Anammox) by measuring ammonia and nitrite in the presence of phosphorous. The results of BCS in the three case studies are compared with other measuring methods.

Finally, **Chapter 13** provides the general outcomes and conclusions of the dissertation and highlights perspectives for future research and applications.

Chapter 2

Preliminary review: a guide for data collection

Abstract

This chapter provides a guide for data collection to optimise anaerobic digestion applications. It reviews data categories that are needed to define the anaerobic model. It introduces data validation and Optimal Experimental Design (OED) procedures to improve the quality and maximise the information content of the collected measurements.

A state of the art of anaerobic digester types is presented. The description of reactor types highlights important features of each reactor to guide hydrodynamic and solid transport modelling assumptions. Wastewater characteristics are reviewed in view of the anaerobic digestion kinetics so that process pathways can be properly defined in the anaerobic model. Data validation tools are introduced since they are necessary to improve the quality of the collected data, eliminate measurement faults and define operating conditions under which the data are to be collected. The concept of OED is also introduced since it will be used to design a monitoring system to maximise the information content of the measurements and enhance model parameter estimation quality.

CHAPTER 2

2.1 Introduction

Optimisation of anaerobic digestion applications is data demanding. Modelling and monitoring are the main activities and the most useful tools to optimise process applications. Recently, a detailed review of anaerobic digestion modelling is reported in the IWA ADM1 report (Batstone et al, 2002). Also, the state of the art of anaerobic digestion and wastewater treatment monitoring applications is reviewed in (Vanrolleghem and Lee 2003). Therefore, this chapter will focus on practical aspects that link modelling and monitoring activities providing a guide for data collection. Also, issues of model implementations will be reviewed in parts I and II of this research, while issues that are more specific to monitoring will be reviewed in part III.

Data collection activities should cover three data categories that are necessary to build a representative model and a monitoring system for an anaerobic process application. The three data categories comprise (1) the anaerobic plant details and (2) wastewater characteristics, and (3) measurements that are collected during the operation of the plant. Figure 2.1 shows a conceptual procedure that links data collection, modelling and monitoring activities for the optimisation of the anaerobic process application. The procedure is applied in two phases. The first phase is during the design of the anaerobic digestion plant and/or its Instrumentation, Control and Automation (ICA) system. The second phase is at the start of the plant and its ICA system operation.

In the design phase data describing the plant layout and the type of the reactor will help the definition of some assumptions that are necessary for the modelling activity. The hydrodynamic and solids' transport parts of the model can be defined. With approximation, the Hydraulic Retention Time (HRT) and the Solids Retention Time (SRT) are defined. According the wastewater characteristics, the kinetics of the process model are defined. For instance, if the wastewater consists mainly of carbohydrates, the process model can be simplified by ignoring protein and fat process pathways. An Optimal Experimental Design (OED) procedure can help to design the monitoring system (see chapter 7). The design of a monitoring system answers the questions concerning what and where to measure and, hence, the wastewater characterisation might need to be extended or the plant layout might need to be adjusted. Accordingly, other iterations through the procedure might be needed till an optimum design of the plant and its ICA components are achieved. Note that iterations of the OED are virtual experiments that can favourably be extended in this phase and be tested on a lab- or a pilot-scale experiment. Also, the modelling activity can be extended to test different control designs.

In the operation phase, the optimum design is implemented in full-scale. The procedure continues but this time real measurements are collected. The collected measurements need to be organised and stored, e.g. in a database. Also, before applying the data in the modelling activity, e.g. for estimating model parameters, data need to be validated. Data validation is indeed another extended topic for research and it mainly aims to control the quality of data, detect faults from the sensors or in the process. In the start of the operation phase OED is useful in two ways. First, it allows to fine-tune the monitoring system, e.g. to determine measurements intervals. Second, it allows to propose an experiment, e.g. by varying the feed flow, to provide data that lead to better confidence in the model parameters. The optimisation procedure during the operation phase can be iterated to design a control model or strategy. Once a satisfactory control strategy is defined, it is applied to the plant and optimal operation of the anaerobic digestion plan is achieved.

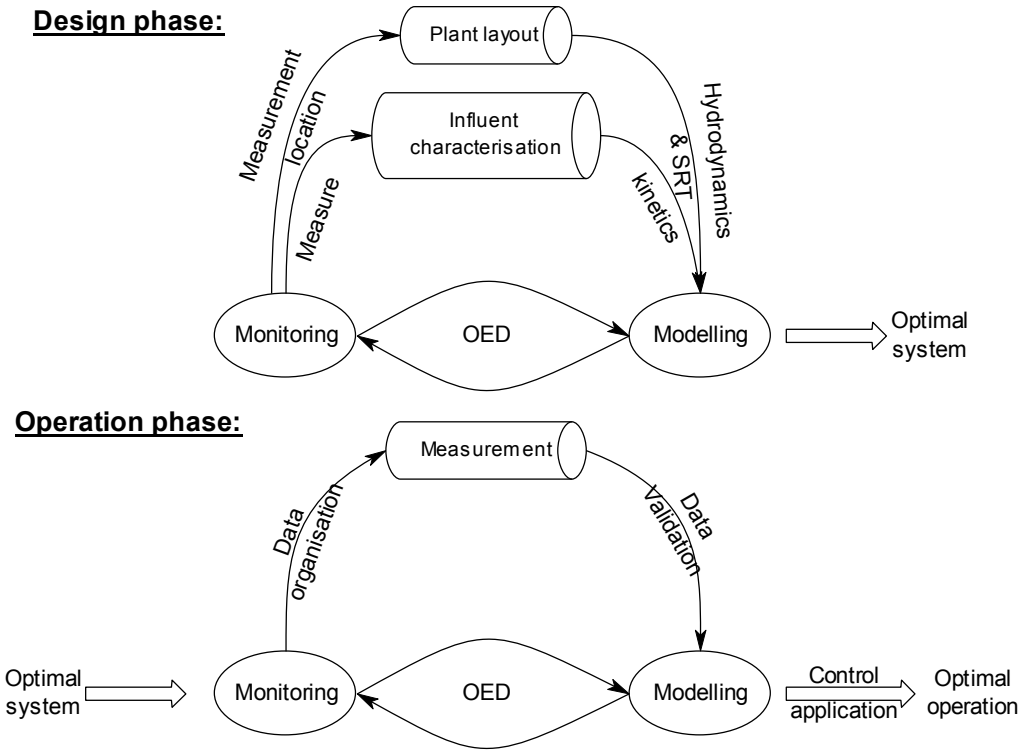

Figure 2.1 A conceptual procedure to link data collection, modelling and monitoring activities for the optimisation of anaerobic process applications.

The modelling and monitoring activities will be looked at from different angles throughout the next chapters of this research. Three objectives are stated for the current chapter. The first objective is to provide a detailed literature review of the anaerobic digestion reactor types to guide the definition of the first data category. The second objective is to review the main wastewater characteristics (the second data category) for anaerobic digestion application. The third objective is to introduce the concepts of data validation and OED

that are important to link data collection, modelling and monitoring activities in the context of process optimisation.

2.2 Plant layout and reactor types

The definition of a plant layout is mainly related to the anaerobic reactor type and its configuration. There are other components of an anaerobic plant that have to be studied for plant modelling, monitoring and control, such as:

- Influent pump configurations
- Possibility of influent dilution and/or recycle rates
- Buffering, hydrolysis and/or acidification in upstream compartments
- Available sensors and off-line analysis
- Available actuators and applied control systems
- Heating systems

These plant components vary widely and, therefore this section will review the major reactor types only.

Different types of digesters are applied for treatment of industrial wastewater at industries such as sugar and distillery, pulp and paper, slaughterhouse, dairy units…etc. (Rajeshwari et al., 2000; van de Steen, 2002). In the following subsections the major digester types are classified and described according their applied flow and solid retention. Advantages of each type are highlighted from the process and application points of view. Due to the slow growth of anaerobic bacteria, it is desired to maintain a long retention of the anaerobic biomass and keep them at high concentrations. Therefore, it is more common, for industrial applications in particular, to apply high rate anaerobic reactor systems. In an anaerobic process, the maximum permissible load is not governed by the maximum rate at which a necessary reactant can be supplied, e.g. oxygen during aerobic processes. Instead, to enable an anaerobic reactor system to accommodate high loading rates for treating a specific wastewater, the following conditions should be optimised:

1. High retention of viable sludge in the reactor under operational conditions.
2. Sufficient contact between viable bacterial biomass and wastewater.
3. High reaction rates and absence of serious transport limitations.
4. The viable biomass should be sufficiently adapted and/or acclimatised.

5. Prevalence of favourable environmental conditions for all required organisms in the reactor.

Considerable efforts have been made in the last two decades to develop high rate anaerobic reactors that fulfil these conditions, first of all in order to enable the application of anaerobic treatment to cold and very low strength wastewaters. Additional reasons were:

1. To reduce the capital expenditure because small reactors are lower in investment.
2. To reduce space requirements, especially because frequently space is the critical factor at industrial locations.
3. To improve the process stability.

Therefore, different configurations of high rate anaerobic reactors have been developed. Generally, these reactor types can be operated in different temperature ranges. As in all biological processes, one can distinguish three temperature ranges in anaerobic biological treatment of waste and wastewater (Batstone et al., 2002):

- a psychrophilic range, from 4-20 °C,
- a mesophilic range, from 20-40 °C,
- and a thermophilic range, from 40-70 °C.

Optimal temperatures for mesophilic and thermophilic anaerobic organisms are approximately 35ºC and 55ºC, respectively. The upper limits of these ranges are defined by the temperature at which the decay rate of the bacteria starts to exceed the growth rate. The temperature dependency of the different groups of organisms follows the Arrhenius equation up to a temperature optimum, followed by a rapid drop to zero. This means that thermophilic bacteria are still quite active in the mesophilic temperature range, and that mesophilic bacteria are still active in the psychrophilic temperature range. Especially, this last feature is very important and one can treat wastewaters at very low temperatures, provided one doesn't have to grow the bacteria at this low temperature. Anaerobic sludge, grown at 35°C, can be used very well to handle wastewater at 10-15 °C. Then, 5-10 % of its activity still remains. Also, at 20°C still volumetric loading rates of 4-5 kg COD m^{-3} d^{-1} can still be effectively treated. In the mesophilic range, it is possible to say that the activities and growth of the bacteria decreases by one half for each 10°C decrease below 35°C.

2.2.1 Continuously Stirred Tank Reactor (CSTR)

The Continuously Stirred Tank Reactor (CSTR) is the most common and easy to operate digester configuration to treat wastewaters with a high concentration of particulates, e.g. in sludge digestion. However, it is not considered to be a high rate reactor. Its function is mainly to stabilise the solid content (sludge) volumes by converting the biodegradable proportions to biogas. It is frequently followed by decanting and drying units. Since the anaerobic digestion process is slow, it is usually operated at high temperatures to increase the process rates by applying heating systems. It has a low COD loading rate and a long retention time (20 days in average). CSTR digestion units are designed in big volumes that make perfect mixing difficult. Mixing is done mechanically or by recycling of flow or the produced biogas. Therefore, the mixing efficiency is an important factor in modelling the solids transport in the reactor and evaluation of the Solids Retention Time (SRT).

2.2.2 Anaerobic Filters (AF)

An anaerobic filter is also called a fixed bed reactors (FBR). *The Upflow Anaerobic Filter (UAF),* was developed in the USA by Young and McCarty (1969). Bonastre and Paris (1989) reviewed anaerobic filter applications at lab-, pilot- and industrial scales. The performance of the UAF is mainly influenced by the sludge retention of the UAF and it is based on the attachment of a biofilm to the solid (stationary) carrier material (e.g. synthetic packing, gravel, coke, bamboo segments). Size and weight are important properties of these materials. The most important are surface properties to increase bacterial attachment and the void ratio to prevent clogging. A pre-acidification step helps in clogging reduction. For acidified wastewaters such as vinasses, a FBR is robust to accommodate hydraulic and organic loads dynamics (Steyer et al., 2002). The sedimentation and entrapment of sludge particles between the intersections of the packing material may cause clogging. However, it also forms very well settling sludge aggregates.

The *Downflow Stationary Fixed Film (DSFF)* and the *Attached Anaerobic Fixed Film (AFF)* reactors are in many ways similar to the UAF except for the flow direction. In a downflow packed bed, hardly any suspended biomass (or bacterial aggregates) can be retained (Kennedy et al., 1991). The system can also treat low strength wastewaters. A pilot-scale study of a DSFF reactor also suggests the design of full-scale plants of this configuration to treat wastewaters like piggery farm slurries (Lomas, 1999; 2000)

2.2.3 Anaerobic Sludge Bed (ASB)

The *ASB-reactor* is based on the formation of easily settling sludge aggregates (flocs or granules) that depend on the type of wastewater, the organic and hydraulic loads (Aiyuk

and Verstraete, 2004) and on the application of an internal Gas/Sludge/Liquid separation system, so called GSL-device (Van Haandel and Lettinga, 1994). The *Upflow Anaerobic Sludge Bed (UASB)* was developed in the Netherlands in the early seventies (Lettinga et al., 1980). As in the UAF-system the wastewater moves in an upward direction through the reactor. However, contrary to the AF system there is generally no packing material in the reactor. Sludge granules are formed due to fluidisation (Guiot et al., 1992). Fluidisation is achieved by mixing of the sludge by the flow and gas release.

Upflow Anaerobic Sludge Bed – Anaerobic filter (UASB-AF): The GSL-device can also be replaced by a packed bed in the upper part of the reactor. This approach is recommended on the basis of results obtained with a hybrid of the UASB-AF system. A configuration of an UAF on top of an UASB reactor was applied to treat wastewaters from a fibreboard production factory (Fernandez et al., 1995). In this configuration, the UASB substitutes the required pre-acidification step for the UAF and helps the clogging reduction. Such combined reactors can maintain high treatment efficiencies at COD-loads considerably higher than those accommodated by upflow and downflow completely packed reactors. Also, these hybrid reactor systems certainly offer quite interesting potentials for the treatment of low strength wastewaters containing a fraction of finely dispersed solids. However, in such a hybrid reactor it remains beneficial to install a GSL-device. This is certainly the case when treating higher strength wastewaters.

2.2.4 Anaerobic Fluidized Bed (AFB)

AFB systems can be considered as a special variant of the sludge bed system. The *FB*-process is based on the occurrence of bacterial attachment to mobile carrier particles, e.g. consisting of fine sand (0.1 - 0.3 mm), basalt, or plastic. The system relies on the formation of a more or less uniform (in thickness, density, strength) attached biofilm and/or particles. In order to maintain a stable situation with respect to the biomass film development, a high degree of pre-acidification was considered necessary (Heijnen, 1989) while dispersed matter should be absent in the feed (Ehlinger, 1994). However, it is virtually impossible to guarantee a stable process performance in practice. The complex dynamic process of film formation, film attachment and release are dependent on the feed composition (Garcia-Encina and Hidalgo, 2005) and therefore the process cannot be controlled sufficiently. Aggregates of very different size and density will always develop in the system, and consequently, at a certain bed expansion, segregation of sludge particles will occur (Hidalgo and Garcia-Encina, 2002). This means that at some time bare carrier particles will start to accumulate in the lower part of the reactor as a kind of stationary bed, while light fluffy aggregates (detached biofilms) will be present in the upper part, at least when they

can be retained. Thus, like UASB reactors, a gas-liquid separator may be needed at the top of the reactor. Moreover, when the biofilm thickness increases in size and the volume of the bed thus increases, a separate system (e.g. recycle pump) is needed to wash part of the media and return it to the reactor.

Anaerobic Attached Fixed Film Expanded Bed (AAFFEB) and *Expanded Granular Sludge Bed (EGSB)* reactors. The *AAFFEB* and *EGSB* reactors are further developed versions of the *AFB*. The *AAFFEB* has a mobile carrier material, e.g. glass, plastic, an ion exchanger, or diatomaceous earth. These media are used for bacterial attachment. The *EGSB* relies on the formation of granular sludge due to the characteristics of the wastewater and the good settling properties of the formed sludge, which will act as a media by itself. The main difference in the design with a normal *AFB* is that the specific external area of the media (or granules) is relatively small, ca.100 $m^2 m^{-3}$. Compared to an UASB, the EGSB differs by having a high height/diameter ratio and sludge bed expansion is realised by recycling the effluent (Seghezzo et al., 1998). To some degree, also settlement of sludge particles occurs in the bed. Because of the high settleability of the sludge, superficial liquid velocities exceeding 6 m/hour, sometimes velocities even higher than 10 $m.h^{-1}$, can be applied. These high liquid velocities, together with the lifting action of gas evolved in the bed, leads to a slight expansion of the sludge-bed. As a result of that an excellent contact between sludge and wastewater prevails in the system, leading to significantly higher loading potentials compared to conventional *UASB*. A combination of EGSB and membranes allows an increase of the liquid flow without losses of the biomass, increases the loading rates and achieves a high efficiency at low temperatures (Chu et al., 2005). These upgraded types of the *AFB* are less sensitive to some toxicity. In this type of reactor, the biogas formed is separated halfway up the reactor by means of baffles, and is then led upwards through a pipe. The lifting forces of the collected biogas are used to induce a recirculation of granular sludge over the lower part of the reactor, which results in improved contact between sludge and wastewater. Thus, the control of the liquid/sludge recirculation depends on the intensity of gas production.

2.2.5 Anaerobic Baffled Reactor (ABR)

An *ABR* is a compartmentalised sludge bed reactor in which the compartments are operated in series. The ABR has been developed since the early 1980s and has several advantages over well established systems such as the UASB and the anaerobic filter (AF) (Barber and Stuckey, 1999). The ABR's advantages are better resilience to hydraulic and organic shock loadings, longer biomass retention times, lower sludge yields, and the ability to partially separate between the various phases of anaerobic catabolism. No special

measures are taken to retain the sludge in the various compartments, except after the last one. Since the superficial liquid velocity in a baffled system is substantially higher than in a single step sludge bed reactor, it is expected that different biomass consortia will develop in each compartment according the substrate availability (Wang et al., 2004). Polymer addition to ABR enhances sludge granulation (Uyanik et al., 2002[a]). Granulation is, however, not necessary for ABR operation. Also, polymer addition increased the population shift of the anaerobic biomass among reactor compartments (Uyanik et al., 2002[b]). Particularly for methanogens, a high aceticlastic methanogens concentration occurred in the last compartments, while the hydrogenotrophic methanogens developed mainly in the first reactors.

2.2.6 Anaerobic Sequencing Batch Reactor (ASBR)

The *ASBR* is another interesting configuration. It consists of a set of anaerobic reactors operated in batch mode using a 'fill and draw' method. A certain amount of raw wastewater is supplied to the anaerobic reactor, after the supernatant liquid of a previously batch has been discharged. Then a 'gentle' type of mixing of the reactor contents is started in order to enable the settled viable sludge to be in contact with the wastewater and to eliminate the biodegradable organics. After a sufficient period of reaction time, the sludge is allowed to settle and the supernatant solution is discharged. The next cycle is then started. An ASBR recovers rapidly from particulate COD, soluble COD and hydraulic overloads (Masse and Masse, 2005). It is less sensitive to particulate and hydraulic shock loads compared to soluble shock loads provided that a high solids retention time is maintained. Performance of the ASBR can be enhanced by changing some operation parameters such as starting the cycle with a low initial concentration and increasing the fill time to the cycle time ratio (Shizas and Bagley, 2002). Granulation proceeds well in an ASBR treating dilute wastewaters, also at lower ambient temperatures (Dague et al, 1997). Despite granulation is not necessary for the ASBR configuration it enhances its performance.

2.2.7 Other reactor configurations

Membrane technology is recently being used in anaerobic digestion to increase sludge retention, i.e. biomass concentration, and therefore the reactor efficiency is increased (Ince et al., 1997). The Staged Sludge Anaerobic Reactor (SSAR) comprises a kind of anaerobic plug flow treatment system (Van Lier et al., 1994) where process stages are phased along

the reactor similar to the ABR reactors. The staging concept could be achieved by having separate compartments or reactors for the subsequent process stages, i.e. liquefying, acidifying and methanogenic reactors in sequence. Liquefying reactors are needed to allow pre-hydrolysis when a high proportion of the COD-load is in the particulate form. They can be combined with acidifying reactors, especially when treating cold wastewaters. Such upstream reactors or compartments also act as buffer tanks to accommodate hydraulic shock loads and prevent biomass washout.

2.3 Wastewater characterisation

2.3.1 COD and oxidation state of carbon

The Chemical Oxygen Demand (COD) and Total Organic Carbon (TOC) are important parameters for the wastewater characterisation and assessment of anaerobic degradability (Hulshoff. Pol., 2002). Also, the determination of their fractions help in the assessment of the corresponding process effects. For an organic compound $C_nH_aO_b$ its oxidation reaction is:

$$C_nH_aO_b + 1/4(4n + a - 2b)O_2 \rightarrow nCO_2 + (a/2)H_2O$$

Accordingly:

$$COD_t = \frac{8(4n + a - 2b)}{(12n + a + 16b)} \text{ g COD/g } C_nH_aO_b$$

$$TOC_t = \frac{12n}{(12n + a + 16b)} \text{ g TOC/g } C_nH_aO_b$$

$$\frac{COD}{TOC} = \frac{8(4n + a - 2b)}{12n}$$

The COD/TOC ratio indicates the complexity of substrates in the wastewater. Generally, if the ratio lies in the range 2 to 3, it is more likely that the substrates are less complex and are anaerobically degradable compounds. Thus if the ratio calculated from the analytical results is out of this range certainly further characterisation of the anaerobic degradability of the wastewater is required.

Including the organic nitrogen in the calculation of the theoretical COD, one considers that organic-N is converted into NH_3-N. This conversion is also what happens in the COD-test. For organic compound $C_nH_aO_bN_d$ the average oxidation number of the C-atom :

$$\text{Oxidation State of Carbon}(OxStC) = \frac{(2b - a + 3d)}{n}$$

Theoretical COD is calculated as the quantity of oxygen consumed in the following chemical oxidation

$$C_nH_aO_bN_d + (n + a/4 - b/2 - 3d/4)O_2 \rightarrow nCO_2 + (a/2 - 3d/2)H_2O + dNH_3$$

2.3.2 Expected gas composition

Three gases are mainly produced in an anaerobic digester: methane, carbon dioxide and hydrogen. Additionally, hydrogen sulphide and/or ammonia are expected for digesters treating wastewaters with high sulphates and/or nitrogen compounds, respectively. Practically, the methane to carbon dioxide ratio is the most important information about the gas composition when controlling the digester. The other gases are of particular importance depending on the composition of the waste or regarding their elimination before the methane/carbon dioxide sensor. In the latter case humidity also comes into the picture. Other factors that may cause more measurement of the gas components are the further processing of the gas (e.g. treatment before power generation), odour control and controlling corrosion /erosion of the transporting pipes.

If the compound $C_nH_aO_bN_d$ is anaerobically degraded, the produced gases can be estimated from the Buswell equation (Buswell et al., 1930)

$$C_nH_aO_bN_d + (n + a/4 - b/2 - 3d/4)\ H_2O \rightarrow$$
$$(n/2 + a/8 - b/4 - 3d/8)\ CH_4 + (n/2 - a/8 + b/4 + 3d/8)\ CO_2 + d\ NH_3$$

Thus, if the influent substrate composition is determined, it is possible to evaluate the produced gas composition. Figure 2.2 shows the theoretical composition of the biogas produced from the anaerobic degradation of different compounds in relation to their carbon oxidation state.

Similarly, the composition of the gas produced from a digester can provide information on the most probable substrate in the influent, provided that the digester is operating under normal operating conditions and with adequate retention time. It should be noted that if other electron acceptors such as sulphate, sulphite, nitrates and nitrite are present, a drop in the methane production will occur. Also, presence of these electron acceptors will cause a drop in the COD measurement compared to the COD of the existing organic compounds. The CO_2 estimated by the Buswell equation will be significantly larger than measured from the biogas for 2 reasons. First, CO_2 is soluble in water. Second, dissolved CO_2 is transformed to bicarbonate.

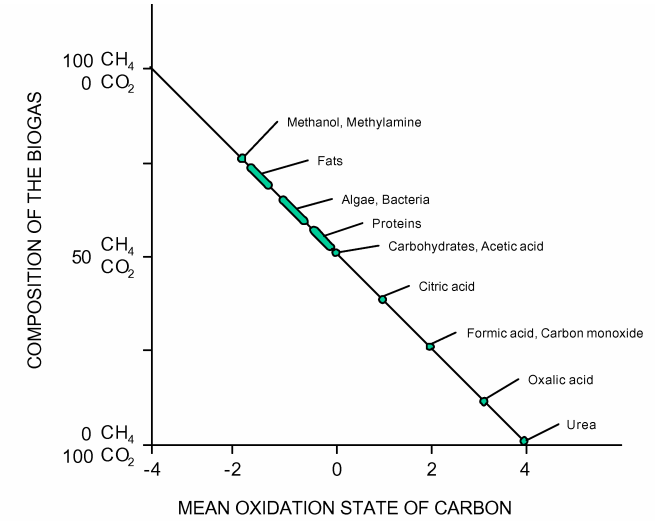

Figure 2.2 Theoretical composition of the biogas produced from the anaerobic degradation of different compounds in relation to their carbon oxidation state (adapted from Hulshoff. Pol., 2002).

2.3.3 Buffering capacity and pH

A very important aspect in the control of the pH in an anaerobic system, is the fact that VFA's are formed, alkalinity is consumed and hence the pH may drop below the optimum for the biological process. When there is enough alkalinity available (bicarbonate), the following reaction will occur, for instance with produced acetic acid:

$$CH_3COOH + Na^+ + HCO_3^- \rightarrow CH3COO^- + Na^+ + CO_2 + H_2O$$

Since bicarbonate is the most crucial substance in the buffering of the reactor content, the most logical chemical for supplementation of bicarbonate alkalinity is sodium bicarbonate. It is the only product which will gently shift the equilibrium to any desired value without disturbing the physical and chemical composition, provided that the sodium concentration is not elevated to a toxic level. Unfortunately, bicarbonate is more expensive than caustic and lime. Alkaline reagents such as caustic soda, soda ash, and lime cannot increase the bicarbonate alkalinity without reacting with soluble CO_2:

$$NaOH + CO_2 \rightarrow NaHCO_3$$

$$Na_2CO_3 + H_2O + CO_2 \rightarrow 2\ NaHCO_3$$

$$Ca(OH)_2 + 2\ CO_2 \rightarrow Ca(HCO_3)_2$$

Addition of these components therefore will result in a lower CO_2-concentration of the biogas. Also, the presence of calcium increases the probability of precipitation. The

impacts of these two side effects should be considered carefully in the monitoring and modelling activities.

The production of methane will perform optimally at pH values between 6.5-7.5. Below a pH of 6.0 methane production from VFA will proceed very slowly. It is very important to maintain the pH of an anaerobic system between the limits between which methanogens are active. Otherwise, acidogens will be more active converting organic substrates to VFA and the resulting VFA accumulation will then further drop the pH to inhibitory levels.

2.3.4 Substrate composition, hydrolysis and degradability

2.3.4.1 Carbohydrates

Most of the carbohydrates are anaerobically biodegradable (Noike et al., 1985). The common polysaccharides and the sugar monomers are easily degraded by anaerobic digestion. Cellulose biodegradation is not easy and less rapid (Noike et al., 1985; Yang et al. 2004). Still, the rate is sufficient and the biodegradation of pure cellulose is not a significant rate limiting. However, the cellulose of plants is never pure. Natural cellulose biodegradation is slower due to the protective effect of lignin (Lubberding, 2000). Anaerobic digestion is, however, useful for treatment of fruit and vegetable wastewater that contains lingo-cellulose in two step reactors (Bouallagui, 2005). If the quantity of particulate COD is high, quantification of lignocellulose might be needed. The particulate degradability can be assessed by comparing the acidified COD (i.e. the COD of VFAs in the reactor) with CODt and CODs in the influent.

2.3.4.2 Proteins and amino acids

Proteins are often easily hydrolysed into amino acids; however they are sometimes coagulated to insoluble forms when exposed to either heat, acids or tannins. Most types of proteins are hydrolysed and degraded anaerobically. In an anaerobic reactor, protein COD is converted to methane and protein organic-N to NH_4^+-N. Therefore, the potential of ammonia toxicity needs to be assessed. Generally, the degradation of proteins is not rate-limiting. In advanced reactor configurations, e.g. in an ABR, the reactor performance remains the same during gradual substitution of carbohydrate by protein (Stamatelatou, 2004).

2.3.4.3 Fats and long chain fatty acids

Fats are polymers of long chain fatty acids (LCFA) linked to a glycerol molecule with ester bonds. The hydrolysis of fats by extracellular lipase enzymes is generally rapid if the fat is soluble. The fats are more soluble if the pH-value is high (pH 8) compared to the pH of

acidifying reactors (5.5 - 6.0) where the fat is mostly insoluble and the hydrolysis is slow. Alkaline pre-treatment enhances the hydrolysis and increases the anaerobic digestion rates (Knezevic et al., 1995; Lin et al., 1997; Rajan et al., 1989). Pretreatment of fats with pancreatic lipase enzyme achieves better reductions of fat particulates compared to alkaline pre-treatment only with NaOH (Masse et al., 2001). Therefore, both the higher pH and the presence of hydrolytic enzymes need to be considered for efficient hydrolysis and anaerobic degradation of fats.

Hydrolysis of fats produces LCFA. The anaerobic degradation of the LCFA monomers of fat is actually not by fermentation but more similar to the anaerobic oxidation that is done by acetogenic bacteria. The most important products of the anaerobic oxidation of long chain fatty acids (LCFA) are acetate and hydrogen gas (67% and 33% respectively). LCFAs have inhibitory effects on acetogens, aceticlastic methanogens and hydrogenotrophic methanogens (Lalman and Bagley, 2000; 2001; 2002).

2.3.4.4 Phenolic Compounds

The phenolic compounds present in wastewater are usually derived from the lignin and tannin of plants. Lignin is apolar and is usually only soluble in alkaline conditions. However, some low molecular weight forms are soluble. The tannins are water soluble compounds. Tannins have ester inter-monomeric bonds that are easily hydrolysed biologically and acidified during anaerobic digestion. Lignin is generally less degradable than tannins.

2.3.4.5 Volatile Fatty Acids (VFA)

VFAs are easily biodegradable substrates. In the anaerobic process they are the intermediate products between the main processes: acidogenesis, acetogenesis and methanogenesis. Some wastewaters are high in VFA concentration, especially those originating from fermentation processes (e.g. vinasses). VFAs have pKa values between 4.7 and 4.9 and when produced they will cause a drop in the pH. Therefore, high VFA levels in wastewaters are favourable to anaerobic digestion provided that the pH is controlled to the optimum level (around 7). The type of VFA produced by anaerobic bacteria depends on the substrate type (Jordening and Winter, 2004). The acidification of LCFA by anaerobic bacteria leads to VFA in the form of acetate only. The acidification of monoscharides by anaerobic bacteria on the other hand produces acetate C_2, propionate C_3 and butyrate C_4. Thermodynamically, the production of C_2 by anaerobic acidifying bacteria is more favourable than respectively C_3 and C_4. Thus, for acidified wastewaters that mainly contain carbohydrates, it is expected that acetate will be the highest proportion of VFA. Under stress conditions to the process, propionate and butyrate concentrations are expected

to increase. For example, at high hydrogen concentration more propionate is produced (Bjornsson et al., 2001). Wastewaters with high protein (amino acids) content mainly yield acetate, butyrate, valerate (C_5) and propionate when acidified. The type of VFA produced depends on the type of amino acids degraded (Batstone et al., 2002).

2.3.5 Precipitation

Precipitation can be implemented as mechanism for partial COD removal with suspended solids in a pre-treatment step. However, it has an adverse effect on high rate reactors (e.g. Upflow Anaerobic Sludge Bed (UASB) and Fixed Bed Reactors (FBR)). The entrapment of the solids in the high rate reactors may cause dilution of the methanogen population while the contact time with the wastewater is relatively short. Some components precipitate due to pH changes and addition of calcium:

- Lignin precipitates by lowering pH below 9 or adding calcium.
- Fat precipitates by lowering pH below 8 or adding calcium
- Some proteins coagulate by lowering pH below 6
- Humic acids coagulate by lowering pH below 5 or adding calcium
- Pectin coagulates by adding calcium
- Protein plus tannins form protein-tannin aggregates
- …

2.3.6 Sulphates

Sulphate reducers are able to outgrow the methanogens (Kalyuzhnyi and Fedorovich, 1998). This is due to the higher energy gained by sulphate reduction compared to methanogenesis. Moreover, the reduction of sulphate to sulphides or H_2S is toxic to methanogens.

2.3.7 Nutrients and trace elements

Nutrients and trace elements are required by the anaerobic bacteria for growth. If limiting, they will eventually wash out of the treatment system. For this reason the wastewater has to contain a number of compounds from which the bacteria can synthesise their cell constituents. The nutrient composition of methanogens is presented in Table 2-1. These include macronutrients like nitrogen, phosphate, and sulphur that are needed in moderate

concentrations. All other elements (the micronutrients or trace elements) that the anaerobic bacteria need for growth must also be present.

Table 2-1 The elemental composition of methane bacteria (according to data published in Rajeshwari et al., 2000).

Macronutrients		Micronutrients	
Element	Concentration mg/kg dry bacteria	Element	Concentration mg/kg dry bacteria
N	65000	*Fe*	1800
P	15000	*Ni*	100
K	10000	*Co*	75
S	10000	*Mo*	60
Ca	4000	*Zn*	60
Mg	3000	*Mn*	20
		Cu	10

In order to ensure that there is a small excess in the nutrients needed, the nutrient concentration in the influent should be adjusted to a value that is at least twice the minimal nutrient concentration required (Rajeshwari et al., 2000).

2.3.8 Toxicity

2.3.8.1 Inorganic toxins

Ammonium: Ammonium nitrogen is present in wastewaters that originally contain high concentrations of proteins or amino acids. Organic nitrogen is also mineralised to ammonium during anaerobic digestion. The toxicity of ammonium is due to the unionised form (free NH_3) (Siegrist and Batstone, 2001). The fraction of free NH_3 is low at a pH value of 7 (about 1% of the (NH_4^++ NH_3) content) but it is about 10 times higher at pH 8. However, ammonia can be stripped by rising the pH to such alkaline level in a pre-hydrolysis/acidification step (Ahn et al., 2004). Anaerobic digestion is found to be still feasible at extreme ammonia concentrations (Koster and Lettinga, 1988).

Sulphur: Wastewater may contain inorganic forms of sulphur like sulphate (SO_4^{2-}) and sulphite (SO_3^{2-}). During the anaerobic digestion, these compounds are microbiologically reduced to hydrogen sulphide (H_2S). The toxicity of H_2S is again due to the unionised form (free H_2S). The concentration of free H_2S which causes 50% inhibition of methanogenic activity in granular sludge is approximately 250 mg S L^{-1} (Koster et al., 1986). For adapted sludge, this 50% inhibition concentration increases to 1000 mg S L^{-1} (Isa et al., 1986). Sulphate is relatively non-toxic. Therefore, the biological reduction of SO_4^{2-} to H_2S during the anaerobic digestion increases the toxicity of sulphur. In contrast, sulphite, SO_3^{2-}, is

more toxic than H_2S. Its biological reduction is very desirable because it will decrease the toxicity of sulphur.

Salt: Salt can cause toxicity problems if the concentration is very high. High concentrations of salts are sometimes present in the wastewaters of industrial processes. Salt toxicity on micro-organisms arises mainly from cations (Isik, 2004). For acidified wastewater, e.g from fermentation processes, high concentrations of salt are sometimes needed to neutralise the high concentrations of VFA. In these cases, the possibility of salt toxicity should be considered. The methanogenic toxicity of various kinds of salts is listed in Table 2-2. The results of this table indicate that monovalent cations are less toxic than divalent cations like calcium (Ca^{2+}). However, the low solubility of Ca^{2+} in the presence of bicarbonate at mild alkaline conditions may result in a low effective concentration in the reactor.

Table 2-2 The 50% inhibitory concentration of salts to the methanogenic activity of digested domestic sludge (Kugelman and McCarty, 1965). pH= 7.0, T= 35°C.

Salt	50% inhibitory concentration ($mg\ L^{-1}$)
Mg^{2+}	1930
Ca^{2+}	4700
K^{+}	6100
Na^{+}	7600

Heavy Metals: Heavy metals are sometimes present in wastewaters. Occasionally, it is necessary to add heavy metals as nutrients to wastewater for anaerobic treatment. However, care should be taken to avoid an overdose which can have a toxic effect. The toxicity of heavy metals depends on the soluble concentration. The soluble concentration of heavy metals would decrease as a result of precipitation reactions with carbonate (CO_3^{2-}) and sulphide (S^{2-}) which are generally present in anaerobic digesters. The precipitation of heavy metals is more effective at increasing pH due to the pH dependency of CO_3^{2-} and S^{2-}. Acidogens are found to be more sensitive to heavy metals than methanogens in granular sludge (Hickey et al., 1989; Lin and Chen, 1999; Lin, 1993). This could be related to the structure of sludge granules in which acidogens at the outside are more exposed to heavy metals. Lin and Chen (1999) found that the 50% inhibition to methanogens depends on the type of VFA, the type of heavy metal and the HRT.

2.3.8.2 Toxicity of organic compounds

As already mentioned, anaerobic bacteria are inhibited by accumulation of process intermediates such as VFA, LCFA and phenols. Also, there are other organic toxicants that

can be further investigated in particular cases such as phenolic amino acids, caramel compounds (e.g. furfurals), xenobiotic compounds, chlorinated hydrocarbons, formaldehyde, cyanide, petrochemicals, detergents and antibiotics.

2.3.9 Flows and seasonal changes

Most of the wastewater treatment systems are subject to seasonal changes, especially in the influent. These changes introduce high levels of uncertainty to the system design and operation. For domestic wastewater treatment, some of the uncertainty is resolved by studying the daily and annual variation of water consumption, the main source of wastewater, as well as the annual variation of rain and infiltration. Similarly, in industrial applications uncertainty can be reduced by investigating the upstream industrial processes, the main source of wastewater. Also, other long-term variation can be estimated from seasonal variation of the sources, e.g. crop harvest seasons for industries based on agricultural products (e.g. grape for vinasses). Moreover, studying the long-term records of the plant help in locating these variations.

2.4 Data validation

2.4.1 Organising data

Data should be stored in a well-defined structure. Variable names should be specified and clearly related to the variable's meaning. The measurement units should be specified in the most practical form. The data can be saved in a standard database or generally in tab delimited text files. Consequently, data sets are made consistent. Data interpolation is required to replace blank or NaN, Not a Number, records. The time scale should be unified for all measured variables. For example the gas flow rate can be measured and recorded more frequently than other variables such as COD. Also, the start of data records may be different and, therefore, unifying the time scale requires the following steps:

1. Set the start instant of the data to the earliest start of the available records so that no data are lost.
2. Set the time unit to a certain unit, e.g. days. However, the resolution is set to to the one of the more frequent records.
3. If records should be available at the same time interval, either interpolate the less frequent series of data or average the more frequent data by using a moving window.

For data averaging or eliminating noise, the Savitzky-Golay (Savitzky and Golay, 1964) smoothing filter is suggested. The same type of filter is described else-where with different

names, e.g. least-squares filter in (Hamming, 1983). Noise, trends and outliers can be removed in different ways (Olsson and Newell, 1999 ; Van Impe et al., 1998).

2.4.2 Quality control of data

Data quality can be checked using statistical process control (SPC) charts. Although statistical control charts are designed for discrete processes to control product quality at a certain set-point, their application can also be extended to check mass conservation and the COD balance in continuous processes. According to Castillo (2002) the assumed in-control model for a statistical control chart is $\forall t : Y_t = \mu + \varepsilon_t \wedge \varepsilon_t \sim (0, \sigma^2) \wedge Cov(\varepsilon_t, \varepsilon_{t+1}) = 0$. In other words, the quality characteristic Y_t is controlled at the expected mean μ and the error ε_t is normally distributed and not correlated over time. Therefore, a control chart can check a variable that is controlled at a set-point μ, e.g. the temperature of the digester, its head space pressure and the reactor pH. Furthermore, it can be used to check the consistency of a set of measurements by applying a continuity check. For instance, the COD balance around the digester can be checked to be within the control chart limits and therefore support the consistency of the gas and COD measurements.

There are different types of statistical control charts. Shewhart charts for averages ($\overline{X}$ - charts) check the control characteristic $\overline{X}$ (average of the control variable in a moving window) to be around the global mean μ and within the control limits. Control limits are estimated as a function of the standard deviation $\mu \pm k\sigma_{\overline{X}}$.

Similar to the $\overline{X}$ chart, the Exponentially Weighted Moving Average (EWMA) chart can be used to monitor the COD balance. This test can be based on theoretical relationships (e.g. simple models, mass balance) to test measured variables. According Castillo (2002) the EWMA is evaluated for the average measurement at each sampling point, $\overline{Y}_t$, according equation (2.1).

$$Z_t = \lambda \overline{Y}_t + (1-\lambda) Z_{t-1} \quad \text{for} \quad t = 1, 2, \ldots \qquad (2.1)$$

where λ is a weight parameter such that $0 < \lambda < 1$. Clearly, as λ approaches 1, more weight is given to the most recent average. As λ decreases, more weight is given to older data and in the limit when $\lambda = 0$ all Z_t values equal Z_0. Similarly, the assignment of a weight $\lambda(1-\lambda)^j$ to values of $\overline{Y}_{t-j}$ estimates Z_t according equation (2.2):

$$Z_t = \lambda \sum_{j=0}^{t-1} \overline{Y}_{t-j} (1-\lambda)^j \qquad (2.2)$$

Analogous to the $\overline{X}$ chart, Z_t is plotted in the EWMA chart with limits at

$$\mu \pm k \frac{\sigma}{\sqrt{n}} \sqrt{\frac{\lambda}{2-\lambda}} \qquad (2.3)$$

In the following example, the experimental data collected from a lab CSTR digester will be tested based on an approximate COD balance around the reactor. The COD balance will be approximated for two reasons. The first reason is that particulate COD in the effluent (i.e. biomass) is not measured. The second reason is that the experimental conditions are very dynamic and thus accumulation terms will introduce an error. Ignoring influent particulate COD, the COD balance at an instance can be approximated by equation (2.4).

ε = influent soluble COD – effluent soluble COD – COD of the off-gas - effluent particulate COD (2.4)

If this balance is performed for an instant of a steady state then ε = 0. However, for an instant of a dynamic state, ε compensates for the COD accumulation, whether it is due to process kinetics (e.g. uptake rates) or inefficient mixing. Performing the COD balance around the reactor avoids the explicit inclusion of the process kinetics. Averaging ε over a period larger than the retention time minimises the influence of the accumulation and the average of ε is approximately 0.

For the present CSTR experiment, the influent and effluent soluble COD are measured. The off-gas COD can be evaluated from the CH_4-flow, ignoring hydrogen. Since the effluent particulate COD is not measured, it can be eliminated from the calculation and hence the average of ε should be a positive value **e** equal to the expected average of the effluent particulate COD. From the experimental data, **e** is evaluated in equation (2.5):

e *(mgCOD/d)* $=(Q_{in}$ *(l/h)*$\cdot$ 24 *(h/d)* $\cdot(COD_{in}$ *(mgCOD/l)* $-COD_{dig}$ *(mgCOD/l)* $))-(Q_{gas}$ *(l/h)*$\cdot$24 *(h/d)*$\cdot P_{ch4}$ *(%)* / 100 *(%)* $\cdot$ 64*(gCOD/Mol)* $\cdot$ 1000 *(mg/g)* / 22.4 *(l/Mol)*)

(2.5)

This gives an *average of* ***e*** *= 1100 (mgCOD/d)*. This data set is globally valid since the calculated average is the accepted average biomass or particulate COD production per day. Figure 2.3 shows the EWMA control chart applied to the COD balance **e** to investigate the

consistency of the lab-CSTR data. The chart indicates that 4 periods are out of the control limits.

Sample points from 11 to 25 and 50 to 62 are out of the Lower Control Limit (LCL). Further investigation to the experiment log book and the simulation of the studied system in chapter 5 shows that these two periods correspond to a partial wash out of the biomass and shock load respectively. Two periods, from sample 30 to 39 and from sample 82 till the end of the experiment, are out of the Upper Control Limit (UCL). Further investigation and simulation showed that the gas composition measurements were not accurate during these two periods. Also, in the last period, extreme hydraulic and organic loads stopped the process.

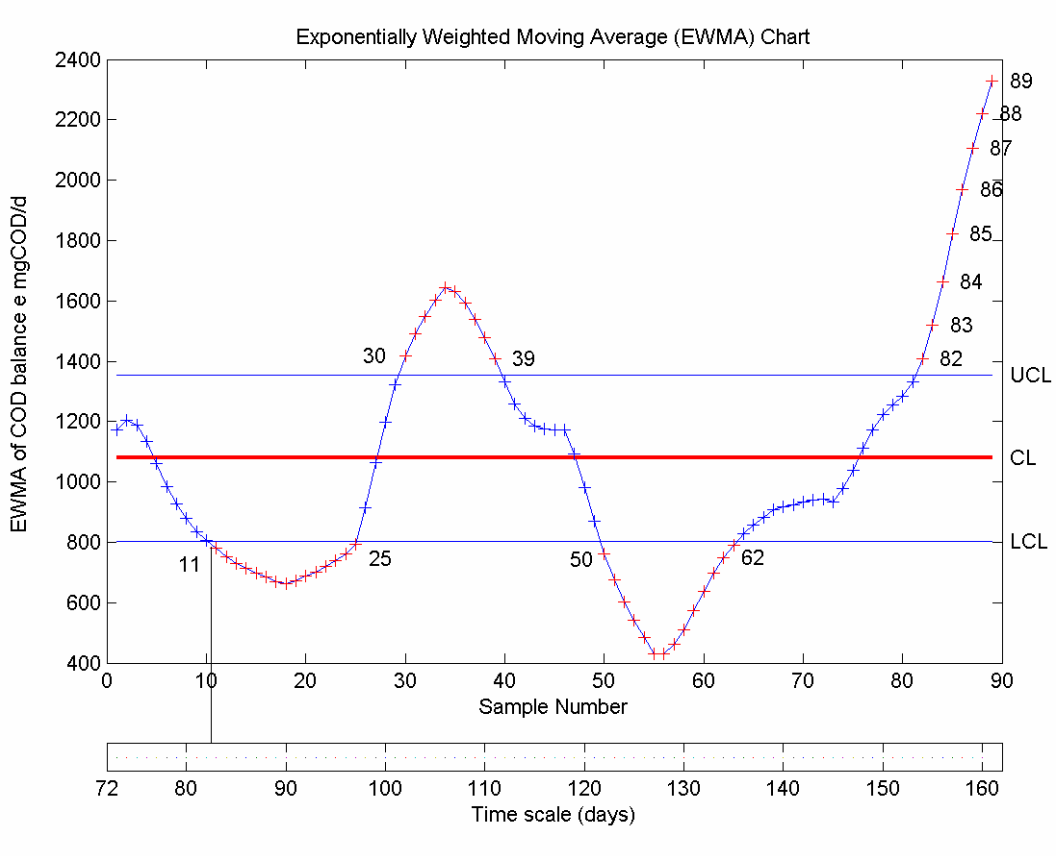

Figure 2.3 EWMA chart of the COD balance around a lab-scale CSTR

A cumulative sum control chart (CSUM) can be configured to show inconsistencies in the measurements. A CSUM chart is based on the concept of Sequential Probability Ratio Tests, SPRTs (Castillo, 2002). The tabular CSUM defines two one-sided cumulative sums, where the first one is calculated for evaluated for the average measurement at each sampling point, $\bar{Y}_t$, using equation (2.6).

$$S_{H,t} = Max(0, \overline{Y}_t - (\mu_0 + K) + S_{H,t-1}) \qquad (2.6)$$

This first sum accumulates deviations that are higher than $(\mu_0 + K)$ where μ_0 is the in-control process mean or target and *K* is the reference value (see below). The second sum is calculated for evaluated for the average measurement at each sampling point, $\overline{Y_t}$, using equation (2.7).

$$S_{L,t} = Max(0, (\mu_0 - K) - \overline{Y}_t + S_{L,t-1}) \qquad (2.7)$$

It accumulates deviations that are less than $(\mu_0 - K)$.

The reference value *K* is usually recommended to be set at half the size of the smallest shift in the mean that one wishes to detect quickly, equation (2.8)

$$K = \frac{\delta \sigma_{\overline{Y}}}{2} \qquad (2.8)$$

where δ is a multiple that allows to measure shift sizes in terms of the standard deviation $\sigma_{\overline{Y}}$ (Castillo, 2002). If individual measurements are used, the overall σ is used instead.

If several consecutive points appear in a $\overline{X}$ chart or EWMA control chart, their error accumulates till it appears in the CSUM chart. Symetric upper and lower limits are defined at $\pm H$ and are applied to calculate the CSUM chart. When the first cumulative sum S_H is higher than $+H$ or the negative of the second cumulative sum S_H is less than –H, it means that something was wrong in the previous period. Typical values for H are four or five times the magnitude of $\sigma_{\overline{Y}}$; or σ in case of the evaluation of individual measurements.

What is interesting about the CSUM chart is that it can be used to test the measurement directly without the need to estimate a quality characteristic such as the COD balance. It does not use a moving window and therefore it is suitable for direct application to process variables that are continuous in time. A drawback of the CSUM chart is that it only detects the inconsistency at the end of the faulty period when the error has accumulated and became significant. However, this drawback doesn't affect the usefulness of the CSUM to test the quality of the collected data sets. Figure 2.4 shows the CSUM applied to the gas flow data collected in the example. It shows accumulated measurement errors detected at point 40 and 100 corresponding to the out-of-UCL periods discovered by EWMA. This further clarifies that the gas measurement contained errors in those periods, refer to chapter 5. The second error at t = 100 didn't pass the UCL. Hence, it is important to realise that the

CSUM chart needs a careful selection of confidence intervals and, hence, H and δ should be tuned carefully.

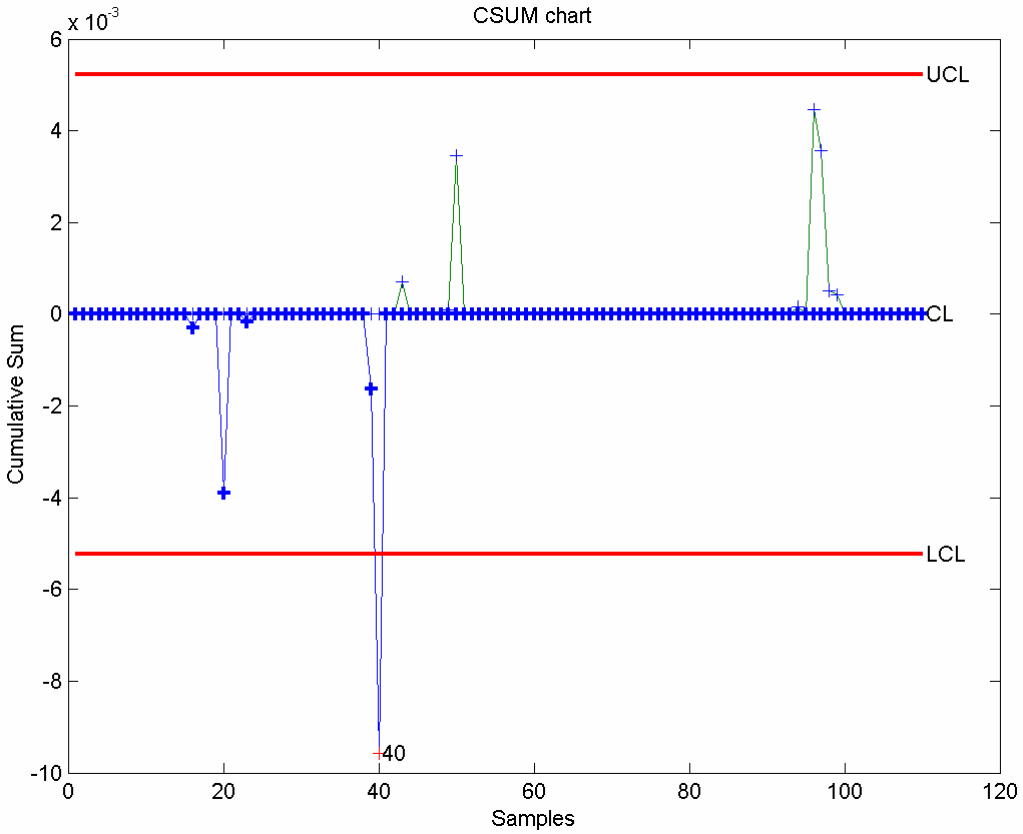

Figure 2.4 CSUM chart for gas flow measurements

The standard MATLAB® functions for $\overline{X}$ and EWMA control charts were updated for use with a moving window. Hence, they can be used for the quality control of a combination of continuous variables, e.g. by applying the COD balance. The CSUM chart has also been implemented to directly check the quality of measurements of any single variable and without the need to apply a moving window.

2.4.3 Fault detection

Figure 2.5 gives a schematic overview of the common faults detected in collected data or measured signals. The faults can be detected by an expert interpretation of the signal and its cross-correlation and cross-covariance plots. The detection of such faults and their reconciliation is important so as to increase the information content about the process.

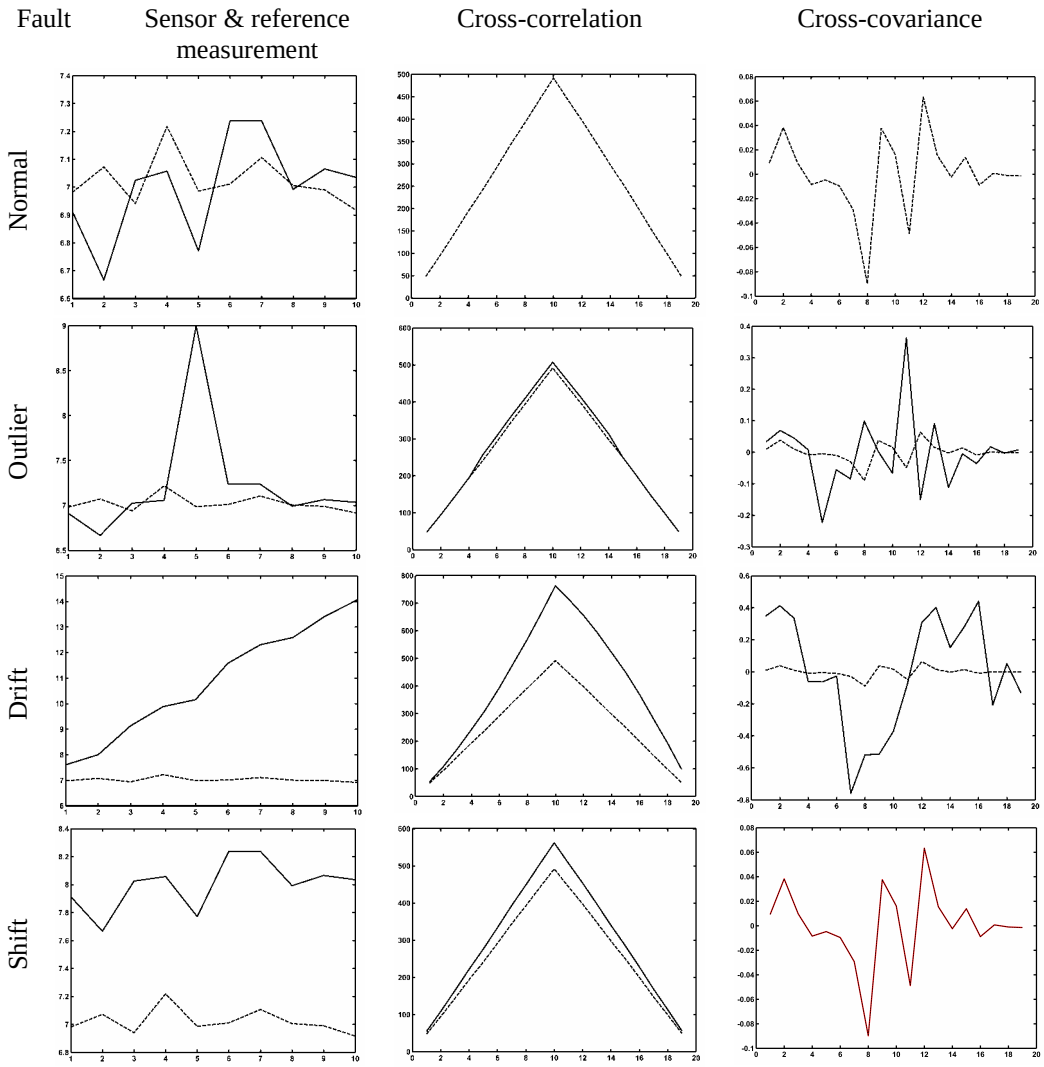

Figure 2.5 Common faults in measured signals and their cross-correlation and cross-covariance (continuous lines represent sensor measurements or function output. In faulty situation, broken lines represent the reference measurement or function output during normal conditions)

However, with large data sets and for on-line monitoring, the fault detection is more complex and is cumbersome if based on human expert judgement. Therefore, many advanced procedures exist to automate the fault detection and make it suitable for on-line use. They can be classified under three main categories. The first is based on fuzzy logic expert systems that give useful information on the process or instrument status, examples are in (Lardon and Steyer, 2003; Lardon et al., 2004; Puñal et al, 2002). The second is based on control models that can be used to check sensor networks, design software sensors and observers, and estimate confidence intervals and a confidence index on the measurement (Alcaraz-Gonzalez et al., 2002; Bastin and Dochain, 1990; Chachuat and Bernard, 2004; Dochain, 2003; Theilliol et al., 2003). The third category covers data-

driven statistical tools such as Principal Component Analysis (PCA), for process monitoring, fault detection and diagnosis (Chiang and Braatz, 2003; Cho et al., 2005; Choi et al., 2005; Choi and Lee, 2004; Ergon, 2004; Lee et al., 2005; Lee et al., 2004[a,b]; Misra et al., 2002, Yoo et al., 2004; Yoo et al., 2003).

2.5 Optimal experimental design

This section reviews the background of an iterative Optimal Experimental Design (OED) procedure. In previous sections of this chapter, possible categories of data that can be collected at an anaerobic digestion plant are described. The necessary data organisation, quality control and fault detection were highlighted. OED helps to limit the data collection to the most useful and economic data set to represent the process within a certain application.

2.5.1 Objectives

According to Dochain and Vanrolleghem (2001), the objectives of using OED are to decide on what manipulations of degrees of freedom should be done, such as:

- which measurements have to be performed,
- which measuring frequencies can or have to be used,
- when measurements should be collected, i.e. in which operation phase,
- where should the measurements be performed,
- what data quality control and data treatment should be used,
- what changes to control variables (e.g. inflow, reactor temperature, recycle flow rate) should be made in the light of plant constraints and available resources, including experimentation time and expenses.

With these manipulations the OED determines an optimal experiment (e.g. operation and data collection scenario) to calibrate and achieve the best fit of a selected model for the process. Thus, the model can be used for diagnosis, prediction and control of an anaerobic digestion plant.

2.5.2 Model calibration and the covariance matrix

The best fit of the model can be achieved by minimising the weighted sum of squared errors between the model predictions and the collected data by changing the model parameters (θ). The quality of the model calibration can be evaluated by analysing the

parameter estimation covariance matrix $C(\theta)$, equation (2.9). This matrix is calculated by many minimisation programs and can also be estimated using different techniques (Dochain and Vanrolleghem, 2001). The diagonal elements are the variances of the parameter estimates and the off-diagonal elements are the covariances between the different parameters. The parameter estimation covariance matrix can then be used to calculate confidence intervals, confidence regions and parameter correlations. Small variances will result in small confidence regions and thus more accurate parameter estimations.

$$C(\theta) = \begin{bmatrix} \sigma_{\theta_i}^2 & cov(\theta_i,\theta_j) & \cdots & cov(\theta_i,\theta_n) \\ cov(\theta_i,\theta_j) & \sigma_{\theta_j}^2 & & \\ \vdots & & \ddots & \\ cov(\theta_i,\theta_n) & & & \sigma_{\theta_n}^2 \end{bmatrix} \tag{2.9}$$

The quality of the model calibration greatly depends on the quality of the performed experiment. In other terms, the parameter estimates and their associated accuracy depends on the quality of the collected data and the operation scenario during which data was acquired. Poorly designed experiments result in poor data and will obviously result in poorly estimated parameters (large variances or strong correlations).

2.5.3 OED and the Fisher Information Matrix

In order to design an experiment that will produce high quality data required for an accurate model calibration, optimal experimental design for parameter estimation (OED-PE) can be used. This is a mathematical technique which provides a solution to the complex problem of choices and constraints resulting in an optimal experiment. The basis of OED-PE is the Fisher Information Matrix (FIM) which under certain conditions (uncorrelated white measurement noise), gives the lower bound of the parameter estimation covariance matrix $C(\theta)$, equation (2.10), according to the Cramer-Rao inequality (Ljung, 1999; Walter and Pronzato, 1997):

$$C(\theta) \geq FIM(\theta)^{-1} \tag{2.10}$$

The Fisher Information Matrix (Mehra, 1974) can be derived from the weighted least squares objective function $J(\theta)$, equation (2.11), of the model calibration minimisation problem:

$$J(\theta) = \sum_{i=1}^{N} (y_i(\theta) - y_i)^T Q_i (y_i(\theta) - y_i) \qquad (2.11)$$

In which y_i and $y_i(\theta)$ are vectors of N measured values and model predictions at times $t_i\ (i = 1 to N)$ respectively. Q_i is a square matrix with user-supplied weighting coefficients, usually taken as the inverse measurement error covariance matrix. The effect of a small parameter change $\partial\theta$ on the objective function, equation (2.11), can be expressed by linearisation of the model along the trajectory:

$$E[J(\theta + \partial\theta)] = \sum_{i=1}^{N} (y_i(\theta + \partial\theta) - y_i)^T Q_i (y_i(\theta + \partial\theta) - y_i) \qquad (2.12)$$

where: $$y_i(\theta + \partial\theta) \approx y_i(\theta) + \left[\frac{\partial y(\theta)}{\partial\theta}\right]_\theta \partial\theta \approx y(\theta) + S_\theta(\theta)\partial\theta \qquad (2.13)$$

In Equation (2.13), $S_\theta(\theta)$ is a vector of output sensitivity functions with respect to the parameters (section 2.5.4). Using equation (2.13), the expected value, equation (2.12), can be rewritten as follows:

$$E[J(\theta + \partial\theta)] = J(\theta) + \partial\theta \left[\sum_{i=1}^{N} S_\theta(\theta)^T Q_i S_\theta(\theta)\right] \partial\theta \qquad (2.14)$$

The term between brackets in equation (2.14) is called the Fisher Information Matrix (FIM). The FIM expresses the information content of the experiment by combining the sensitivity functions $S_\theta(\theta)$ and the measurement error Q_i. As already discussed, the FIM is an approximation of the inverse of the parameter estimation covariance matrix. This relationship is illustrated in Figure 2.6 for a 2 parameter estimation problem. The figure represents the confidence regions of two parameters (θ_1 and θ_2). The size, shape and orientation of the confidence ellipse is determined by the eigenvalues and eigenvectors of the FIM. The largest axis is inversely proportional to the square root of the smallest eigenvalue ($\lambda_{min}(FIM)$), the smallest axis is inversely proportional to the square root of the largest eigenvalue ($\lambda_{max}(FIM)$). In this way, the properties of the FIM determine the properties of the confidence region and thus the accuracy of the parameter estimates.

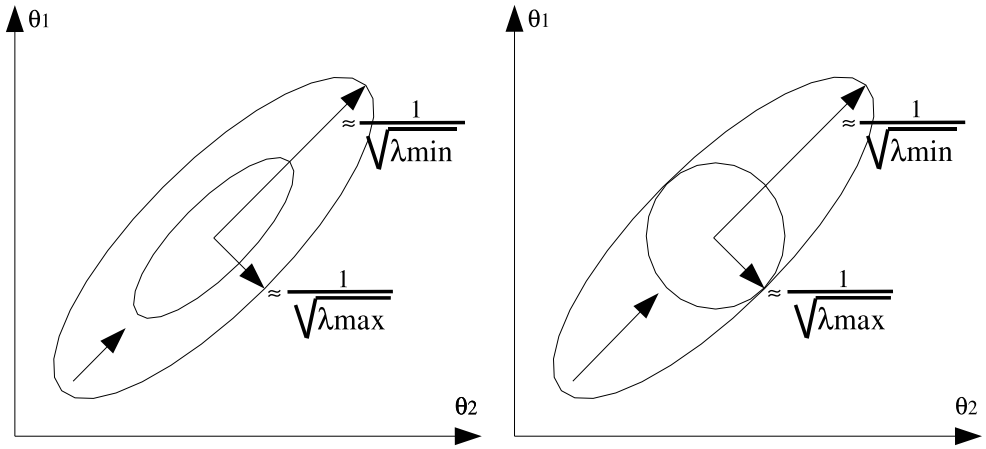

Figure 2.6 Confidence ellipse of two parameters: (left) Effect of the D-criterion on changing the ellipse, (right) Effect of the Modified E-criterion.

The information content of the experiment can be optimised by considering different measures of the FIM, Table 2-3 lists these criteria. The D- and A-optimal design criteria aim at minimising the volume of the confidence ellipse. This is illustrated in Figure 2.6 (left). The modified E optimal design criterion on the other hand aims at reducing parameter correlations by getting the shape of the confidence region as close to a circle as possible, which is illustrated in Figure 2.6 (right). The best value one can obtain for the modified E criterion is 1. However, one must be aware that such optimum only guarantees the confidence region is a circle, but it can be a very large circle (Dochain and Vanrolleghem, 2001).

Table 2-3 Different optimal design criteria based on FIM properties adapted from (Dochain and Vanrolleghem, 2001)

Name	Criterion
A-optimal design	$min\left[tr\left(FIM^{-1}\right)\right]$
Modified A-optimal design	$max\left[tr\left(FIM\right)\right]$
D-optimal design	$max\left[det\left(FIM\right)\right]$
E-optimal design	$max\left[\lambda_{min}\left(FIM\right)\right]$
Modified E-optimal design	$min\left[\frac{\lambda_{max}(FIM)}{\lambda_{min}(FIM)}\right]$

tr(): sum of eigenvalues, det(): product of eigenvalues

2.5.4 Local sensitivity analysis using finite differences

In order to calculate the Fisher Information Matrix a sensitivity analysis has to be performed first. Sensitivity analysis studies the sensitivity of the outputs of a system to changes in the parameters, inputs or initial conditions. Sensitivity analysis can be divided into two large categories: local and global sensitivity analysis. Local sensitivity analysis

methods refer to small changes of parameters, whereas global methods refer to the effect of simultaneous, possibly orders-of-magnitude parameter changes. For a detailed review of existing sensitivity techniques reference is made to the reviews of (Turanyi, 1990) and (Rabitz et al., 1983). The *FIM* is based on local sensitivity functions which will be discussed in detail in the next paragraphs.

The sensitivity of a state variable y to a parameter θ can be expressed as a sensitivity function, equation (2.15). A state variable y is called sensitive to θ if small changes in θ produce significant changes in y.

$$S(t) = \frac{\partial y(t)}{\partial \theta} \tag{2.15}$$

This partial derivative can be analytically solved if the analytical solution of the model equations is known. Unfortunately, this is rarely the case and numerical methods have to be used in order to approximate the sensitivity function, equation (2.15). Local sensitivity analysis techniques evaluate this partial derivative at one specific parameter value, also called the nominal parameter value. Many techniques exist to calculate local sensitivity functions. Most of these techniques require complex manipulations of the model equations. Such manipulations are often not practically feasible and most of the time a symbolic software is needed. The simplest way of calculating local sensitivities is to use the finite difference approximation. This technique is also called the brute force method or indirect method. It is very easy to implement because it requires no extra code beyond the original model solver. The partial derivative defined in equation (2.15) can be mathematically formulated by equation (2.16) (forward difference).

$$\frac{\partial y_i}{\partial \theta_j} = \lim_{\Delta\theta_j \to 0} \frac{y_i(t, \theta_j + \Delta\theta_j) - y_i(t, \theta_j)}{\Delta\theta_j} \tag{2.16}$$

However, according to De Pauw and Vanrolleghem (2003), the practical implementation of equation (2.16) has two major drawbacks. The resulting sensitivity function relates to the $(\theta_j + \Delta\theta_j/2)$ parameter set and it does not provide any information on the quality of the sensitivity function. If sensitivities are required around the nominal values of the parameters, then the central difference formula should be used, equation (2.17). Although this method requires $2p$ model evaluations, it is innovative in the sense that it can be used to provide additional information concerning the quality of the sensitivity function.

$$\frac{\partial y_i}{\partial \theta_j} \approx \frac{y_i(t, \theta_j + \Delta\theta_j) - y_i(t, \theta_j - \Delta\theta_j)}{2\Delta\theta_j} \tag{2.17}$$

According to De Pauw and Vanrolleghem (2003) the central difference method is implemented by two sensitivity functions, equations (2.18) and (2.19), by respectively increasing and decreasing the nominal parameter value by $\xi\theta_j$. The centralised sensitivity is calculated as the average of both sensitivity functions. The perturbation factor ξ is selected such that it allows a minimum difference between both sensitivity functions for accurate sensitivity and therefore accurate FIM evaluation.

$$\frac{\partial y}{\partial \theta_{j+}} = \frac{y(t,\theta_j + \xi\theta_j) - y(t,\theta_j)}{\xi\theta_j} \tag{2.18}$$

$$\frac{\partial y}{\partial \theta_{j-}} = \frac{y(t,\theta - \xi\theta_j) - y(t,\theta_j)}{\xi\theta_j} \tag{2.19}$$

To make the numerical error and the error introduced by the nonlinearity of the model as small as possible the difference between these two sensitivity functions should be minimal. Several criteria can be used to quantify this difference.

1. Sum of squared errors (SSE).

$$\frac{\sum\left(\frac{\partial y}{\partial \theta_+} - \frac{\partial y}{\partial \theta_-}\right)^2}{N} \tag{2.20}$$

   For this criterion, the squared error between both sensitivity functions is calculated and summed over all times where the sensitivity is required (N).

2. Sum of absolute errors (SAE).

$$\frac{\sum\left|\frac{\partial y}{\partial \theta_+} - \frac{\partial y}{\partial \theta_-}\right|}{N} \tag{2.21}$$

   For this criterion, the absolute error between both sensitivity functions is calculated and summed over all times where the sensitivity is required (N).

3. Maximum relative error (MRE).

$$\left|\frac{\frac{\partial y}{\partial \theta_+} - \frac{\partial y}{\partial \theta_-}}{\frac{\partial y}{\partial \theta_+}}\right|_{MAX} \tag{2.22}$$

   This criterion returns the maximum value of the relative difference between both sensitivity functions. One should be careful with this criterion because $\partial y/\partial\theta_+$ or $\partial y/\partial\theta_-$ may become 0. In this special case the criterion can be specified to return 0.

4. Ratio between sensitivities (RATIO).

$$\left| 1 - \frac{\frac{\partial y}{\partial \theta -}}{\frac{\partial y}{\partial \theta +}} \right|_{MAX} \qquad (2.23)$$

This criterion is based on the ratio of the sensitivity functions. The ideal case is when this ratio equals 1, because then both sensitivity functions are equal. The criterion returns the maximum deviation from this ideal situation. Like the MRE criterion one should be careful if $\partial y/\partial \theta_+$ becomes 0. In this special case the criterion can be specified to returns 0.

The optimum perturbation factor was determined for accurate sensitivity analysis of the anaerobic digestion model AM2, described in chapter 3, before its implementation in the protocol and the OED in chapter 7. Figure 2.7 illustrates the use of these criteria for the sensitivity of organic substrate (S_1) to the maximum specific growth rate for acidogenic bacteria ($\mu_{max,1}$).

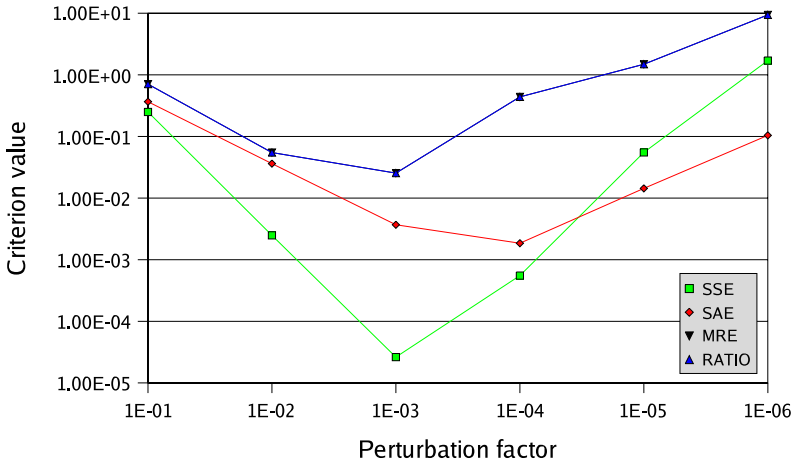

Figure 2.7 Different criteria calculated for the sensitivity of organic substrate (S_1) to the maximum specific growth rate ($\mu_{max,1}$) for acidogenic biomass in the AM2 model (Bernard et al., 2001; 2002)

The figure clearly illustrates the nonlinearity effects of the model for perturbation factors larger than 10^{-3}. An example of the calculated sensitivity functions is given in Figure 2.8 for a perturbation factor 10^{-1}. It is clear that the $\partial y/\partial \theta_-$ differs from $\partial y/\partial \theta_+$ due to nonlinearities. The sensitivity at 10^{-3} is also shown and it has less nonlinearity effect. Figure 2.9 illustrates the effect of numerical errors for perturbation factors lower than 10^{-3} and shows the effect of numerical errors (the spike at 40 days) at a perturbation factor of 10^{-3}.

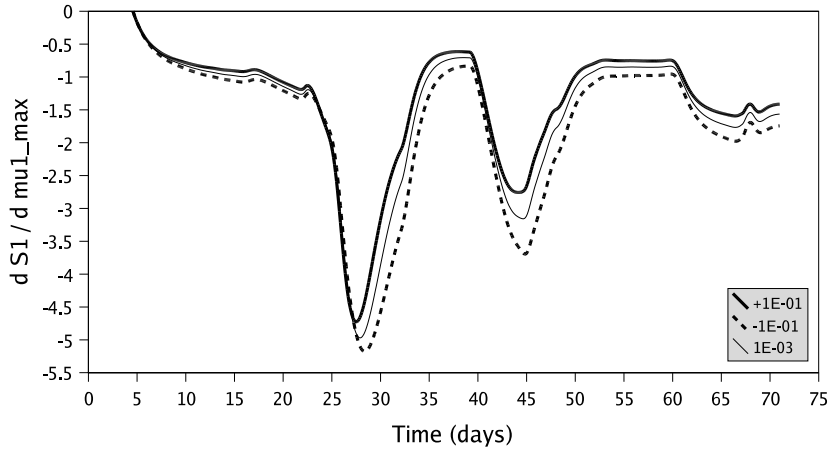

Figure 2.8 Effect of the nonlinearity of the model on the sensitivity calculations. Perturbation factor 1E± 1.

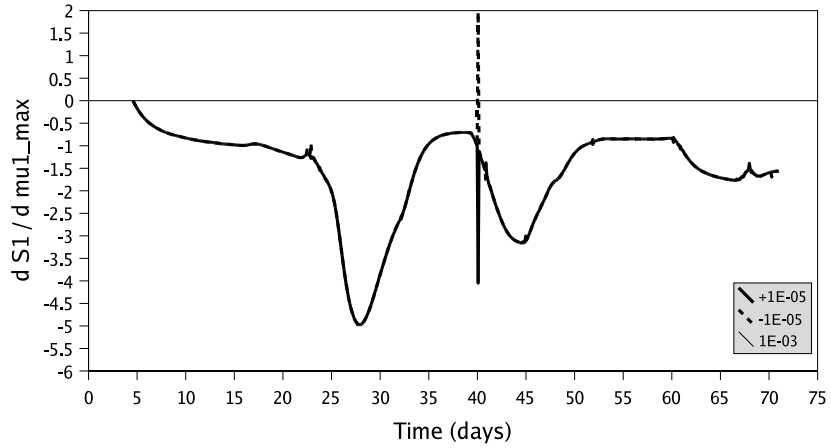

Figure 2.9 Effect of numerical error on the sensitivity calculations. Perturbation factor 1E± 5.

Therefore, the perturbation factor is set to 10^{-3} for accurate sensitivity analysis, and the FIM and OED evaluations for the AM2 model implementation that is illustrated in chapter 7.

2.5.5 Iterative optimal experimental design procedure

Figure 2.10 shows the procedure for optimal experimental design according (Dochain and Vanrolleghem, 2001). The procedure is general and it can be implemented to calibrate an existing model on lab- and pilot-scales. Moreover, it can be adapted to select a model for a full-scale plant and define the operating scenario and the monitoring system of full scale plants.

Before starting experimental design, a preliminary model (control model) should be available. In most cases the control model is fitted to data acquired from initial experiments. For anaerobic digestion plants this is usually based on the long-term data that is already available on the plant. If the plant is new, its detailed design can be used to configure a reference model (more complex) to generate the expected data of the plant. The control model is then fitted to this generated data. If no data is available, there is no reference model and if, on top of that, no initial experiments can be performed, a proper set of default parameter values can be used. Once the model is identified, the iterative procedure is started. Based on the control model an experiment is proposed by choosing certain experimental degrees of freedom. This experiment is then simulated on the computer and an objective function is evaluated. Typically this objective function is a design criterion from the Fisher Information Matrix, Table 2-3, which summarises the information content of the proposed experiment and is also a measure for the accuracy of the parameter estimates (in case this experiment would be performed in reality and the model would be fitted to the acquired data). A (nonlinear) optimisation algorithm is used to propose different experiments and find an "optimal" experiment in the sense that it maximizes the parameter estimation accuracy and/or minimizes parameter correlations. In the light of defined constraints, the optimal experiment can relate to the operating conditions of the plant and measurement settings or an initial experiment that is performed when the anaerobic digestion and/or the monitoring system are commissioned. Based on the data of this experiment the model can be refitted and the accuracy of the parameter estimates evaluated. If the required accuracy is not yet reached, a further iteration can be performed, leading to an even better "optimal" experiment (operating conditions and measurement settings). Finally a calibrated model is available for its intended use, e.g. planning control strategies.

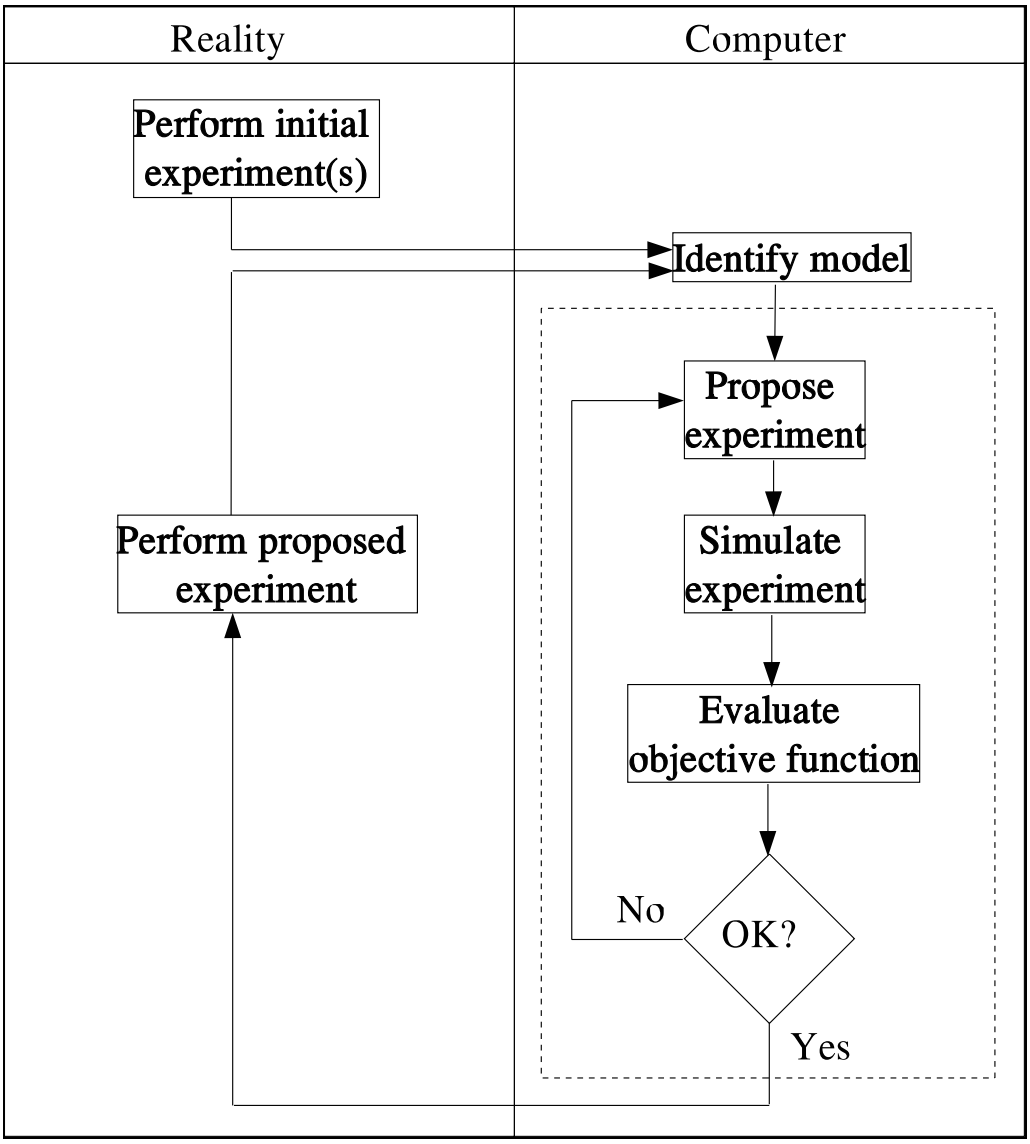

Figure 2.10 General procedure for optimal experimental design (Dochain and Vanrolleghem, 2001)

2.6 Conclusions

For optimisation of anaerobic digestion applications, the main data categories and procedures of data validation and Optimal Experimental Design (OED) were reviewed. This review can guide data collection for better definition of models and optimum design of monitoring systems.

The anaerobic process is optimal in the mesophilic and thermophilic temperature ranges. The anaerobic biomass is active at lower temperatures but they grow slowly. To avoid expensive heating systems, different reactor configurations have been designed to increase the process rate and compensate for the slow growth.

Data of plant layout and reactor types guide the definition of hydrodynamic and solid transport assumptions. For a CSTR, the efficiency of the mixing system is important to define the Solids Retention Time, SRT, in the anaerobic model. For anaerobic filters a high recycling flow rate is needed, which makes that they can be considered as CSTR but with a high SRT. Anaerobic sludge beds have a high SRT too. Their hydrodynamic model will depend on the applied flow distribution and velocity, especially in the upflow configuration. They can be modelled as a series of CSTR's but this will require different sampling points along the reactor. Optimal Experimental Design can be used to locate the most informative sampling locations. Accordingly, the reactor layout may change and a redefinition of the model might be needed. Therefore, with an approximation for these configurations, e.g. for an UASB, the reactor could be considered as a CSTR but the cross-sectional distribution of flow should be guaranteed and the SRT should be estimated carefully. Similarly, fluidised bed reactor modelling will be dependent on the upflow velocity but also on the expansion of the bed that will depend on the media and/or the sludge granule properties. The hydrodynamics of baffled reactors will be dependent on the location of baffles, the configuration of compartments and the developed flow pattern. In general, they can be modelled as a series of CSTR's. The sequencing batch reactor modelling will depend on the phased operation and whether the settling phase needs to be modelled or not. Other plant components like membrane separators or liquefying and acidifying compartments may need to be integrated with the main reactor model.

The reviewed wastewater characteristics guide the data collection and support the model kinetics selection. If the content of particulates is high, disintegration and hydrolysis steps need to be considered. Also, substrate composition and degradability are important to define the process pathways in the model. The main pathways of carbohydrate, fat and protein degradation are different, e.g. in terms of their hydrolysis rates and the produced VFA's. Also, some general properties of wastewater such as precipitation, pH, availability of enough nutrients and trace elements will influence the modelling activity and may need process optimisation in terms of pre-separation of precipitates, pH adjustment and dosing of nutrients. These options will need more parameters to be characterised in the wastewater. Toxicant components need to be investigated since they may require implementation of some inhibition mechanisms in the model and therefore more measurements might be required. Flow dynamics and seasonal changes of the wastewater are important variations that may require more than one modelling scenario. The study of the oxidation state of substrate and wastewater COD and evaluation of the expected gas composition are useful to properly design the physicochemical part of the model. Also, they will influence the gas phase measurement in the design of the monitoring system.

In the operation phase, the collected measurements need to be organised and validated so that the model parameters can be estimated accurately. Simple statistical quality control tools were useful to understand operation dynamics. Examples were given for a CSTR experiment showing washout of biomass, overload conditions and some measurement faults can be detected by simple SPC charts. Prior detection of these conditions was useful for the model application illustrated in chapter 5. More advanced fault detection procedures exist and they are much more useful and applicable on-line. They are briefly classified in this review but no more details are given since fault detection is indeed another extended area for research.

An Optimal Experimental Design procedure is reviewed highlighting its concept. OED is important to achieve a complementary link between modelling and monitoring activities. It helps to properly design the monitoring system and maximise the information content of the collected measurement. On the other hand, it improves model parameter estimation results. The reviewed procedure depends on evaluation of the covariance between model parameters and, thus, model parameter correlations. This information is necessary to improve the model structure and reduce the number of parameters to be estimated. The numerical evaluation of the OED depends on sensitivity analysis and therefore sensitivity analysis is introduced. The introduction of the sensitivity analysis is important to highlight the associated computation problems and the necessity to select an appropriate perturbation factor. The main computational problems arise from simulation numerical errors and the nonlinearity of models that are expected to a large extent in complex anaerobic models. The introduction of the OED procedure is necessary for its application in chapter 7. It will be implemented to design the monitoring system using a control model (AM2). Therefore, in this chapter, the appropriate perturbation factor for sensitivity calculation is checked for this control model to guarantee the accurate OED results as will be presented in chapter 7.

Part I
Modelling

Chapter 3

WEST: Implementation of Anaerobic Digestion Models

Abstract

WEST implementations of three anaerobic digestion models are discussed in this chapter. The IWA Anaerobic Digestion Model No.1 (ADM1) is illustrated in detail to highlight the necessary updates to be made to the model for a successful implementation. The structure of the ADM1 is introduced and its relevance for modelling the anaerobic digestion of different wastewater types is highlighted. The mass balance of the model is extended to ensure carbon and nitrogen balances. The implemented inhibition terms are clearly defined. The pH calculation is updated for a feasible Differential Equations (DE) implementation. A mathematical procedure is proposed and implemented to solve the set of non-linear algebraic equations for the pH calculation. The external calculation is nested with the simulation that uses a DE solver to achieve a DAE implementation of the model and improve the simulation speed. The necessary updates in the standard Model Specification Language (MSL) code to build ADM1 as a multiphase model with multiple matrices are illustrated. Possible simplifications to the gas transfer and pH modelling are introduced using two examples of simpler anaerobic digestion models compared to ADM1, the detailed model of Siegrist and the simplified model for control applications, AM2.

CHAPTER 3

3.1 Introduction to ADM1 model

The International Water Association (IWA) Anaerobic Digestion Model no.1 (ADM1) is implemented in WEST and used throughout this research as a reference model. As shown in Figure 3.1 the IWA ADM1 model (Batstone et. al, 2002) considers the conversion processes in the digester from the most complex (substrate) to the simplest components. In other words, it starts from the disintegration of composite particulate till the gas formation.

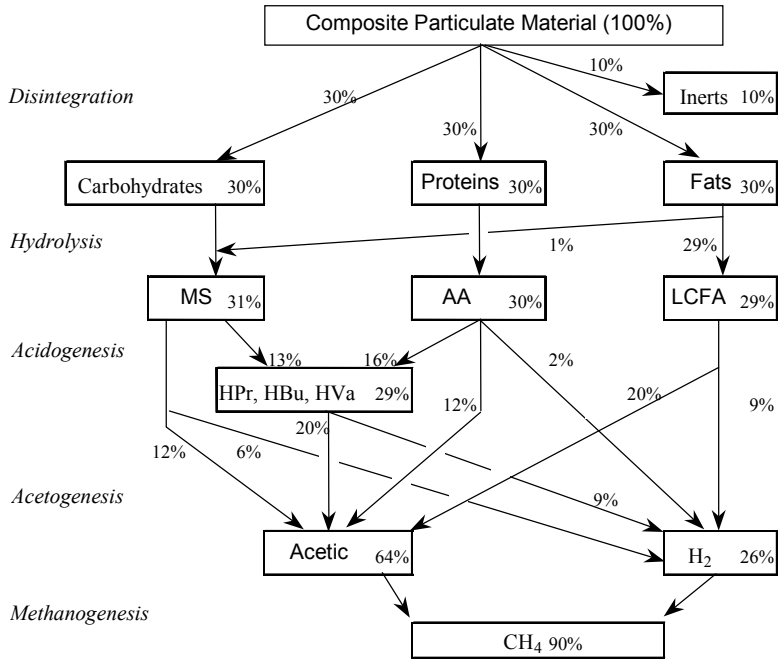

Figure 3.1 COD flux for a particulate composite comprised of 10% inerts, and 30% each proteins, carbohydrates and fats (in terms of COD). Propionic acid (10%), butyric acid (12%) and valeric acid (7%) are grouped in the diagram for simplicity (Batstone et. al, 2002).

However, in some industrial applications such as the case studies that are presented in chapter 5 and 6, the supplied wastewater is simpler. The process for the supplied wastewater mainly takes the path of carbohydrates that is shown in Figure 3.1. Moreover, in the case of treating vinasses, chapter 5, the waste is already acidified and the process starts mainly with the acetogenesis step. However, implementation of the extended ADM1 to such applications is important for two reasons. First, it is possible to still find considerable fractions of composite particulate in these wastewaters that originates from plant sources (e.g. grapes used in wineries, barley used in breweries and distilleries). These materials remain useful though. For a cost effective manufacturing process, they can be separated and used for animal feed. Second, the decay of biomass produced in the digestion processes is modelled; the decaying species are lumped and added to the

composite particulates. Therefore, it is advantageous that all digestion paths described in Figure 3.1 are included, even to describe the digestion of relatively simple wastewaters as vinasses.

The biogas is a valuable product of the anaerobic process and an important control parameter of the processes. The anaerobic reactor is a closed system. Therefore, it is essential to also consider the gas - liquid transfer and evaluate the flow of gas components. In the IWA ADM1, the gas transfer between two compartments (i.e gas compartment and liquid compartment), shown in Figure 3.2, is modelled by considering three gas components of the biogas: methane, carbon dioxide and hydrogen. Their concentrations are evaluated in both phases.

Also, the anaerobic process is sensitive to pH changes. There are buffering systems such as VFAs (acetate, propionate, butyrate and valerate), bicarbonate and ammonia affecting the pH. Those buffers were considered in the ADM1 by their corresponding dissociation reactions that can be modelled by either differential equations (DE implementation) or by algebraic equations of equilibrium (DAE implementation). From either implementations, the hydrogen ion concentration and the pH are calculated. Ion concentrations are used to estimate inhibition factors that are also considered in the model. All these reaction rates add more state variables that are in most cases not measured online and require a lot of effort for off-line analysis. It also implies a burden on the numerical solver used for simulation. The solver should be able to handle this large number of equations with different time constants: slow (biological), intermediate (physical) and fast (chemical).

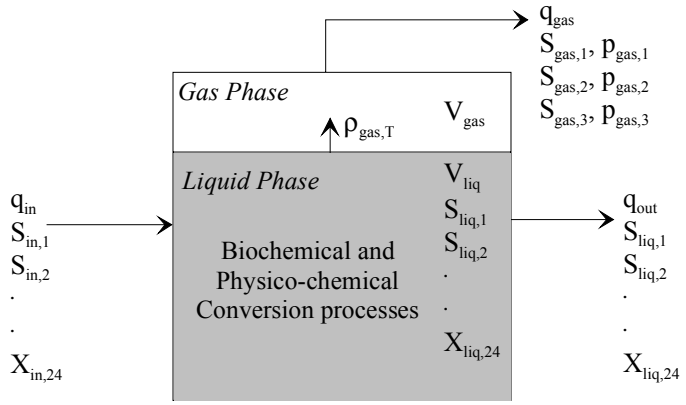

Figure 3.2 Schematic diagram of a typical single-tank digester (Batstone et al, 2002)

Therefore, ADM1 should be seen as a detailed reference model that helps the understanding of the process/process changes, validating simple models, generating balanced sets of data and optimal experimental design. Of course, ADM1 is not a model to be used in on-line control, but it could be used to evaluate control systems and strategies.

Therefore, another model was implemented to base control systems on, AM2, and it is also presented in this chapter. Both models are used in chapter 7 to design a protocol to set up a digester monitoring system.

3.2 Extending ADM1 elemental balance

According the IWA ADM1 report (Batstone et al, 2002), the COD balance of the model is implicit since all the COD components of the model are presented in COD units, Table 3-1. In the report, a carbon balance was considered only when inorganic carbon is the carbon source for, or a product of, catabolism or anabolism (i.e. uptake of sugars, amino acids, propionate, acetate and hydrogen).

Table 3-1 ADM1 components and units

Model component	Descriptions	Unit
S_{su}	Monosaccharides	(kgCOD m^{-3})
S_{aa}	Amino Acids	(kgCOD m^{-3})
S_{fa}	Fatty Acids	(kgCOD m^{-3})
S_{va}	Total Valerate	(kgCOD m^{-3})
S_{bu}	Total Butyrate	(kgCOD m^{-3})
S_{pro}	Total Propionate	(kgCOD m^{-3})
S_{ac}	Total Acetate	(kgCOD m^{-3})
S_{h2}	Hydrogen gas	(kgCOD m^{-3})
S_{ch4}	Methane gas	(kgCOD m^{-3})
S_{IC}	Inorganic carbon	(kmole C m^{-3})
S_{IN}	Inorganic nitrogen	(kmole N m^{-3})
S_I	Soluble inerts	(kgCOD m^{-3})
X_c	Composites	(kgCOD m^{-3})
X_{ch}	Carbohydrates	(kgCOD m^{-3})
X_{prot}	Proteins	(kgCOD m^{-3})
X_{li}	Lipids	(kgCOD m^{-3})
X_{su}	Sugar degraders	(kgCOD m^{-3})
X_{aa}	Amino Acids degraders	(kgCOD m^{-3})
X_{fa}	Fatty Acids degraders	(kgCOD m^{-3})
X_{c4}	Valerate and Butyrate degraders	(kgCOD m^{-3})
X_{pro}	Propionate degraders	(kgCOD m^{-3})
X_{ac}	Acetate degraders	(kgCOD m^{-3})
X_{h2}	Hydrogen degraders	(kgCOD m^{-3})
X_I	Particulate inerts	(kgCOD m^{-3})

In the implementation of this work, the carbon balance is considered for all biological reactions to prevent carbon leaks due to differences in the model fraction parameters. This is achieved by defining the carbon content C_i of all model components and closing the carbon balance for each reaction with the inorganic carbon, S_{IC}. Accordingly, the stoichiometry of S_{IC} is defined by (3.1) for all reactions.

$$\forall : j = 1-19 \quad \nu_{10,j} = -\sum_{i=1-9,11-24} C_i \nu_{i,j} \tag{3.1}$$

Equation (3.1) results in the update of column 10 of the model matrix, Table 3-2. Similarly, by defining the nitrogen content N_i of all model components, equation (3.2) is applied to achieve the nitrogen balance and update column 11 of the matrix.

$$\forall : j = 1-19 \quad \nu_{11,j} = -\sum_{i=1-10,12-24} N_i \nu_{i,j} \tag{3.2}$$

the particulates stoichiometry will not be affected, Table 3-3.

Closing carbon and nitrogen balances is important to adequately model a system. Inorganic carbon and nitrogen are influencing the model kinetics through the pH and inhibition terms. The inorganic carbon sources the bicarbonate concentration and buffers the process in the optimum pH range. A pH inhibition term is connected to all uptake reactions. Inorganic nitrogen sources the ammonium concentration. Ammonium is an alkalinity source that resists a pH drop. Ammonia is the other component of the inorganic nitrogen and its toxicity to acetate uptake is considered in the model. Also, insufficient nitrogen is considered in the model since it limits biomass growth.

Another reason to close the inorganic carbon and nitrogen balance is concerned with pre- and post-treatment processes, i.e. in context of plant-wide modelling, Chapter 8 and 9. For instance, applying the model for sludge digestion, alkalinity (bicarbonate) and ammonia are components of the conventional activated sludge processes and models. Also, the digester effluents are high in ammonia concentrations that might call for the application of advanced processes for ammonia removal. Therefore, an accurate estimation of inorganic carbon and nitrogen in ADM1 is also important when it is used to evaluate these processes or when it is linked to their models.

Table 3-2 Updated Petersen matrix of the IWA Anaerobic Digestion Model No.1 (for soluble components)

i	Component →	1	2	3	4	5	6	7	8	9	10	11	12	Rate (ρ_j, kg COD.m^{-3}.d^{-1})
j	Process ↓	S_{su}	S_{aa}	S_{fa}	S_{va}	S_{bu}	S_{pro}	S_{ac}	S_{h2}	S_{ch4}	S_{IC}	S_{IN}	S_I	
1	Disintegration										$-\sum_{i=1-9,11-24} C_i\nu_{i,1}$	$-\sum_{i=1-12,14-27} N_i\nu_{i,1}$	$f_{sI,xc}$	$k_{dis}X_c$
2	Hydrolysis of Carbohydrates	1									$-\sum_{i=1-9,11-24} C_i\nu_{i,2}$			$K_{hyd,ch}X_{ch}$
3	Hydrolysis of Proteins		1								$-\sum_{i=1-9,11-24} C_i\nu_{i,3}$			$K_{hyd,prot}X_{prot}$
4	Hydrolysis of Lipids	$1-f_{fa,li}$		$f_{fa,li}$							$-\sum_{i=1-9,11-24} C_i\nu_{i,4}$			$K_{hyd,li}X_{li}$
5	Uptake of Sugars	-1				$(1-Y_{su})f_{bu,su}$	$(1-Y_{su})f_{pro,su}$	$(1-Y_{su})f_{ac,su}$	$(1-Y_{su})f_{h2,su}$		$-\sum_{i=1-9,11-24} C_i\nu_{i,5}$	$-(Y_{su})N_{biom}$		$k_{m,su}\frac{S_{su}}{K_{s,su}+S_{su}}X_{su}I_1$
6	Uptake of Amino Acids		-1		$(1-Y_{aa})f_{va,aa}$	$(1-Y_{aa})f_{bu,aa}$	$(1-Y_{aa})f_{pro,aa}$	$(1-Y_{aa})f_{ac,aa}$	$(1-Y_{aa})f_{h2,aa}$		$-\sum_{i=1-9,11-24} C_i\nu_{i,6}$	$-\sum_{i=1-10,12-27} N_i\nu_{i,6}$		$k_{m,aa}\frac{S_{aa}}{K_{s,aa}+S_{aa}}X_{aa}I_1$
7	Uptake of LCFA			-1				$(1-Y_{fa})0.7$	$(1-Y_{fa})0.3$		$-\sum_{i=1-9,11-24} C_i\nu_{i,7}$	$-(Y_{fa})N_{biom}$		$k_{m,fa}\frac{S_{fa}}{K_{s,fa}+S_{fa}}X_{fa}I_2$
8	Uptake of Valerate				-1		$(1-Y_{c4})0.54$	$(1-Y_{c4})0.31$	$(1-Y_{c4})0.15$		$-\sum_{i=1-9,11-24} C_i\nu_{i,8}$	$-(Y_{c4})N_{biom}$		$k_{m,c4}\frac{S_{va}}{K_{s,c4}+S_{va}}X_{c4}\frac{1}{1+S_{bu}/S_{va}}I_2$
9	Uptake of Butyrate					-1		$(1-Y_{c4})0.8$	$(1-Y_{c4})0.2$		$-\sum_{i=1-9,11-24} C_i\nu_{i,9}$	$-(Y_{c4})N_{biom}$		$k_{m,c4}\frac{S_{bu}}{K_{s,c4}+S_{bu}}X_{c4}\frac{1}{1+S_{va}/S_{bu}}I_2$
10	Uptake of Propionate						-1	$(1-Y_{pro})0.57$	$(1-Y_{pro})0.43$		$-\sum_{i=1-9,11-24} C_i\nu_{i,10}$	$-(Y_{pro})N_{biom}$		$k_{m,pro}\frac{S_{pro}}{K_{s,pro}+S_{pro}}X_{pro}I_2$
11	Uptake of Acetate							-1		$(1-Y_{ac})$	$-\sum_{i=1-9,11-24} C_i\nu_{i,11}$	$-(Y_{ac})N_{biom}$		$k_{m,ac}\frac{S_{ac}}{K_{s,ac}+S_{ac}}X_{ac}I_3$
12	Uptake of Hydrogen								-1	$(1-Y_{h2})$	$-\sum_{i=1-9,11-24} C_i\nu_{i,12}$	$-(Y_{h2})N_{biom}$		$k_{m,h2}\frac{S_{h2}}{K_{s,h2}+S_{h2}}X_{h2}I_1$
13	Decay of X_{su}										$-\sum_{i=1-9,11-24} C_i\nu_{i,13}$	$-\sum_{i=1-10,12-24} N_i\nu_{i,13}$		$k_{dec,Xsu}X_{su}$
14	Decay of X_{aa}										$-\sum_{i=1-9,11-24} C_i\nu_{i,14}$	$-\sum_{i=1-10,12-24} N_i\nu_{i,14}$		$k_{dec,Xaa}X_{aa}$
15	Decay of X_{fa}										$-\sum_{i=1-9,11-24} C_i\nu_{i,15}$	$-\sum_{i=1-10,12-24} N_i\nu_{i,15}$		$k_{dec,Xfa}X_{fa}$
16	Decay of X_{c4}										$-\sum_{i=1-9,11-24} C_i\nu_{i,16}$	$-\sum_{i=1-10,12-24} N_i\nu_{i,16}$		$k_{dec,Xc4}X_{c4}$
17	Decay of X_{pro}										$-\sum_{i=1-9,11-24} C_i\nu_{i,17}$	$-\sum_{i=1-10,12-24} N_i\nu_{i,17}$		$k_{dec,Xpro}X_{pro}$
18	Decay of X_{ac}										$-\sum_{i=1-9,11-24} C_i\nu_{i,18}$	$-\sum_{i=1-10,12-24} N_i\nu_{i,18}$		$k_{dec,Xac}X_{ac}I_{dec,Xac}$
19	Decay of X_{h2}										$-\sum_{i=1-9,11-24} C_i\nu_{i,19}$	$-\sum_{i=1-10,12-24} N_i\nu_{i,19}$		$k_{dec,Xh2}X_{h2}$

Table 3-3 Petersen matrix of the IWA ADM1 (for particulate components

i	Component →	13	14	15	16	17	18	19	20	21	22	23	24	Rate (ρ_j, kg COD.m^{-3}.d^{-1})
j	Process ↓	X_c	X_{ch}	X_{prot}	X_{li}	X_{su}	X_{aa}	X_{fa}	X_{c4}	X_{pro}	X_{ac}	X_{h2}	X_I	
1	Disintegration	-1	$f_{ch,xc}$	$f_{prot,xc}$	$f_{li,xc}$								$f_{xI,xc}$	$k_{dis}X_c$
2	Hydrolysis of Carbohydrates		-1											$K_{hyd,ch}X_{ch}$
3	Hydrolysis of protein			-1										$K_{hyd,prot}X_{prot}$
4	Hydrolysis of Lipids				-1									$K_{hyd,li}X_{li}$
5	Uptake of Sugars					Y_{su}								$k_{m,su}\frac{S_{su}}{K_s+S_{su}}X_{su}I_1$
6	Uptake of Amino Acids						Y_{aa}							$k_{m,aa}\frac{S_{aa}}{K_{s,aa}+S_{aa}}X_{aa}I_1$
7	Uptake of LCFA							Y_{fa}						$k_{m,fa}\frac{S_{fa}}{K_{s,fa}+S_{fa}}X_{fa}I_2$
8	Uptake of Valerate								Y_{c4}					$k_{m,c4}\frac{S_{va}}{K_{s,c4}+S_{va}}X_{c4}\frac{1}{1+S_{bu}/S_{va}}I_2$
9	Uptake of Butyrate								Y_{c4}					$k_{m,c4}\frac{S_{bu}}{K_{s,c4}+S_{bu}}X_{c4}\frac{1}{1+S_{va}/S_{bu}}I_2$
10	Uptake of Propionate									Y_{pro}				$k_{m,pro}\frac{S_{pro}}{K_{s,pro}+S_{pro}}X_{pro}I_2$
11	Uptake of Acetate										Y_{ac}			$k_{m,ac}\frac{S_{ac}}{K_s+S_{ac}}X_{ac}I_3$
12	Uptake of Hydrogen											Y_{h2}		$k_{m,h2}\frac{S_{h2}}{K_{s,h2}+S_{h2}}X_{h2}I_1$
13	Decay of X_{su}	1				-1								$k_{dec,Xsu}X_{su}$
14	Decay of X_{aa}	1					-1							$k_{dec,Xaa}X_{aa}$
15	Decay of X_{fa}	1						-1						$k_{dec,Xfa}X_{fa}$
16	Decay of X_{c4}	1							-1					$k_{dec,Xc4}X_{c4}$
17	Decay of X_{pro}	1								-1				$k_{dec,Xpro}X_{pro}$
18	Decay of X_{ac}	1									-1			$k_{dec,Xac}X_{ac}I_{dec,Xac}$
19	Decay of X_{h2}	1										-1		$k_{dec,Xh2}X_{h2}$

3.3 Model inhibition terms

In the ADM1 model report (Batstone et al, 2002), different inhibition term relationships are suggested with emphasis in modelling the effects of pH, insufficient nitrogen inhibition and hydrogen inhibition. The implemented inhibition terms are listed in Table 3-4.

Table 3-4 Implemented inhibition terms

Description	Inhibition form	To process rates ρ_j
Empirical inhibition by pH	$I_{pH} = \exp\left\{-3\left(\frac{pH - pH_{UL}}{pH_{UL} - pH_{LL}}\right)^2\right\}$, when $pH < pH_{UL}$; and $I_{pH} = 1$, when $pH > pH_{UL}$	All substrate uptake processes, $\forall j = 5-12$
Inhibition for growth due to insufficient inorganic nitrogen	$I_{NH,\lim} = \frac{1}{1 + K_{I,IN} / S_{I,IN}}$	All substrate uptake processes, $\forall j = 5-12$
Non-competitive inhibition by H_2	$I_{h2} = \frac{1}{1 + S_{I,h2} / K_{I,h2}}$	acidogenic processes, $\forall j = 7-10$
Non-competitive inhibition by ammonia	$I_{nh3} = \frac{1}{1 + S_{I,NH3} / K_{I,NH3}}$	acetate uptake process, $j = 11$

The inhibition factors I_1, I_2 and I_3 that are assigned to the model kinetics (Table 3-2 and Table 3-3) are calculated by using the inhibition terms (Table 3-4) according equations (3.3), (3.4) and (3.5), respectively.

$$I_1 = I_{pH} \cdot I_{IN,\lim} \tag{3.3}$$

$$I_2 = I_{pH} \cdot I_{IN,\lim} \cdot I_{h2} \tag{3.4}$$

$$I_3 = I_{pH} \cdot I_{IN,\lim} \cdot I_{NH3} \tag{3.5}$$

3.4 Chemical equilibrium reactions and pH calculation

Two approaches are suggested in the ADM1 report (Batstone et al, 2002) to calculate ion concentrations and the pH. The first models the buffering systems as a system of Differential Equations (DE implementation). In the second approach the buffering systems are modelled by algebraic equations and thus the whole model consists of Differential-Algebraic Equations (DAE implementation). Both implementations aim to determine the pH from the charge balance of the model components, equation (3.6).

$$S_{H^+} + S_{cat} + S_{nh4^+} - S_{an} - S_{oh^-} - S_{hco3^-} - \frac{S_{ac^-}}{64} - \frac{S_{pro^-}}{112} - \frac{S_{bu^-}}{160} - \frac{S_{va^-}}{208} = 0 \quad (3.6)$$

In this section, an update is proposed to the DE implementation and a mathematical solution is illustrated for the DAE implementation.

3.4.1 DE implementation of acid-base equilibrium

In the model report, the DE implementation is suggested by calculating the ion concentrations according to the equilibrium reactions suggested in Table 3-5. However, the DE implementation of acid-base reactions as such is not possible because the acid form of the components is not included in the components vector of ADM1. Indeed, in addition to total concentrations, ion concentrations need to be added to the ADM1 model component vector. To link the biological reaction matrix computation to the acid-base computations as suggested in Table 3-5, a set of algebraic equations need to be added according equation (3.7):

$$S_i = S_{i,a} + S_{i,b} \qquad \text{and } i = 4,5,6,7,10,11 \qquad (3.7)$$

In other words, concentrations should be constrained so that the total concentrations of buffer components are sums of their dissociated and undissociated forms. This troubles the model calculations since the S_i are calculated dynamically from the biological reactions as function of transport and uptake rates, equation (3.8). This leads to a double definition problem, i.e. two equations exist for the evaluation of each component.

$$\frac{dS_i}{dt} = \frac{Q}{V}(S_{i,in} - S_{i,out}) - S_i \cdot \rho_i \qquad (3.8)$$

Q , V and ρ are the flow, reactor volume and reaction specific rate, respectively.

Table 3-5 IWA ADM1 suggested DE implementation of acid-base reactions, adapted from Batstone et al.(2002)

Component i		4a	4b	5a	5b	6a	6b	7a	7b	10a	10b	11a	11b	Rate (ρ_j, all in kg COD.m^{-3}.d^{-1} except inorganic carbon and nitrogen in kmole.m^{-3}.d^{-1})
j	process	S_{hva}	S_{va^-}	S_{hbu}	S_{bu^-}	S_{hpro}	S_{pro^-}	S_{hac}	S_{ac^-}	S_{co2}	S_{hco3^-}	S_{nh4^+}	S_{nh3}	
A1	Valerate acid-base	1	-1											$k_{B,va}(S_{va^-} \cdot S_{H^+} - K_{a,va} \cdot S_{hva})$
A2	Butyrate acid-base			1	-1									$k_{B,bu}(S_{bu^-} \cdot S_{H^+} - K_{a,bu} \cdot S_{hbu})$
A3	Propionate acid-base					1	-1							$k_{B,pro}(S_{pro^-} \cdot S_{H^+} - K_{a,pro} \cdot S_{hpro})$
A4	Acetate acid-base							1	-1					$k_{B,ac}(S_{ac^-} \cdot S_{H^+} - K_{a,ac} \cdot S_{hac})$
A5	Inorganic carbon acid-base									1	-1			$k_{B,co2}(S_{hco3^-} \cdot S_{H^+} - K_{a,co2} S_{co2})$
A6	Inorganic nitrogen acid-base											1	-1	$k_{B,nh}(S_{NH_3} \cdot S_{H^+} - K_{a,nh} \cdot S_{NH_4^+})$
	Valeric acid ($kgCOD/m^3$)													*Kinetic parameters* : $k_{B,i}$: rate coefficient for the base to acid reaction. May be optimised for each acid- base reaction or initially set to $10^8 M^{-1} d^{-1}$.
	Valerate ($kgCOD/m^3$)													
	Butyric acid ($kgCOD/m^3$)													
	Butyrate ($kgCOD/m^3$)													
	Propionic acid ($kgCOD/m^3$)													
	Propionate ($kgCOD/m^3$)													
	Acetic acid ($kgCOD/m^3$)													
	Acetate ($kgCOD/m^3$)													
	Carbon dioxide ($kmoleC/m^3$)													
	Bicarbonate ($kmoleC/m^3$)													
	Ammonium ($kmoleN/m^3$)													
	Ammonia ($kmoleN/m^3$)													

One solution to this problem is to change the biological reactions into terms of either the acid or base forms, but this requires a different definition of kinetic parameters. Another solution is suggested here by calculating the acid/base reaction rates as functions of the total concentrations and the ionised forms of the buffer components, Table 3-6. Using acetate as an example of the model buffer components, its acid/base reaction rate is derived from the dissociation reaction, equations (3.9) to (3.14).

$$HAc \underset{k_B}{\overset{k_A}{\rightleftharpoons}} Ac^- + H^+ \tag{3.9}$$

At equilibrium:

$$k_A \cdot \{HAc\} = k_B \cdot \{Ac^-\} \cdot \{H^+\} \tag{3.10}$$

and equilibrium constant:

$$K_{a,ac} = \frac{k_A}{k_B} = \frac{\{Ac^-\} \cdot \{H^+\}}{\{HAc\}} \tag{3.11}$$

substituting k_A from (3.11) in (3.10):

$$K_{a,ac} \cdot k_B \cdot \{HAc\} = k_B \cdot \{Ac^-\} \cdot \{H^+\} \tag{3.12}$$

due to a shift from equilibrium in direction of acid formation the net reaction rate is:

$$\rho_{ac} = k_B \left(S_{ac^-} \cdot H^+ - K_{a,ac} \cdot S_{hac} \right) \tag{3.13}$$

Equation (3.13) is the reaction rate suggested in Table 3-5. The acid concentration can be substituted by the total concentration according (3.7):

$$\rho_{ac} = k_B \cdot \left(S_{ac^-} \cdot \left(S_{H^+} + K_{a,ac} \right) - K_{a,ac} \cdot S_{ac} \right) \tag{3.14}$$

Applying the reaction rates according equation (3.14) eliminates the acid concentrations from the model components and achieves a direct relation between biological and acid-base model matrices. The updated matrix for chemical reactions and DE implementation is presented in Table 3-6. The updated matrix makes the simultaneous calculation of the biological and chemical reactions possible. However, the DE implementation will be slow

in simulation due to combining the fast chemical process rates and the comparably slow biological process rates that increases the model stiffness.

Table 3-6 Updated DE implementation of acid-base reactions for IWA ADM1

Component i		4b	5b	6b	7b	10b	11b	Rate (ρ_j, all in kg COD.m^{-3}.d^{-1} except inorganic carbon and nitrogen in kmole.m^{-3}.d^{-1})
j	process	S_{va^-}	S_{bu^-}	S_{pro^-}	S_{ac^-}	S_{hco3^-}	S_{nh3}	
A1	Valerate acid-base	-1						$k_{B,va}(S_{va^-}\cdot(S_{H^+}+K_{a,va})-K_{a,va}\cdot S_{va})$
A2	Butyrate acid-base		-1					$k_{B,bu}(S_{bu^-}\cdot(S_{H^+}+K_{a,bu})-K_{a,bu}\cdot S_{bu})$
A3	Propionate acid-base			-1				$k_{B,pro}(S_{pro^-}\cdot(S_{H^+}+K_{a,pro})-K_{a,pro}\cdot S_{pro})$
A4	Acetate acid-base				-1			$k_{B,ac}(S_{ac^-}\cdot(S_{H^+}+K_{a,ac})-K_{a,ac}\cdot S_{ac})$
A5	Inorganic carbon acid-base					-1		$k_{B,co2}(S_{hco3^-}\cdot(S_{H^+}+K_{a,co2})-K_{a,co2}S_{IC})$
A6	Inorganic nitrogen acid-base						-1	$k_{B,nh}(S_{NH_3}\cdot(S_{H^+}+K_{a,nh})-K_{a,nh}\cdot S_{IN})$
		Valerate (kgCOD/m^3)	Butyrate (kgCOD/m^3)	Propionate (kgCOD/m^3)	Acetate (kgCOD/m^3)	Bicarbonate (kmoleC/m^3)	Ammonia (kmoleN/m^3)	*Kinetic parameters* : $k_{B,i}$: rate coefficient for the base to acid reaction. May be optimised for each acid-base reaction or initially set to 10^8M^{-1} d^{-1}.

3.4.2 DAE implementation of acid-base equilibrium

According the ADM1 report and for the proposed DAE implementation, the ion concentrations are calculated from the algebraic equations in Table 3-7 column (1). Using a DAE solver, these equations and equation (3.6) can be solved simultaneously with the differential equations pertaining to the biological reactions. When implementing the pH calculation by the algebraic equations, it is assumed that the chemical equilibrium is reached instantaneously. When using a DE solver for the model, the solution of the algebraic equations should be carefully looked after to avoid very slow simulations. WEST® uses a set of DE solvers but also allows the implementation of C++ functions to perform some external calculation that can be linked to the model. Therefore, this feature was used and a C++ function is programmed to solve the set of algebraic equations externally at each integration step of the DE solver. The idea of external calculation of pH is not new and it was already successfully applied in Matlab/Simulink for modelling the advanced nitrogen removal processes SHARON-Anammox (Hellinga et al., 1999; Volcke et al., 2002). The nested solution of the model system of equations is found to be successful in improving the simulation speed. However, the implementation required an update to the standard model declarations used in WEST® as will be illustrated in section 3.6.

The system of algebraic equations for pH calculation is nonlinear. The Newton-Raphson nonlinear procedure is used to solve the system of equations for H^+. To this end, the ion concentrations (Table 3-7 column (1)) are substituted in equation (3.6). The resulted

equation is $f(H^+) = 0$ since the total concentrations are known at every integration step of ADM1 model. In a next integration step of the model, the total concentrations change, e.g. due to the uptake processes. Accordingly, a small shift δ will occur in H^+ to maintain the charge balance, i.e. $f(H^+ + \delta) = 0$. Based on a Taylor expansion of this function, equation (3.15), a small value of δ can be evaluated according equation (3.16). The calculation procedure requires the evaluation of both the function $f(H^+)$, and the derivative $f'(H^+)$ whose terms can be obtained from Table 3-7.

$$f(H^+, \delta) \approx f(H^+) + f'(H^+)\delta + \frac{f''(H^+)}{2}\delta^2 + ... \tag{3.15}$$

$$\delta = -\frac{f(H^+)}{f'(H^+)} \tag{3.16}$$

Since the dynamics of H^+ in the system is rarely linear, the approximation in equation (3.16) will not reach the solution in one step. A new H^+ is obtained iteratively according the Newton-Raphson procedure with the application of some convergence conditions according (3.17).

$$H^+_{i+1} = H^+_i - \frac{f(H^+_i)}{f'(H^+_i)} \qquad i < N \qquad \frac{f(H^+_i)}{f'(H^+_i)} > tol \tag{3.17}$$

The trials and the updates of the H^+ estimate continue until a maximum number of trials N or an acceptable tolerance tol is reached. Table 3-7 lists the functions that allow to calculate the ion concentrations of standard ADM1 buffer components and their derivatives. The standard ADM1 components are dealt with as monoprotic buffers. In chapter 4, the procedure will be more generalised to also include diprotic and triprotic buffers. This generalisation enables the inclusion of other buffer components in the ADM1 model and makes the procedure suitable for the pH calculation in other models. In the generalised procedure the functions and derivatives will be calculated recursively according their declaration in the model.

Table 3-7 IWA ADM1 DAE implementation functions

	(1)	(2)
Unknown Algebraic	Ion concentration functions	First derivative with respect to S_{H^+}
S_{OH^-}	$S_{OH^-} = \frac{K_w}{S_{H^+}}$	$S'_{OH^-} = -\frac{K_w}{\left(S_{H^+}\right)^2}$
S_{va^-}	$S_{va^-} = \frac{K_{a,va} S_{va,total}}{K_{a,va} + S_{H^+}}$	$S'_{va^-} = -\frac{K_{a,va} S_{va,total}}{\left(K_{a,va} + S_{H^+}\right)^2}$
S_{Bu^-}	$S_{Bu^-} = \frac{K_{a,bu} S_{bu,total}}{K_{a,bu} + S_{H^+}}$	$S'_{Bu^-} = -\frac{K_{a,bu} S_{bu,total}}{\left(K_{a,bu} + S_{H^+}\right)^2}$
S_{Pro^-}	$S_{Pro^-} = \frac{K_{a,pro} S_{pro,total}}{K_{a,pro} + S_{H^+}}$	$S'_{Pro^-} = -\frac{K_{a,pro} S_{pro,total}}{\left(K_{a,pro} + S_{H^+}\right)^2}$
S_{Ac^-}	$S_{Ac^-} = \frac{K_{a,ac} S_{ac,total}}{K_{a,ac} + S_{H^+}}$	$S'_{Ac^-} = -\frac{K_{a,ac} S_{ac,total}}{\left(K_{a,ac} + S_{H^+}\right)^2}$
$S_{HCO_3^-}$	$S_{HCO_3^-} = \frac{K_{a,CO2} S_{IC,total}}{K_{a,CO2} + S_{H^+}}$	$S'_{HCO_3^-} = -\frac{K_{a,CO2} S_{IC,total}}{\left(K_{a,CO2} + S_{H^+}\right)^2}$
$S_{NH_4^+}$	$S_{NH_4^+} = \frac{S_{H^+} S_{IN}}{K_{a,NH_4} + S_{H^+}}$	$S'_{NH_4^+} = \frac{K_{a,NH_4} S_{IN}}{\left(K_{a,NH_4} + S_{H^+}\right)^2}$

3.5 Gas-liquid transfer reactions

Gas transfer is modelled according to the current gas concentrations in gas and liquid compartments, Table 3-8.

Table 3-8 Gas liquid transfer reactions

i	Component →	S_{h2}	S_{ch4}	S_{IC}	$S_{gas,h2}$	$S_{gas,ch4}$	$S_{gas,co2}$	Rate (ρ_j)
j	Process ↓	Liquid-phase			Gas-Phase			
G1	H_2 Transfer	-1			1			$K_L a(S_{h2} - R \cdot T_{op} \cdot K_{H,h2} S_{gas,h2})$
G2	CH_4 Transfer		-1			1		$K_L a(S_{ch4} - R \cdot T_{op} \cdot K_{H,ch4} S_{gas,ch4})$
G3	CO_2 Transfer			-1			1	$K_L a(S_{co2} - R \cdot T_{op} \cdot K_{H,co2} S_{gas,co2})$
		Hydrogen (kg COD m^{-3})	Methane (kg COD m^{-3})	Inorganic carbon (kmole C m^{-3})	Hydrogen (kg COD m^{-3})	Methane (kg COD m^{-3})	Carbon dioxide (kmole C m^{-3})	Gas flow: $q_{gas} = \frac{RT_{opt}}{P_{atm} - p_{H2O}} \cdot V_{liq} \cdot \left(\frac{\rho_{h2}}{16} + \frac{\rho_{ch4}}{64} + \rho_{CO2}\right)$

3.6 Update of WEST® standard model declaration

A model is declared in WEST® on the basis of its Petersen matrix definition. The declaration of biodegradation models was standardised on the basis that every model will be defined by one matrix. However, ADM1 is a multiphase model that is defined by three matrices: for the biological, chemical equilibrium and gas-liquid transfer reactions. In this section, the standard declaration of biological models in the WEST® Model Specification Language (MSL) is briefly illustrated. Second, the necessary updates of the standard declaration are illustrated for ADM1. The updates give an example for future implementation of multiphase models, i.e. complex models whose reactions are defined with more than one Petersen matrix.

3.6.1 Standard model declaration in WEST®

A general description of the MSL structure can be found in detail in the WEST® - Modelbase technical reference. The concept of its formalism can be found in detail in (Vangheluwe, 2000). Briefly, the MSL has a hierarchal structure of classes where a new model is extended from one of them. At the top of the hierarchy the types of the models' components and reactions are declared.

For example, writing ADM1 in MSL by only considering its Petersen matrix of biological reactions, starts with the definition of the matrix dimension by two enumerated arrays for components and reactions, BOX 3-1:

BOX 3-1

```
TYPE ADM1Components
  "The biological components considered in the ADM1 model"
  = ENUM { H2O_An, S_INN, S_IC, S_ch4, S_h2, S_aa, S_ac, S_bu, S_fa, S_Inert,
     S_pro, S_su, S_va, X_aa, X_ac, X_c, X_c4, X_ch, X_fa, X_h2, X_Inert, X_li,
     X_pr, X_pro, X_su, S_an, S_cat};
TYPE ADM1Reactions
  "The anaerobic reactions between biological components considered in the ADM1
     model"
  = ENUM {decay_aa, decay_ac, decay_c4, decay_fa, decay_h2, decay_pro, decay_su,
     dis, hyd_ch, hyd_li, hyd_pr, uptake_aa, uptake_ac, uptake_bu, uptake_fa,
     uptake_h2, uptake_pro, uptake_su, uptake_va,};
OBJ NrOfADM1Components "The number of anaerobic components considered in the ADM1
     model"
  : Integer := Cardinality(ADM1Components);
OBJ NrOfADM1Reactions "The number of anaerobic reactions considered in the ADM1
     model"
  : Integer := Cardinality(ADM1Reactions);
```

After the definition of the matrix dimensions using the cardinality function, the type and classes of the interface terminals of the model can be defined, BOX 3-2:

BOX 3-2

```
TYPE ADM1ConcTerminal
  "
   The variables which are passed to and from the digester
  "
 = PhysicalQuantityType[NrOfADM1Components;];

CLASS InADM1ConcTerminal SPECIALISES ADM1ConcTerminal; //inflow

CLASS OutADM1ConcTerminal SPECIALISES ADM1ConcTerminal;//outflow
```

A model class is created either by extending a previous model class or by defining the model as a new class with one of the general model types. ADM1 is a new category and therefore it should be created as a new class within the DAE model type. This type has a structure of 7 blocks, as shown in BOX 3-3:

BOX 3-3

```
CLASS ADM1
 (* class = "anaerobic_digester"; category = "" *)
 "anaerobic digester"
SPECIALISES PhysicalDAEModelType :=
   {:
comments <- "ADM1 model for anaerobic digestion ";
interface <-
  {
.................
  };
parameters <-
  {
.................
};
state <-
{
.................
};
initial <-
{
.................
};
independent <-
     {
.................
};
equations <-
{
.................
};
   :};
```

A general comment is added to the “comments” block such as the model name. In the interface the reactor terminals are defined (inflow, outflow and Gas). In the “parameters” block the model parameters are defined. The model stoichiometry is also defined in the “parameters” block. The standard definition of the stoichiometry is defined as a two-dimensional matrix $n \times m$ where n is the number of reactions and m is the number of components, BOX 3-4 :

BOX 3-4

```
OBJ AnaerobicStoichiometry (* hidden = "1" *)"A matrix structure containing the
     stoichiometry       of       anaerobic       biological       processes":
     Real[NrOfADM1Reactions;][NrOfADM1Components;];
```

In the "state" block, model state variables and kinetic reactions are defined. The standard declaration of the kinetic reactions is in the following BOX 3-5:

BOX 3-5

```
OBJ AnaerobicKinetics (* hidden = "1" *) "A vector containing kinetics for all
     anaerobic reactions" : QuantityType[NrOfADM1Reactions;];
```

In the "initial" block, known functions of parameter values are defined. For instance, stoichiometry is defined in this section as shown in the following example BOX 3-6:

BOX 3-6

```
// process : decay of amino acid degrading organisms
parameters.AnaerobicStoichiometry[decay_aa][X_c]:= 1;
parameters.AnaerobicStoichiometry[decay_aa][X_aa]:= -1;
parameters.AnaerobicStoichiometry[decay_aa][S_IC]:=parameters.C_biom-
     parameters.C_Xc;
parameters.AnaerobicStoichiometry[decay_aa][S_INN]:=parameters.N_biom-
     parameters.N_Xc;
```

The functions in the "initial" block are calculated once at the start of the simulations. In the "independent" block, the independent variable is declared, e.g. the time. In the "equations" block all model equations that will be calculated during the simulation are defined. Equations are needed to calculate the kinetic reactions, influxes, conversion terms, rate equations, out-fluxes and concentrations. Examples are only given below for the standard forms of equations of kinetic reactions, conversion terms and rate equations, since these are the main forms of the equations block that will be updated / extended during building ADM1 as a multiphase model, section 3.6.2.

- Standard kinetic equation example, BOX 3-7 :

BOX 3-7

```
// decay of amino acid degrading organisms
 state.AnaerobicKinetics[decay_aa]=parameters.kdec_xaa* state.C_An[X_aa];
```

- Standard conversion terms function example, BOX 3-8 :

BOX 3-8

```
  { FOREACH Comp_Index IN {1 .. NrOfADM1Components }:
      state.AnaerobicConversionTermPerComponent[Comp_Index] =
       SUMOVER Reaction_Index IN {1 .. NrOfADM1Reactions}:
        (parameters.AnaerobicStoichiometry[Reaction_Index][Comp_Index]
         * state.AnaerobicKinetics[Reaction_Index])
        * parameters.V_liq;};
```

Note that with this nested FOREACH – SUMOVER loop all conversion terms for all components will be generated.

– Standard mass balance equations generator example, BOX 3-9 :

BOX 3-9

```
{FOREACH Comp_Index IN {1 .. NrOfADM1Components}:
  DERIV(state.M_An[Comp_Index],[independent.t]) =
   state.AnaerobicInFluxPerComponent[Comp_Index]
   - state.AnaerobicOutFluxPerComponent[Comp_Index]
   + state.AnaerobicConversionTermPerComponent[Comp_Index];
};
```

Note that this FOREACH-DERIV loop generates all differential equations in the model, if one matrix for the model is assumed.

The MSL code that is shown in BOX 3-1 to BOX 3-9 illusterates the main parts to define and build a one phase (one matrix) model using the WEST standard model definition. The boxes indicate the locations where the code should be updated to include multiple phases (more than one matrix) such as for ADM1. In fact, the definitions and equations are not repeated for every model. They are built once for a model category whose underlying models are extended from it with their particular upgrades. For instance, the Activated Sludge Model (ASM) blocks are built once for common ASM definitions. Then, ASM1, ASM2…etc. can be extended from the ASM category with a few statements necessary to reflect each particular model. In the case of ADM1, it is a new category in WEST and, therefore, all blocks have to be defined. However, when ADM1 is extended; the model will not need to be redefined. Only the particular changes are needed when starting from the standard ADM1, e.g. when upgrading ADM1 with cyanide kinetics as in chapter 6.

3.6.2 ADM1 updates in the MSL declaration

A possibility to implement ADM1 is to include all model matrices in one matrix dimensioned with a super array of all components and a super array of all reactions. However, splitting the ADM1 into three different matrices to separate chemical, physical (gas transfer) and biological reactions is found more practical and applicable, for two reasons. First, including the ion component concentrations together with the total concentrations, as in the super array implementation, will violate the assumptions of the Petersen matrix that all components should not be part of others, allowing continuity checks, e.g. for COD, C and N mass balances. Solving this problem using acid and ion components instead of total concentration components introduces other difficulties in defining the stoichiometry of the biological part for both ion and acid forms. Moreover, the ADM1 biological kinetic and yield parameters are defined for total concentration components, according the ADM1 report. Second, declaring such big matrix will reserve unneeded memory locations for all arrays that are dimensioned on the basis of the Petersen matrix dimension. Splitting the arrays is more applicable since a digester consists of two

compartments of liquid and gas. In the gas phase, only gas components need to be considered and therefore it is better to declare them in a separate array. A separate array declaration of gas phase components is also needed to configure the gas outlet terminal of the digester.

Consequently, the ADM1 is implemented by its three matrices, biological, chemical and physical gas-liquid transfer processes. In the following the necessary updates for the MSL code is illustrated for the DAE implementation, i.e. with the external calculation of pH presented in section 3.4.2.

In addition to the declaration of the biological matrix, BOX 3-1, declarations for chemical reactions and gas transfer should be added, BOX 3-10 .

BOX 3-10

```
TYPE ADM1IonComponents
  "The ion components considered in the ADM1 model"
  = ENUM {S_ac_ion, S_bu_ion, S_pro_ion, S_va_ion, S_hco3_ion, S_nh3};

TYPE ADM1GasVesselComponents
  "The gaseous components considered in the ADM1 model in the gas phase"
  = ENUM {S_ch4_gas, S_co2_gas, S_h2_gas};

TYPE ADM1GasComponentsInliquid
    "The gaseous components considered in the ADM1 model dissolved in the liquid
     phase"
  = ENUM {S_ch4_liq, S_IC_liq, S_h2_liq};

TYPE ADM1IonReactions
  "The equilibrium reactions between biological components considered in the ADM1
     model"
  =  ENUM {dissociation_va, dissociation_bu, dissociation_pro, dissociation_ac,
     hco3_co2, ammonia_production};

TYPE ADM1GasTransfer
  "The anaerobic gas transfer considered in the ADM1 model"
  = ENUM {transfer_ch4, ransfer_co2, transfer_h2};

OBJ NrOfADM1GasComponents "The number of anaerobic components considered in the
     gas phase"
  : Integer := Cardinality(ADM1GasVesselComponents);

OBJ  NrOfADM1GasComponentsInliquid "The number of gaseous anaerobic components
     dissolved in the liquid phase"
  : Integer := Cardinality(ADM1GasComponentsInliquid);
OBJ NrOfADM1IonComponents "The number of anaerobic ion components considered in
     the ADM1 model"
  : Integer := Cardinality(ADM1IonComponents);

OBJ NrOfADM1IonReactions "The number of anaerobic ion reactions considered in the
     ADM1 model"
  : Integer := Cardinality(ADM1IonReactions);

OBJ NrOfADM1GasTransfer "The number of anaerobic gas transfers considered in the
     ADM1 model"
  : Integer := Cardinality(ADM1GasTransfer);
```

The ion components and reactions are declared in BOX 3-10 for the DE implementation. However, they are not needed in the DAE implementation as the reactions are assumed to have an instantaneous equilibrium. The gas components are declared in the liquid and the gas phases separately. The separate declaration of the gas components is necessary for the conversion terms, BOX 3-16, and for the definition of the gas outlet, BOX 3-11.

BOX 3-11

```
CLASS ADM1GasOutFromTheADVessel
  "
   The variables that pass the gas outlet
  "
  = PhysicalQuantityType[NrOfADM1GasComponents;];
```

The 7 blocks of model definitions, in BOX 3-3, should be updated. In the parameters block and in addition to the declaration of the stoichiometry of biological reactions in BOX 3-4, the stoichiometry of the gas reactions should be declared as shown in BOX 3-12. No stoichiometry is needed for the ion reactions since they will be evaluated externally in the DAE implementation.

BOX 3-12

```
OBJ  AnaerobicGasStoichiometryInLiquid (* hidden = "1" *)"A matrix structure
     containing stoichiometry related to gas components in the liquid phase":
 QuantityType[NrOfADM1GasTransfer;][NrOfADM1GasComponentsInliquid;];

OBJ  AnaerobicGasStoichiometryInGas (* hidden = "1" *)" A matrix structure
     containing stoichiometry related to gas components in the gas phase ":
     QuantityType[NrOfADM1GasTransfer;][NrOfADM1GasComponents;];
```

Similarly and in addition to the declaration of the biological reaction kinetics in the state block, BOX 3-5, gas transfer kinetics are declared, BOX 3-13.

BOX 3-13

```
   OBJ GasKinetics (* hidden = "1" *) "A vector containing kinetics for all
     anaerobic gas transfers" : QuantityType[NrOfADM1GasTransfer;];
```

In addition to the definition of the biological stoichiometry values in the initial block as shown in BOX 3-6, the gas transfer stoichiometry is also defined. BOX 3-14 shows an example of declaring the methane transfer stoichiometry.

BOX 3-14

```
// process : transfer of CH4
    parameters.AnaerobicGasStoichiometryInLiquid[transfer_ch4][S_ch4_liq] := -1;
    parameters.AnaerobicGasStoichiometryInGas[transfer_ch4][S_ch4_gas] := 1;
```

In the equations block, the important updates are the addition of gas transfer kinetics and the update of the equation form of the conversion terms and rate equations. Examples of the updates to BOX 3-7, BOX 3-8 and BOX 3-9 are given in the following boxes:

- Example of the gas kinetics to be added, BOX 3-15:

BOX 3-15

```
// process: transfer_ch4
    state.GasKinetics[transfer_ch4]=  parameters.kla  *  (  state.C_An[S_ch4]  -
     parameters.KH_ch4  *  state.C_AnGas[S_ch4_gas]  *  parameters.R  *  parameters.T
     );
```

– Example of the update to the conversion terms, BOX 3-16:

BOX 3-16

```
  {
// conversion terms of inorganic carbon in the liquid phase
      state.AnaerobicConversionTermPerComponent[S_IC]=
     parameters.AnaerobicGasStoichiometryInLiquid[transfer_co2][S_IC_liq]
         * state.GasKinetics[transfer_co2] * parameters.V_liq +
        ( SUMOVER Reaction_Index IN {1 .. NrOfADM1Reactions}:
             (parameters.AnaerobicStoichiometry[Reaction_Index][S_IC]
                    * state.AnaerobicKinetics[Reaction_Index])
                   * parameters.V_liq) ;

// conversion terms of methane in the liquid phase (are not presented below)
…… Similar as before …….
……..
// conversion terms of hydrogen in the liquid phase(are not presented below)

…… Similar as before …….
……..

// conversion terms of other liquid components
   { FOREACH Comp_Index IN {S_aa .. S_cat}:
      state.AnaerobicConversionTermPerComponent[Comp_Index] =
       SUMOVER Reaction_Index IN {1 .. NrOfADM1Reactions}:
        (parameters.AnaerobicStoichiometry[Reaction_Index][Comp_Index]
         * state.AnaerobicKinetics[Reaction_Index])
        * parameters.V_liq;};

// gas phase conversion terms (they are liquid volume specific)
       {FOREACH Comp_Index IN {S_ch4_gas .. NrOfADM1GasComponents}:
             state.AnaerobicGasConversionTermPerComponent[Comp_Index] =
              SUMOVER Reaction_Index IN {1 .. NrOfADM1GasTransfer}:
   (parameters.AnaerobicGasStoichiometryInGas[Reaction_Index][Comp_Index]
             * state.GasKinetics[Reaction_Index])* parameters.V_liq;

   };
```

Instead of generating the conversion terms with one FOREACH – SUMOVER construct, BOX 3-8, new complex equations need to be implemented as shown in BOX 3-16. The main reason of this complexity is because the concentrations of gas components in the liquid phase link the biological and gas transfer matrices. The conversion terms of gas components due to biological reactions and gas transfer should be defined by one equation for each gas component. It is not possible for one gas component to define two conversion terms since it will not be possible in MSL to generate one rate equation using the two conversion terms and it is not possible to define two rate equations for one component. After defining the gas conversion terms in the liquid, the remaining liquid components can be defined by one FOREACH – SUMOVER nested loop. Similarly the conversion terms

of gas components in the gas phase can be generated by another FOREACH – SUMOVER nested loop.

- An example of the additional loop to generate the gas rate equations is shown in BOX 3-17:

BOX 3-17

```
{FOREACH Comp_Index IN {1 .. NrOfADM1GasComponents}:
      DERIV(state.M_AnGas[Comp_Index],[independent.t]) =
              - state.AnaerobicGasOutFluxPerComponent[Comp_Index]
       + state.AnaerobicGasConversionTermPerComponent[Comp_Index];
    };
```

It can be seen that including the gas transfer matrix into the model increased the complexity of the model MSL definition. The degree of complexity would rather increase even further if the chemical reactions matrix is added for the DE implementation. Conversely, the DAE implementation didn't increase the complexity and achieved the same simulation speed and accuracy. The only MSL code that had to be added to the equations block is a C++ function call, BOX 3-18.

BOX 3-18

```
state.S_h_ion=
     Newton_Raphson(parameters.Ka_nh4,parameters.Ka_co2,parameters.Ka_ac,paramete
     rs.Ka_bu,parameters.Ka_va,parameters.Ka_pro,parameters.Ka_h2o,

       state.C_An[S_INN],state.C_An[S_IC],state.C_An[S_ac]/64,state.C_An[S_bu]/16
     0,state.C_An[S_va]/208,state.C_An[S_pro]/112,state.C_An[S_cat],state.C_An[S_
     an],previous(state.S_h_ion));
```

The function passes the acidity constants, the total concentrations of buffer components and the previously calculated H^+ concentration to start the Newton Raphson iterative procedure and returns the H^+ concentration.

The present ADM1 implementation in WEST was validated on steady and dynamic states and compared with implementations on other simulation platforms, see chapter 5.

3.7 Simplification of pH and gas transfer modelling

Anaerobic digestion models can be simplified by applying some assumptions to approximate the gas transfer and the pH calculations. Hence, an anaerobic digestion model can be defined by biological reactions only. Consequently, at each simulation time step, pH and gas flow are calculated as functions of other model components. In this section, the simplification of gas transfer and pH calculations are illustrated in two simpler models compared to ADM1. The first is the Siegrist model that is implemented in WEST according to (Siegrist et al., 1991; 1993; 1995). Looking for simplifications, it should be noted that in this study an older version of this model is considered and not the last Siegrist

et al. (2002) model. The latter is more similar to ADM1 and is therefore not a good example of a simplified model. The second simple model is AM2 that is implemented in WEST according to (Bernard et al., 2001; 2002).

3.7.1 Siegrist model

There are some simplifications in the biological reactions of the Siegrist model compared to ADM1. The main biological simplifications consist in combining the fermentation pathways of amino acids and sugars and considering only the acetate and propionate forms of volatile fatty acids. The major simplifications in the model compared to ADM1 were in the pH and gas calculations.

Similar to ADM1, the Siegrist model considers methane, carbon dioxide and hydrogen. The Siegrist model simplification in the gas transfer consists in assuming that the gas transfer is due to gas stripping and no diffusion is considered from the gas phase to the liquid. The stripping rate is considered proportional to the total gas flow that is either determined by the initial value at the start of the simulation or from the previous value during the simulation by equation (3.18).

$$\rho_{\text{stripping},t+\delta t} = \frac{q_{gas}}{V_{liquid} \cdot \frac{R \cdot T}{P}} \tag{3.18}$$

Note that the liquid volume V_{liquid}, the universal gas constant R, the operational temperature, T, and the total pressure, P, are constants and therefore equation (3.18) reflects the proportional relation between the general stripping rate, $\rho_{\text{stripping},t+\delta t}$, and the total gas flow q_{gas}. The stripping rate of each gas component is calculated as the product of its liquid concentration, $\rho_{\text{stripping},t+\delta t}$ and the Henry coefficient H. For example, the methane stripping rate can be calculated from equation (3.19).

$$\rho_{stripping,CH_4} = -H_{CH_4} \cdot \rho_{stripping,t+\delta t} \cdot S_{CH_4,liq} \tag{3.19}$$

According equation (3.19), the transfer rates will be functions of the liquid concentrations only. Therefore, stripping reactions can be added to the model biological matrix. The stripped amount of each gas can be calculated at each step and therefore the corresponding volume can be calculated since the pressure is assumed constant. Summing the produced volumes of the three gases will be the current gas flow and it will be used to calculate the stripping rate for the next time step, and so on.

For the pH calculation the model only considers the bicarbonate system, CO_2 and HCO_3^-. Both components and H^+ are considered in the model matrix. The kinetics are based on the carbon system equilibrium and the consumption and release of H^+. In other words, the reversible reaction, (3.20), is presented in kinetics for both directions. The rate equations are considered for bicarbonate protolysis, equation (3.21), and for CO_2 deprotolysis, equation (3.22).

$$HCO_3^- + H^+ \underset{k_2}{\overset{k_1}{\rightleftharpoons}} CO_2 + H_2O \tag{3.20}$$

$$\rho_{hco3} = k_1 \cdot S_{hco3} \cdot S_{H^+} \tag{3.21}$$

$$\rho_{co2} = k_2 \cdot S_{co2} \tag{3.22}$$

Accordingly, the H^+ and therefore the pH are calculated. This simplification is valid in cases of treating wastewaters that have a high bicarbonate alkalinity. The model was validated and gives practical results with sludge digestion, see chapter 8. However, during overloads and VFA accumulation, the approximation of the pH calculations is not valid and the VFA should be considered, as illustrated for the ADM1.

3.7.2 AM2 model

According (Bernard et al., 2001; 2002), the AM2 model is based on only two reactions: acidogenesis step, reaction (3.23), and the methanogenesis step, reaction (3.24).

$$k_1 S_1 \xrightarrow{r1} X_1 + k_2 S_2 + k_4 CO_2 \tag{3.23}$$

$$k_3 S_2 \xrightarrow{r2} X_2 + k_5 CO_2 + k_6 CH_4 \tag{3.24}$$

The growth of acidogens is assumed to follow Monod kinetics and the growth of methanogens is assumed to follow Haldane kinetics. The inhibition of methanogenesis due to VFA accumulation is considered. Rates are given in equations (3.25) and (3.26).

$$r1 = \mu_{1\max} \frac{S_1}{S_1 + K_{S1}} \cdot X_1 = \mu_1(S_1) X_1 \tag{3.25}$$

$$r2 = \mu_{2\max} \frac{S_2}{S_2 + K_{S2} + \frac{S_2^2}{K_{I2}}} \cdot X_2 = \mu_2(S_2) X_2 \tag{3.26}$$

Also, the model considers gas stripping of CO_2 and CH_4. Because of its simplicity and the few rate equations, the model is implemented in WEST directly by the set of rate equations in (3.27) and not as a Petersen matrix. However, the Petersen matrix of the model can be easily constructed.

$$(\text{AM2}) \begin{cases} \dot{X}_1 &= (\mu_1(S_1) - \alpha D)X_1 \\ \dot{X}_2 &= (\mu_2(S_2) - \alpha D)X_2 \\ \dot{Z} &= D(Z_{in} - Z) \\ \dot{S}_1 &= D(S_{1in} - S_1) - k_1\mu_1(S_1)X_1 \\ \dot{S}_2 &= D(S_{2in} - S_2) + k_2\mu_1(S_1)X_1 - k_3\mu_2(S_2)X_2 \\ \dot{C} &= D(C_{in} - C) - q_c(\xi) + k_4\mu_1(S_1)X_1 + k_5\mu_2(S_2)X_2 \end{cases} \tag{3.27}$$

Also, because of the simplicity of the model, the gas flow and the pH can be derived mathematically from the model equations, the alkalinity expressions and gas laws. Details can be found in Bernard et al. (2001). The gas flows can be estimated from equations (3.28) to (3.31):

$$q_M(S_2, X_2) = k_6\,\mu_2(S_2)X_2 \tag{3.28}$$

$$q_c(\xi) = k_L a(CO_2 - K_H P_c(\xi)) \tag{3.29}$$

$$P_c = \frac{-\phi(\xi) + \sqrt{\phi(\xi)^2 - 4K_H P_T CO_2}}{2K_H} \tag{3.30}$$

$$\phi(\xi) = CO_2 + K_H P_T + \frac{q_M(S_2, X_2)}{k_L a} \tag{3.31}$$

It should be noted that estimated gas flows are liquid volume specific and, therefore, the total gas flows are calculated by multiplying the estimated specific rates by the liquid volume. The pH can be calculated from the hydrogen ion concentration that is calculated by equations (3.32) and (3.33).

$$h = \frac{-\psi(\xi) + \sqrt{\psi(\xi)^2 + 4K_a K_b Z(C - Z + S_2)}}{2Z} \tag{3.32}$$

$$\psi(\xi) = K_a(Z - S_2) - K_b(C - Z) \tag{3.33}$$

Although the gas and pH formulas are relatively complex, they could be implemented and simulated easily in WEST. Further simplifications to the model done for control application were presented in Bernard (2002). In chapter 7, the AM2 model implementation is validated and the model is used for numerous simulations of an iterative optimal experimental design procedure. The simplicity of the model enabled fast simulations and the numerous simulations could be performed in a reasonable time.

3.8 Conclusions

Anaerobic digestion modelling is described using three standard models that were applied throughout this research. Key updates were necessary to have a successful implementation of the standard IWA ADM1 model. The inorganic carbon and nitrogen components of the model were used to close the carbon and nitrogen balance over all reactions to guarantee mass continuity. It was necessary to clearly state the implemented inhibition terms since this was only loosely specified in the ADM1 model report to allow more flexibility of the model application. For pH simulation with ADM1, some updates were necessary to the description of the DE implementation in the model report. For the DAE implementation of the model, the algebraic equations for pH calculation should be solved externally, e.g. following the procedure presented in this chapter. In this way the models can be solved with simple DE solvers and have improved simulation speed. To have a successful implementation of multiphase models in WEST, updates were necessary to the WEST standard model declarations as presented for ADM1. There are possible simplifications of pH and gas transfer modelling in anaerobic reactors as presented by the two simpler models (Siegrist and AM2). However, these simplifications are only valid if the assumptions of both models are acceptable for the desired modelling application. More specifically, the simplifications of the gas transfer modelling in the Siegrist et al. (1995) model are valid only if there is a continuous gas flow through the liquid compartment of the anaerobic reactor to strip the gas components, e.g. by applying gas recycling for mixing. The pH simulation of the Siegrist et al. (1995) model is valid only if there is sufficient bicarbonate alkalinity in the treated wastewaters to buffer the reactor contents. Therefore, the simplifications in the Siegrist et al. (1995) model are quite useful to simplify the modelling of high-rate reactors, especially if high bicarbonate alkalinity is available. AM2 simulation is accurate if the considered acetogenesis and methanogenesis steps are the main steps in the anaerobic reactor, i.e. the influent wastewater to the anaerobic reactor is low in organic particulates and is to a large extent acidified.

Chapter 4

General ion recruiting procedure for pH calculation

Abstract

Generalising the calculation of pH requires the definition of general formulas and a calculation procedure of molar and equivalent ion concentrations, respectively, that recruits all ions of buffer systems in a solution. The general procedure for pH calculation is iterative and requires the evaluation of the derivative of the total equivalents with respect to the hydrogen ion concentration. The general procedure is programmed to be run by a stand-alone programme or can be linked to the WEST simulator for pH simulation with any model. The general pH-calculation is built as a hierarchy of three functions. This substructure of the procedure is useful for other applications. It is used to calculate the net cation concentration, i.e. the total alkalinity, for example when the pH measurement is available. It is also used in another procedure that simulates titration experiments for samples with known buffer composition. The titration simulation procedure is used to implement a Titrimetric Analyser Simulator (TAS) in WEST. The TAS was validated with real titration experiments performed with mixtures with different concentrations of mono-, di- and tri-protic buffers.

CHAPTER 4

4.1 Introduction

In chapter 3, a procedure is presented for external pH calculation for the DAE implementation of the anaerobic digestion model no.1 (ADM1). The application of the procedure considerably improved the simulation speed when using DE solvers, for instance available in the WEST simulator. The procedure was developed for monoprotic buffers that are considered in the standard ADM1. In this chapter, the procedure is generalised for any combination of buffer systems. The general procedure is suitable for upgrading ADM1 with other buffer components, implementation of pH calculation with other models, calculation of the total alkalinity (net cation concentration) and simulation of titration experiments. The structure of the general function consists of three functions that work together in the hierarchy depicted in Figure 4.1.

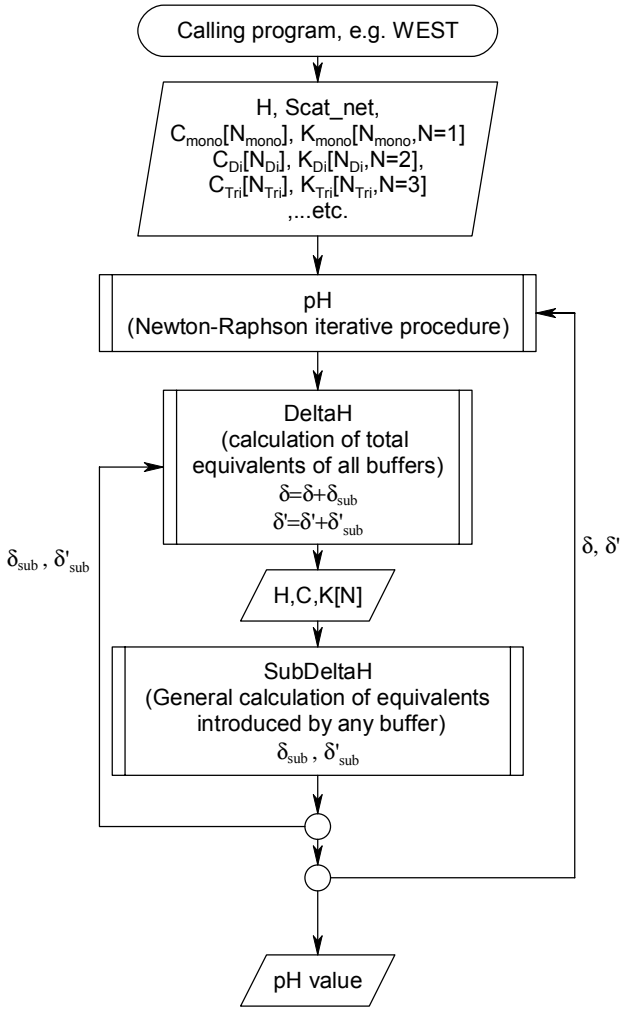

Figure 4.1 General ion recruiting procedure for pH calculation

The steps to build up the general procedure will be described in detail in sections 4.2 to 4.6 in bottom-up direction according to Figure 4.1. Generally, the pH calculation is performed in four steps:

1. Use the algorithm for systematic equations to calculate the ion molar concentrations and their derivatives (sections 4.2 and 4.3, respectively).
2. Use the function SubDeltaH to recruit ions and calculate the equivalents introduced by a buffer component and the corresponding derivative term, i.e. how much do the equivalents change with a pH change (section 4.4).
3. Calculations with function DeltaH that evaluates the total net equivalents, i.e. the sum of all negative ions minus the sum of all positive ions, and the corresponding total of derivatives section 4.5.
4. Apply the Newton-Raphson iterative procedure for pH calculation in which the charge balance is followed to iteratively determine the true hydrogen ion concentration (section 4.6).

Then the implementation of the general procedure in WEST is presented in section 4.7. The implementations of the DeltaH and SubDeltaH functions for calculation of total alkalinity and use in the Titrimetric Analyser Simulator are presented in sections 4.8 and 4.9. Conclusions are drawn in the last section.

4.2 General functions of ion concentrations

The molar concentration of an ion can be defined as a function of the total concentration of its corresponding buffer component. The Matlab symbolic toolbox was used to define general molar concentration functions for ions of mono-, di- and tri-protic buffers.

For a monoprotic buffer, x_0, x_1, C_T, K_1 and H are defined as symbols of acid, ion and total concentrations, acidity constant and hydrogen ion concentration, respectively. From the mass conservation and the equilibrium of the dissociation reaction, the simultaneous linear functions f_0 and f_1 can be defined, equations (4.1) and (4.2).

$$f_0 = C_T - x_0 - x_1 = 0 \tag{4.1}$$

$$f_1 = x_1 - \frac{K_1}{H} \cdot x_0 = 0 \tag{4.2}$$

The two functions can be solved for x_0 and x_1 using the symbolic toolbox. The concentration of the acid form x_0 is not considered any further in the present calculation.

Using the symbolic toolbox "pretty" function, the x_1 symbolic function is presented by equation (4.3).

$$x_1 = \frac{K_1 C_T}{H + K_1} \tag{4.3}$$

Similarly, for a di-protic buffer these linear algebraic functions are defined. The first function f_0 is calculated from the mass balance and is extended with the second ion x_2. The second function f_1 is evaluated from the first dissociation reaction (i.e. release of the first hydrogen ion) and, therefore, it will be the same as equation (4.2). A third equation, f_2, is produced from the second dissociation reaction and describes the release of the second hydrogen ion, equation (4.6).

$$f_0 = C_T - x_0 - x_1 - x_2 = 0 \tag{4.4}$$

$$f_1 = x_1 - \frac{K_1}{H} \cdot x_0 = 0 \tag{4.5}$$

$$f_2 = x_2 - \frac{K_2}{H} \cdot x_1 = 0 \tag{4.6}$$

The symbolic solution of the three functions leads to the following molar concentration functions of the di-protic buffer ions, equations (4.7) and (4.8).

$$x_1 = \frac{K_1 \cdot C_T \cdot H}{H^2 + K_1 \cdot H + K_1 \cdot K_2} \tag{4.7}$$

$$x_2 = \frac{K_1 \cdot K_2 \cdot C_T}{H^2 + K_1 \cdot H + K_1 \cdot K_2} \tag{4.8}$$

Note that for the carbon system as a di-protic buffer, x_0, x_1 and x_2 refer to the molar concentrations of H_2CO_3, HCO_3^- and CO_3^{2-}, respectively. Similarly, 4 linear equations can be defined from the tri-protic buffer mass balance and its three dissociation reactions. From the simultaneous solution of the 4 equations the molar concentration of ions of the tri-protic buffer can be calculated from equations (4.9), (4.10) and (4.11).

$$x_1 = \frac{K_1 C_T H^2}{H^3 + K_1 H^2 + K_1 K_2 H + K_1 K_2 K_3} \tag{4.9}$$

$$x_2 = \frac{K_1 K_2 C_T H}{H^3 + K_1 H^2 + K_1 K_2 H + K_1 K_2 K_3} \tag{4.10}$$

$$x_3 = \frac{K_1 K_2 K_3 C_T}{H^3 + K_1 H^2 + K_1 K_2 H + K_1 K_2 K_3} \tag{4.11}$$

The unionised form (the acid form) x_0 is not stated since it will not be used in further calculations. For phosphorous as a tri-protic buffer x_0, x_1, x_2 and x_3 are analogous to the molar concentration of H_3PO_4, $H_2PO_4^-$, HPO_4^{2-} and PO_4^{3-}, respectively. Comparing with the general titration curve model (Van Vooren, 2000) the term of the tri-protic buffer can be derived as $x_1 + 2x_2 + 3x_3$, i.e. by considering the charge of each ion and calculating total equivalents.

4.3 Derivatives of ion concentration functions

For the calculation of pH, the iterative procedure of Newton-Raphson will be applied. It requires the derivative of the concentration functions. Having the symbolic definition of the ion concentration functions in the Matlab symbolic toolbox, the derivative of the functions is obtained with respect to H. Using the "pretty" function of the toolbox derivatives can be nicely arranged as follows.

For a mono-protic buffer, the derivative of x_1 is presented by the following equation (4.12).

$$\frac{dx_1}{dH} = -\frac{K_1 C_T}{\left(H + K_1\right)^2} \tag{4.12}$$

For di-protic buffers derivatives of x_1 and x_2 are presented by equations (4.13) and (4.14)
.

$$\frac{dx_1}{dH} = \frac{K_1 C_T}{H^2 + K_1 H + K_1 K_2} - \frac{K_1 C_T H \left(2H + K_1\right)}{\left(H^2 + K_1 H + K_1 K_2\right)^2} \tag{4.13}$$

$$\frac{dx_2}{dH} = -\frac{K_1 K_2 C_T \left(2H + K_1\right)}{\left(H^2 + K_1 H + K_1 K_2\right)^2} \tag{4.14}$$

Finally, for a tri-protic buffers derivatives of x_1, x_2 and x_3 are presented by equations (4.15), (4.16) and (4.17).

$$\frac{dx_1}{dH} = \frac{2K_1C_TH}{H^3 + K_1H^2 + K_1K_2H + K_1K_2K_3} - \frac{K_1C_TH^2\left(3H^2 + 2K_1H + K_1K_2\right)}{\left(H^3 + K_1H^2 + K_1K_2H + K_1K_2K_3\right)^2} \quad (4.15)$$

$$\frac{dx_2}{dH} = \frac{K_1K_2C_T}{H^3 + K_1H^2 + K_1K_2H + K_1K_2K_3} - \frac{K_1K_2C_TH\left(3H^2 + 2K_1H + K_1K_2\right)}{\left(H^3 + K_1H^2 + K_1K_2H + K_1K_2K_3\right)^2} \quad (4.16)$$

$$\frac{dx_3}{dH} = -\frac{K_1K_2K_3C_T\left(3H^2 + 2K_1H + K_1K_2\right)}{\left(H^3 + K_1H^2 + K_1K_2H + K_1K_2K_3\right)^2} \quad (4.17)$$

4.4 Recruiting ion equivalents concentration

It can be seen that the ion concentration and derivative functions consist of common fractions whose numerators and denominators are evolving systematically with the increase of the number of ions and the ion charge. For instance, equations (4.9) to (4.11) have a common denominator and numerators that build up with increasing sequence of acidity constants and a decreasing power of the hydrogen ion concentration. The functions are expressed in molar units. The pH calculations depend on the charge balance and, therefore, the functions' units should be converted from molar concentrations to equivalents. When a buffer is added to a solution the hydrogen concentration will shift with a value δ to balance the total equivalents of the ions of the introduced buffer. For each buffer, the ion concentration functions have the same denominator. Equivalents introduced by a buffer B_j that has a number of ions N can be generalised for all buffers, equation (4.18).

$$\delta_{B_j} = \frac{\sum_{i=1}^{N} num_{i,B_j}}{denom_{B_j}} \quad (4.18)$$

The total equivalents are then calculated by recruiting equivalents of all ions and buffers in the solution according the developed recruiting algorithm given in Figure 4.2. Applying this so called SubDeltaH function to a tri-protic buffer (N=3) as an example, the for-loop in the procedure iterates 3 times (i = 1 : N) the buffer ions are recruited in the equivalents calculation as follows:

$@\ i = 1$:

$num = K_1H^2C_T$

$denom = H^3 + K_1H^2$

$@\ i = 2$:

$num = K_1 H^2 C_T + 2K_1 K_2 H\ C_T$

$denom = H^3 + K_1 H^2 + K_1 K_2 H$

$@\ i = 3$:

$num = K_1 H^2 C_T + 2K_1 K_2 H\ C_T + 3K_1 K_2 K_3 C_T$

$denom = H^3 + K_1 H^2 + K_1 K_2 H\ + K_1 K_2 K_3$

At the end of the for loop, the equivalents introduced by the tri-protic buffer are calculated:

$$SubDelta = \frac{num}{denom} = \frac{K_1 H^2 C_T + 2K_1 K_2 H\ C_T + 3K_1 K_2 K_3 C_T}{H^3 + K_1 H^2 + K_1 K_2 H\ + K_1 K_2 K_3}$$

A similar generalisation can be done for the derivatives. Because of the systematic evolution of the derivative formulae terms with respect to buffer type and ion order, the derivative formulae can be presented by the general equation (4.19). the total derivative of the ion equivalents can be calculated by recruiting ion derivatives according SubDeltaH, Figure 4.2.

$$\frac{d\,\delta_{B_j}}{dH} = \frac{\sum_{i=1}^{N} diffnum1_{i,B_j}}{denom_{B_j}} - \frac{\sum_{i=1}^{N} num_{i,B_j} \cdot diffnum2_{i,B_j}}{\left(denom_{B_j}\right)^2} \qquad (4.19)$$

In both equations (4.18) and (4.19) N is the number of ions of one buffer component, i.e. equal to the number of its acidity constants. The input of the function SubDeltaH is the total concentration C of the buffer component, an array of the buffer component acidity constants, the array dimension and the current concentration of the hydrogen ion, H . The function outputs are the total equivalents and the total derivative values that are passed by reference to other calling procedures.

The flow chart in Figure 4.2, generated automatically from the C++ code by a special software tool, shows the implemented SubDeltaH function and exactly reflects the algorithm. It can be seen that the function is very compressed and contains no “if” structures. Therefore, the function execution is fast and can be linked to models without noticeable reduction of their simulation speed.

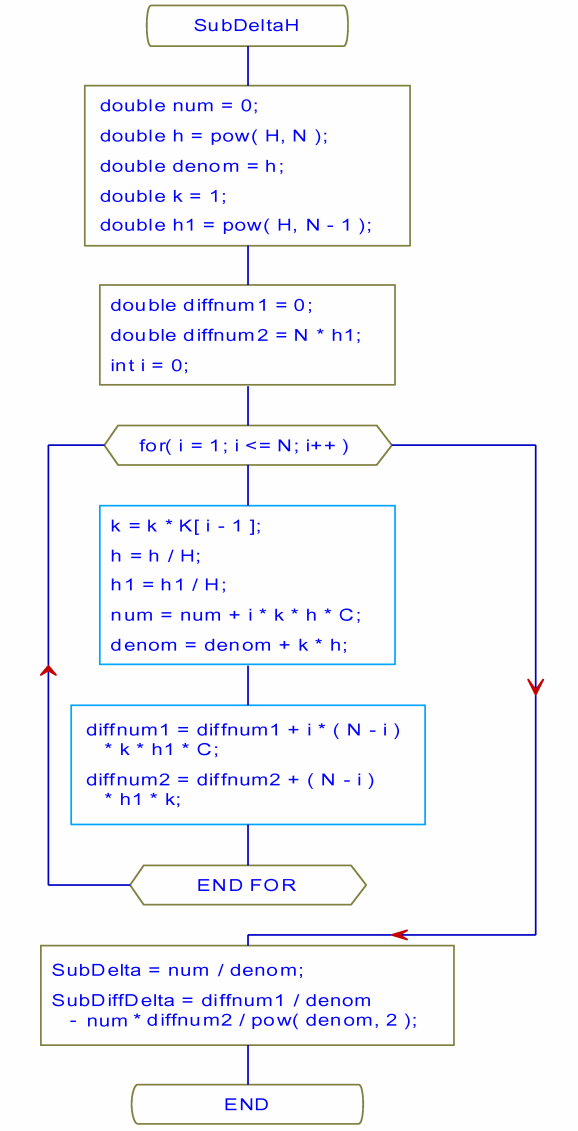

Figure 4.2 General procedure of ion recruiting for calculation of total equivalents and derivatives effected by a buffer component

4.5 Calculation of total equivalents

The function DeltaH has three jobs to do. First it receives the input data of all buffers in the system from the calling programme and loops to pass the data buffer component by buffer component to SubDeltaH. Therefore, the structure of DeltaH will depend on how the buffer data are declared in the calling programme. Its second job is to sum the total equivalents and derivatives for all buffers at a given pH. Some important aspects need to be considered for the general application of the procedure. The net cation concentration is known and passed with the DeltaH arguments so that it will be added to the δ value but not to its derivative, the derivative of the cation concentration is zero. For consideration of OH^-, the water buffer is passed to the DeltaH function as a mono-protic buffer. The water

buffer is considered according equation (4.20) and the OH^- is calculated by equation (4.21).

$$K_w^\dagger = \frac{[OH^-][H^+]}{[H_2O]} \tag{4.20}$$

$$[OH^-] = \frac{C_w K_w^\dagger}{K_w^\dagger + H^+} \tag{4.21}$$

Where the water concentration is usually considered constant such as $C_w = [H_2O] + [OH^-] \approx [H_2O] = 55.5$ mol/l and $K_w^\dagger = \frac{K_w}{[H_2O]}$.

The third job of the DeltaH function is concerned with buffers that have positive ions. Taking NH_4^+ as an example, its concentration is passed to the function with a negative sign so that its concentration is subtracted from δ. Also, their equilibrium constants are defined by the corresponding K_b value and not by the K_a value. More specifically, the concentration function of mono-protic buffers, equation (4.3), is considered for negatively charged ions. Two other forms are possible to present the concentration of positively charged ions as function of their total concentrations, e.g. for ammonia in equations (4.22) and (4.23). Note that buffers of positively charged ions are usually mono-protic.

$$NH_4^+ = \frac{C_T H^+}{K_a + H^+} \tag{4.22}$$

$$NH_4^+ = \frac{C_T K_b}{K_b + OH^-} \tag{4.23}$$

Equation (4.23) has the same form of equation (4.3) defined in the function SubDeltaH. Upon the negative sign of the input concentration to the function DeltaH, K_b and OH^- are passed to the K_a and H^+ arguments of SubDeltaH, respectively. Therefore, the general structure of the function SubDeltaH is unchanged and the calculation for positively charged ions remains correct.

4.6 General procedure for pH calculation

Figure 4.3 shows the Newton-Raphson iterative procedure for pH calculation. Starting with an initial pH-value, the iterative procedure calls the DeltaH function that calculates the estimated value of δ and its derivative. Accordingly, it updates the concentration of the hydrogen ion. The procedure iterates in the “while” loop till an acceptable tolerance is

reached or till the maximum number of iterations is exceeded. Then the estimated pH-value is passed on to the calling programme.

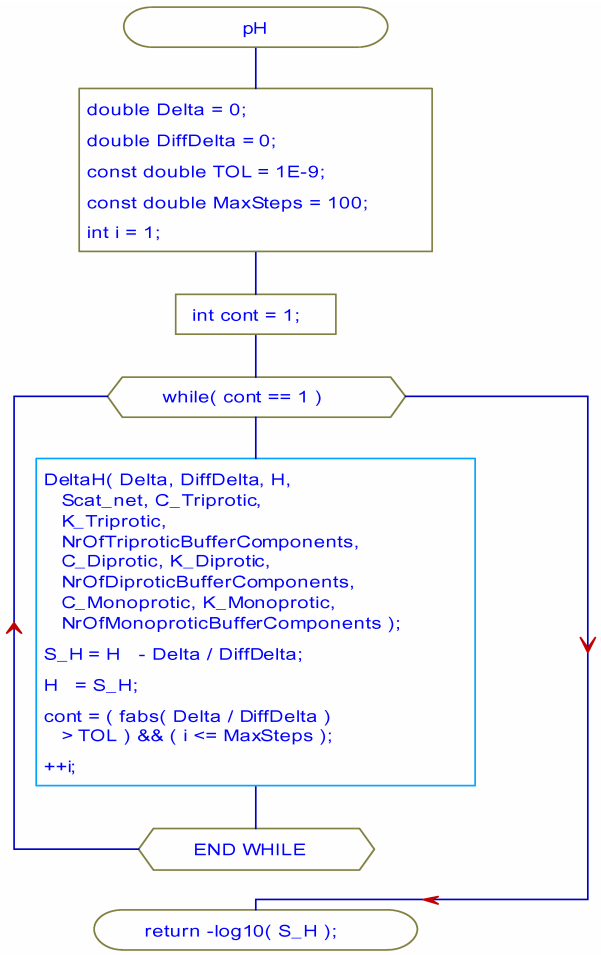

Figure 4.3 General iterative procedure for recursive pH calculation

The input of the general pH calculation procedure is an initial H^+ to start the iteration, the net cation concentration and the arguments of the buffer components. Arguments of buffer components are acidity constants, total concentrations and number of mono-, di- and tri-protic buffer components. The arguments can be declared and passed by a main C++ programme or a simulator. In this work, the function was implemented for general pH calculation in the WEST simulator, and was used for pH-calculation in an extended version of the ADM1 model that has phosphorous and cyanide as additional buffer components, see chapter 6.

4.7 WEST: implementation of the general pH function

All buffer components are defined once for all models in the WEST MSL library. Three enumerated arrays are defined in the top of the MSL tree for mono-, di-and tri-protic buffers, example in BOX 4-1.

BOX 4-1

```
TYPE MonoproticBufferComponents
  "Monoprotic buffer components"
  = ENUM { water, ammonia, phenol, sulphide, VFA,.............};
TYPE DiproticBufferComponents
  "Diprotic buffer components"
  = ENUM { carbon, ......};

TYPE TriproticBufferComponents
  "Triprotic buffer components"
  = ENUM { phosphorus, ............};

OBJ NrOfDiproticBufferComponents "The number of diprotic buffer components"
  : Integer := Cardinality(DiproticBufferComponents);

OBJ NrOfTriproticBufferComponents "The number of triprotic buffer components"
  : Integer := Cardinality(TriproticBufferComponents);

OBJ NrOfBufferComponents "The number of buffer components"
  : Integer := Cardinality(BufferComponents);
```

There are two ways to declare the general pH calculation with models in the MSL library. The first is by doing the declarations once for all models, BOX 4-2. A new general model class "PhysicalDAEModelType_WithpH" is extended from the general model class "PhysicalDAEModelType". Consequently, all model classes that apply the general pH calculations are extended from the new class.

BOX 4-2

```
CLASS PhysicalDAEModelType_WithpH
  SPECIALISES PhysicalDAEModelType :=
  {:
    parameters <-
   { OBJ K_Triprotic  "": Real[NrOfTriproticBufferComponents;][3;];
     OBJ K_Diprotic  "": Real[NrOfDiproticBufferComponents;][2;];
     OBJ K_Monoprotic  "": Real[NrOfMonoproticBufferComponents;][1;];};
  state <-
   {OBJ C_Triprotic "":MolConcentration[NrOfTriproticBufferComponents;];
    OBJ C_Diprotic "": MolConcentration[NrOfDiproticBufferComponents;];
    OBJ C_Monoprotic"":MolConcentration[NrOfMonoproticBufferComponents;];
    OBJ S_cat_net "cations of strong bases - anions of strong acids":Real;};
:};
```

The second way is to define the declarations in the "parameters" and "state" blocks in each model. Of course, the first way is more efficient. In both ways, the acidity constants are defined in the "initial" block. Total concentrations are defined only for buffer components that are relevant to each model in its "equations" block, BOX 4-3. The call of the general pH function can be included in the "equations" block of each model or declared once in the "equations" block of the new general model class. The standard function call is shown in BOX 4-3. After passing the previous state of the hydrogen ion concentration and the net cation concentration, other defined buffer characteristics arrays are passed by reference and, therefore, using less memory and achieving better simulation speed.

BOX 4-3

```
  initial <-
{..............
parameters.K_Monoprotic[M_water][1] :=parameters.Ka_h2o/55.5;
arameters.K_Monoprotic[M_ammonia][1] :=parameters.Ka_nh4;
.........
parameters.K_Diprotic[carbon][1] := parameters.Ka_co2;
parameters.K_Diprotic[carbon][2] := 4.69e-11;
...........
parameters.K_Triprotic[T_phosphorus][1] := 7.11e-3;
parameters.K_Triprotic[T_phosphorus][2] := 6.23e-8;
parameters.K_Triprotic[T_phosphorus][3] := 4.55e-13;};


  equations <-
{
state.C_Monoprotic[M_water]=55.5;
state.C_Monoprotic[M_ammonia]=-state.C_An[S_INN];
...........
state.C_Diprotic[D_carbon]=state.C_An[S_IC];
...........
state.C_Triprotic[T_phosphorus]=state.C_An[S_phos];
..............
state.pH_=pH(previous(state.S_h_ion),state.S_cat_net,
ref(state.C_Triprotic[T_phosphorus]),
ref(parameters.K_Triprotic[1][1]),NrOfTriproticBufferComponents,
ref(state.C_Diprotic[1]),
ref(parameters.K_Diprotic[1][1]),NrOfDiproticBufferComponents,
ref(state.C_Monoprotic[1]),
ref(parameters.K_Monoprotic[1][1]),NrOfMonoproticBufferComponents);
..............};
```

4.8 Total alkalinity calculation

Alkalinity can be defined as the excess of positively charged ions of strong bases over the anions of the strong acids. Total alkalinity is the net cation concentration. According to the charge balance, the alkalinity can also be presented by the ion equivalent concentrations of n buffer components (e.g. weak acids) minus the hydrogen ion concentration, equation (4.24).

$$Cat_{net} = Alk_{total} = \sum_{j}^{n} \delta_{B_j} - H^+ \qquad (4.24)$$

Concentrations of buffer components are easier to be determined than determining the cation concentration, see part III. Also, pH is easily measurable on-line. However, application of pH-dependent models such as the ADM1 model requires the estimation of the influent cation and anion concentrations for accurate simulations of pH. Using the available data of the influent buffer concentrations and a pH measurement, a function (called Cat) is implemented to calculate the net cation concentration. The function is simple, as shown in Figure 4.4. It calls the DeltaH function to calculate δ and applies equation (4.24).

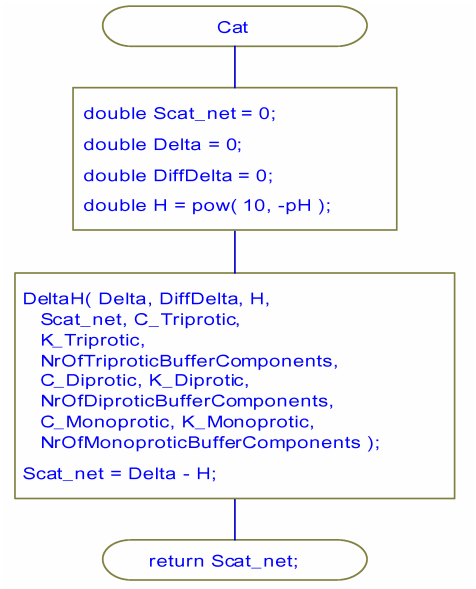

Figure 4.4 Simple net cation calculation using calculated total equivalents

A node has been defined in the WEST modelbase to calculate the net cation concentration in flow streams. The node has two influent interfaces, one is for the buffer component concentrations and the other is for the pH measurement. The cation calculator is defined in the MSL library, BOX 4-4, by extending the new general model class "PhysicalDAEModelType_WithpH" that is defined for pH calculation with the interface definitions and the "Cat" function call.

BOX 4-4

```
CLASS CationCalculator
EXTENDS PhysicalDAEModelType_WithpH WITH
 {:
  interface <-
   {
    OBJ Inflow (* terminal = "in_1" *) "Inflow" :
        InBuffer := {: causality <- "CIN" ; group <- "Influent" :};
    OBJ Inflow_pH (* terminal = "in_2" *) "Inflow" :
         InpH := {: causality <- "CIN" ; group <- "Influent pH" :};
    OBJ Outflow_cat (* terminal = "out_1" *) "Outflow filtered" :
         OutCat := {: causality <- "COUT" ; group <- "Effluent_cat" :};
  };
  state <-
    {
    OBJ test "" : Real ;
    };

  equations <-
   {
    state.test=Cat(independent.t,interface.Inflow_pH[pH_m]
     ,ref(state.C_Triprotic[T_phosphorus]),ref(parameters.K_Triprotic[1][1]),NrOf
     TriproticBufferComponents,ref(state.C_Diprotic[1]),ref(parameters.K_Diprotic
     [1][1]),NrOfDiproticBufferComponents,ref(state.C_Monoprotic[1]),ref(paramete
     rs.K_Monoprotic[1][1]),NrOfMonoproticBufferComponents);
    interface.Outflow_cat[cat]=state.test;
    };
 :};
```

The cation calculator node can be used to calculate the dynamic evolution of the influent cation concentration as is, for instance, necessary for ADM1 application. It is applied in chapter 6 to calculate the evolution of the cation concentration of the applied cassava wastewater. It would not have been possible to simulate the experiment presented in chapter 6 without this cation calculation.

4.9 Titrimetric Analyzer Simulator (TAS)

All titrimetric methods are based on the charge balance among dissociated buffers and the shift introduced to this chemical equilibrium by step wise addition of base or acid. A general charge balance can be performed according (4.24).

After addition of titrant (strong acid) to this equilibrium the H^+ will shift to achieve a new point of equilibrium and the concentration of the titrant acid in the sample C_a can be calculated from (4.25) :

$$C_a = H^+ - \sum_j^n \delta_{B_j} \tag{4.25}$$

Considering the volume change of the sample and the dilution of original ion concentrations due to the addition of acid, equation (4.25) can be expressed in terms of N_a, V_a and V_s which are the normality and the volume of the acid added and the volume of the sample, respectively. The result is equation (4.26).

$$\frac{V_a \cdot N_a}{(V_a + V_s)} = H^+ - \frac{V_s}{(V_a + V_s)} \sum_j^n \delta_{B_j} \tag{4.26}$$

V_a can then be calculated directly from (4.27)

$$V_a = \frac{V_s}{N_a - H^+} \cdot \left(H^+ - \sum_j^n \delta_{B_j} \right) \tag{4.27}$$

In case of up titration, the volume of added base, V_b, can be calculated from equation (4.28) that is also derived from the charge balance. There is no need to include the added OH^- since water is considered with the buffers B_j.

$$V_b = \frac{V_s}{N_a + H^+} \cdot \left(\sum_j^n \delta_{B_j} - H^+ \right) \tag{4.28}$$

To simulate titration curves of different buffer combinations, a Titrimetric Analyser Simulator (TAS) is built in WEST. Figure 4.5 shows the procedure that is implemented in C++ and is linked to TAS as an external function.

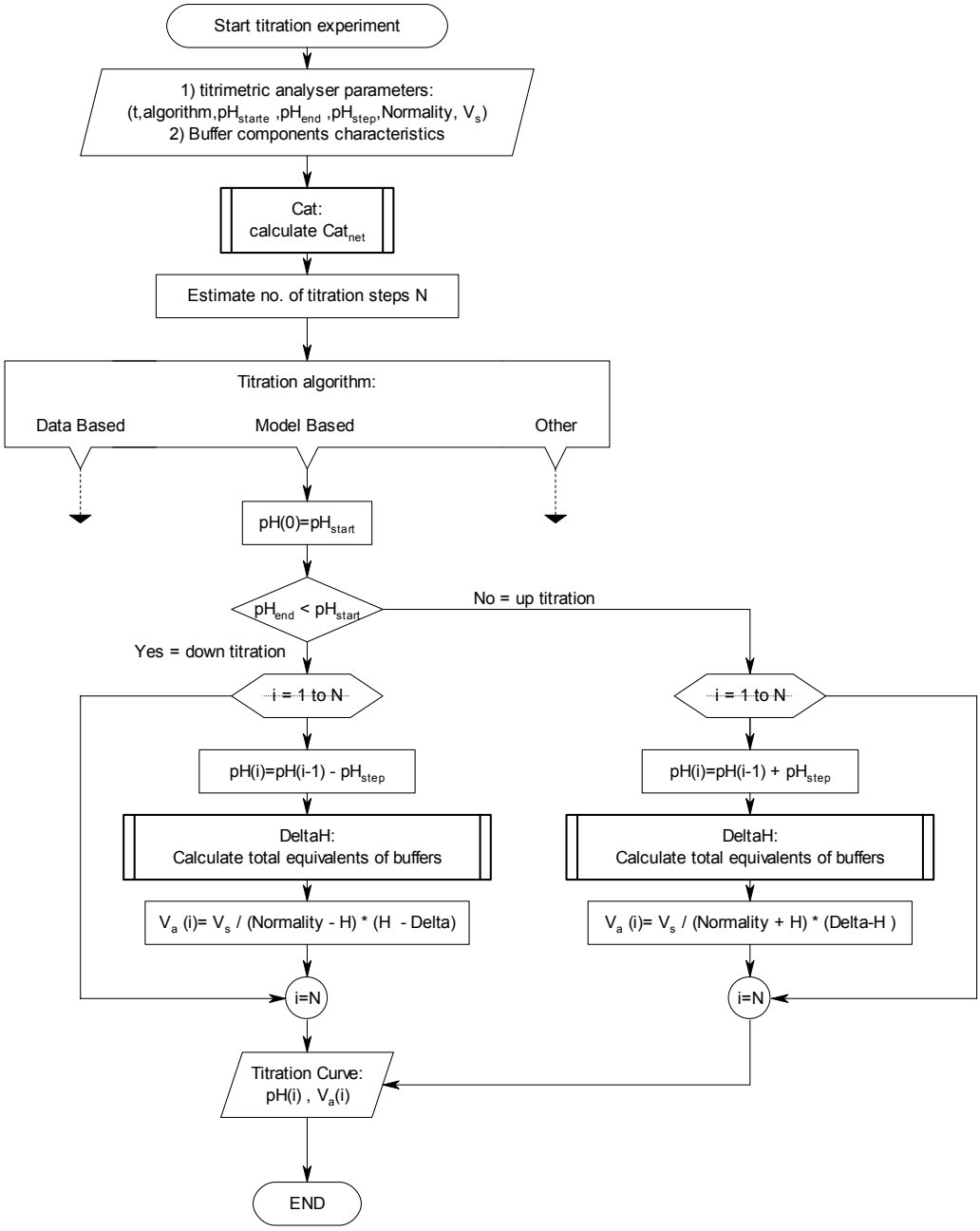

Figure 4.5 Titration procedure of Titrimetric Analyser Simulator (TAS)

Accordingly, a titration curve can be produced by evaluating the volume of added acid or base at stepwise increments of pH, i.e. H^+. Such titration curve can also be produced in real titration experiments by estimating the acid/base dose using the same procedure, i.e. using a model-based titration algorithm as recommended by Van Vooren (2000). The procedure is modular and can be extended by data-based and other algorithms so that different algorithms can be compared before the implementation to real analysers.

The procedure uses the previously illustrated Cat and DeltaH functions for the calculation of the net cation concentration and the total equivalents concentration, respectively. The titrimetric analyser parameters and the characteristics of the buffer mixture are input to the function from a main program or the TAS. The net cation concentration is calculated and the number of titration steps is estimated. The calculation proceeds according to the selected titration algorithm. For an ideal titration curve with the model-based algorithm, a decision is made for down or up titration according the defined titration experiment parameters. A loop is started to calculate the accumulative acid/base addition according the desired pH increment. In each iteration, the function DeltaH is called to evaluate the total equivalents of the defined buffers and equation (4.27) or (4.28) is calculated to evaluate the added acid or base volume. The loop continues till the number of titration steps is reached. The output is an array of pH and V_a values.

4.9.1 WEST: implementation and validation of TAS

The Titrimetric Analyser Simulator (TAS) was defined in the WEST MSL library by extending the new general model class “PhysicalDAEModelType_WithpH” that is defined for pH calculation with the interface definitions and equations, and the titration function call. The inflow interface of the TAS was declared for all defined buffer components. A dynamic inflow stream with varying concentrations of buffer components was sampled at regular time steps and the titration curves were simulated for each sample.

The TAS was first validated by using real titration curves obtained by titrating standard solutions. The titration experiments were performed using the titrimetric lab setup illustrated in detail in chapter 10. Titration experiments were performed using standard solutions of mono-, di- and tri-protic buffers. The titration was configured to achieve a small increment of 0.1 pH so that detailed titration curves were produced. Figure 4.6 shows the titration of lactate and acetate mixtures as examples of mono-protic buffers. The initial pH of the samples was adjusted by addition of strong base to start the titration from a pH above 7. Down titration was performed till pH 2.5 by stepwise addition of HCL 0.5N. Acetate and lactate have pKa values around 4.75 and 3.85, respectively. The simulation

was performed for the designed sample concentrations and titration experiment parameters. It can be seen in Figure 4.6 that the simulated titration curves, solid lines, agree with the titration data points. Similarly high slopes are simulated in the buffering zones of the added buffers, i.e. around their pKa values. Both simulated and experimental titration slopes are almost flat above pH 6.5 since there is no influence of the buffers in this zone. Close to the end of the titration curves, the slope decreases due to the decrease of the acetate and lactate buffering capacity, but a small slope is maintained due to the water buffer. Adding the water buffer to the simulated buffers is necessary to correctly simulate the end part of the titration curves. Generally, the simulated titration curves agree well with the measured titration points at the different tested concentration levels. However, at high concentrations a less accurate fit occurs because of the higher ionic strength.

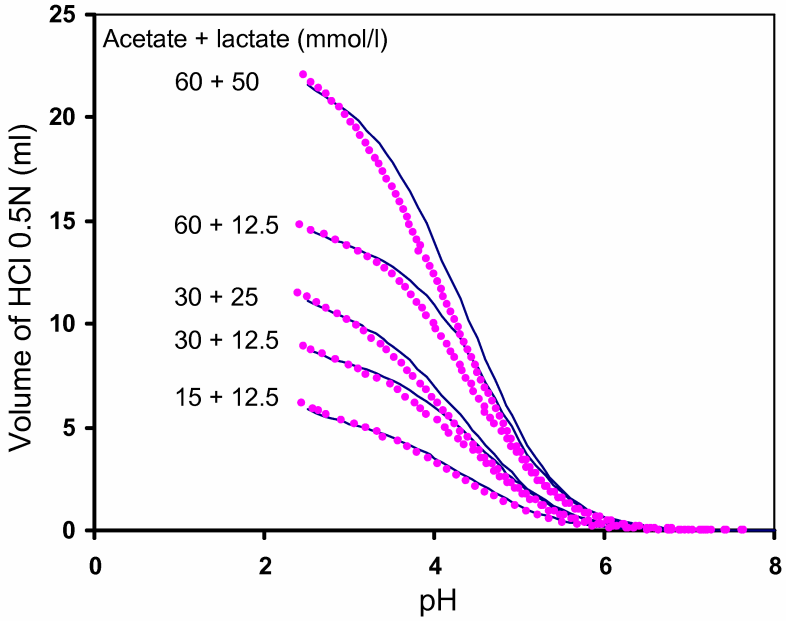

Figure 4.6 Validation of TAS with titration data of mono-protic buffers,
• data ____ simulation

Figure 4.7 shows the titration of mixtures of inorganic carbon and phosphorus solutions as examples of di- and tri-protic buffers. The initial pH of samples was again adjusted by addition of strong base to start the titration from a pH above 11. Down titrations were performed till pH 2.5 by stepwise addition of HCL 0.5N. The carbon buffer has two buffering zones at its pKa values, around 6.35 and 10.3 pH. The phosphorus buffer is tri-protic and has three buffering zones around pH values of 2.15, 7.2 and 12.3. Simulations were performed for the designed sample concentrations and titration experiment parameters. The simulated titration curves agree with the titration data points. Following the direction of the titration experiment, 5 slopes can be seen in the titration curve of each

experiment. The high slope due to the carbonate buffer around pH 10.3 is simulated for the different carbon concentrations and it agrees with the titration data. A small slope is in the range of pH 9 to pH 8 due to the little influence of the existing buffers in that range. Another high slope is well simulated in the overlapping buffering zones of carbon and phosphorous around pH 6.35 and 7.2. At the end of the titration curves, the slope increases again due to the start of the water buffer and another buffering zone of phosphorous at 2.15. Generally, the simulated titration curves agree well with the measured titration points at the different tested levels of concentrations.

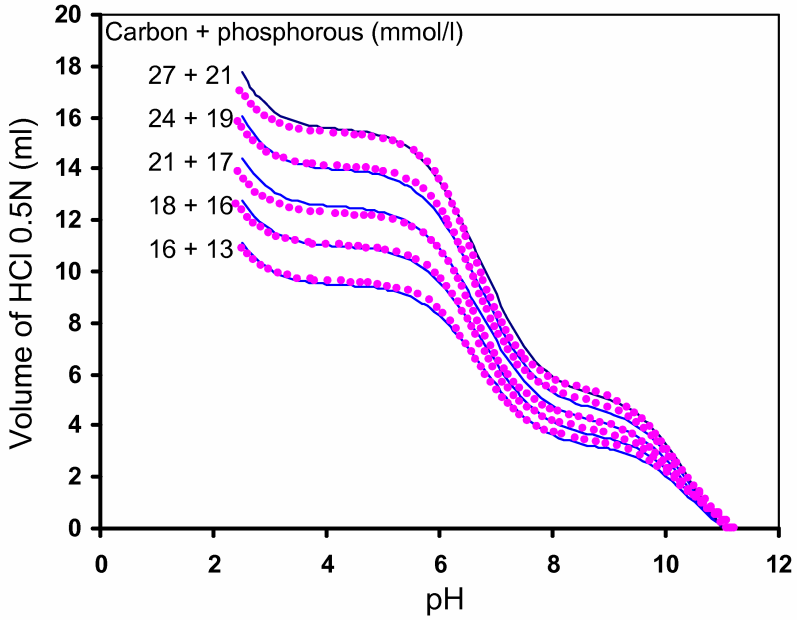

Figure 4.7 Validation of TAS with titration data of di- and tri- protic buffers
• data ____ simulation

The titration procedure was used for the preliminary evaluation of the Buffer Capacity Software BCS, as illustrated in chapter 11. Concentrations of buffering components were defined for simulation of titration curves using the TAS. The simulated concentrations are exactly retrieved with BCS, that in fact uses a different interpretation methodology. This reproducibility of concentration results proves the correctness of both TAS and BCS implementations and their underlying theories. The TAS was also used to design the experimental protocol to test a real titrimetric analyser as illustrated in chapter 12.

4.10 Conclusions

It was possible by using the Matlab symbolic toolbox to mathematically derive general formulas for ion concentrations present in a solution and observe their systematic evolution with the buffer types and ion order. Accordingly, general forms for recruiting equivalent

ion concentrations in a solution and their derivatives with respect to the hydrogen ion concentration could be developed and programmed in a simple and general function "SubDeltaH" to evaluate the total equivalents effected by any buffer component. It was then possible to programme a higher level function "DeltaH" that arranges the properties of any group of buffers (including the water buffers) in a sample, iterates all buffers, by calling "SubDeltaH", and calculate the total equivalents δ in the sample and the corresponding H^+-derivative. This generalisation was useful to simplify different calculation and simulation procedures that are dependent on the charge balance and pH. The generalised calculation of total equivalents was implemented in three procedures. First, it is implemented in an iterative procedure to calculate the pH of a known buffer mixture. Second, it is implemented for the calculation of cation concentrations in flows of known buffer composition and pH. Third, it is implemented for the simulation of titration experiments.

The iterative pH-calculation procedure is implemented in the WEST simulator to simulate the pH for any model with any buffer combination and it allowed to improve the simulation speed in comparison with alternative pH-calculation methods. For instance, the implementation of the pH procedure with the ADM1 model significantly improved its simulation speed and made its extension with more buffer components easier. Furthermore, cation calculations in digester influents are useful to correctly simulate the digester pH.

Finally, a Titrimetric Analyser Simulator (TAS) was implemented in the WEST simulator. The TAS was validated with titration experiments of standard solutions of mono-, di- and tri-protic standard solutions. The TAS will be useful to design experimental protocols to test real titrimetric analysers, check their titration algorithms and interpretation methods. Furthermore, the TAS can be implemented in testing and simulating titrimetric monitoring and control designs.

Chapter 5

Conceptual approach for ADM1 application

Abstract

This chapter introduces a conceptual approach to apply the IWA Anaerobic Digestion Model no. 1 to simulate digester dynamics. The illustrated modelling approach avoids laborious measurements to characterise the influent according the extensive list of components defined in the model. It rather uses the model to make a better characterisation of the inflow. The model is applied to simulate a digester that was originally designed as a CSTR, i.e. with solids retention time equal to the hydraulic retention time. Because it is not practical to completely achieve the CSTR condition, an update to the model is introduced to describe the effect of hydrodynamics on solids retention. The solids retention time is modelled proportional to the hydraulic retention time, i.e. with less efficient retention during overload conditions. The update is also useful for the simulation of high rate reactors. The application of the approach to a real wastewater treatment with important dynamics shows excellent simulation results.

CHAPTER 5

5.1 Introduction

Practical measurements in digester follow-up are mainly based on available cost-effective methods that allow frequent measurements. Therefore, control strategies are developed on the basis of these measurements and on their on/off-line availability at reasonable price. Examples are pH, flow, gas pressure and gas flow which are practically available at anaerobic digesters and wastewater treatment plants in general (Vanrolleghem and Lee, 2003).

Alkalinity and VFA measurements are available off-line and much efforts are invested to make them available on-line, e.g. by using titration (Di Pinto *et al.*, 1990; Hawkes *et al.*, 1993; Guwy *et al.*, 1994, Van Vooren *et al.*, 2001; Bouvier et *al.*, 2002; Feitkenhauer *et al.*, 2002), using gas / high pressure liquid chromotgraphy (Zumbusch *et al.,* 1994; Banister and Pretorius, 1998; Pind *et a*l., 2001) and using intermediate infrared absorption (Steyer *et al.*, 2001).

Since such measurements are more oriented towards control of the digester, they are more suitable for use with simple models that are developed in view of control systems, e.g. the two-step mass balance model developed by Bernard *et al.* (2001). However, when more insight into the process dynamics is needed, models need to be adapted to cope with the complex characteristics of the wastewater and the way the biomass interacts with it. This means that an extension of the anaerobic digestion model is needed to involve more components that have a role in the process. Also, a better characterisation of the influent wastewater must be performed. For example, the model developed by Mosey (1983) and the consequent expansion and enhancements in (Costello *et al.,* 1991; Romli, 1993; Ramsay, 1997; Batstone et al., 2000[a]; Batstone et al., 2000[b]) and finally the IWA ADM1 (Batstone et al., 2002) are a reflection of their development.

This work is one of the first contributions to apply the IWA ADM1 model to simulate an experiment with important process dynamics treating a complex wastewater. Practical measurements, the model, information about the wastewater composition and knowledge about the industrial process producing the wastewater are used to expand the influent characteristics and define reactor behaviour.

5.2 Methods and materials

5.2.1 Anaerobic digestion model and its implementations

The model used in the present simulation is the IWA Anaerobic Digestion Model no. 1. The IWA report (Batstone et al., 2002) provides a complete description of the model.

However, for a successful implementation of the model, updates are necessary as illustrated in chapter 3. The present simulation uses a set of ADM1 parameters suggested in (Rosen and Jeppsson, 2002). Although this set of parameters was selected from the IWA ADM1 report for anaerobic digestion of secondary sludge, it is used for the present type of distillery wastewater. It is conceived that mainly the wastewater fraction parameters are the ones that should change with the change of wastewater source. As an initial set of parameters it gives good simulation results provided that the influent is characterised in detail and, thus, the influence of the fraction parameters is reduced.

The simulation was performed using ADM1 implementations on three different simulation platforms, AQUASIM®, WEST® and MATLAB SIMULINK®. The gas transfer is modelled on the first platform using a diffusive link between liquid and gas compartments and, therefore, the transfer is treated mathematically by partial differential equations and the gas flow is calculated for restricted flow through an orifice that is proportional to the piping resistance coefficient. In the second and third implementations, the gas components are modelled by differential equations in both liquid and gas phases and gas flow is estimated as a function of the gas transfer rates and the headspace pressure.

5.2.2 Reactor and wastewater composition

A lab-experiment was performed at the Department of Chemical Engineering, University of Santiago de Compostela, Spain. The reactor is a lab-scale CSTR, Figure 5.1, with a 2 liters liquid volume. It is equipped with pH and temperature probes, a stirrer to provide 200 r.p.m. and a condensation system in the gas outlet. A gas flow meter measures the gas production every 15 minutes. The temperature is fixed by a thermostatic jacket at 37 ºC. The reactor is fed by diluted fresh wastewater. The reactor was inoculated with sludge produced at a pilot-scale plant treating dextrose with a specific methanogenic activity of 0.27 kg COD/m^3·d, and its initial concentration in the reactor was 6 g VSS/l. The gas composition was measured with a thermal conductivity gas chromatography (HP 5890 SerieII), with helium as carrier gas.

Wastewater composition: The wastewater was collected from an alcoholic distillery plant and contained a high amount of TKN mainly in the form of protein. Average concentrations of the distillery wastewater are listed in Table 5-1 Due to the high concentration of wastewater, it is diluted before it is introduced into the reactor. This complex wastewater probably contains some unmeasured compounds that could have slight toxic effects in some microbial populations. This fact appears as an extra source of uncertainties.

Figure 5.1 Experimental setup: transducers and data logging systems are to the right, the reactor, pH probe, gas flow sensor and gas sampling are in the middle and the thermal conductivity probe, influent /effluent pump and effluent sampling are to the left.

Table 5-1 Average concentrated wastewater concentrations produced at the industrial plant

Characteristic	Unit	Average value
Total COD	(g/l)	75
Soluble COD	(g/l)	71
TOC	(g/l)	29.2
COD/TOC	(ratio)	2.6
Acetate	(g/l)	6.39
Propionate	(g/l)	0.07
nBuH	(g/l)	0.47
TSS	(g/l)	1.7
VSS	(g/l)	1.63
Protein	(g/l)	4.0
NH_4^+-N	(g/l)	0.126
NO^{x-}	(g/l)	0
SO_4^{2-}	(g/l)	0.709
PO_4^{3-}	(g/l)	0.114
Sugars	(g/l)	6.4

Influent records: Influent flow and pH were recorded on-line. TOC, soluble COD, total volatile fatty acids (VFA), total alkalinity (TA) and partial alkalinity (PA) were analysed off-line and recorded on a daily basis.

Digester/effluent records: pH, gas flow and gas composition (%CO_2 and %CH_4) were measured on-line. Specific VFA gas chromatography analysis, TA and PA, total organic carbon and COD were measured in the digester on a daily basis.

5.2.3 Conceptual approach for influent characterisation

Figure 5.2 shows the applied approach to extend the influent characterisation for ADM1. Conceptually, the approach is visualised by a triangle where one dimension represents the information about the wastewater and the second dimension represents the practical measurement in both the influent and the digester. Extending either dimension will increase the information space and help the extension of the influent characterisation along the diagonal. Different methods can be used to define the interaction between information sources from both dimensions. For instance:

- The measurement of total VFA can be subdivided into VFA fractions in proportion to the different VFA's in the wastewater.

- COD measurements in the influent in comparison with the average wastewater COD can define a dilution term that defines the influent profile for the components for which only the average concentration in the wastewater is known.

- From a COD-balance of the previous two steps an extra COD amount can be estimated and further distributed to the most expected components in the wastewater. The time evolution of these components can be estimated by assigning new parameters to their influent concentrations. These parameters are then estimated by fitting the VFA and CODs measured in the digester. VFA sums the most sensitive components in the model.

- From partial and total alkalinity measurement in the influent, an initial estimate of the inorganic carbon and cation concentration can be evaluated, assuming that the anions will balance with the influent concentration of ammonium. For a further enhancement of the estimates, a distributed parameter can be assigned to each component. Each parameter is distributed according to major perturbations in the digester operation. The parameters are estimated (PE) by fitting the pH measurement in the digester. The ADM1 is very sensitive to the pH due to the inhibition terms. The pH depends on different buffering components, the cation and anion concentrations.

- Similarly, other rules can be exploited for further extension and time distribution of influent components.

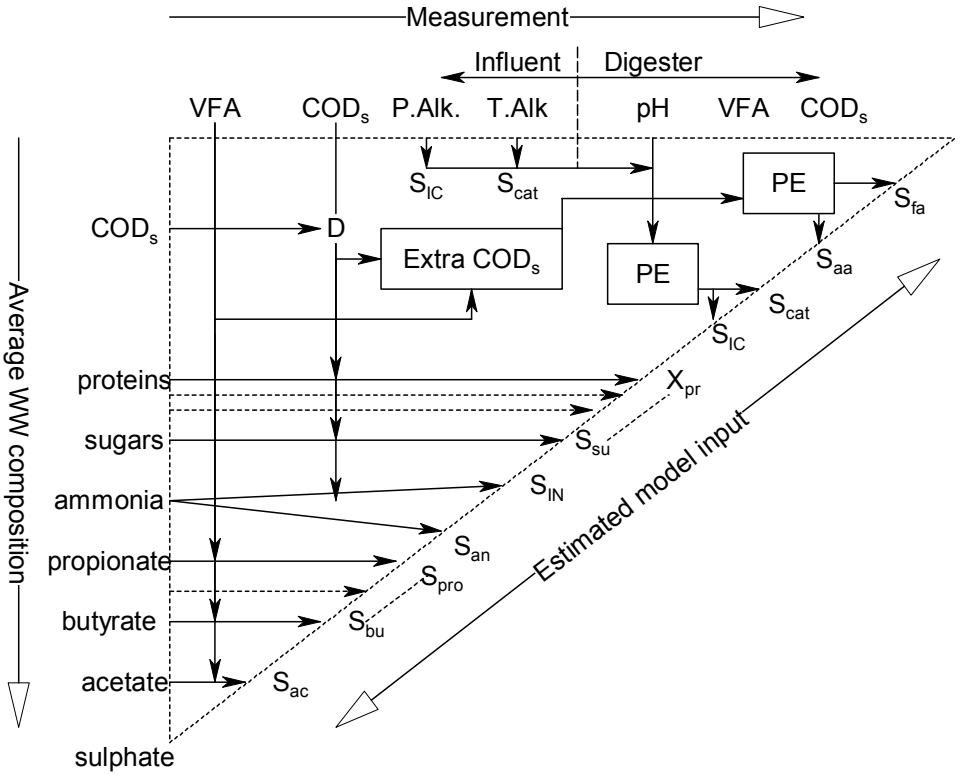

Figure 5.2 ***Applied methodology for influent distribution (explanation, see text).***

5.2.4 Influent characterisation

In a first step, information about the wastewater composition was used to extend the practical set of measurements to the IWA ADM1 influent characteristics. The IWA ADM1 has a detailed structure that presents most of the anaerobic digestion process pathways and possible inhibitions. Therefore, in a second step, the certainty encapsulated in the detailed structure of the model is used to resolve uncertainties encountered during influent characterisation.

First step in extending the practical measurements. Based on the wastewater average composition, it is concluded that the main part is in the form of soluble COD (CODs). A dilution term (D) is estimated at every measuring point as the ratio of the average CODs composition to the CODs measurement.

$$CODs_{in}.(WW+W) = CODs_{composition}.WW \tag{5.1}$$

$$D = \frac{(WW+W)}{WW} = \frac{CODs_{composition}}{CODs_{in}} \tag{5.2}$$

where:

WW is assumed average wastewater produced by the plant

W is assumed water added for dilution

This factor is then used to estimate unmeasured components. For example the influent inorganic nitrogen $S_{IN_{in}}$ is in the form of ammonium:

$$S_{IN_{in}} = \frac{S_{NH_4^+-N}}{14 \cdot D} \tag{5.3}$$

Similarly, other unmeasured components are estimated from the wastewater composition. Also, information about the type of waste and the manufacturing process helps in the determination of the molecular weights and COD contents that are needed to convert the measurement units to the model COD units. Influent soluble sugar, $S_{su_{in}}$, is estimated from the sugar composition assuming that it is mainly consisting of monosaccharides. Influent composite particulates, $X_{C_{in}}$, are estimated from the total suspended solids, TSS, composition assuming that they have the same composition of biomass since $X_{C_{in}}$ is used within the model as a sink for decaying biomass. Influent inert particulates are estimated as the difference between TSS and volatile suspended solids, VSS. Particulate protein was estimated from the wastewater composition and it was assumed to have an equal molecular weight and COD content since its molecular formula is not known. This assumption will affect the predictions of the amino acids and their conversion to different volatile fatty acids, inorganic nitrogen, inorganic carbon and hydrogen gas in the reactor.

VFA-specific components were estimated from the daily measurement of the total VFA concentration. The fractions of acetate, propionate and butyrate were estimated according to their average proportions in the wastewater. The influent soluble COD measurement was found to be higher than the sum of the COD of the estimated influent sugars and VFAs. This extra COD was redistributed using the ADM1 model in the next step.

Estimate of inorganic carbon. If anions in the influent are mainly due to bicarbonate and VFA and the influent-pH is in the optimum range of 6 to 8, the estimate of the inorganic carbon is straightforward from the practical measurement of total alkalinity (TA). TA is determined by the volume of acid added to a sample till the pH reaches 4.3 and will be equivalent to the total concentration of cations (Bernard *et al.*, 2001). The total VFA concentration can be estimated, e.g. by recording the volume of acid added to the titrated

sample at pH 5.75 and then the total acid till pH 4.3 (Ripley et al., 1986). The inorganic carbon will be mainly due to bicarbonate (Van Haandel and Lettinga, 1994) and it will equal the total cation concentration minus the VFA concentration.

In the present case study anions other than bicarbonate and dissociated VFA are expected in the influent. We assume that anions (San) of strong acids eg. (Cl^-) will be in chemical equilibrium with ammonium NH_4^+ and thus will equal its concentration. Influent anions of other acids (in oxidised form, e.g. SO_4^{2-}) will influence the charge balance with the influent cations. In the digester, such anions are not considered any further in the charge balance since they are expected to be reduced due to acidification while evaluated cations remain and influence the charge balance.

Total alkalinity will not correspond to VFAs and bicarbonate but also to the other ions (Lahav et al., 2002). Since the additional ions in the influent are not measured, IWA ADM1 itself is used to resolve this uncertainty. First, the inorganic carbon is estimated from the partial alkalinity (PA). PA is the amount of acid added to a sample till it reaches pH 5.75. In this narrow range most of the influence of the different buffering system is avoided. However, VFA has a considerable influence on the PA measurement in this range (Lahav and Loewenthal, 2000). The total VFA is measured in the influent and thus a proportion of the VFA is deducted from the partial alkalinity value to get an initial estimate of the inorganic carbon (bicarbonate).

Use of the ADM1 to better characterise the influent composition. Better characterisation is needed with two objectives in mind. The ADM1 model will be used to improve the initial estimate of cations and distribute the detected extra COD to the different model components. These two objectives are met by defining parameters (multipliers / fractions) to the concerned influent components and estimate them by fitting the digester COD, acetate, propionate, pH as follows.

Enhancing the initial estimate of the influent cations. The pH is measured in the influent and thus an initial estimate of the cations is obtained as the sum of bicarbonate and dissociated VFA (as acetate), equation (5.4):

$$S_{Cat-initial} = \frac{IC \cdot Ka_{HCO_3}}{Ka_{HCO_3} + \{H^+\}} + \frac{VFA \cdot Ka_{acetate}}{Ka_{acetate} + \{H^+\}} \qquad (5.4)$$

A parameter P_{cat} is added to the model according equation (5.5).

$$\text{Influent } S_{cation} = P_{cat} \,.\, S_{cat\text{-}initial} + \text{external cation pulses} \qquad (5.5)$$

External cation pulses are recorded base additions to adjust the influent pH. With a sensitivity analysis it was shown that the IWA ADM1 is very sensitive to this. The parameter P_{cat} is then estimated by fitting the most sensitive and measured state variables. The parameter P_{cat} is used to scale the estimated cation concentration to compensate for the extra ions expected in the influent. Provided that the wastewater is from the same origin, the cation concentration will vary according to the dynamics of the other influent concentrations. Therefore, different values $P_{cat,i}$ can be estimated in equation (5.6) according to the major changes observed in the influent concentrations, e.g. COD.

$$P_{cat\,0\to t} = \left\{ P_{cat}(1)_{0\to t_1}, P_{cat}(2)_{t_1\to t_2}, ...P_{cat}(n)_{t_{n-1}\to t} \right\} \qquad (5.6)$$

In the present case study P_{cat} was estimated in two intervals from day 0 to 100 and from day 100 till the end of the experiment. Indeed the influent COD concentration was reduced by 50% after 100 days.

Distribute the detected extra COD to model components. The influent wastewater contains protein. Amino acids are expected from hydrolysis of their proteins and therefore their concentration has to be estimated. The wastewater is produced from an industrial process that depends on the fermentation of grains (e.g. barley). Grain contains some oil that will not be processed during the industrial processes. Oil is expected to hydrolyse to long chain fatty acids (LCFA) in the wastewater and therefore needs to be estimated as well. Extra COD can be attributed to fatty acids and amino acids by estimating two fraction parameters, equations (5.7), (5.8). To allow more degrees of freedom and check the assumption, two fraction parameters are added in equations (5.9) and (5.10) to estimate some extra acetate and propionate since they are already high in the influent. The sum of these fraction parameters is expected to be less than 1 since some of the extra COD is expected to be inert soluble or particulate matter which passed the filtration that was performed prior to the COD measurement. This fraction is determined by equation (5.11).

$$S_{aa_{in}} = f_{aa} \cdot COD_{extra} \qquad (5.7)$$

$$S_{fa_{in}} = f_{fa} \cdot COD_{extra} \qquad (5.8)$$

$$S_{ac_{in\_adjusted}} = S_{ac_{in\_estimated}} + f_{ac} \cdot COD_{extra} \qquad (5.9)$$

$$S_{pro_{in\_adjusted}} = S_{pro_{in\_estimated}} + f_{pro} \cdot COD_{extra} \tag{5.10}$$

$$S_{inert/escaped\_paticulate} = \left(1 - f_{aa} - f_{fa} - f_{ac} - f_{pro}\right) \cdot COD_{extra} \tag{5.11}$$

Parameter estimation resulted in a small value of f_{ac} and f_{pro} that can be ignored. Therefore, the confidence was increased that the extra measured COD is mainly due to fatty acids and amino acids, which can be expected in the influent.

5.2.5 Changes in particulate dynamics

The IWA ADM1 model was used to evaluate whether the observed process dynamics were either due to wash-out of biomass or due to a higher retention. However, in view of this a minor update had to be made to the model. For a perfect CSTR the rate of change of the particulate concentration is calculated according equation (5.12). Originally, it is recommended in the model report (Batstone et al., 2002) that for the description of a higher solids residence time (SRT) in a biofilm or a high-rate reactor, the retention time can be extended by implementing an extra residence time, equation (5.13) above the hydraulic retention time in the second term (particulate mass flow out) on the right hand side of the particulate concentration mass balance.

$$\frac{dX_{liq,i}}{dt} = \frac{qX_{in,i}}{V_{liq}} - \frac{qX_{liq,i}}{V_{liq}} + \sum_{j=1-19} \rho_j \nu_{i,j} \tag{5.12}$$

$$\frac{dX_{liq,i}}{dt} = \frac{qX_{in,i}}{V_{liq}} - \frac{X_{liq,i}}{t_{res,X} + V_{liq}/q} + \sum_{j=1-19} \rho_j \nu_{i,j} \tag{5.13}$$

and in terms of the flux rate of change equation (5.14) :

$$\frac{V_{liq} \cdot dX_{liq,i}}{dt} = qX_{in,i} - \frac{V_{liq} \cdot X_{liq,i}}{t_{res,X} + V_{liq}/q} + V_{liq} \sum_{j=1-19} \rho_j \nu_{i,j} \tag{5.14}$$

The second term represents the particulate mass outflow $J_{X_{out}}$:

$$J_{X_{out}} = \frac{V_{liq} \cdot X_{liq,i}}{t_{res,X} + V_{liq}/q} = \frac{V_{liq} \cdot X_{liq,i}}{SRT} \tag{5.15}$$

In the present implementation, $J_{X_{out}}$ is calculated in a different way, equation (5.16), i.e. we apply a factor f_{Xout} :

$$J_{X_{out}} = f_{Xout} \cdot q \cdot X_{liq,i} \tag{5.16}$$

Equating equation (5.15) and (5.16) results in equation (5.17) :

$$f_{Xout} = \frac{V_{liq} / q}{SRT} = \frac{HRT}{SRT} \tag{5.17}$$

Equation (5.17) defines a proportional relation between *HRT* and *SRT*. During hydraulic overloads applied to high-rate reactors, the HRT will drop and the SRT will drop proportionally rather than having a fixed difference. In terms of the solid retention time, reactors theoretically vary from a completely stirred tank reactor CSTR to a perfectly fixed bed reactor PFBR. For a CSTR f_{xout} equals one and for a PFBR f_{xout} is 0. In the original implementation the corresponding values of $t_{res,X}$ range from 0 to infinity respectively. For estimation of f_{xout}, minimum and maximum boundaries can be easily assigned making it easier to estimate.

Moreover, values > 1 can be assigned to f_{xout} to simulate biomass washout events (e.g. more biomass flocs in the effluent of a CSTR due to a defect in mixing or floating of the sludge bed in a UASB). In the present case study washout is simulated this way between day 55 and day 85. This effect can also be simulated by assigning a negative value to $t_{res,X}$ but its magnitude should be assigned carefully. If $t_{res,X}$ is assigned a value higher than the HRT, the result will be, according equation (5.14), as if biomass was added to the reactor and not washed out. This event is likely to happen when the HRT is very small during hydraulic shocks.

5.3 Results and discussions

5.3.1 Simulated dynamics

"All anaerobic processes simulated by the ADM1, both biological and physico-chemical, except perhaps disintegration and hydrolysis, are affected by either competition for substrate, inhibition by H_2S, or the acid-base reactions and gas–liquid transfer of H_2S. Because of its complexity, the sulphate reduction system was not included in the ADM1. The ADM1 is therefore incapable of modelling systems with low to medium amounts of sulphide (>0.002 M influent SOx)." (Batstone et al., 2002). In the presented experiment, the influent contains low concentrations of sulphate varying from 0.001 to 0.002 mol/l. The ADM1 simulated the experiment dynamics nicely (Figures 5.3, 5.4 and 5.5). Influent sulphates increased up to 0.003 during the high organic load applied in the last 7 days of

the experiment. At these low sulphate concentrations, a careful estimate of the cations is necessary to compensate for the presence of sulphate since the major influence will be due to its effect on the acid-base reactions. Sulphates will be reduced to S^{2-} which due to acidification in the reactor will be converted to $HS^- \leftrightarrow H_2S$ (with a lower equivalent concentration compared to the original sulphates). The equilibrium $HS^- \leftrightarrow H_2S$ will be determined by the reactor pH. Influent cations that were associated with sulphates will remain influencing the charge balance and therefore the calculations of the pH in the reactor.

It can be seen from the simulations that the results from the three IWA ADM1 implementations on different simulation platforms are the same. The dynamics to the digester are caused mainly by three perturbations and the process crash at the end of the experiment. Biomass washout from day 55 to day 85 produced the first perturbation accompanied by an increase of the hydraulic and organic overload. The second perturbation is due to two consequent doses of bicarbonate at day 68 and day 70. The third perturbation is due to a sudden increase of the OLR (shock load) during the period 117 to 125 days. From day 165 till the end of the experiment, two step increases of the OLR stopped the process.

5.3.2 Liquid phase simulation results

Figure 5.3 and Figure 5.4 show the soluble COD and the VFA results, respectively.

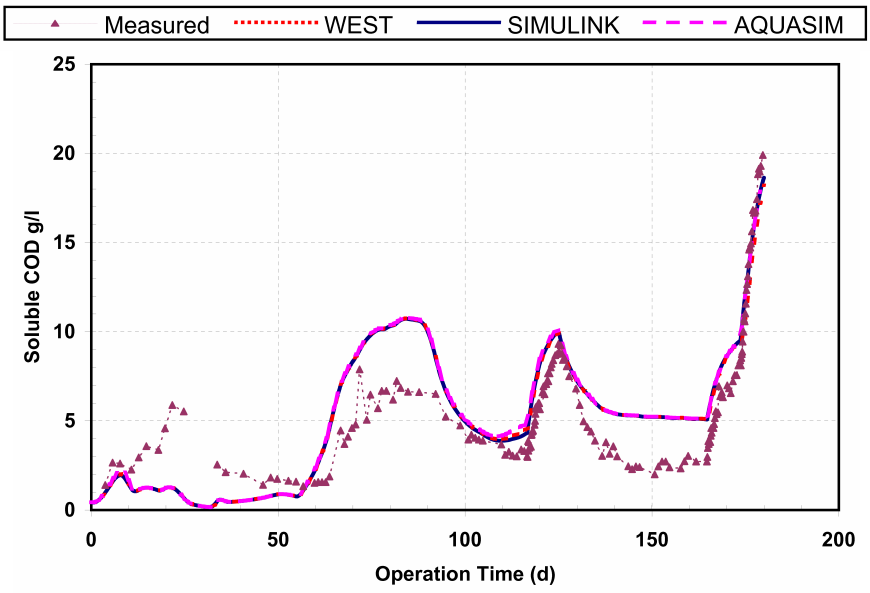

Figure 5.3 CODs results

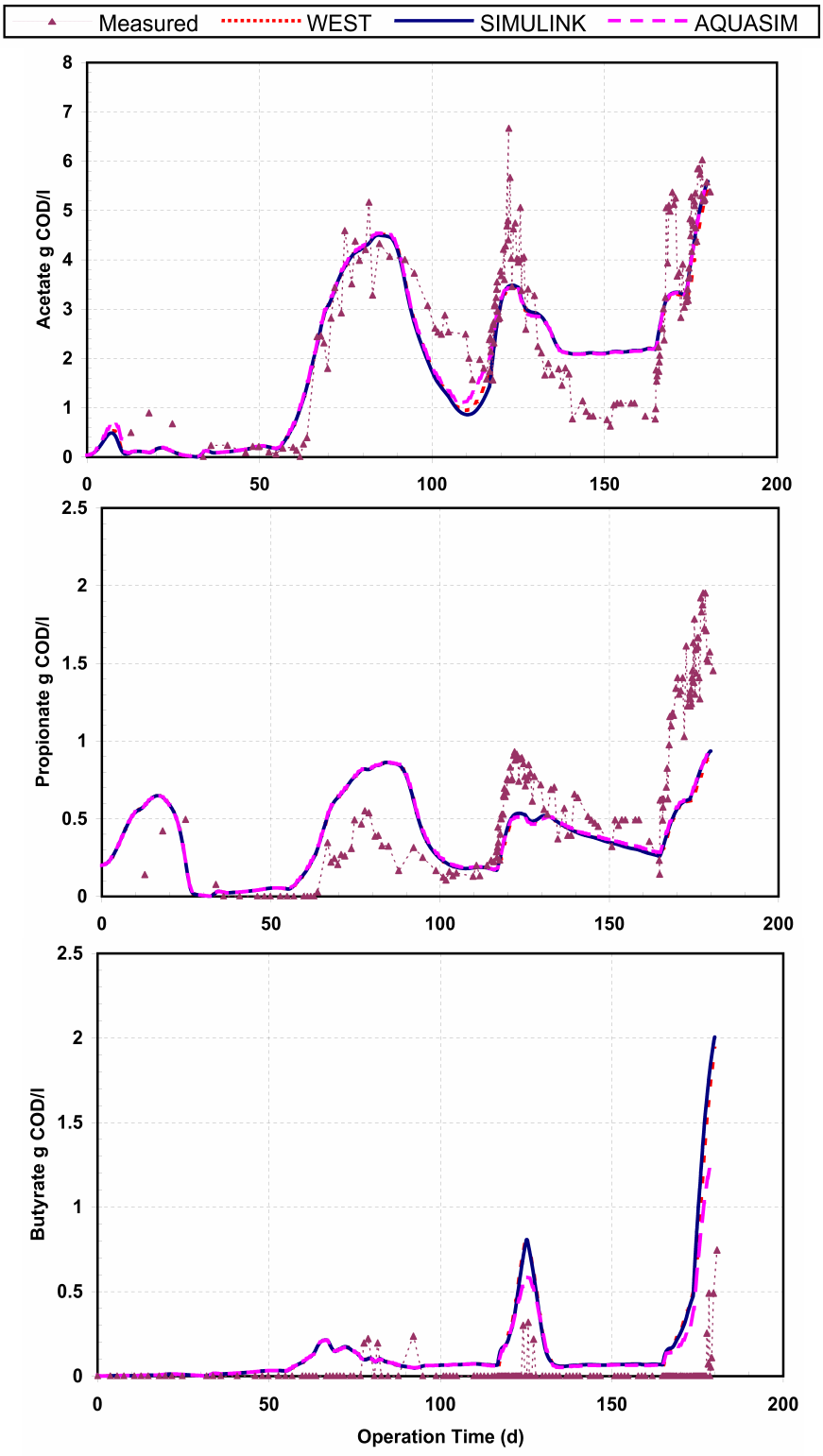

Figure 5.4 VFA results

The first and third perturbations lead to two peaks in acetate, propionate and soluble COD from day 60 to day 108 and from day 118 to day 137. Estimation of the LCFA from the extra COD in the influent produced a better fit to the first acetate peak. Indeed, according

to the model stoichiometry, the uptake of LCFA yields VFA in the form of acetate only. Similarly, the estimation of the influent amino acids enhanced the fit during the second peak and produced the corresponding peak in butyrate (similarly in valerate, not shown). According the model stoichiometry, the uptake of amino acids produces all VFAs. Especially valerate is only produced through the uptake of amino acids. Moreover, CODs is calculated by summing all soluble components considered in the model (e.g. sugar, inerts, VFAs,…etc.) and results are showing a good fit to the measurements. This confirms the validity of the extra CODs distribution in the influent. The acetate simulation results are slightly higher during the period 140 to 160. This could be related to uptake by sulphate reducing bacteria. This is not accounted for in the model. A corresponding effect will be shown in the simulation results of the gas phase.

Figure 5.5 shows the alkalinity results. The TA simulation results are calculated by summing the bicarbonate and all ionised forms of VFA (scaled to meq/l). A nice fit to the TA measurements can be observed. Thus, the TA in the reactor is mainly due to bicarbonate and VFA in contrast to the situation in the influent that is influenced by other ions.

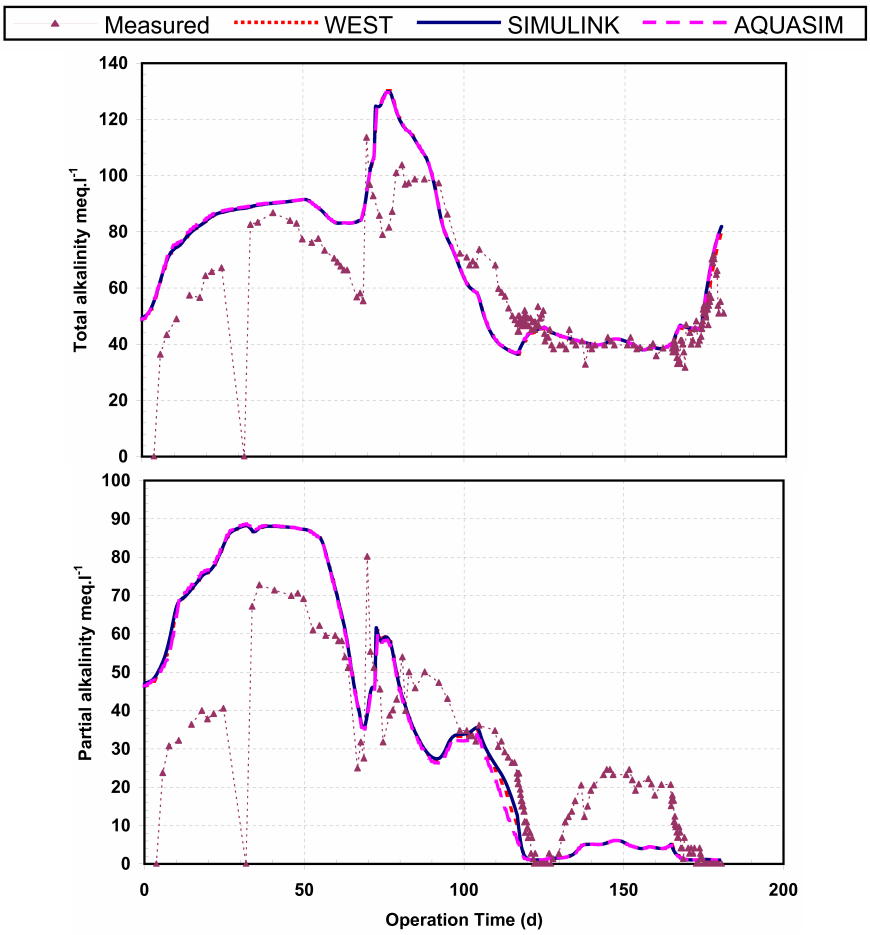

Figure 5.5 Alkalinity results

The PA results are the meq/l of the simulated bicarbonate. It corresponds with the dynamics of the PA measurements, but the simulation tends to underestimate the measurements when the VFA concentrations increase during the first and third perturbations. The PA measurements are indeed slightly influenced by the presence of VFA. Therefore, a reduction proportional to the VFA concentrations was required during the estimation of the influent inorganic carbon (see above, influent characterisation). During the period between day 140 to 160, a larger underestimation of PA is observed. In addition to the VFA influence, the HS^- buffer with a pKa of 7.05 will influence the PA simulation due to the expected sulphate reduction activity. This effect is not shown in the total alkalinity results for two reasons. First, the acetate is overestimated in the same period. Second, through the charge balance, the better estimate of the influent cations conceals the effect of sulphate reduction (change of equivalent concentration: $SO_4^{2-} \rightarrow S^{2-} \rightarrow HS^- \leftrightarrow H_2S$).

5.3.3 Gas phase and pH simulation results

Figure 5.6 shows the experimental and simulation results of pH. The pH simulation is fitting the measurements. To achieve this excellent fit, the influent cations concentration had to be adjusted according to the introduced conceptual approach. This leads to a better estimation of the inhibition factors and therefore a better simulation of the other variables. In the beginning of the experiment, however, the simulated pH is higher than the measurement but it adapts to the measurement after 40 days. This is similar for the alkalinity results. This is mainly due to the initial conditions. Better estimates of the initial values can be obtained by fitting the first 40 to 60 days of VFA measurements. However, in this experiment it was difficult since the VFA measurements were less frequent during this start-up period.

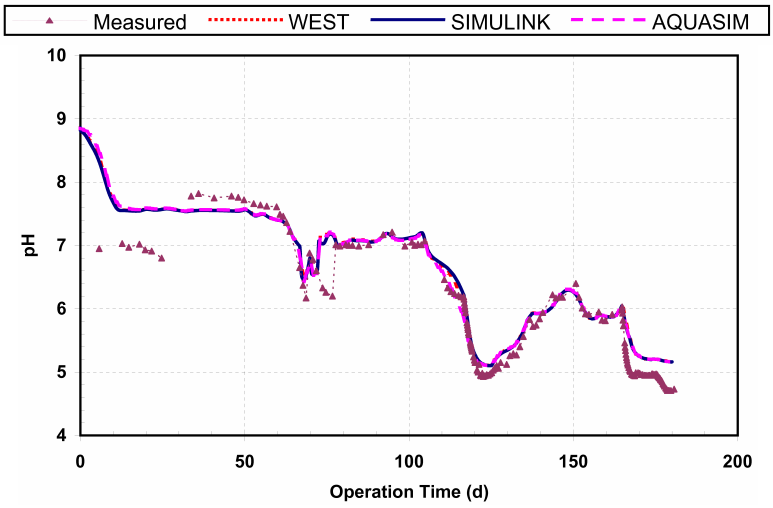

Figure 5.6 pH experimental and simulation results

The gas phase dynamics are shown in Figure 5.7. The % CH_4 is calculated from the ratio of the simulated methane partial pressure to the simulated total pressure including adjustment for the water vapour pressure. Similar to the CH_4 concentration, the %CO_2 is calculated from the partial pressure of CO_2. Although the calculation procedure of the gas transfer and flow applied in the AQUASIM implementation is different than in the SIMULINK and WEST implementations, the simulation results are almost the same. Good results are obtained during the first perturbation.

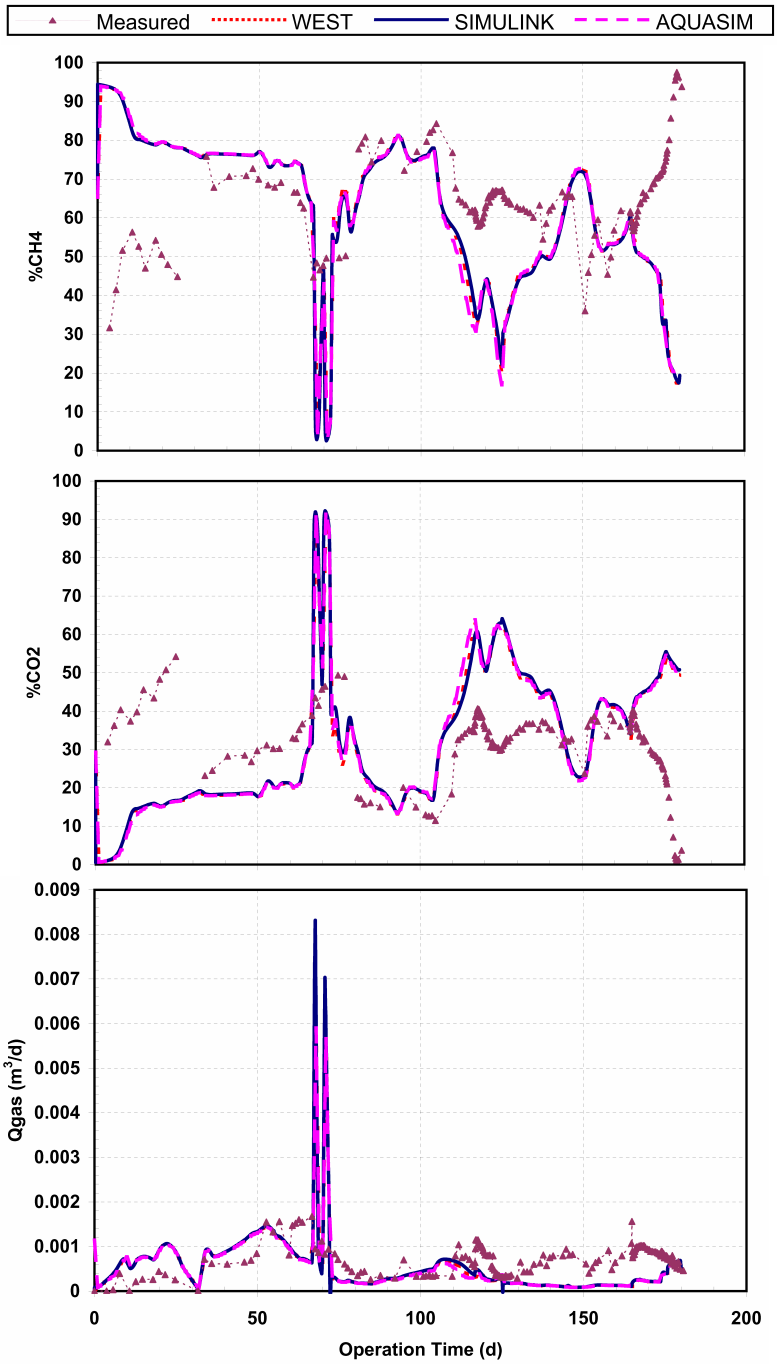

Figure 5.7 Gas phase dynamics

In the second perturbation immediate stripping of the added bicarbonate in the form of CO_2 occurred and the result was reflected in the percentage of methane and the total gas flow. However, the measured gas composition and flow are lower and thus a lower transfer rate should be considered. Another interpretation is a limitation of the gas sensor to measure such large difference in gas composition. Further study is clearly needed. After the start of the third perturbation, a worse fit to the measurements is shown. These overloads are accompanied by a drop in the pH from 6 to 5, thus leading to inhibition of all biological reactions. An increase is shown in the hydrogen concentration leading to inhibition of acetogenesis.

During the third perturbation and during the extreme overload at the end of the experiment, the simulation results show lower methane and higher CO2 concentrations while there is a decrease in the simulated gas flow. These results could be attributed to inhibition phenomena but it is more likely due to the production of other gases that influenced the gas measurement. During overload, hydrogen sulphide is produced in addition to the produced hydrogen. Higher concentrations of sulphates are applied to the reactor (>0.002 mole/l). Hydrogen sulphide and hydrogen were not considered in the measurement method of the gas composition while it will be accounted for in the gas flow measurement. This indeed can contribute to the difference.

5.4 Conclusions

Information about the wastewater composition and knowledge of the upstream industrial processes was used successfully to extend the concise set of practical measurement and achieve a detailed characterisation of the influent wastewater. This detailed characterisation of the influent produced good simulation results using a default set of parameters that was selected for a different type of waste. The detailed structure of the IWA ADM1 model helped to distribute the COD measurements to expected components leading to better simulation results. Also, the ADM1 model was used to enhance the estimation of the influent cation concentration. This was necessary to achieve good simulation results in the presence of unmeasured anions and sulphates. The increase of the sulphate concentration in the influent to levels higher than 0.002 mole/l and the drop of the pH caused a disturbance to the gas measurements that may be due to hydrogen sulphide production. A model extension might be necessary to describe this phenomenon.

A change was made to the method to describe the SRT in proportion to the HRT. It uses a parameter with known bound for high rate anaerobic reactors, therefore leading to better parameter identifiability. Moreover, the newly introduced parameter can be used to detect/estimate the washout of biomass from the reactor.

Chapter 6

Extension of ADM1 with irreversible toxicity: application to cyanide

Abstract

In this chapter, the IWA Anaerobic Digestion Model no.1 (ADM1) is updated to study and simulate the effect of irreversible toxicity on the anaerobic digestion process. The irreversible toxicant studied is cyanide. Inhibition of cyanide to acetate uptake is modelled by introducing two populations of aceticlastic methanogens. The model is also extended with the hydrolytic pathway for cyanide degradation. The uptake of cyanide hydrolysis end products is modelled to be achieved by hydrogenotrophic methanogens. The chemical equilibrium reactions of ADM1 are extended by the cyanide and phosphorous related equilibria to correctly simulate reactor pH. To help the simulation of the reactor pH, a method that estimates the cation concentration in the influent to high rate reactors is updated. An experiment using 3 lab-scale Upflow Anaerobic Sludge Bed (UASB) is used to achieve a preliminary estimate of the introduced model parameters and validate the model.

CHAPTER 6

6.1 Introduction

Cyanide is produced in many different industrial wastewaters and it is harmful to the environment if disposed without treatment (Gijzen et al. 2000, Raybuck, 1992). The treatment of cyanide wastewaters from mining operations, electroplating processes, coal gasification and from other industries is attracting public and regulatory attention (Bozzi et al., 2004). Also, production of cassava starch from cassava roots is an agricultural industry that produces cyanide-rich wastewater. Khoa (1998) reported an average concentration of 11 – 32 mg CN/l in cassava wastewater in Vietnam. Cassava crop production and starch industry is a wide agricultural and industrial sector in the tropics. Indonesia produces 15 – 16 million tons of cassava and the production of cassava starch from this crop is 1.2 – 1.3 million tonnes per year (Widyatmika, 2004).

Many industrial wastewaters are rich in cyanide but low in biodegradable substrate. For the treatment of these wastewaters, aerobic microbiological degradation of cyanide has been evolving rapidly. Akcil et al. (2003) demonstrated that *Pseudomonas sp* degrade cyanide into formate and ammonia. For the removal of ammonia, nitrification is applied and since it is carried out by autotrophic bacteria, no biodegradable soluble substrate is needed as a carbon source. Therefore, aerobic treatment is successfully applied to treat low COD wastewaters such as mining effluents.

However, cassava wastewater is rich in biodegradable substrates, mainly in the form of carbohydrates. Therefore, aerobic treatment will be less efficient due to the toxicity of cyanide towards heterotrophs and the excess of oxygen for COD removal. Recently, high rate anaerobic reactors have been tested for the treatment of cassava and starch processing wastewaters (Annachhatre and Amornkaew 2001; Gijzen et al. 2000; Siller and Winter, 1998). All come to the conclusion that the inhibitory effects of cyanide to the anaerobic process were temporary and reversible if a sufficiently long acclimatisation period is allowed. However, at first sight, these practical results seem to contradict with the theoretical classification of cyanide as biocidal inhibitor, i.e. a reactive toxicant whose toxicity is normally irreversible, in the IWA Anaerobic Digestion Model no.1 (ADM1) report (Batstone et al., 2002).

Therefore to clarify this contradiction, the work presented in this chapter is aimed to study the effect of cyanide, its degradation in anaerobic treatment, extend the ADM1 model with cyanide kinetics and validate the model with experimentation. The experiment uses 3 UASB lab scale reactors with sludge adapted to cyanide to test and model the response of the process to different levels of cyanide concentration. For the first time, the different

pathways suggested in literature for cyanide toxicity and inhibition to aceticlastic methanogens and cyanide anaerobic degradation have been formulated in a proposed scenario that is likely to resolve the contradiction between the theoretical classification of the cyanide toxicity and the achieved practical results. The IWA ADM1 is extended with the proposed scenario. The performed experiment has been used to achieve the first estimates of the introduced parameters and validate the extended model predictions.

6.2 Methods

6.2.1 Lab-setup and wastewater

A lab-experiment was done at the International Institute for Infrastructural, Hydraulic and Environmental Engineering (UNESCO-IHE), Delft, The Netherlands. Three laboratory scale UASB reactors (named R1, R2, R3), with 3 L effective volume each, were used to treat cassava starch wastewater with a cyanide concentration of up to 25 mgCN/L. Figure 6.1 shows the schematic layout of one reactor.

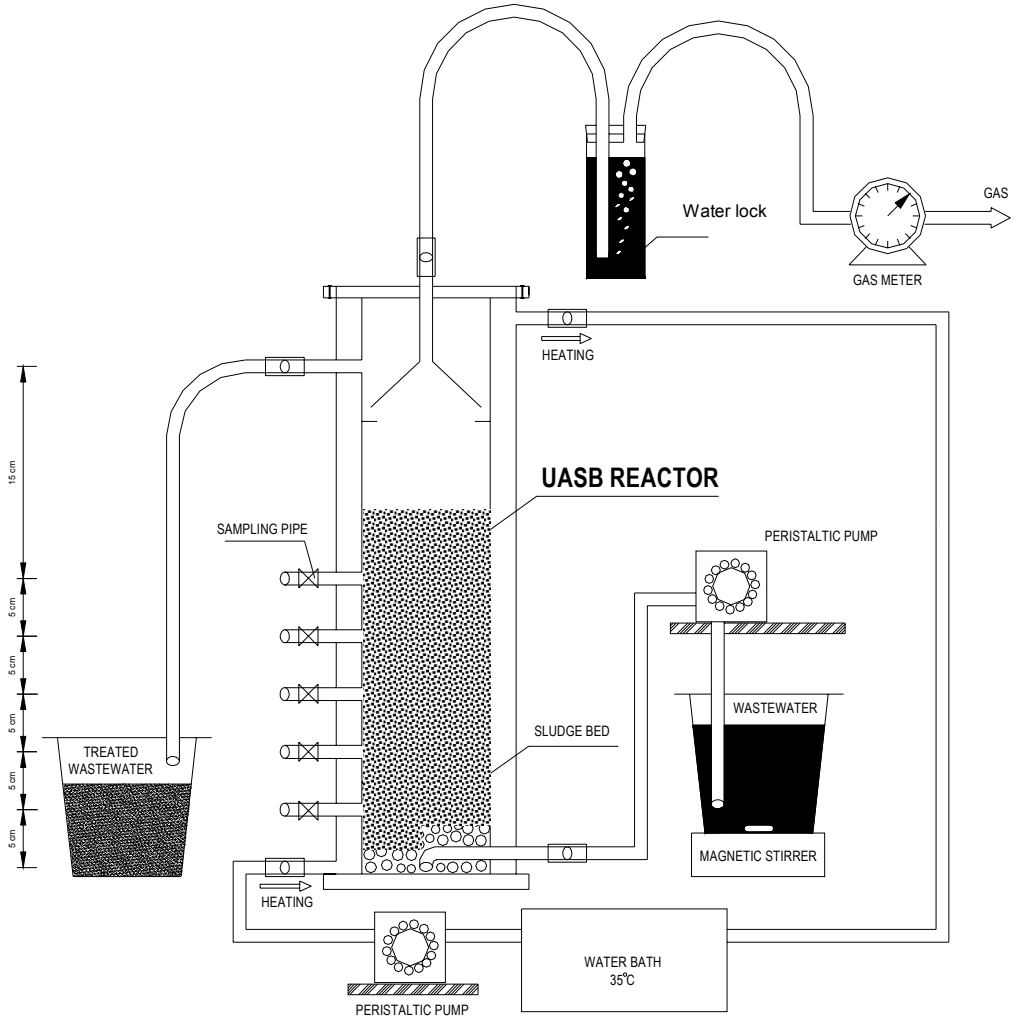

Figure 6.1: layout of one of the experiment UASB reactors

The wastewater was prepared from commercially grinded cassava and only the settled supernatant was used as reactor's influent. The influent wastewater fractions comprise six components: carbohydrates, protein, lipids, acetate, soluble inert and particulate inert COD. Acetate was the only VFA found in the influent wastewater. The average concentration of the influent acetate is 9.5% of the total influent COD. On average, only 0.4% of the influent COD is in the form of protein. Measurements of the acetate and protein were conducted randomly from several influent batches. Lipid content in the influent was not measured but it is predicted to be low according the raw cassava composition and assumed to be 1% of the total influent COD. Particulate and soluble inert fractions in the influent were adjusted based on the effluent COD_s and COD_t. The supernatant already contained a cyanide concentration of 1.5 – 5 mgCN/L. KCN was used as an additional source of cyanide. Carbonate and phosphate buffers and NaOH were added to the wastewater for pH regulation. All three reactors were seeded with granular sludge from an industrial UASB reactor of a potato chip industry that adapted to the new wastewater in 80 to 90 days. The Hydraulic Retention Time (HRT) in the three reactors was maintained at 12 hours through the whole experiment. Temperature in the reactors was maintained at 35^0C using a double-jacketed reactor. The organic load per unit of volume of reactors ranged from 3.6 to 11.1 g COD/L.day.

6.2.2 Experiment protocol

The adaptation during 80 - 90 days was obtained by a stepwise increase in organic load without any addition of external cyanide. By the end of the adaptation period, the three reactors achieved COD removal efficiencies higher than 90%. The cyanide concentration to R3 was increased to 5 mg CN/L on day 99. Then, from day 160, the cyanide load was gradually increased till 15 mg CN/L. R2 received an additional cyanide concentration of 20 mg CN/L starting from day 160. R1 was kept as a control reactor without any addition of external cyanide.

6.2.3 Measurements

Measurements of flow, COD, VFA, biogas flow, methane content, ammonium and pH were conducted. Free CN was measured on a daily basis starting from the external addition of KCN. Bicarbonate alkalinity was estimated on a daily basis from the last phase of the experiment starting from day 161 onwards. Flow was measured by measuring the effluent volume over one day. COD measurements are based on the closed reflux method by digestion with $K_2Cr_2O_7$ and by analysing the concentration of green Cr^{3+} photometrically. VFA is measured using gas chromatography (GC). Biogas flow is measured using a wet

test gas meter. The methane content in the biogas is measured using the GC method, by injecting a small gas sample to the gas chromatograph equipped with a FID detector. This detector was only capable of measuring the content of CH_4 and H_2. It is assumed that the amount of hydrogen in the biogas is negligible compared to the amount of methane. Therefore the biogas is assumed to only consist of CH_4 and CO_2. The gas chromatograph was calibrated first for methane measurement using pure methane gas. Ammonium was measured by a standard colorimetric technique as NH_4^+- N. Bicarbonate alkalinity is approximately estimated by titrating a filtered sample to pH 4.4. Free cyanide in the samples was measured using Dr Lange field kit (LCK 315 for free cyanide) after applying the necessary dilution. pH is measured immediately after collecting the sample and without stirring the sample to prevent the influence of CO_2 stripping. Total suspended solids and volatile suspended solids were occasionally measured according section 2540G of the Standard Methods for the Examination of Water and Wastewater (1992).

6.2.4 ADM1 updates

Two simulation platforms: WEST and AQUASIM were used for simulation. Two identical implementations of standard ADM1 on each platform that have been validated with dynamic experiment in Chapter 5 were extended with the following updates.

6.2.4.1 Modelling UASB high solids retention

The UASB is classified as a high rate reactor because of the high Solids Retention Time (SRT) compared to the Hydraulic Retention Time (HRT), i.e. leading to higher biomass concentrations and therefore more activity. A fraction parameter f_{Xout} is used as the ratio of the particulates leaving the reactor to the total particulates in the reactor. It can be proven that this ratio is also equivalent to the HRT to SRT ratio. The parameter f_{Xout} has known boundaries ranging from 1 to 0 for CSTR and PFBR (Perfectly Fixed Bed Reactor) and is therefore better identifiable compared to the implementation of additional solids retention that has an upper bound of infinity. In WEST the implementation of f_{Xout} is used directly to reduce the particulates outfluxes. In AQUASIM it is not possible to apply it directly since the fluxes are calculated by the programme according to the definitions of links between compartments. Therefore, the liquid phase was designed to consist of two compartments: a large compartment that is having a volume almost equal to the liquid volume in the real reactor and a very small compartment that is linked to the main compartment by advective link. To apply the higher SRT, the outflow of all particulates is returned to the first compartment by a factor (1- f_{Xout}).

6.2.4.2 *Extension of ADM1 with cyanide*

Figure 6.2 shows the updated pathway of ADM1 for the cyanide kinetics. Kinetics are suggested according observations and conclusions found in literature described in the following subsections. The update to the ADM1 Petersen matrix is listed in Table 6-1.

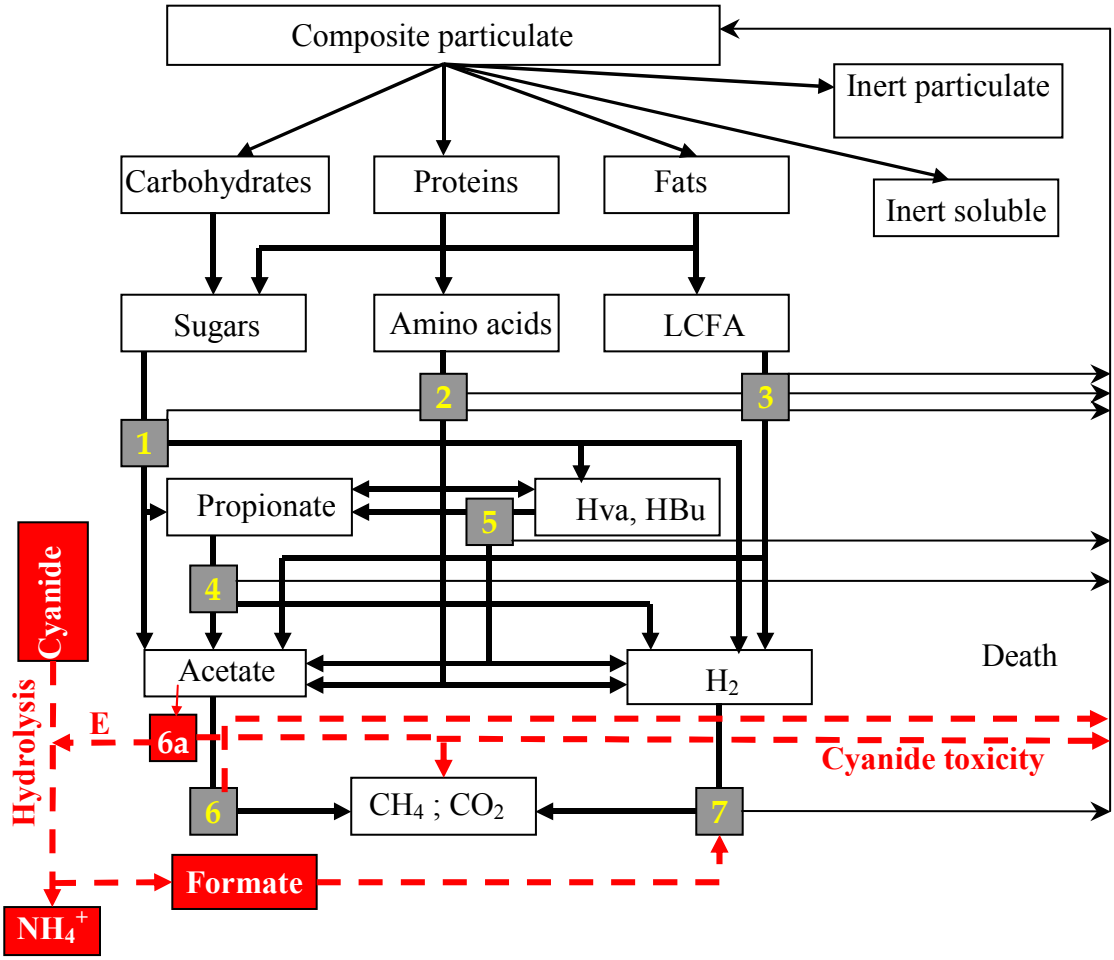

Figure 6.2: Biochemical processes in the model: (1) acidogenesis from sugars; (2) acidogenesis from amino acids; (3) acetogenesis from LCFA; (4) acetogenesis from propionate; (5) acetogenesis from butyrate and valerate; (6) unadapted aceticlastic methanogenesis; (6a) adapted aceticlastic methanogenesis and cyanide hydrolysis; (7) hydrogenotropic methanogenesis. Dashed lines represents the extension from ADM1

Irreversible toxicity is modelled as a decay factor to the acetate degraders' decay processes. Irreversible enzyme inhibition is modelled as an inhibition factor to acetate uptake processes. The observed reversible effect after acclimatisation of sludge is modelled by a population shift between two acetate degraders species that have different tolerance to cyanide toxicity. Cyanide degradation is modelled as enzymatic hydrolysis of cyanide to formate and ammonia, in proportion to the concentration of the most cyanide tolerant acetate degraders. Another reaction is added for methanogenesis from formate.

Table 6-1 ADM1 updated biological reactions matrix

Component → i		7	9	10	11	12a	12b	13	22	22a	23	Rate (ρ_j, kg COD.m^{-3}.d^{-1})
j	Process ↓	S_{ac}	S_{ch4}	S_{IC}	S_{IN}	S_{cya}	S_{fo}	X_c	X_{ac}	$X_{ac,cya}$	X_{h2}	
4a	Hydrolysis of cyanide				1	-1	16					$k_{hyd,cya} \cdot X_{ac,cya} \cdot S_{cya}$
11	Uptake of Acetate	-1	$(1-Y_{ac})$	$-\sum_{i=1-9,11-24} C_i \nu_{i,11}$	$-(Y_{ac}) \cdot N_{bac}$				Y_{ac}			$k_{m,ac} \cdot \frac{S_{ac}}{K_S + S_{ac}} \cdot X_{ac} \cdot I_4$
11a	Uptake of Acetate by cyanide tolerant methanogens	-1	$(1-Y_{ac,cya})$	$-\sum_{i=1-9,11-24} C_i \nu_{i,11}$	$-(Y_{ac,cya}) \cdot N_{bac}$					$Y_{ac,cya}$		$k_{m,ac,cya} \cdot \frac{S_{ac}}{K_{S,cya} + S_{ac}} \cdot X_{ac,cya} \cdot I_4$
12	Uptake of Formate		$(1-Y_{X_{h2},fo})$	$-\sum_{i=1-9,11-24} C_i \nu_{i,12}$	$-(Y_{X_{h2},fo}) \cdot N_{bac}$		-1				$Y_{X_{h2},fo}$	$k_{m,fo} \cdot \frac{S_{fo}}{K_{S,fo} + S_{fo}} \cdot X_{h2} \cdot I_3$
18	Decay of X_{ac}							1	-1			$k_{dec,Xac} \cdot X_{ac} \cdot I_{dec,Xac}$
18a	Decay of $X_{ac,cya}$							1		-1		$k_{dec,Xac,cya} \cdot X_{ac,cya} \cdot I_{dec,Xac,cya}$
		Total acetate (kg COD·m^{-3})	Methane gas (kg COD·m^{-3})	Inorganic Carbon (k-mole C·m^{-3})	Inorganic nitrogen (k-mole N·m^{-3})	Cyanide concentration (k-mole N·m^{-3})	Formate concentration (kg COD·m^{-3})	Composites (kg COD·m^{-3})	Acetate degraders (kg COD·m^{-3})	Acetate degraders (kg COD·m^{-3})	Hydrogen degraders (kg COD·m^{-3})	Inhibition factors: $I_3 = I_{pH,Xac} \cdot I_{IN,\lim} \cdot I_{NH3,Xac}$ $I_{cya} = \frac{K_{I,cya}}{K_{I,cya} + S_{cya}}$ $I_4 = I_3 \cdot I_{cya}$ decay factors: $I_{dec,Xac} = \frac{S_{cya}}{K_{I_{cya},Xac}} + 1$ $I_{dec,Xac,cya} = \frac{S_{cya}}{K_{I_{cya},Xac,cya}} + 1$

6.2.4.3 Cyanide irreversible toxicity and inhibition

Generally, cyanide is classified as an irreversible enzyme inhibitor and therefore considered toxic (Mathews et al., 2000; Speece, 1996). Applications of anaerobic digestion for the treatment of cassava wastewaters show that, among the anaerobic processes, methanogenesis is the most sensitive to cyanide toxicity (Annachhatre and Amornkaew, 2001; Cuzin and Labat, 1992; Gijzen et al., 2000; Siller and Winter, 1998). In Gijzen et al. (2000), sludge activity measurements demonstrated that the effect of CN-inhibition on methanogenic activity was more pronounced for aceticlastic than for hydrogenotrophic methanogens.

Therefore, in this chapter, modelling the toxicity and inhibition of cyanide will only consider the acetate degraders. Irreversible toxicity of cyanide is applied as a decay factor that is calculated as a function of the cyanide concentration, increasing the decay rate with the increase of the cyanide concentration, according to equation (6.1).

$$I_{dec,Xac,cya} = 1 + \frac{S_{cya}}{K_{I_{cya,Xac}}} \tag{6.1}$$

The inhibition of cyanide is modelled as the term shown in equation (6.2).

$$I_{cya} = \frac{K_{I,cya}}{K_{I,cya} + S_{cya}} \tag{6.2}$$

The inhibition term is applied to the ADM1 acetate uptake kinetics so that it decreases the acetate uptake with an increase in cyanide concentration. Cyanide inhibition occurs by blocking the active site of enzymes and therefore limits the substrate uptake (Mathews et al., 2000).

6.2.4.4 Reversibility and acclimatisation

Despite of the irreversible toxicity of cyanide, a reversible effect to methanogenesis has also been observed in high-rate anaerobic reactors after acclimatisation (Annachhatre and Amornkaew, 2001; Cuzin and Labat, 1992; Gijzen et al., 2000; Siller and Winter, 1998). The reversible effect can be explained by a population shift in the aceticlastic methanogens. Methanogenic species types and their relative population levels in reactor biomass depend on wastewater characteristics as well as on the maintained operational/environmental conditions (Jawed and Tare, 1999; Novaes 1986). Within the order *Methanosarcinales*, there are two acetate degrading genera; *Methanosaeta* (within

the order *Methanosaetaceae*), and *Methanosarcina* (within the order *Methanosarcinaceae*). The two genera have different acetate affinity thresholds, and within each genus, member species have different tolerances to temperature, pH, and, importantly in this context, toxic compounds. Therefore, it is possible to have a shift from one species of *Methanosaeta* to another. *Methanosarcina* is generally regarded as being more tolerant to toxic compounds than *Methanosaeta*. However, Fang and Zhang (2004) found in an UASB treating wastewaters with a high concentration of phenol, that also acts as an irreversible toxicant, that the majority of aceticlastic methanogens were *Methanosaeta*. This could be explained by their different morphology and granulation properties, which may mean that the different genera are exposed to different toxicant levels. In general, it can be accepted that every species has a different tolerance to toxicants, either because of the resistance of the genus or due to its aggregation and morphology properties. In the present experiment the bacterial population was not examined in view of identifying the species that is most dominant.

However, in the model extension two populations of acetate degraders were considered to model the observed reversible toxicity and acclimatisation effects. One acetate degraders population is considered to be more tolerant to cyanide toxicity $X_{ac,cya}$ while the other population X_{ac} is less tolerant. The different levels of tolerance to cyanide are effected through the decay factor. $X_{ac,cya}$ will have a lower decay factor compared to X_{ac}. This is achieved by having two $K_{I_{cya,Xac}}$ parameters. Namely, $K_{I_{cya,Xac}}$ is assigned to the X_{ac} decay and $K_{I_{cya,Xac,cya}}$ is assigned to $X_{ac,cya}$ decay. During parameter estimation $K_{I_{cya,Xac,cya}}$ is constrained to have a higher value than $K_{I_{cya,Xac}}$.

6.2.4.5 Enzymatic hydrolysis of cyanide

Fallon et al. (1991) observed a strong correlation between microbial activity and cyanide removal in anaerobic digestion and suggested that the removal mechanism depends on microbial activity. They evaluated different anaerobic enrichment cultures in the presence of cyanide. All yielded positive cultures but it was not possible to find organism(s) responsible of cyanide metabolism. Cyanide hydrolysis to formate and ammonia is a thermodynamically favourable reaction, $\Delta G^{\circ\prime}$=-15.6 kJ. Fallon (1992) reported that the cyanide transformation is analogous to the hydrolysis pathways of aerobes. Two pathways were suggested. One pathway leads directly to formate and ammonia while the other includes some intermediates that end rapidly into the same products, reactions (6.3) and(6.4):

$$HCN + 2H_2O \rightarrow HCOOH + NH_3 \qquad (6.3)$$

$$HCN + H_2O \rightarrow HCONH_2 + H_2O \rightarrow HCOOH + NH_3 \qquad (6.4)$$

These hydrolytic reactions are achieved in aerobic systems by enzymes called cyanidases (Raybuck, 1992). Aerobic degradation is carried out by heterotrophs such as *Pseudomonas* that can grow on methanol and acetate as carbon source. Therefore, analogous to aerobic systems, cyanide hydrolysis is modelled as function of aceticlastic methanogens but related to the most tolerant group only, $X_{ac,cya}$. The hydrolysis kinetics are given in equation (6.5) and the stoichiometry is modelled according reaction (6.3). This requires the addition of formate to the ADM1 model components. Equation (6.5) assumes that the cyanide concentration is low compared to the enzyme affinity for cyanide (Mathews et al., 2000). For model simplification, it is assumed that the enzyme concentration is proportional to the biomass concentration. Therefore, the hydrolytic enzyme efficiency $K_{hyd,cya}$ in equation (6.5) is specific to the aceticlastic methanogens and not to the enzyme concentration. $K_{hyd,cya}$ is considered as a second order rate constant for a reaction between the enzymes (presented by the biomass concentration) and cyanide.

$$\rho_{\text{hyd,cya}} = k_{hyd,cya} \cdot X_{ac,cya} \cdot S_{cya} \qquad (6.5)$$

6.2.4.6 Uptake of cyanide hydrolysis products

Ammonium will be a source of nitrogen for growth. Fallon (1992) suggested that methanogenesis could play a role of removal of the end product of cyanide hydrolysis so that the cyanide hydrolysis remains thermodynamically favourable. Two reactions, (6.6) and(6.7), are possible for formate conversion.

$$HCOO^- + H_2O \rightarrow H_2 + HCO_3^- \quad , \Delta G^{\circ'} = 1.3 \text{ kJ} \qquad (6.6)$$

$$4HCOOH \rightarrow CH4 + 3\ CO_2 + 2H_2O \quad , \Delta G^{\circ'} = -281 \text{ kJ} \qquad (6.7)$$

Reaction (6.6) will proceed if the product concentration is zero (Hoh and Cord-Ruwisch, 1996). This is only possible if the hydrogenotrophic methanogens are sufficiently active to maintain a low hydrogen partial pressure. This pathway is not further considered here. Reaction (6.7) is the direct methanogenesis from formate. All hydrogenotrophic methanogens are capable of utilising formate as substrate for metabolism. Also, among the aceticlastic methanogens, *Methanosarcina* is capable of utilising formate for methanogenesis. However, uptake of acetate by *Methanosarcina* is inhibited by low

concentrations of cyanide but growth and methanogenesis on H_2 and CO_2 or methanol is not inhibited (Smith et al., 1985). Therefore, *Methanosarcina* growth and methanogenesis on formate might not be inhibited by cyanide too. In the present modelling, both pathways suggested for methanogenesis from formate have been tried. No significant difference between both pathways was observed due to the low concentration of formate. Therefore, the uptake of formate by hydrogenotrophic methanogens will be used as the main pathway since it is not proven that *Methanosarcina* will become dominating. The kinetics used was in a similar form as the ADM1 acetate uptake kinetics but as function of hydrogenotrophic biomass since it is a heterotrophic uptake (metabolism of soluble carbon source), i.e. inhibition terms to formate uptake are considered similar to the acetate uptake.

6.2.4.7 Equilibrium and pH calculation

The system of equilibrium equations for pH calculation is listed in Table 6-2 and Table 6-3. Cyanide is a buffering component and therefore it should be considered in the chemical equilibrium equations for pH calculation. Also, phosphorus should be considered since it was added during the experiment to buffer the reactor in the normal pH range. The cyanide ion concentration is calculated as a function of its total concentration in a way similar to other monoprotic buffers such as VFA's. Phosphorus is a triprotic buffer and for generality its three ions $H_2PO_4^-, HPO_4^{2-}, PO_4^{3-}$ should be considered in the chemical equilibria and the pH calculation. The concentration of each ion in the phosphorous buffering system can be calculated as function of the total phosphorus concentration. However, the functions get more complex compared to the ones only involving monoprotic buffers. However, the equations are still systematic. In WEST, a general pH calculation procedure has been developed for such systems.

The general pH calculation calculates the chemical equilibrium and the involved ions according their buffer system definitions: monoprotic, diprotic or triprotic. Therefore, the carbon system was considered as diprotic buffer in the updated WEST ADM1 model. The system of equations that is generated recursively in WEST was implemented directly in AQUASIM as a set of equilibrium processes, according the buffer components that are present in the current experiment. However, it should be noted that it was not possible to include the carbon system as a diprotic buffer equilibrium in AQUASIM. The reason is probably that the carbon system is also involved in different reactions, i.e. physical gas-liquid transfer reactions and biological reactions. The different rates of reactions created a computational problem for the AQUASIM solver. Therefore, in AQUASIM, the carbon system is implemented dynamically as a bicarbonate monoprotic buffer (Table 6-3).

Table 6-2 Chemical equilibrium equations for pH calculation

Equation	Unknown Algebraic
$S_{H^+} + S_{cat} + S_{nh4^+} - S_{an} - S_{oh^-} - S_{hco3^-} - \frac{S_{ac^-}}{64} - \frac{S_{pro^-}}{112} - \frac{S_{bu^-}}{160} - \frac{S_{va^-}}{208} - S_{h2po4^-} - 2S_{hpo4^{2-}} - 3S_{po4^{3-}} - S_{CN^-} = 0$	S_{H^+}
$S_{OH^-} - \frac{K_w}{S_{H^+}} = 0$	S_{OH^-}
$S_{va^-} - \frac{K_{a,va} S_{va,total}}{K_{a,va} + S_{H^+}} = 0$	S_{va^-}
$S_{Bu^-} - \frac{K_{a,bu} S_{bu,total}}{K_{a,bu} + S_{H^+}} = 0$	S_{Bu^-}
$S_{\Pr o^-} - \frac{K_{a,pro} S_{pro,total}}{K_{a,pro} + S_{H^+}} = 0$	$S_{\Pr o^-}$
$S_{Ac^-} - \frac{K_{a,ac} S_{ac,total}}{K_{a,ac} + S_{H^+}} = 0$	S_{Ac^-}
$S_{cya^-} - \frac{K_{a,cya} S_{cya,total}}{K_{a,cya} + S_{H^+}} = 0$	S_{cya^-}
$S_{h2po4^-} - \frac{K_{a,h3po4} S_{IP} S_{H^+}^2}{A} = 0$	S_{h2po4^-}
$S_{hpo4^{2-}} - \frac{K_{a,h3po4} S_{IP} S_{H^+} K_{a,h2po4^-}}{A} = 0$	$S_{hpo4^{2-}}$
$S_{po4^{3-}} - \frac{K_{a,h3po4} S_{IP} K_{a,h2po4^-} K_{a,hpo4^{2-}}}{A} = 0$	$S_{po4^{3-}}$
$S_{IP} - S_{h3po4} - S_{h2po4^-} - S_{hpo4^{2-}} - S_{po4^{3-}} = 0$	S_{h3po4}
$S_{NH_4^+} - \frac{S_{H^+} S_{IN}}{K_{a,NH_4} + S_{H^+}} = 0$	$S_{NH_4^+}$
$S_{IN} - S_{NH_3} - S_{NH_4^+} = 0$	S_{NH_3}

$$A = S_{H^+}^3 + K_{a,h3po4} S_{H^+}^2 + K_{a,h3po4} K_{a,h2po4^-} S_{H^+} + K_{a,h3po4} K_{a,h2po4^-} K_{a,hpo4^{2-}}$$

Table 6-3 Dynamic calculation for the carbon buffering system equilibrium (as bicarbonate only)

i	Component í	S_{co2}	S_{hco3-}	Rate (ρ_i, kmole.m^{-3}.d^{-1})
Process	Inorganic carbon acid base	1	-1	$k_{B,co2}(S_{hco3^-} \cdot S_{H^+} - K_{a,co2} S_{co2})$
		Carbon dioxide (kmoleC/m^3)	Bicarbonate (kmoleC/m^3)	$k_{B,CO2}$: rate coefficient for the base to acid reaction. May be optimised or initially set to 10^{-8}M^{-1} d^{-1}

6.2.5 Estimation of the influent cation concentration

Based on partial and total alkalinity measurements, the cation concentration can be estimated and further refined by fitting the pH in the reactor. However, in the present experiment the alkalinity measurements were not frequent enough to allow this estimation. Therefore, the method was adapted by first estimating the VFA fraction (as Acetate) in the acidogenic compartment, as explained below.

It can be assumed that a fraction of the input X_{ch} will hydrolyse in a small acidogenic compartment located at the reactor inlet. The fraction of acetate in the reactor inlet was estimated by fitting the approximate steady state in the period 75 to 95 days that was achieved after adaptation of the inoculated biomass and assuming the reactor pH is constant at the observed value of 7.25 during this period. This fraction is used to estimate the acetate profile and hence calculate the cation influent concentration profile by performing a charge balance of the influent. The estimated cation profile was further filtered using a Savitzky-Golay filter (Orfanidis, 1996). Filtering was done using a 3rd order polynomial and a frame width of 21 days. The estimated profile was then checked and found to agree with the staggered alkalinity measurements.

Note that for further simulation, the measured feed characteristics were used with an average acetate fraction of the influent wastewater of 9.5%.

6.3 Results and discussions

6.3.1 Achieved treatment efficiencies

After the acclimatisation period, the three reactors achieved high treatment efficiencies for the rest of the experiment. All reactors had a satisfactory COD removal efficiency of 92% in average. The methane content of the biogas was slightly above 75% in average for the three reactors. The average cyanide removal efficiency was ranging between 70% and 80%. In situ methanogenic activity tests also gave similar results for the three reactors.

6.3.2 Model calibration

Values were assumed to the newly introduced model parameters and further enhanced by trial and error simulations. Initial values of the model state variables were obtained by simulating the average feed to the reactor for 1000 days. The solids retention time (SRT) of the reactor was found around 80 days, by fitting the simulated Mixed Liquor Volatile Suspended Solids MLVSS with the measured MLVSS of the R2 experiment by accordingly adjusting the f_{Xout} parameter. Sensitivity analyses were performed for the newly introduced parameters and the default acetate-related parameters: maximum specific

uptake rates: $k_{m,ac}$, $k_{m,ac,cya}$, $k_{m,fo}$; half saturation values: $k_{s,ac}$, $k_{s,ac,cya}$, $k_{s,fo}$; decay factors: $K_{I,cya,Xac}$ $K_{I,cya,Xac,cya}$; inhibition factor to uptake $K_{I,cya}$; decay parameters: $k_{dec,Xac}$, $k_{dec,Xac,cya}$; yield parameters: Y_{Xac}, $Y_{Xac,cya}$, $Y_{X_{h2},fo}$; specific efficiency of the cyanide hydrolytic enzyme: $K_{hyd,cya}$.

$Y_{Xac,cya}$, $k_{dec,Xac,cya}$ and $K_{I,cya,Xac,cya}$ (set 1) were found to be the most influential parameters for almost all model variables. Acetate, cyanide, gas components and pH were also sensitive to the other parameters. Especially cyanide is sensitive to $K_{hyd,cya}$ and acetate is sensitive to $K_{I,cya}$ with a higher sensitivity during cyanide overloads. Using the R2 data set and according the sensitivity results, four model calibration runs were performed to obtain the preliminary estimates of the listed parameters and initial acetate degraders' concentrations, using the simplex algorithm (Nelder and Mead, 1965). The preliminary estimates of the parameters are listed in Table 6-4.

Table 6-4 ***Parameters estimated during calibration***

Parameters	Unit	Definition	Estimates
$k_{m,ac}$	d^{-1}	Monod maximum specific uptake rate of acetate by normal acetate degraders	8
$k_{m,ac,cya}$	d^{-1}	Monod maximum specific uptake rate of acetate by cyanide tolerant acetate degraders	11.88
$k_{m,fo}$	d^{-1}	Monod maximum specific uptake rate of formate by hydrogenotrophic methanogens	6
$k_{s,ac}$	kg COD·m^{-3}	half saturation constant of acetate uptake by normal acetate degraders	0.15
$k_{s,ac,cya}$	kg COD·m^{-3}	half saturation constant of acetate uptake by cyanide tolerant acetate degraders	0.5
$k_{s,fo}$	kg COD·m^{-3}	half saturation constant of formate uptake by hydrogenotrophic methanogens	0.15
$K_{I,cya,Xac}$	--	decay factor of normal acetate degraders	3E-005
$K_{I,cya,Xac,cya}$	--	decay factor of cyanide tolerant acetate degraders	4.7E-004
$K_{I,cya}$	kmole·m^{-3}	50% inhibitory concentration of cyanide to acetate degraders	1E-004
$k_{dec,Xac}$	d^{-1}	first order decay rate of normal acetate degraders	0.02
$k_{dec,Xac,cya}$	d^{-1}	first order decay rate of cyanide tolerant acetate degraders	0.01
Y_{Xac}	--	yield of normal acetate degraders on acetate	0.05
$Y_{Xac,cya}$	--	yield of cyanide tolerant acetate degraders on acetate	0.07
$Y_{X_{h2},fo}$	--	yield of hydrogenotrophic methanogens on formate	0.01
$K_{hyd,cya}$	d^{-1}(kgCOD·m^{-3})$^{-1}$	Aceticlastic biomass specific efficiency of cyanide hydrolytic enzyme	0.6

Acetate, cyanide, gas flow and pH were selected to fit the listed parameters because they are the most sensitive variables to these parameters and they are the most frequently measured in this experiment. In the first run, set 1 and the initial population of X_{ac} and $X_{ac,cya}$ were used to fit the measured acetate, cyanide and biogas flow data. In a second fitting run, $K_{hyd,cya}$ was added to the list of parameters and pH measurement was added to the list of measurements. In a third run, only acetate measurements were used to estimate $K_{I,cya}$. In a fourth run the estimated parameters obtained so far were excluded from the optimisation and the other newly introduced parameters were estimated using the four available measurements.

6.3.3 Experiment simulation and model validation

The data set from R 2 was used to calibrate the model. Data from reactor 1 and 3 were used to validate the model. Although the model was calibrated on one step increase of cyanide, experiment R2, the model has been validated on two quite different scenarios. The model is first validated with the normal cyanide level in the influent, experiment R1. The model is then validated further with a gradual increase in cyanide, experiment R3. The model could simulate the performance of the three reactors and simulation results were comparable to the measurements, as shown below.

6.3.3.1 Cyanide simulation results

Figure 6.3 shows the cyanide simulation results in the effluent compared to the influent cyanide concentration of the three reactors. Although only reactor 2 data was used for calibration, the simulation results of reactor 1 and 3 agree with the measurements. The model could accurately simulate the cyanide concentration in the effluent in response to the low concentration of 1 to 5 mg CN/l in the feed to R1, the step increase on day 160 from 1.5 to 25 mg CN/l to R2 and the gradual increase from 1.5 to 15 mg CN/l to reactor 3. Both implementations (WEST and AQUASIM) give the same simulation results with slight difference because of the different modelling of the carbon system equilibrium and the corresponding effect on the pH.

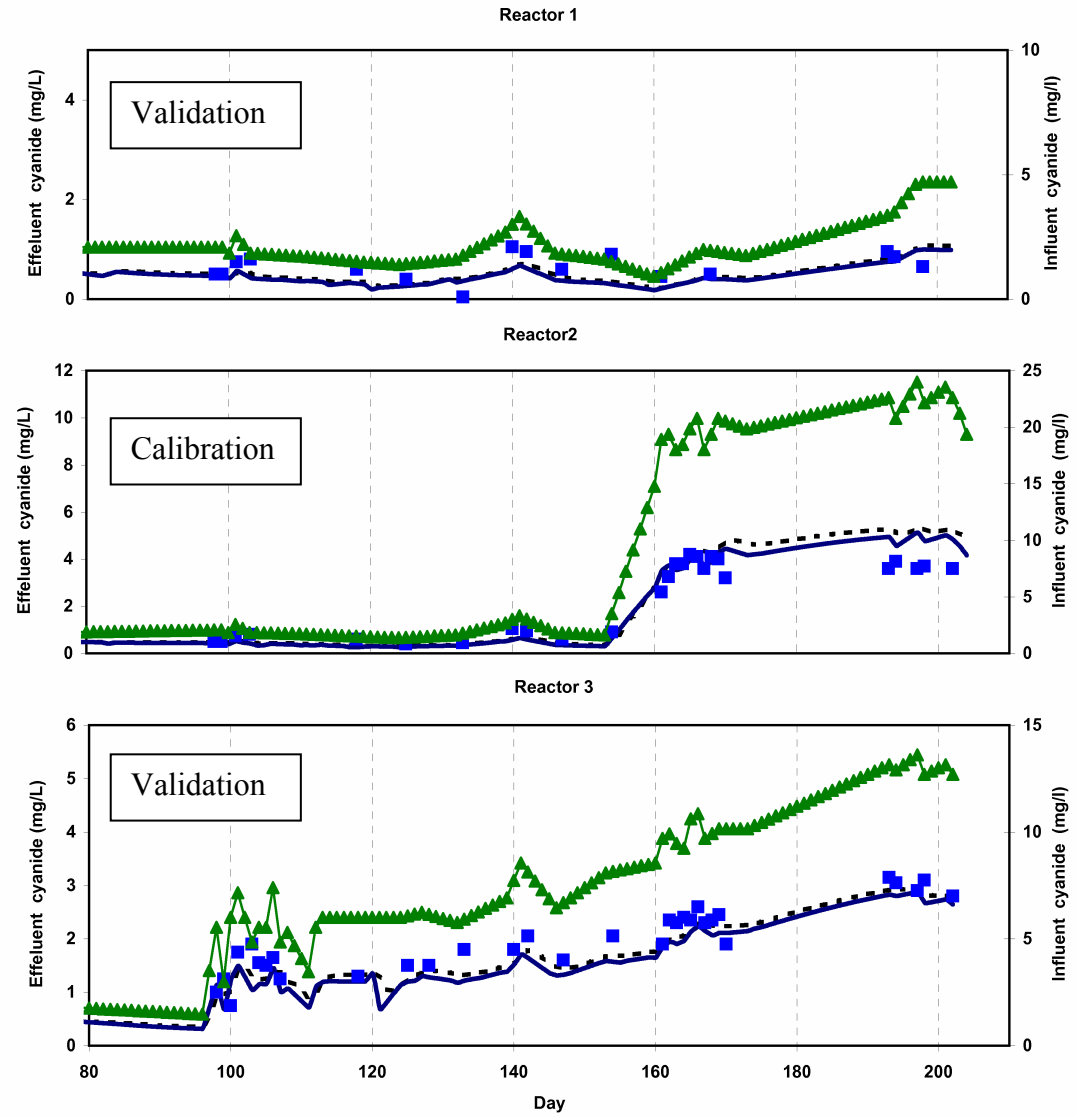

Figure 6.3: Cyanide simulation results: measurements ■; simulation with WEST implementation ——; simulation with AQUASIM implementation .....; influent cyanide concentration —▲—

6.3.3.2 *Acetate simulation results*

Figure 6.4 shows the acetate results in the reactor effluent compared to the COD load to the reactors. The COD load to the three reactors was the same except for a few instances of problems with the feed pumps, mainly on day 86 and on day 120. Recall that the three reactors are fed with the same wastewater, have the same volume and run to have the same hydraulic retention time. The main trend of the COD load was gradually decreasing towards the end of the experiment and consequently acetate should have followed the same trend.

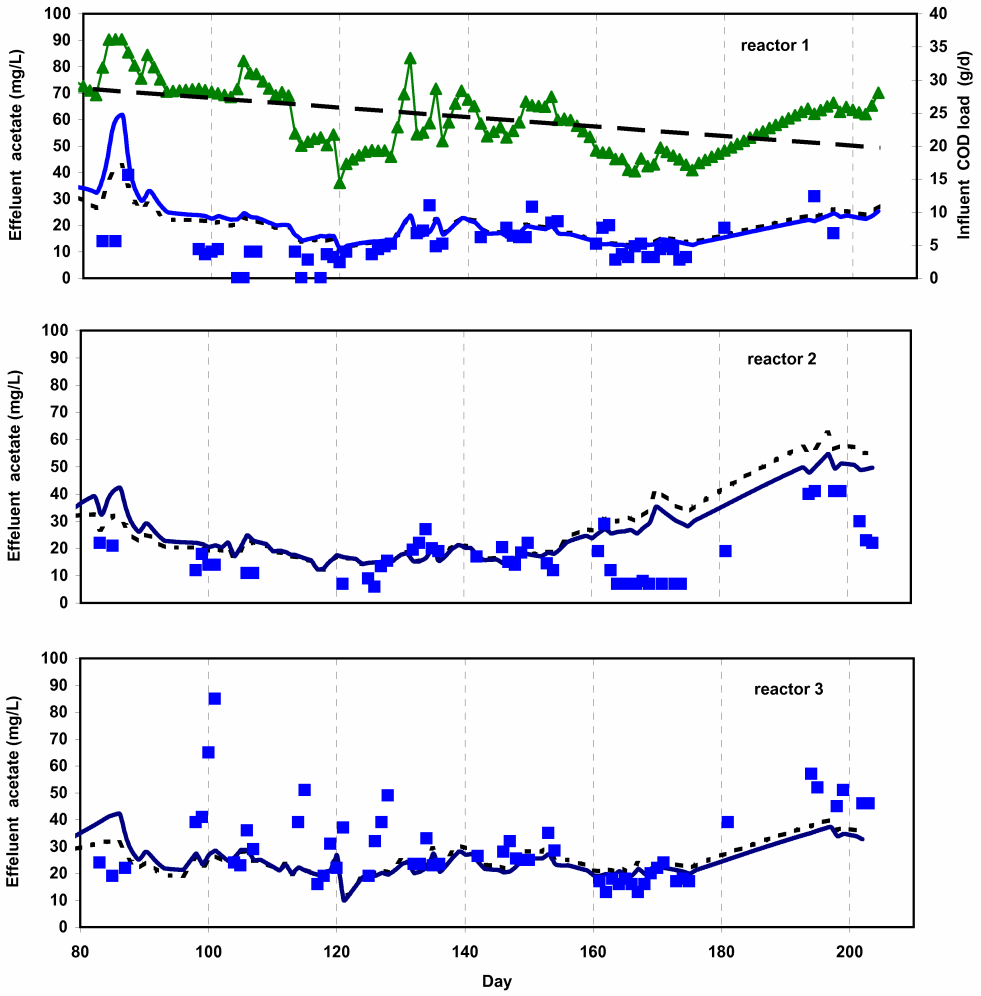

Figure 6.4: Acetate simulation results: measurements ■; simulation with WEST implementation ——; simulation with AQUASIM implementation .....; COD load to reactors —▲—, trend line of COD load — —

However, in the three reactors, the acetate concentration was rising because of the introduced cyanide and the model could nicely capture these dynamics. The main kinetics that enabled the model to show these correct responses are the cyanide inhibition terms introduced in the acetate uptake kinetics and the modelled population shift of the acetate degraders. Still, some differences with the measured data remain. At the end of the experiment, insufficient measurements of acetate in the period 175 to 195 were available to allow the reliable estimation of the corresponding model parameters. Also, some variations in the acetate measurements for R3 in the period 100 to 130 could not be captured by the model. With further investigation to this period of R3, it was found that the ammonia concentration in the reactor followed the same trend as the acetate results and to a higher extent compared to the normal levels detected throughout the experiment. Such effect could be related to some cassava granules that accidentally entered the reactor with the decanted wastewater. Also, in the acetate simulation results there were slight differences

between the WEST and AQUASIM results due to the difference in modelling the carbon system equilibrium.

6.3.3.3 Gas flow simulation results

Figure 6.5 shows the gas flow results in the three reactors.

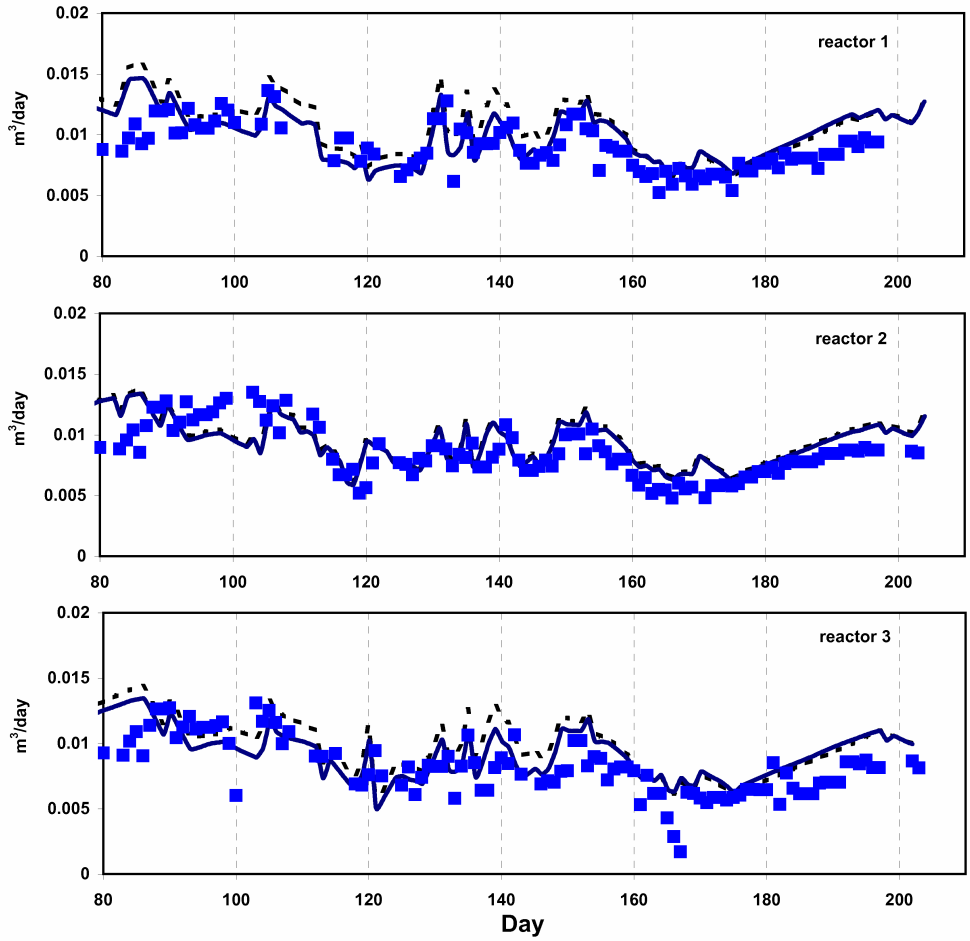

Figure 6.5: Gas flow simulation results: measurements ■ ; simulation with WEST implementation ——— ; simulation with AQUASIM implementation .....

The gas flow dynamics correspond to the COD load dynamics. The pH in the reactors was kept slightly above 7 and therefore no pH dynamics affect the gas flow. The gas flows from the three reactors are simulated very well by the model except at the points of different inflows due to a fault in the influent pump, e.g. on day 120.

6.3.3.4 pH simulation results

In Figure 6.6, the three reactors have the same pH that is slightly above pH 7. The simulated pH is close to the measurements due to the good estimate of the influent cation concentration that was kept the same for the three reactors. In the present experiment no

major influence of the cyanide on the pH is observed due to the low levels of cyanide and the phosphorus buffering at 7.25. There are some differences in pH simulation between WEST and AQUASIM because of the differences in the built-in methods that are used to interpolate the influent cation concentrations. Note that influent cations were estimated by the charge balance and, only, on days when the influent pH was recorded. Thus, the pH simulation is very sensitive to the cation (total alkalinity) records in the influent. However, the simulation of other variables was not affected since the pH was simulated within the optimum range for the process, i.e. there was no significant inhibition by pH.

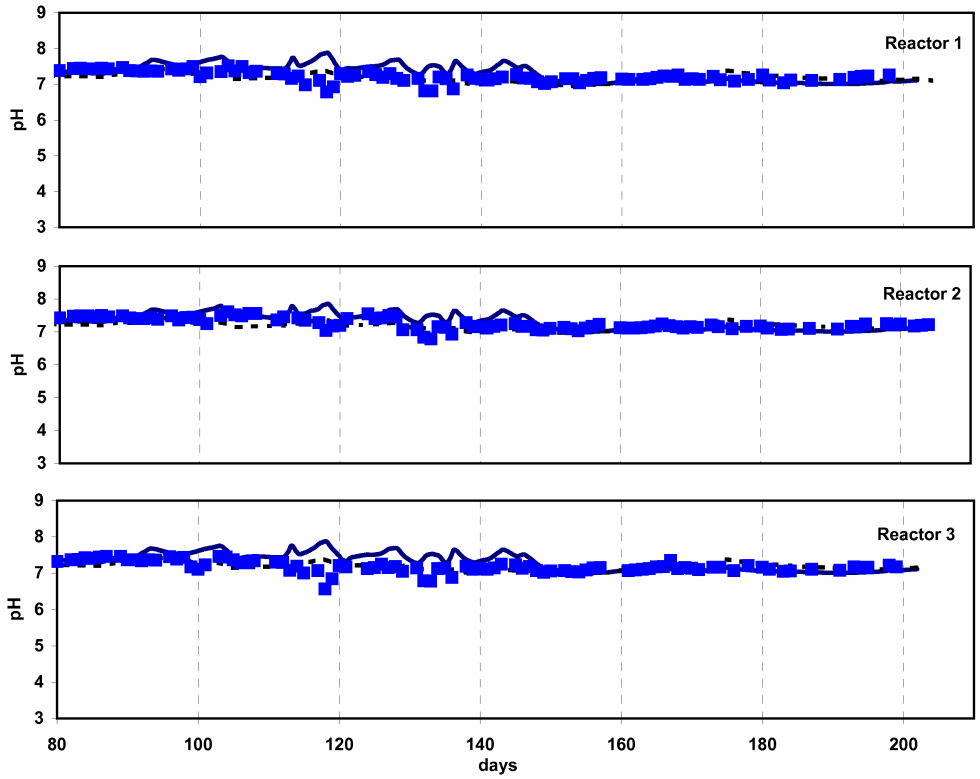

Figure 6.6: pH simulation results: measurements ■ ; simulation with WEST implementation ——; simulation with AQUASIM implementation.....

6.3.3.5 Shift in aceticlastic methanogens

Figure 6.7 shows the simulated population shift in aceticlastic methanogens in relation to the cyanide load. Two populations of aceticlastic methanogens were modelled. The initial concentration of cyanide tolerant aceticlastic methanogens is estimated to be 10 times the less tolerant population (see section 6.3.2). During the first 80 days of the adaptation period with the influent cassava wastewater and a cyanide concentration less than 5mgCN/l, 90% of the population shift is achieved. In R1 the cyanide load was gradually

increasing to 5mgCN/l and this was accompanied with a gradual decrease in the less tolerant aceticlastic methanogenic population. In R3 the cyanide influent concentration was increased to 5mg CN/l on day 98 and gradually increased till 15 mgCN/l at the end of the experiment. The decrease of the less tolerant aceticlastic methanogens was faster in R3 compared to R1. In R2 the increase of the cyanide influent concentration occurred suddenly at day 160 and to a higher level of 25 mgCN/l. As a result, the less tolerant aceticlastic methanogens decreased immediately.

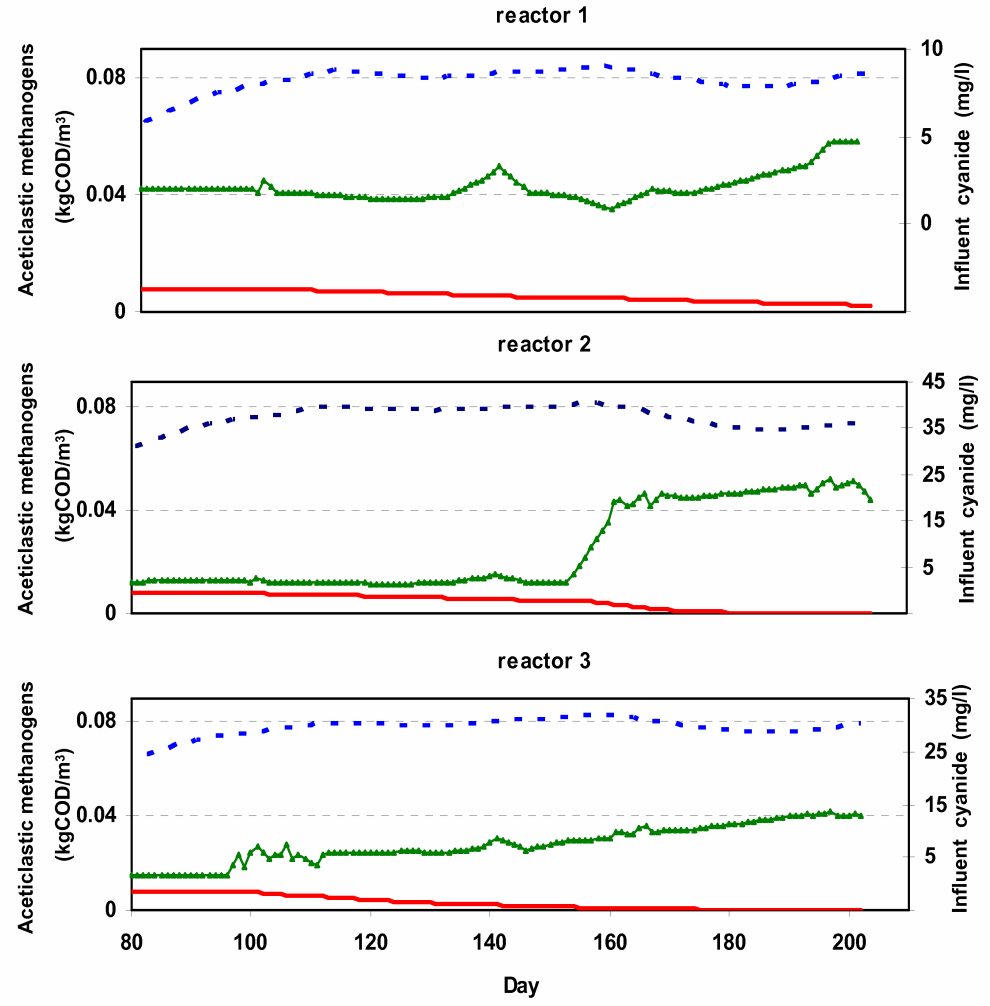

Figure 6.7: Simulated population shift in aceticlastic methanogens: influent cyanide load ; simulation of cyanide tolerant aceticlastic methanogens ; imulation of normal aceticlastic methanogens

Comparing the simulation results of the less tolerant aceticlastic methanogens in the three reactors, two conclusions can be drawn. First, for a cyanide concentration less than 5 mg/l both aceticlastic methanogens will be present and should be considered in the model. At higher cyanide concentrations the tolerant population will be the only one present and the

model can be simplified to only consider this population. Second, if no acclimatisation period is provided and an increase of cyanide levels above 5 mg CN/l occurs, drop of methane production and acetate uptake will occur.

The evolution of the more tolerant population, in the period starting at day 160 to the end of the experiment, shows a drop in the population size. The drop is proportional to the influent cyanide concentration level in each reactor during this period. The drop is mainly due to the inhibition term assigned to the acetate uptake and it was necessary to adequately simulate the acetate accumulation in R2 and R3 during this period.

6.4 Conclusions

The experiment performed with different cyanide concentrations in the wastewater shows the potential use of UASB reactors for the treatment of cassava and cyanide contaminated wastewaters. It allows a high removal efficiency of COD and cyanide, and a high biogas production. The ADM1 model extended in this work could adequately simulate the process dynamics in three reactors with different cyanide loads. The proposed approach of using two aceticlastic biomass populations with different cyanide tolerances helped in resolving the contradiction of the observed reversible effect of cyanide to anaerobic process while cyanide is classified as irreversible toxicant. The use of two biomass populations is especially important if selection of cyanide tolerant biomass is not likely to occur completely. This is expected if provided acclimatisation is insufficient and/or the applied cyanide load is low, e.g. less than 5mgCN/l.

Sensitivity analysis has shown that yield and decay parameters of the cyanide tolerant aceticlastic methanogens are the most important parameters. Therefore, the sensitivity analysis supports the importance of modelling the population shift and shows that the parameters are practically identifiable from experimental data.

The modelled hydrolytic pathway for cyanide degradation as function of the proposed cyanide tolerant aceticlastic methanogens concentration helps to accurately simulate the cyanide dynamics in the three reactors, with only one reactor being used for calibration. The introduction of the cyanide inhibition term in the acetate uptake kinetics helped to predict the acetate accumulation during the cyanide overload, even after the accumulation of the tolerant acetoclastic methanogens had occured. According the present experiment, if the sludge is acclimatised sufficiently long to cyanide loads above 5 mg CN/l, a single population of aceticlastic methanogens would suffice to adequately model the cyanide effects, provided that the inhibition term is applied to the acetate uptake. After a reasonable

acclimatisation period, the biogas in the reactors will follow the influent COD dynamics and can be accurately simulated.

Finally, it is important to measure the cation concentration in the influent and to extend the model with the introduced buffer components to obtain the right pH simulation and achieve reasonably accurate simulations.

Overall, the model could adequately predict the process dynamics in the presence of irreversible toxicity. Hence, the model can be used to study the feasibility of anaerobic treatment of wastewaters contaminated with irreversible toxicants such as cyanide.

Chapter 7

Protocol to design and set up the monitoring system

Abstract

In this chapter, a control model for anaerobic digestion of vinasses is validated. A general protocol is designed and implemented to set up the monitoring system and the sensor network at an anaerobic digestion plant. The protocol starts with data collection. It processes the information that can be collected at an existing anaerobic digestion plant or that is simulated for a new plant according to its design parameters. After optimising the process and selecting a control model, an iterative Optimal Experimental Design (OED) procedure is used to improve the practical identifiability of the control model parameters. The OED implementation in the protocol determines the needed measurements and measurement intervals. Using the OED procedure, influent dynamics of an optimal experiment is designed to achieve the highest confidence in the parameter estimates of the selected model. To test the approach, a virtual plant has been developed using a more detailed reference model, ADM1. A detailed example is given for the protocol implementation by applying it to the virtual plant. The virtual plant can be used to generate the data needed for the protocol application to a new plant.

CHAPTER 7

7.1 Introduction

Anaerobic digestion modelling and monitoring are complementary. The first key step to better monitor the anaerobic digestion process consists of increasing the information flow from the process by implementing new sensors (Bernard et al., 2004). Mathematical models, of increasing complexity, can optimise the information from a sensor network to predict the evolution of the anaerobic process, provided that the influent concentrations are known. Models are applied for optimal management, design of automatic controllers ensuring process stability, and they give tools to test several feeding strategies and forecast their consequence on the process viability (Puñal et al., 2003; Mailleret et al., 2003, 2004). Therefore, a procedure to optimally design the sensor network should be based on a selected model for a certain application and hence be nested with the model selection.

A modular and reliable system was designed to support remote telemonitoring and telecontrol (TELEMAC) of anaerobic digestion wastewater treatment units with no local expertise available to them. TELEMAC was a European project funded by the European Information Society Technologies (IST) Program (i.e., IST-2000-28156 project). The project was particularly focusing on the treatment of vinasses. Two main modules of the project comprise the development of anaerobic models for normal and abnormal operating conditions of digesters and development of sensors to be installed in the system monitoring network. The AM2 model was developed through the project (based on an improvement of AM1 by Bernard et al., 2001), for use in monitoring and control systems.

In this chapter, the AM2 implementation that is illustrated in chapter 3 is validated with anaerobic digestion of vinasses. A protocol is designed to set up the TELEMAC system and particularly its sensor network. The protocol is based on the AM2 model and the optimal design procedure reviewed in chapter 2. For generality of the protocol application, the protocol allows for process optimisation and upgrade of the model. The protocol is tested using a virtual plant that is based on the ADM1 model presented in chapter 3.

7.2 Validation of AM2 and its implementation

The model AM2 is described in chapter 3 and was implemented in WEST. In this section, the WEST implementation is compared with a standard FORTRAN implementation of the model and experimental data. The experimental data are collected from a dynamic experiment applied to the fixed bed reactor that will be described briefly in chapter 12. The fixed bed configuration was chosen to enable the application of rapid dynamics and validate the model and its implementation in response to these dynamics. Figure 7.1 shows the soluble COD and VFA results. Both implementations give exactly the same simulated

results. The experiment has three perturbations of COD shock loads that started at days 20, 40 and 60. The simulation results agree with measured data and correspond with the perturbations. The model is able to predict high overloads, e.g. the COD increase to 5 g COD/l and VFA accumulation to 35 mmol/l during the first perturbation. The model slightly underpredicts the fast shock loads, e.g. the spike at day 70.

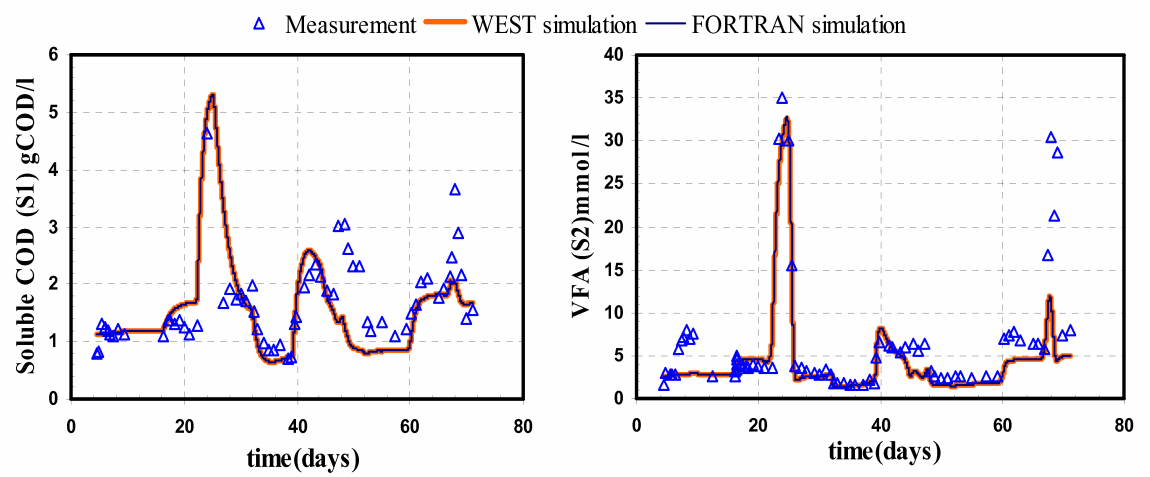

Figure 7.1 Validation results of AM2 WEST implementation: (left) soluble COD results (right) VFA results.

Figure 7.2 compares the simulated results of the methane flow to the measured data. The measured methane flow is evaluated from the total gas flow and the measured gas composition of methane and carbon dioxide. Therefore, validation in this figure is actually for both gas flow and composition measurements. Simulation results of CO_2 are not presented since it is reflected to this figure too. Both implementations show similar simulation results except for a slight difference in the highest peak during the first perturbation. Such difference is due to the use of different solvers in the two implementations. The FORTRAN implementation uses the stiff solver DASSL (Petzold, 1983). The WEST implementation uses the non stiff Runge Kutta solver. In general, the model nicely simulates the gas measurements. A clear difference is, however, present at the peak of the first perturbation. Either the model underpredicts the methane gas flow or there was a drift in the gas measurements under such high overload.

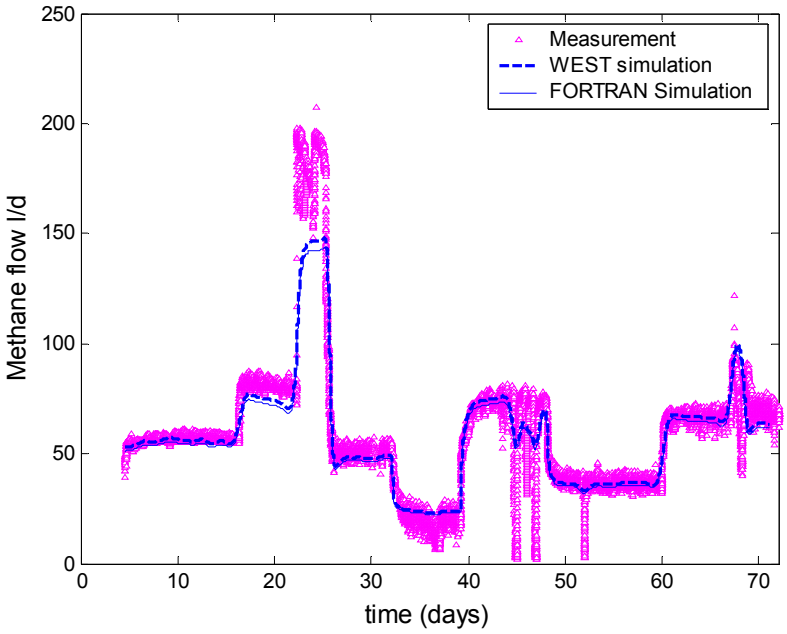

Figure 7.2 Validation results of AM2 WEST implementation: methane flow

Figure 7.3 shows the pH results. Both implementations have the same simulation results. The pH spikes at the first two perturbations are overscaled by the model while it is underscaled at the third perturbation. The pH dynamics are very rapid and such spikes are occurring for a short time. Therefore, it is more important to observe that the trend of the pH changes is well simulated.

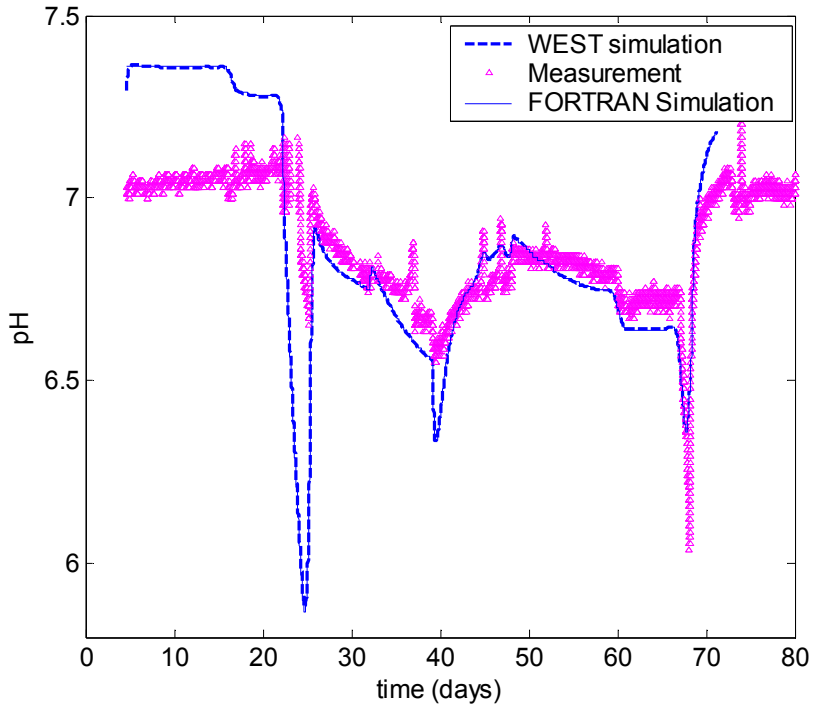

Figure 7.3 Validation results of AM2 WEST implementation: pH

In conclusion, the WEST implementation of the AM2 model is correct. Rapid dynamics of COD overload, VFA accumulation, gas flow and pH change can be simulated. Therefore, the model implementation can be used further in the protocol to design and set up the monitoring system.

7.3 Protocol description

The general protocol to set up the TELEMAC system at a new treatment plant is shown in Figure 7.4. It starts with data collection. Data collection, especially characterisation of the influent can be extended to a very detailed, laborious analysis but preferably it is not. In the application of the presented protocol it is advised to split the data collection into stages. Data is collected under three main categories: plant layout, influent characterisation and study of long-term data collected at the treatment plant. Also, information about sensors that are already installed at the plant or designed for the plant should be documented. The quality of the collected data should be checked and filtered. Trends should be detected to determine measurement bias and seasonal changes. Checklists can be made for data categories, sensors and data quality checks. Chapter 2 reviewed in detail the information and tools that help in constructing the checklists highlighting common anaerobic digestion problems and possible remedies.

The intended first applications of the TELEMAC system are devoted to the treatment of vinasses. For most of those plants it is expected that the protocol will proceed in the yes directions at the mentioned two check nodes, Figure 7.4. The control model AM2 is applied with the protocol in this chapter. This model is already validated on vinasses applications. In case of unexpected problems at these plants or for application to other types of waste that is not strictly suitable for the TELEMAC system, process optimisation can be an option. Examples of problems that might be found are high solids contents, large variations in the influent, more particulates than expected and so on. Such problems can be solved by minor updates to the plant design or operation instead of investing in a monitoring system that is more extended than the TELEMAC system. If the AM2 model is not able to describe the process dynamics, the process probably needs to be optimised and upgrade variants may have to be added to the model, e.g. describing toxicity. These 2 back loops are not expected to cycle more than two to three times. Otherwise, a more detailed model than AM2 needs to be implemented and, therefore, a more complex monitoring system will be needed.

The model is tested using the long-term data that is already available on the plant or for a new plant using simulated data obtained with a more detailed model. Once the selected

model is identified satisfactorily, the iterative procedure of optimal experimental design that is reviewed in chapter 2 can be applied.

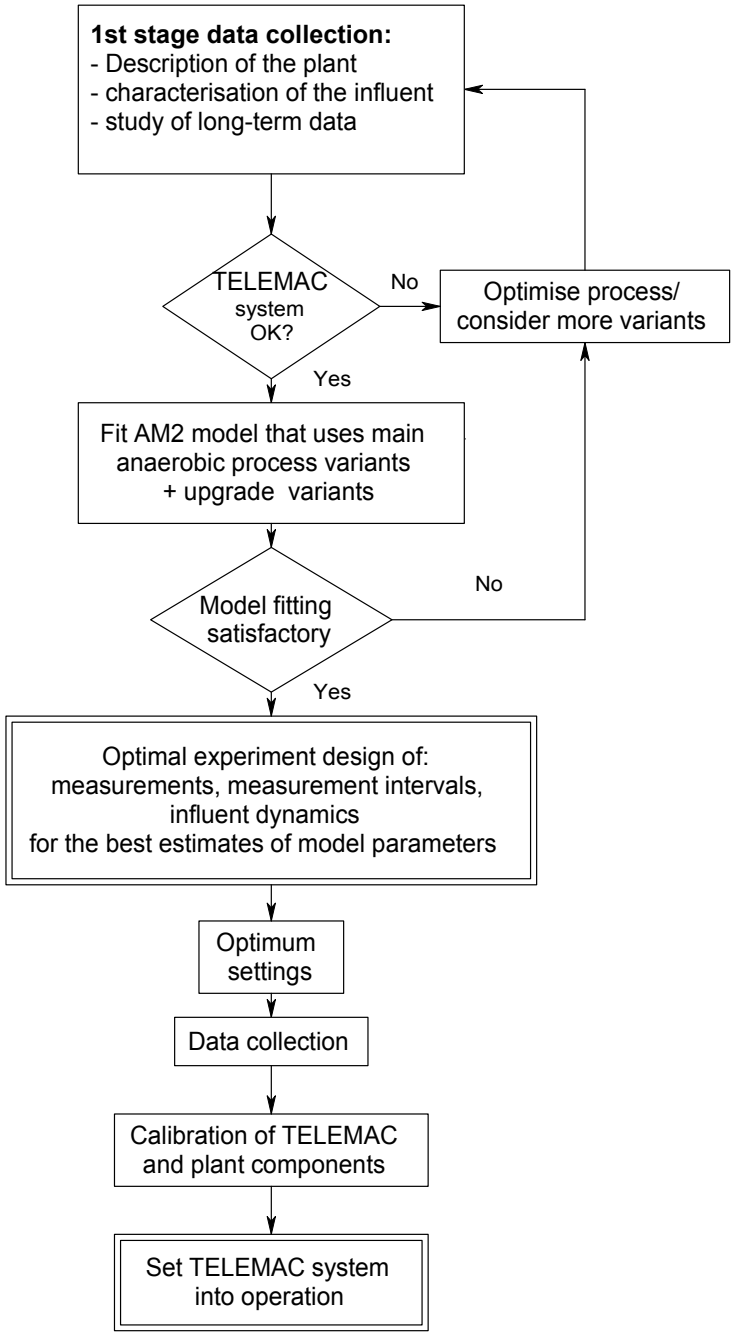

Figure 7.4 General protocol to optimise and set up the TELEMAC system

Briefly, the iterative procedure operates as in Figure 7.5. First, it designs an experiment based on the current model. An experiment is proposed by choosing certain experimental degrees of freedom. Sensors to be installed, measurement intervals and sensors noise levels are examples of the experimental degrees of freedom. They are also important settings of the sensor network (see on-line sensor combinations, section 7.4.2) and the monitoring

system. These degrees of freedom can be constrained in the ranges defined for the present and/or planned installation. The proposed experiment is then simulated on the computer and an objective function is evaluated. Typically this objective function is a design criterion from the Fisher Information Matrix (see chapter 2). The matrix summarises the information content of the proposed experiment and is a measure for the accuracy of the parameter estimates (in case this experiment would be performed in reality and the model would be fitted to the acquired data). A (nonlinear) optimisation algorithm is used to propose different experiments and find optimum settings of the monitoring system, in the sense that it maximizes the parameter estimation accuracy and/or minimizes parameter correlations.

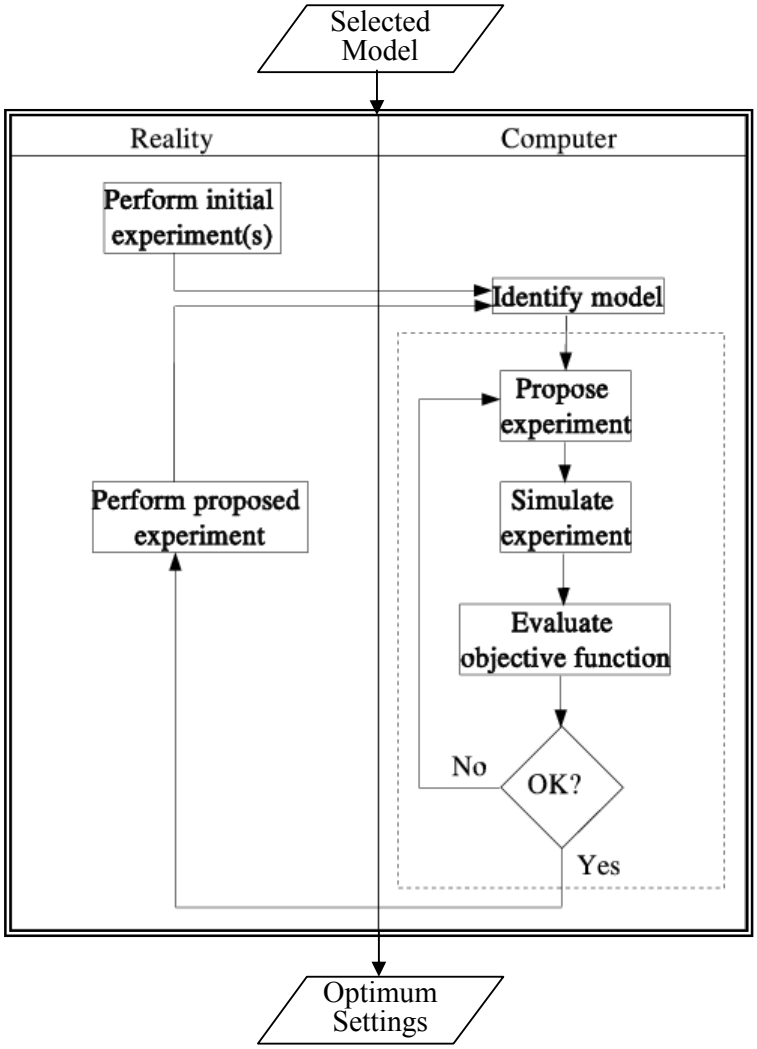

Figure 7.5 General procedure for optimal experimental design (adapted from Dochain and Vanrolleghem, 2001)

Practical identifiability of model parameters increases with the applied experiment dynamics. An experiment can be performed after the installation of the monitoring system to get the most accurate parameter estimates over an extended operation range. Further

degrees of freedom can be exploited with the variation of the hydraulic or the COD-load to design that experiment. The experimental procedure is repeated and, once the "optimal" experiment is found, it can be performed in reality. Based on the data of this experiment the model can be refitted and the accuracy of the parameter estimates evaluated. If the required accuracy is not yet reached another iteration can be performed, leading to an even better "optimal" experiment.

At the end of the iterative procedure, optimum settings of the monitoring system are defined and a calibrated model is available for its intended use. Optimum settings are applied to the sensor network; data is collected for the calibration of other plant components and control modules. Finally, the TELEMAC system is set into operation.

7.4 Virtual case study

The idea of the virtual case study is to test the proposed protocol and give an example of its application to design the monitoring system of a new plant. The example builds a virtual anaerobic digester and runs the optimal experimental design tools to reliably set up the TELEMAC system on that plant. The virtual plant is created using a reference model (IWA ADM1 model) to emulate a real digester treating vinasses. The ADM1 model implementation is illustrated in chapter 3. The type of vinasses and description of the influent characterisation are described in the following sections. The ADM1 implementation on the WEST® simulation is extended to generate all possible measurements in practical units.

Two data sets are generated. The first is presenting a long-term data set that is expected as a record of data available at an anaerobic digestion treatment plant (the virtual plant in this case study). This first data set is then used to fit the control model AM2 and get an initial estimate of its parameters. Then the optimal experiment design (OED) is used to evaluate the available TELEMAC sensors and their settings in terms of increased confidence in parameter estimates.

Allowing some degrees of freedom to the inflow, OED is used to design an optimal experiment with step inflow and TELEMAC sensors. The optimal experiment is then applied to the virtual plant to generate a second data set. This second data set is then used to fit the control model AM2 and evaluate the improvement of the confidence in its parameters. The simulation results of AM2 for both data sets together with the OED analysis and prediction are illustrated in section 7.4.3.

7.4.1 Description and modelling of the virtual plant

7.4.1.1 Virtual plant description

The implemented virtual digester is a scaled-up version of the lab CSTR system which is illustrated in chapter 5. The ADM1 model was applied and validated to successfully simulate 180 days experiment using that system. The 2 litres CSTR is fed by an alcoholic distillery wastewater with characteristics mentioned in chapter 5. A scale factor of 10^6 is used to size that reactor to the virtual plant and approximate a real digester. Thus, the volume of the virtual plant is 2000 m^3 and the liquid flow is multiplied by the same scale factor. The process parameter values used in the lab experiment are also used with the virtual plant.

During the lab experiment, the influent records were: flow and pH (on-line); TOC, soluble COD, total volatile fatty acids (VFA), total alkalinity (TA) and partial alkalinity (PA) were analysed off-line and recorded on a daily basis. The digester/effluent records were: pH, gas flow and gas composition (%CO_2 and %CH_4) (on-line); specific VFA gas chromatography analysis, TA and PA, total organic carbon and COD (on daily basis). More detailed influent characteristics were estimated using ADM1 and the default parameter set. For the virtual treatment plant concentrations in the influent were maintained the same and simulation was performed for the 180 days of the experiment. The simulation results of the concentrations in the virtual plant were exactly the same as those simulated for the lab-scale reactor which validates the modelling scaling assumption.

Since the lab experiment was designed to achieve an extreme overload towards the end of the experiment with some intermediate shock loads, it is not practical to consider the whole experiment period for the normal digester of the virtual plant. Such abnormal conditions wouldn't be allowed on a real plant. Thus, only the first 50 days are considered to avoid extreme loading and shocks. Also, the influent flow is smoothened to avoid the rapid dynamics of the lab-scale influent since these are not feasible for a normal digester. The result is a dynamic flow with a gradual increase in the influent through the designated 50 days. Accordingly, the hydraulic retention in the virtual plant is varying from 20 to 8 days, which can be accepted for a real digester. For SRT, AM2 was validated and calibrated by using FBR data and, therefore, the fraction of the biomass leaving the reactor (α in AM2 and f_{xout} in ADM1) was set around a value of 0.5. To better imitate the reality of seasonal changes in a real digester influent, the influent is extended steady for 10 more days and then the first 50 days are mirrored. This forms a 110 days period that can then be repeated to study the long-term dynamics, as shown in the flow profile of Figure 7.6.

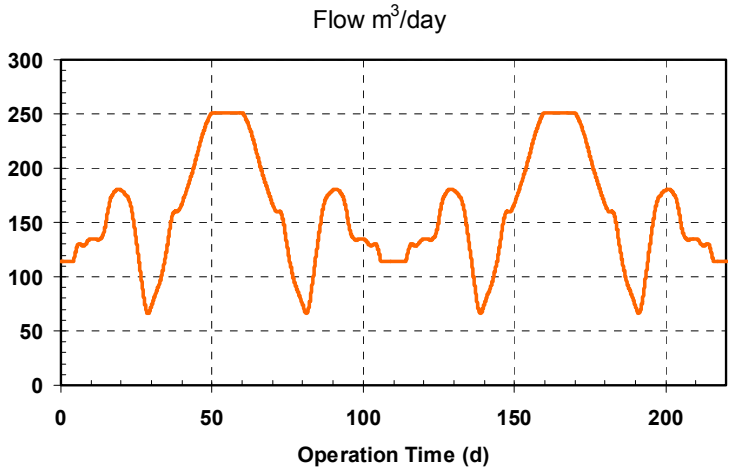

Figure 7.6 Designed long-term flow profile to the virtual plant

7.4.1.2 Influent characteristics

The detailed influent characteristics previously estimated with the ADM1 were used to generate the influent characteristics for AM2. The ADM1 and AM2 models are described in chapter 3. Two influent scenarios were generated for the AM2 to apply the OED steps. The first scenario is for the long-term data as would be typically collected from a digestion plant records. The second scenario is the one determined by the optimal experiment design. Briefly, the AM2 influent is calculated from an ADM1 specified influent. Table 7-1 lists the input variables for AM2. ADM1 state variables were illustrated in Table 3-1.

Table 7-1 AM2 state variables

State Variable Description	Name	Units
Organic Substrate concentration	S_1	g/l
VFA concentration	S_2	mmol/l
Concentration of acidogenic bacteria	X_1	g/l
Concentration of methanogenic bacteria	X_2	g/l
Total alkalinity	Z	mmol/l
Inorganic carbon concentration	C	mmol/l

Two important assumptions need to be clearly stated for AM2. The first is that total alkalinity is equivalent to the net cation concentration. The second is that the influent S_I is estimated from the practically measured total CODs less the COD of the measured total VFA. It is assumed that the VFA concentration is equivalent to a mixture of 70% of acetate and 30% of propionate. As a result 1g VFA (i.e S_2)=1.2 g COD and 1 mole S_2 = 64.2 g. Despite the fact that it is straightforward to sum all ADM1 soluble COD components minus VFA to calculate S_I, the second assumption is exploited and S_I is calculated as function of CODs mg/l and VFA in mg/l. This is mainly done to take into account the

effect of the second assumption as will happen in reality for an AM2 influent characterisation. Thus the AM2 influent characteristics are calculated as follows:

CODs (mg/l) = $(S_i + S_{su} + S_{aa} + S_{fa} + S_{va} + S_{bu} + S_{pro} + S_{ac})$ .1000
VFA (mg/l) = $(S_{va}$ *102 /208+ S_{bu} *88 /160+ S_{pro} *74 /112+ S_{ac} *60/64) .1000
S_1 = (CODs – VFA *1.2)/1000
S_2 = VFA /64.2
$X_1 = X_2 = 0$
$Z = S_{cat} - S_{an}$
$C = S_{ic}$ *1000

Note that S_{ic} will be mainly equal to the bicarbonate concentration since it is expected to be measured after the addition of the cations to the influent to rise the pH.

The above estimated concentrations are projected to one-day intervals. In practice and at a digestion plant without on-line monitoring of the influent, these measurements are expected to be collected off-line on a daily basis. However, the flow was assumed to be recorded on-line and was thus collected every 30 min.

7.4.1.3 Long-term data

The long-term data was generated using the virtual plant. Since the long-term flow profile is assumed to be a repeated cycle of 110 days, the data was only generated for one period of 110 days. The data expected to be recorded at any digestion plant is assumed to be CODs, pH and total gas flow. It is expected that at a normal plant, the pH and the gas flow are collected on-line. Feasible measurement intervals are assumed to be 5min and 30min, respectively. For CODs the measurement is assumed to be performed off-line on a daily basis. Thus, the long-term measurements are interpolated from the virtual plant results at those intervals. Nevertheless, noise is expected in the measurements and thus the signal is not expected to be smooth as simulated. Thus, a Matlab function was programmed to automatically interpolate individual records from the virtual plant and generate the noised signal. White noise N(0, E) was generated and introduced to the simulation signal. E is the corresponding error levels. Figure 7.7 shows examples of the CODs and gas flow (generated) measured signal.

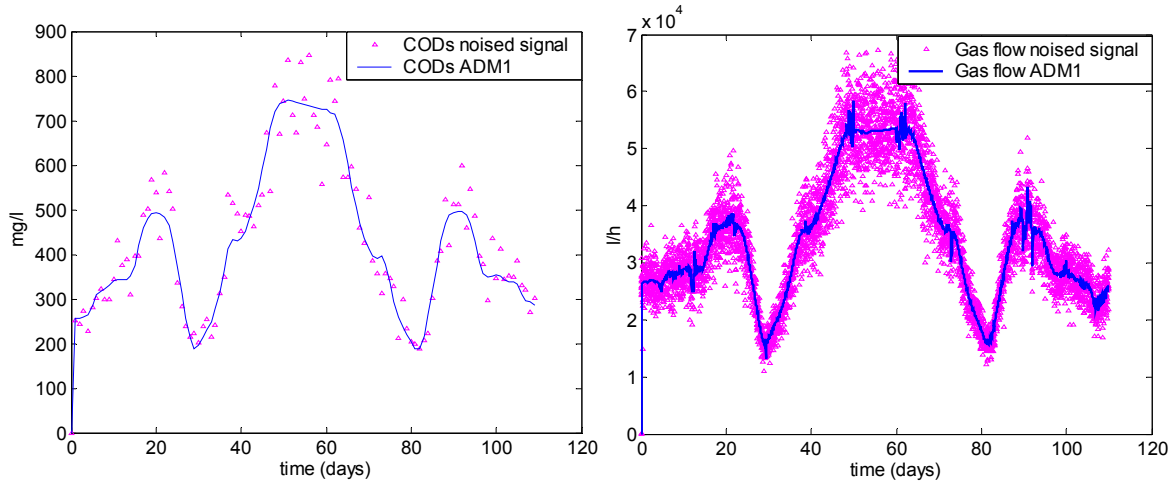

Figure 7.7 Example virtual plant simulated and noised signals (CODs to the left, Gas flow to the right)

Although the concept of white noise in the measurement is not new, the way it is used to investigate the effect of different noise levels (error in the measurement) on practical identifiability is innovative. Traditionally, the intention is to filter the measured signal from noise to clarify the signal trend. In the present application, noise is automatically generated on a predefined error level and added to the signal that is generated by the virtual plant (simulated by the reference model).

7.4.2 On-line sensors

Figure 7.8 shows a possible arrangement and expansion of the monitoring system at an anaerobic digestion plant. The third set presents the planned TELEMAC extension of the monitoring system with on-line measurements for VFA, $\%CO_2$ and $\%\ CH_4$. These additional on-line measurements will be provided by titrimetric and gas sensors developed within TELEMAC (Bernard et al., 2005). To test the added value of these sensors using the Optimal Experimental Design (OED) procedure, the corresponding simulation signals were generated from the virtual plant. The simulated signals are interpolated and noised at the intervals and error levels that are expected for these additional on-line measurements.

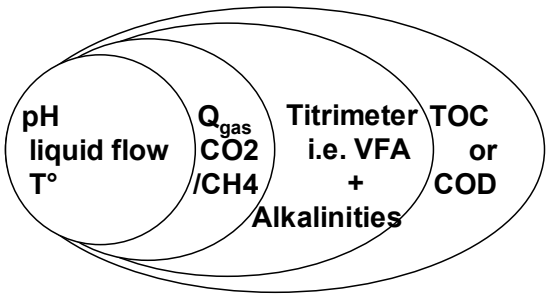

Figure 7.8 Possible sensor arrangements and expansion at anaerobic digestion plants

7.4.3 Optimal experimental design

7.4.3.1 Model calibration for long-term data

Using the long-term data described in Section 7.4.1.3, model AM2 was calibrated. Initial conditions for the state variables S_1, S_2, X_1, X_2, C and Z were obtained after running a long-term simulation with a steady-state influent file. This influent file was constructed by averaging all influent components of the long-term data over the period of 110 days. The initial conditions are listed in Table 7-2 and will be assumed fixed during the model calibration.

Table 7-2 Initial condition for AM2 state variables based on a steady state influent file

Name	Value
S_1 (g/l)	0.241
S_2 (mmol/l)	0.521
X_1 (g/l)	0.455
X_2 (g/l)	0.296
Z (mmol/l)	69.72
C (mmol/l)	71.89

Default AM2 parameters were assumed as initial parameter estimates. They are listed in Table 7-3.

Table 7-3 Default AM2 parameters used as initial parameter values

Name	Value
k_1 (-)	42.14
k_2 (mmol/g)	116.5
k_3 (mmol/g)	268
k_4 (mmol/g)	50.6
k_5 (mmol/g)	343.6
k_6 (mmol/g)	453
μ_{m1} (1/d)	1.2
μ_{m2} (1/d)	0.74
K_{S1} (g/l)	7.1
K_{S2} (mmol/l)	9.28
K_{I2} (mmol/l)	256
α (-)*	0.5
$k_l a$ (1/d)	19.8

**In ADM1 is called f_{xout}*

Model AM2 was fitted to the three available measurement variables: soluble COD (COD_s), pH and the gas flow rate (Q_{TOT}) with measurement errors 7, 1 and 2 % respectively. Measurement errors are used as weights in the parameter estimation objective function (weighted least squares) and the optimal experimental design. These measurement errors were assumed to be representative for a real case study. The model was calibrated using a constrained, derivative free optimisation algorithm, known as Simplex (Nelder and Mead, 1965). The model calibration resulted in parameter values and estimation standard deviations listed in Table 7-4. Figure 7.9, Figure 7.10 and Figure 7.11 show the fit of the model to the long-term data generated by the virtual plant, with $f_{xout} = \alpha = 0.5$. The model was able to describe the data adequately enough to be used as the starting point for the experimental design. The fit on the soluble COD measurements (COD_S) is less accurate than the fit on the other measurements because of the low quantity of data and the high measurement error. This causes the contribution of the COD_S to the optimisation objective function to be relatively small compared to the contributions of pH and total gas flow (Q_{TOT}) leading to a less accurate fit to this variable.

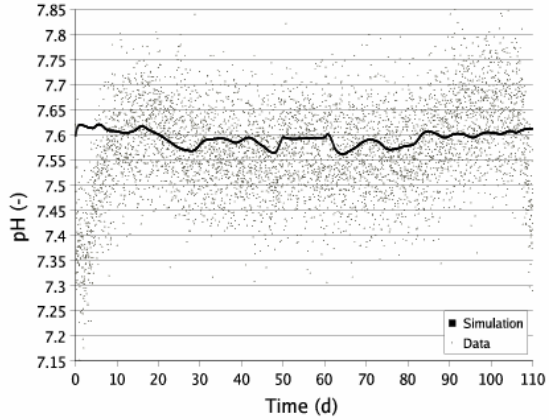

Figure 7.9 Optimal AM2 model fit to the long-term pH measurements

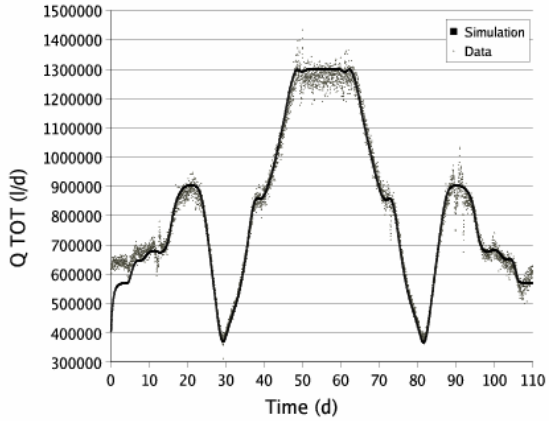

Figure 7.10 Optimal AM2 model fit to the long-term gas flow rate measurements

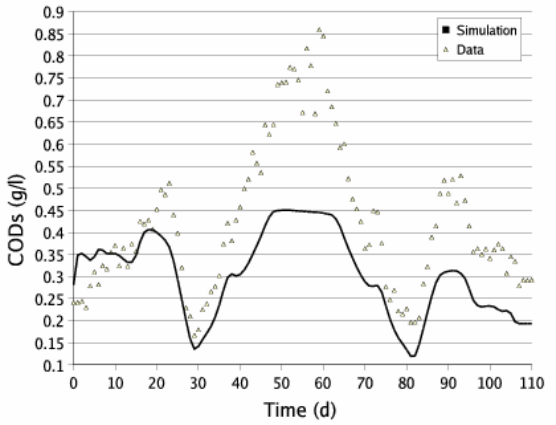

Figure 7.11 Optimal AM2 model fit to the long-term COD_s measurements

Together with the estimated parameters the Fisher Information Matrix (FIM) is calculated for the long-term simulation and the existing data collection plan. The inverse of this FIM is used as an approximation of the parameter estimation covariance matrix, as reviewed in chapter 2. Based on this covariance matrix the estimation standard deviations are calculated and presented in Table 7-4 as percentages of the parameter values. From Table 7-4 we can conclude that the confidence on the parameter estimates is very low (large estimation standard deviations). The information contained in the three available measurements for these parameters is very low. In fact, only parameters k_1, k_2 and α could be estimated with adequate accuracy. To increase the confidence on the parameter estimates, optimal experimental design should be used to come up with experiments (operation scenarios) which yield data with a higher information content. This will be discussed in the next sections.

Table 7-4 Estimates of AM2 parameters and their standard deviations found by fitting the model to the long-term data

Name	Value	Standard deviation	Error(%)
k_1	20.63	1.53	7.43
k_2	243.17	19.03	7.83
k_3	344.55	56.18	16.31
k_4	30.42	7.83	25.74
k_5	184.44	31.01	16.81
k_6	466.25	75.86	16.27
μm_1	1.65	1.24	75.13
μm_2	0.70	1.31	186.77
K_{S1}	8.37	6.79	81.12
K_{S2}	7.17	15.02	209.61
K_{I2}	349.42	19.94E+03	57.07E+02
α	0.56	0.04	6.51
k_{la}	16.63	3.36	20.26

7.4.3.2 Evaluation of added sensors

To improve the information content of the experiment, the added value provided by TELEMAC sensors will be investigated. *VFA* measurements (state variable S_2 in the AM2 model), CH_4 and CO_2 flow measurements will be considered. CH_4 and CO_2 flow measurements can be calculated from the total gas flow rate and the percentages of CH_4 and CO_2 in the gas provided by the gas sensor. With the availability of *VFA* measurements, the AM2 state variable S_1 (organic substrate) can also be calculated as the *CODs* value minus the amount of *VFA* expressed as *COD*. In total six measurements will be considered in this proposed experiment (operation scenario): S_1, S_2, pH, Q_{TOT}, Q_{CH_4} and Q_{CO_2}. The total experiment time is again assumed to be 110 days. Table 7-5 lists the additional measurements together with the proposed measurement interval and measurement error.

Table 7-5 Measurement interval and error for the additional TELEMAC sensor measurements

Name	Measurement interval	Measurement error (%)
VFA (mmol/l)	2 hours	2
$\boldsymbol{CH_4}$ flow rate (l/d)	30 minutes	2
$\boldsymbol{CO_2}$ flow rate (l/d)	30 minutes	2

To illustrate the increase in information content that an experiment with these measurements would have, the FIM was calculated for the experimental conditions and parameter values used in the previous section with and without considering the additional measurements. Again, the information content of the newly proposed experiment is expressed in terms of the predicted standard deviations of the parameters. In Table 7-6 a comparison is made between the experiment with and without the TELEMAC sensor measurements. It can clearly be seen that the confidence on almost all parameters increases indicating that with the additional measurements the model parameters could be estimated with considerably higher accuracy.

Table 7-6 Added value of the TELEMAC sensors (VFA, CH4 and CO2) on the parameter estimation standard deviations

		Without TELEMAC sensors		With TELEMAC sensors	
Name	Value	Standard deviation	Error(%)	Standard deviation	Error(%)
k_1	20.63	1.53	7.43	0.23	1.14
k_2	243.17	19.03	7.83	2.91	1.20
k_3	344.55	56.18	16.31	2.73	0.79
k_4	30.42	7.83	25.74	1.44	4.73
k_5	184.44	31.01	16.81	2.21	1.20
k_6	466.25	75.86	16.27	3.08	0.66
μm_1	1.65	1.24	75.13	0.53	32.21
μm_2	0.70	1.31	186.77	0.06	8.42
K_{S1}	8.37	6.79	81.10	2.84	33.92
K_{S2}	7.17	15.02	209.60	0.63	8.83
K_{I2}	349.42	19.94E+03	57.07E+02	81.42E+02	23.30E+02
α	0.56	0.04	6.51	3.40E-03	0.61
k_{la}	16.63	3.36	20.26	0.72	4.36

Inhibition parameter K_{I2}, however, still shows very low confidence, probably because the reactor is not operated at inhibiting conditions. This parameter will not be considered further. However it is feasible to design an experiment for which this parameter does become identifiable, for example by running the reactor at high VFA, S_2, concentrations.

By considering the TELEMAC sensors, errors on the parameter estimates could be reduced by a factor 5-20. This shows the importance of these sensors and the need for their development.

7.4.3.3 Design of an optimal experiment influent profile

After the check of the added value of the TELEMAC sensors, an experiment was designed using the optimal experimental design procedure in order to further improve the accuracy of the AM2 model parameters. The measurements considered for this experiment included the already available measurements on the plant and the TELEMAC sensors. They are listed in Table 7-7 together with the measurement interval and error. The total experiment time considered here is 1 month (28 days), rather than 110 days as before. The associated influent concentrations with the proposed flow are assumed the same as those of the long-term data in the period from day 41 to 69. This mainly presents the middle period of the assumed seasonal change.

Table 7-7 Measurements considered for the design of the optimal experiment with their measurement interval and error.

Name	Model name	Interval	Error (%)
Organic substrate (g/l)	S_1	0.5 days	7
VFA (mmol/l)	S_2	2 hours	2
pH (-)	***pH***	30 minutes	1
Total gas flow rate (l/d)	Q_{TOT}	30 minutes	2
CH_4 gas flow rate (l/d)	Q_{CH_4}	30 minutes	2
CO_2 gas flow rate (l/d)	Q_{CO_2}	30 minutes	2

The experimental manipulation under investigation here is the influent flow profile. The profile consists of step changes in the influent flow rate at the end of every week, resulting in 3 steps during the entire experiment. Upper and lower bounds for the flow rate are 250000 l/d and 66000 l/d respectively. This corresponds with the maximum and minimum allowable hydraulic retention time of the plant. Figure 7.12 shows an example flow profile, including the upper and lower bounds. Using computer simulations this profile is optimised in order to maximise the D criterion of the FIM, which corresponds with a minimisation of the volume of the confidence region of the parameters (see chapter 2). For the design of the experiment it is assumed that the concentrations of the influent components (S_1, S_2, Z and C) are constant. They are taken as the average values of the influent components of the long-term data. In reality this will of course not be the case but

taking the averages is a good approximation because the real fluctuations cannot be known in advance. Moreover, additional dynamics in the real influent will only further increase the information content of the data.

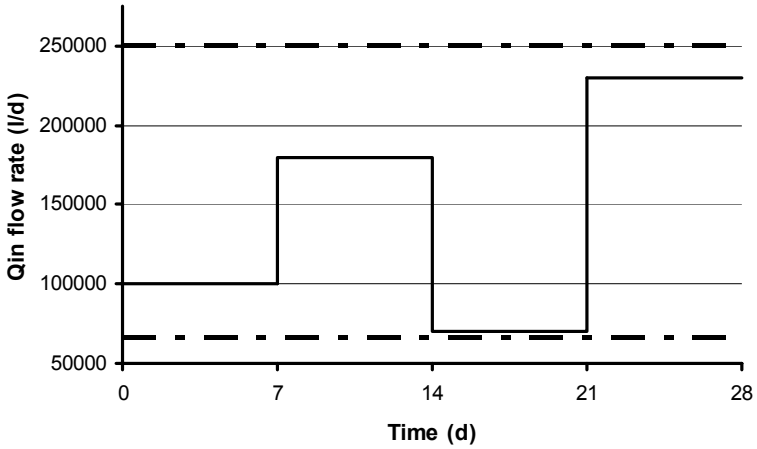

Figure 7.12 Example influent flow profile, including upper and lower bounds

Figure 7.13 represents the evaluation of the D-criterion during the optimisation of the influent flow rate. The optimisation algorithm used was again Simplex (Nelder and Mead, 1965). For each experiment an influent flow rate profile is proposed by the optimiser. Using this profile, a sensitivity analysis of the measured state variables to the parameters is performed and the FIM is calculated. From this FIM, the D-criterion is calculated and new experiments are proposed by the optimiser based on previous D-criterion values. This process continues until the D-criterion reaches its maximal value, i.e. the "optimal" experiment has been found. In this case the optimum is reached after approximately 90 proposed and simulated experiments.

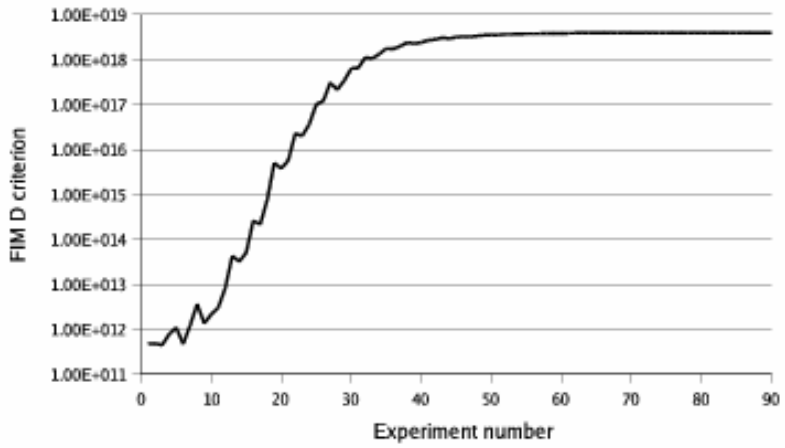

Figure 7.13 Evolution of the FIM D-criterion during the course of the experimental design optimization

Figure 7.14 shows the influent profile at the start of the optimisation (dotted line), experiment 1, and the optimal flow profile (full line), experiment 90. It can clearly be seen that the optimal profile is an alternation of the minimum and maximum allowable flow rate

(bang-bang profile). This introduces the maximal amount of dynamics in the system and thus the highest possible information content of the data.

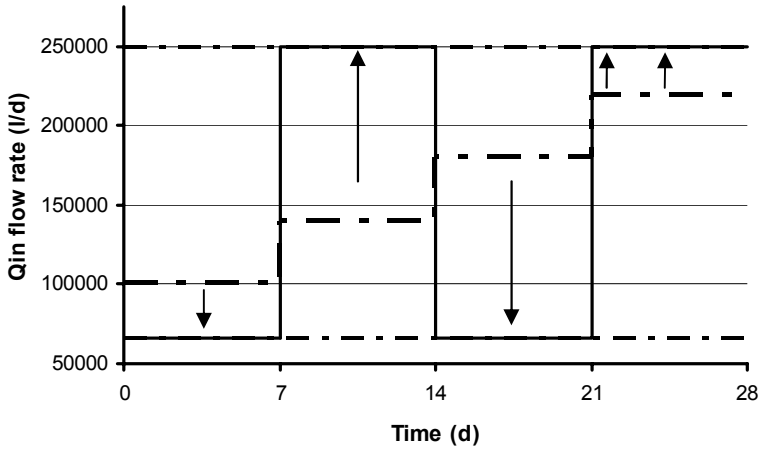

Figure 7.14 Initial (dotted line) and optimal (full line) influent flow profile. Upper and lower flow rate bounds are included as dashed lines. Arrows indicate the shift from initial to optimal influent flow profile

The optimal experiment results in a FIM which can be used to predict what the parameter estimation standard deviations would be once the experiment would be performed in reality and the model is fitted to the data, Table 7-8.

Table 7-8 Predicted parameter estimation standard deviations in case the model would be fitted to the data of the optimal experiment

Name	Value	Std. Dev.	Error (%)
k_1	20.63	0.46	2.21
k_2	243.17	9.16	3.77
k_3	344.55	11.84	3.44
k_4	30.42	14.57	47.93
k_5	184.44	19.18	10.4
k_6	466.25	9.46	2.03
μm_1	1.65	0.15	9.21
μm_2	0.70	0.01	2.02
K_{S1}	8.37	0.84	10.03
K_{S2}	7.17	0.13	1.8
α	349.42*	0.02	2.69
k_{la}	0.56	1.34	8.07

**It is not a reliable value since no particulate measurement were used*

Once the optimal experiment was determined it was performed in reality, in this case on the virtual plant. The optimal experiment with step changes of the hydraulic load is simulated using the virtual plant. The measurements assumed available at the plant, including the TELEMAC sensors, are generated at the designed sensor intervals and error levels. AM2 is fitted to the generated data to check the OED predictions of the confidence in AM2 parameters.

Model fits on all 6 measurements are shown in Figure 7.15. The model is able to describe the data accurately, except for the pH where there is a slight offset. However, it is still within the noise band of the measurement.

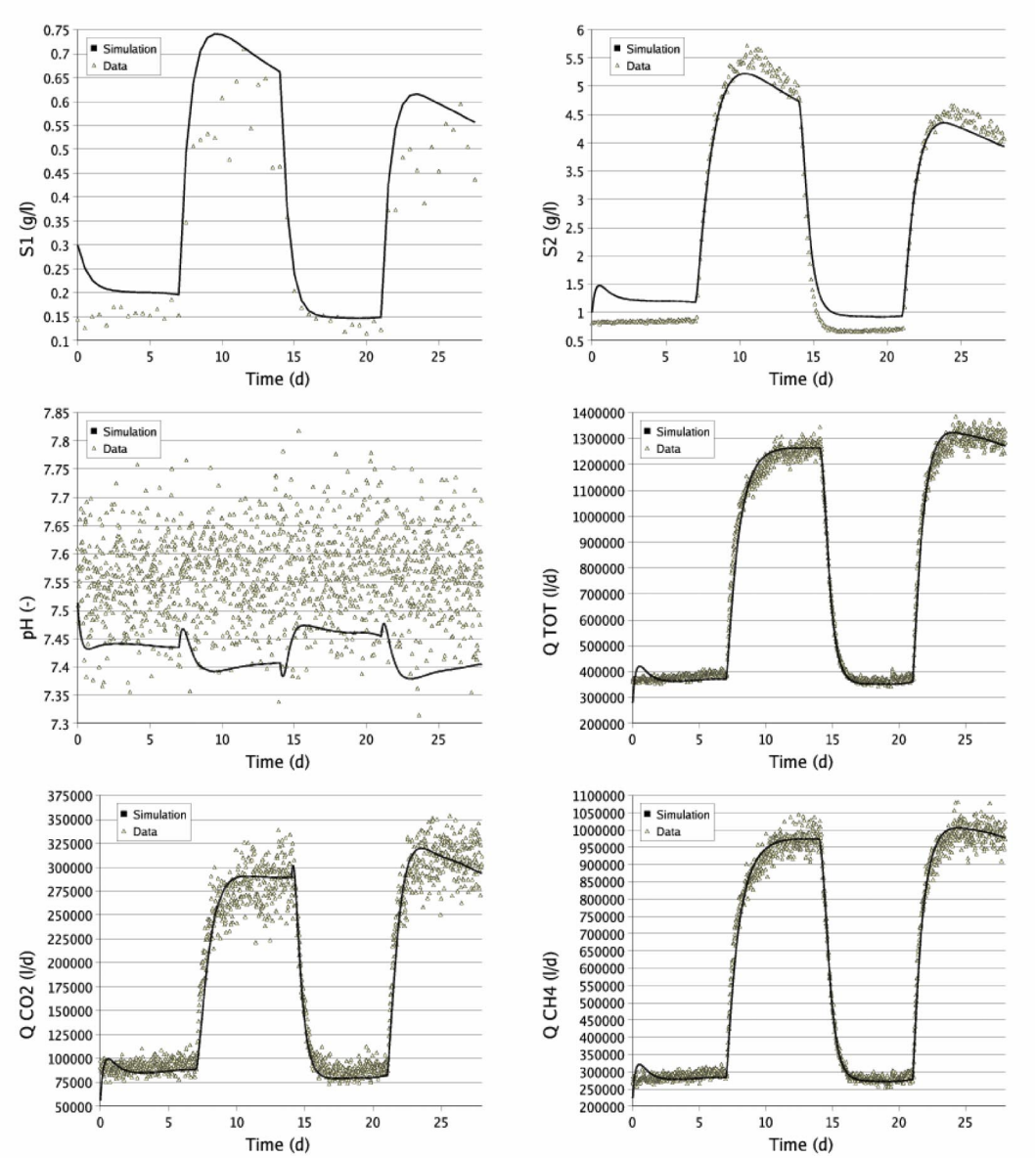

Figure 7.15 AM2 model fit on optimal experiment measurements that are generated by the virtual plant

The Simplex optimisation algorithm (Nelder and Mead, 1965) was started from different initial parameter values to ensure the convergence to a global minimum. At the best fit, the parameter estimation standard deviations were calculated based on the parameter estimation covariance matrix (inverse Fisher Information Matrix). Table 7-9 shows the estimated parameter values, the predicted estimation standard deviations from the experimental design procedure and the calculated estimation standard deviations after the model fit. From the table, it can be concluded that all parameters were fitted with high

confidence and that the experimental design procedure was able to predict the estimation standard deviations very well.

Table 7-9 Optimal parameter values for the AM2 model fitted to the optimal experiment data. OED-predicted and real parameter estimation standard deviations are also listed.

Name	Value	Standard Deviation	Error (%)	Predicted error (%)
k_1	11.00	0.40	3.64	2.21
k_2	175.87	6.61	3.76	3.77
k_3	262.94	10.07	3.83	3.44
k_4	14.11	1.98	14.04	47.93
k_5	134.81	5.72	4.24	10.40
k_6	251.36	9.43	3.75	2.03
μm_1	0.55	0.02	4.01	9.21
μm_2	0.42	0.04	8.36	2.02
K_{S1}	3.13	0.10	3.08	10.03
K_{S2}	15.44	1.24	8.06	1.80
α	0.59	0.03	4.60	2.69
k_{la}	18.83	1.56	8.29	8.07

Summarising, Figure 7.16 shows the improved confidence in model stoichiometric and kinetic parameters by implementing TELEMAC sensors and performing an optimal experiment. The stoichiometric parameters k_1 to k_6 are improved significantly by inclusion of the TELEMAC sensors. The designed experiment improves the confidence in the acidifiers kinetic parameters with a slight reduction in the confidence of the stoichiometric parameters. Similarly, the physical parameters, i.e. the fraction of bacteria in the liquid phase α and the gas transfer rates k_{la}, were improved. However, information about the reactor (the virtual plant) were incorporated, e.g. measurement were generated by the virtual plant using f_{xout} = 0.56 and k_{la}=20.

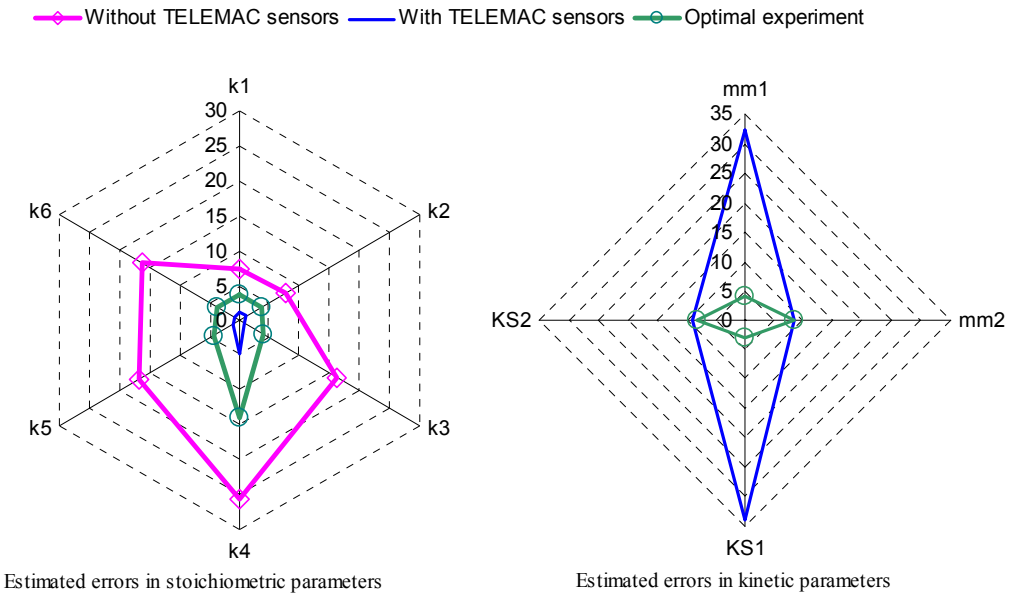

Figure 7.16 Improved confidence in model parameters expressed in % error. (Note mm1 and mm2 are μm_1 and μm_1 respectively)

The provided case study of the virtual plant helped in illustrating the steps of the protocol and the optimal experimental design. Furthermore, the virtual plant example can be applied to a new plant design, evaluate and design its monitoring system and operation strategy at an early stage, even before the plant construction.

7.5 Conclusions

The simple control model AM2 was successfully implemented in the WEST simulation platform, and was validated with another standard implementation in FORTRAN and experimental data of a pilot-scale fixed bed reactor treating vinasses.

A simple protocol to set up the monitoring system was designed and successfully validated using a virtual plant. The application of the Optimal Experimental Design procedure shows the benefit of the additional sensors, the increased precision of the control model parameter estimates and therefore the increased robustness of the model in simulating and controlling the process.

The virtual case study reported here is the first application in the scientific community that uses a reference model for an anaerobic digestion process as a data generator to evaluate methodologies and validate other simple models. Practical measurements are calculated in the common units that are used at industrial applications and are evaluated as functions of ADM1 state variables and parameters.

For the first time, OED was applied to anaerobic digestion. A range of experimental degrees of freedom has been considered: type of measurement, measurement frequencies and influent flow profile. This technique has proven itself to be highly valuable for the design of experiments in order to improve the control model calibrations. The OED application showed the value of on-line monitoring of pH, VFA and gas flow and composition. Therefore, having an on-line titrimetric analyser is very useful since it provides the VFA, pH and other buffers' measurement. Also, it measures bicarbonate alkalinity that can be related to the gas results.

Accordingly, the monitoring system can be designed, confidence in the control model parameters can be increased and therefore the anaerobic digestion plant can be successfully managed and controlled.

Part II

Plant-wide modelling

Chapter 8

Anaerobic digestion models in plant-wide modelling

Abstract

In this chapter, the integration of an Anaerobic Digestion Model (ADM) with the standard Activated Sludge Models (ASMs) is introduced in view of plant-wide application. A flexible approach is presented and illustrated through an example of integrating the Siegrist ADM and ASM1. In the example the IWA/COST benchmark model of activated sludge systems is extended with an anaerobic digestion unit. To simulate the practice of sludge treatment in this example, two process units are added and configured to act as a thickener and a centrifuge before and after the digester respectively. To increase flexibility for further applications, two interfaces between activated sludge and digester model components are created. The structure of the transformers is briefly described. Results of the benchmark simulation are shown to highlight the effect of supernatant recycling and the plant-wide output.

CHAPTER 8

8.1 Introduction

Anaerobic digestion receives a growing attention in the field of wastewater treatment. Figure 8.1 shows possible locations of digesters for wastewater treatment in agricultural, farming, residential, commercial and industrial areas. Since anaerobic digestion is a closed system, it can be located nearby these areas without nuisance, e.g. odour. It can be scaled and configured for different types of wastes from these activities and utilise the produced gas for energy production. In this context, anaerobic digestion can serve as a primary treatment upstream the main wastewater treatment plant and can be favourably located at the pollution source.

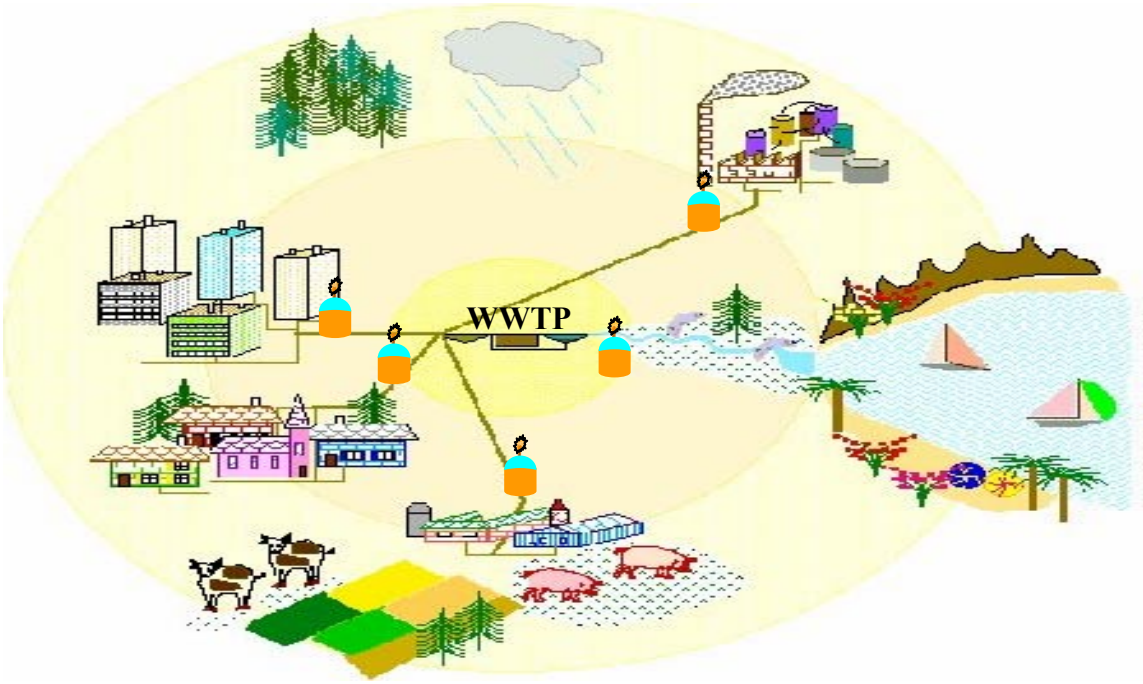

Figure 8.1 Possible locations of a digester( )

Moreover, at conventional wastewater treatment plants, anaerobic digestion is employed for sludge treatment and stabilization. It considerably reduces the amount of sludge produced. However, the cost of waste sludge treatment constitutes approximately 35% of the capital cost and 55% of the annual operation and maintenance costs of a wastewater treatment plant (Cinar et al., 2004; Knezevic et al., 1995). As compensation, the lower amounts of sludge reduce the cost of final disposal. The reduction of sludge volumes is turned mainly to bio-gas that can be used as clean energy source, e.g. generating electrical power for plant operation. For industries, anaerobic treatment could be a good option for wastewater treatment as an alternative to connecting to the sewer and paying higher tariffs. Other loads can be connected to the digesters at the conventional plant such as truck loads from decentralised systems or sludge from other treatment plants. To study such scenarios

and evaluate plant-wide control systems and operating strategies, integrated modelling of anaerobic digestion and other plant processes is very valuable.

The question tackled in this chapter is how to connect models so that control systems, sensors and subsequent treatment processes can be evaluated at the plant-wide level. Also, this chapter aims at enabling different comunity sectors to assess the aforementioned possible solutions. For this purpose, a standard benchmark system, the BSM1 developed for activated sludge systems (Spanjers et al., 1998; Copp, 2002), is extended with the sludge treatment line including the anaerobic digester. The flexible approach of transformers is introduced to interface anaerobic process models with other process models so that anaerobic digestion applications can be evaluated in the context of stand-alone application at one of the community sectors or in an integrated manner relevant to all sectors of a community and the stakeholders.

8.2 Interfacing methodology

The Siegrist ADM (Siegrist et al, 1990, 1993 & 1995) has been chosen for illustration of the extended benchmark plant in this chapter. All modelling and simulation was performed in the WEST software (Hemmis NV, Kortrijk, Belgium), (Vanhooren et al, 2003), using the Model Specification Language, MSL (Vangheluwe, 2000). The objectives, flexibility and easiness are stated for the presented transformation approach. Flexibility is achieved by building the two transformer nodes outside the digester model node. The feed to the digester can be implemented by either external loads or treatment plant sludge or both. An external load could be a pipe line from an industry or truck loads (Jeppsson et al., 2004) from septic tanks whose wastewater characteristics are more relevant to the ADM state vector.

Similarly, the effluent liquors from the anaerobic digester can be channelled to a post-treatment or recycled back to the inlet of the treatment plant. Therefore, two transformers have to be developed for connecting the Siegrist ADM with ASM1 (Henze et al., 2000) and vice versa. The easiness objective was pursued by direct assignment of fractions among model components as shown in Figure 8.2.

For each transformer fraction parameters need to be defined. Fraction parameters should be consistent so that they maintain continuity, i.e. fulfil the COD and Nitrogen balance. Therefore, these fractions depend on state variable definitions and units of both models. Appendix 3 lists the values of the mass fractions and the nitrogen content parameters that were used in this case study. For an application to a real wastewater treatment plant, these

parameters can be estimated from actual measurements and a sludge characterisation. Table 8-1 lists the state variables of ASM1. Table 8-2 lists the state variables of the Siegrist ADM. It should be noted, however, that in the WEST implementation the transformers and the models have flux terminals and therefore concentration units are converted to flux units at the interfaces by multiplying with the flow rate. Also, for the continuity check in WEST, outfluxes from the nodes will have a negative sign while influxes will have a positive sign. This sign rule will be reflected in the following transformer equations.

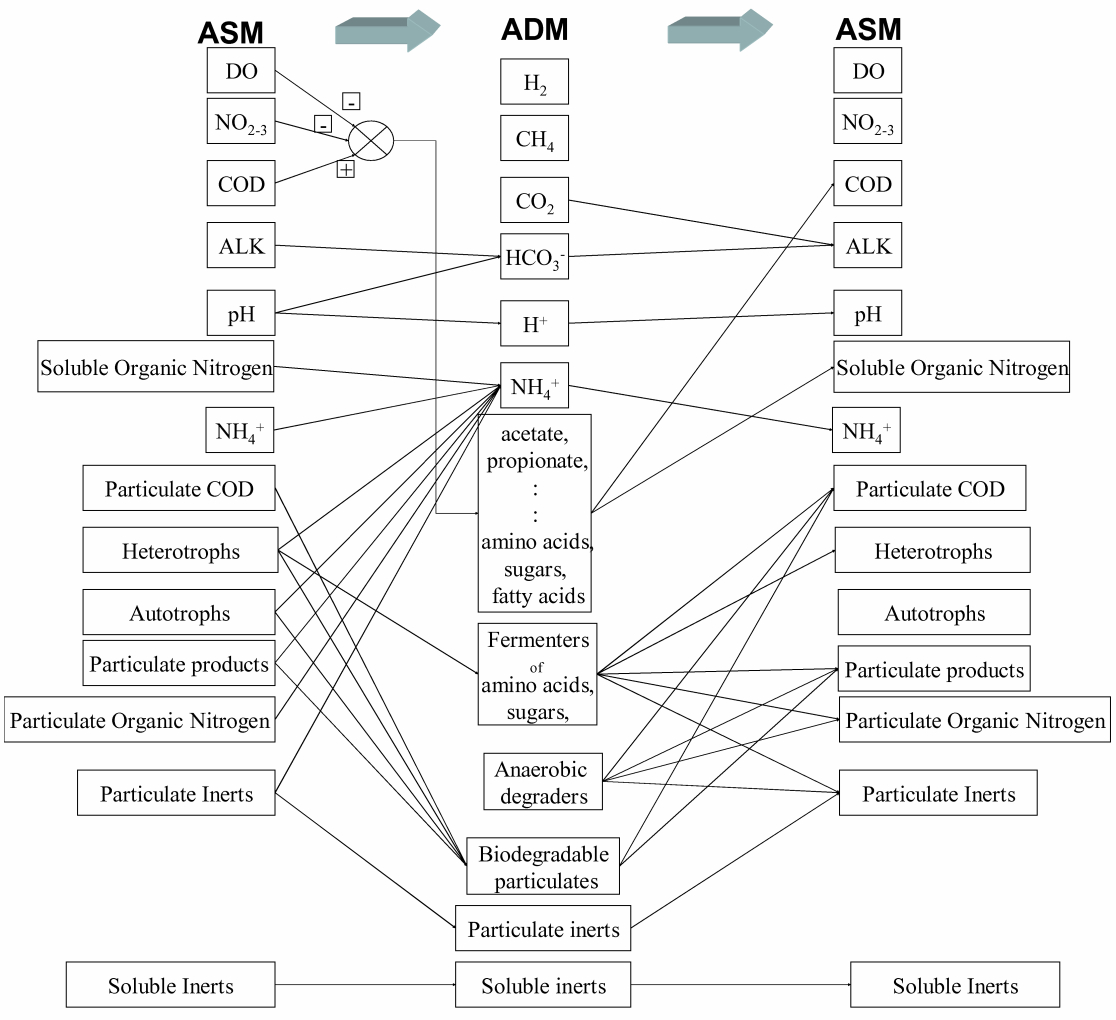

Figure 8.2 Direct assignments between model components in the proposed transformers

Table 8-1 ASM1 state variables

State Variable Description	Symbol	Units
Soluble inert organic matter	S_i	g COD m^{-3}
Readily biodegradable substrate	S_s	g COD m^{-3}
Particulate inert organic matter	X_i	g COD m^{-3}
Slowly biodegradable substrate	X_s	g COD m^{-3}
Active heterotrophic biomass	X_{bh}	g COD m^{-3}
Active autotrophic biomass	X_{ba}	g COD m^{-3}
Particulate products arising from biomass decay	X_p	g COD m^{-3}
Oxygen	S_o	g COD m^{-3}
Nitrate and nitrite nitrogen	S_{no}	g N m^{-3}
$NH_4^+ + NH_3$ nitrogen	S_{nh}	g N m^{-3}
Soluble biodegradable organic nitrogen	S_{nd}	g N m^{-3}
Particulate biodegradable organic nitrogen	X_{nd}	g N m^{-3}
Alkalinity	S_{alk}	mol L^{-1}

Table 8-2 Siegrist et al.(1995) anaerobic digestion model state variables

State Variable Description	Symbol	Units
Hydrogen	S_{H2}	g COD m^{-3}
Methane	S_{CH4}	mol m^{-3}
Carbon dioxide	S_{CO2}	mol m^{-3}
Bicarbonate	S_{HCO3}	mol m^{-3}
Protons	S_H	mol m^{-3}
Ammonia	S_{NH4}	g N m^{-3}
Acetate	S_{ac}	g COD m^{-3}
Propionate	S_{pro}	g COD m^{-3}
Amino acids and sugars	S_{AS}	g COD m^{-3}
Long chain fatty acids	S_{FA}	g COD m^{-3}
Inert soluble organic matter	S_{IN}	g COD m^{-3}
Particulate biodegradable organic matter	$X_{S(SIEG)}$	g COD m^{-3}
Biomass capable of fermenting	X_{AS}	g COD m^{-3}
Biomass capable of anaerobic oxidation of long chain fatty acids	X_{FA}	g COD m^{-3}
Biomass capable of anaerobic oxidation of propionate	X_{pro}	g COD m^{-3}
Biomass capable of converting acetate to methane	X_{AC}	g COD m^{-3}
Biomass capable of converting hydrogen to methane	X_{H2}	g COD m^{-3}
Inert particulate organic matter	X_{IN}	g COD m^{-3}

8.2.1 ASM1 to Siegrist ADM transformer

8.2.1.1 Soluble components

Hydrogen and methane are zeros, equation (8.1), since they are not expected in the aerobic effluent.

$$S_{H2} = S_{CH4} = 0. \tag{8.1}$$

Knowing the pH, the CO_2 and HCO_3^- concentrations can be estimated from the bicarbonate equilibrium. Neither the pH nor the proton concentration is defined in the ASM1 model. Therefore, as an approximation, pH is assumed fixed and the proton concentration to the digester is set as a parameter $S_{H\,IN}$ of the transformer. In real case, the pH value can be set to the average pH in the sludge stream feeding the digester. The pH value is practically less than 8 and, therefore, carbonate concentration can be ignored. From the ASM1 S_{alk} concentration, the influent S_{CO2} and S_{HCO3} can be calculated from equations (8.2) and (8.3) respectively.

$$S_{CO2} = -\left(\frac{S_{H\,IN} \cdot S_{alk}}{S_{H\,IN} + K_{a,HCO3}}\right) \tag{8.2}$$

$$S_{HCO3} = -\left(\frac{K_{a,HCO3} \cdot S_{alk}}{S_{H\,IN} + K_{a,HCO3}}\right) \tag{8.3}$$

where $K_{a,HCO3}$ is the acidity constant of bicarbonate.

Readily biodegradable substrate S_S is reduced to compensate for the depletion of the remaining dissolved oxygen S_O and nitrates S_{NO}. A temporary state is calculated for the S_S influx, equation (8.4). This equation applies logic rules to check the sufficiency of S_S and subtract the remainder of the necessary COD from X_S if needed. If S_S remains, it will be split into acetate S_{AC}, propionate S_{PRO}, amino acids and sugar S_{AS}, and fatty acids S_{FA} according to predefined fractions according equations (8.5), (8.6), (8.7) and (8.8). Note that hydrolysis is not considered in the Siegrist ADM.

$$\text{TemporaryInFlux}_{SS} = S_S - S_O - 2.86 \cdot S_{NO} \begin{cases} < 0 \rightarrow \begin{cases} \text{InFlux}_{SS} = 0. \\ \text{InFlux}_{XS} = X_S + \text{TemporaryInFlux}_{SS} \end{cases} \\ > 0 \rightarrow \begin{cases} \text{InFlux}_{SS} = \text{TemporaryInFlux}_{SS} \\ \text{InFlux}_{XS} = X_S \end{cases} \end{cases} \tag{8.4}$$

$$S_{AC} = -f_{AC\_S} \cdot \text{InFlux}_{SS} \quad (8.5)$$

$$S_{PRO} = -f_{PRO\_S} \cdot \text{InFlux}_{SS} \quad (8.6)$$

$$S_{AS} = -f_{AS\_S} \cdot \text{InFlux}_{SS} \quad (8.7)$$

$$S_{FA} = -f_{FA\_S} \cdot \text{InFlux}_{SS} \quad (8.8)$$

where f_{AC_S}, f_{PRO_S}, f_{AS_S} and f_{FA_S} are fractions of remaining S_S to S_{AC}, S_{PRO}, S_{AS} and S_{FA} respectively. To guarantee continuity of COD f_{FA_S} is calculated from the other fractions, equation (8.9).

$$f_{FA\_S} = 1 - (f_{AC\_S} + f_{PRO\_S} + f_{AS\_S}) \quad (8.9)$$

Inerts will be passed through as such, equation (8.10).

$$S_{IN} = S_I \quad (8.10)$$

8.2.1.2 Particulate components

Fermenters (degraders of sugars and amino acids) could be estimated as a predefined fraction of heterotrophs, as some of the heterotrophs are capable of fermenting, equation (8.11).

$$X_{AS} = f_{AS\_H} \cdot X_{BH} \quad (8.11)$$

where f_{AS_H} is the fraction of X_{bh} (heterotrophs in ASM1) that is capable of fermenting.

Degraders of fatty acids, propionate, acetate and hydrogen are absent in the aerobic biomass, equation (8.12).

$$X_{FA} = X_{PRO} = X_{AC} = X_{H2} = 0. \quad (8.12)$$

Slowly biodegradable substrate X_s in ASM1 will be added to particulate biodegradable organic matter $X_{S(SIEG)}$ after possible compensation for influent S_o and S_{no}. Other particulate matter in ASM is assigned in fractions to $X_{S(SIEG)}$, equation (8.13).

$$X_{S(SIEG)} = -\left(InFlux_{XS} + f_{XS(SIEG)\_I} \cdot X_I + f_{XS(SIEG)\_H} \cdot X_{BH} + f_{XS(SIEG)\_A} \cdot X_{BA} + f_{XS(SIEG)\_P} \cdot X_P\right) \quad (8.13)$$

where $InFlux_{XS}$ is calculated from equation (8.4). $f_{XS(SIEG)\_I}$, $f_{XS(SIEG)\_H}$, $f_{XS(SIEG)\_A}$ and $f_{XS(SIEG)\_P}$ are predefined fractions of X_i, X_{bh}, X_{ba} and X_p to $X_{S(SIEG)}$, respectively. Note that some of the aerobically inerts may be anaerobically degradable.

Remaining fractions of the aerobic particulates are assigned to anaerobic inert particulates, equation (8.14).

$$X_{IN} = -\left(\left(1-f_{XS(SIEG)\_I}\right)\cdot X_I + f_{XIN\_H}\cdot X_{BH} + \left(1-f_{XS(SIEG)\_A}\right)\cdot X_{BA} + \left(1-f_{XS(SIEG)\_P}\right)\cdot X_P\right) \tag{8.14}$$

where f_{XIN_H} is the remaining inert fraction of the heterotrophs and is calculated from equation (8.15).

$$f_{XIN\_H} = 1-\left(f_{XS(SIEG)\_H} + f_{AS\_H}\right) \tag{8.15}$$

8.2.1.3 Nitrogen

The ammonia concentration should be calculated to maintain the nitrogen mass balance between incoming ASM fractions and outgoing Siegrist ADM fractions in either soluble or particulate form. Thus, appropriate fractions should be assigned for each, equation (8.16).

$$\begin{aligned} S_{NH4} = &-((S_{NH} + S_{ND} + X_{ND}) + i_{XB}\cdot(X_{BH} + X_{BA}) + i_{XP}\cdot(X_P + X_I)) \\ &+(i_{S\_AS}\cdot S_{AS(SIEG)} + i_{XS(SIEG)}\cdot X_{S(SIEG)} + i_{X(SIEG)}\cdot X_{AS} + i_{X\_IN}\cdot X_{IN}) \end{aligned} \tag{8.16}$$

where i_{XB}, i_{XP}, i_{S_AS}, $i_{XS(SIEG)}$, $i_{X(SIEG)}$ and i_{X_IN} are the mass of nitrogen per mass of COD of the corresponding components. Note that S_{NH4} is the outflux and should have a negative sign. If $S_{NH4} > 0$, parameters for fractionating ASM components must be changed.

8.2.2 Siegrist ADM to ASM1 transformer

8.2.2.1 Soluble components

Ammonia and inerts will pass through from the ADM to ASM, equations (8.17) and (8.18).

$$S_{nh} = -S_{NH4} \tag{8.17}$$

$$S_i = -S_{IN} \tag{8.18}$$

Readily biodegradable substrate S_s is estimated from the total acetate S_{ac}, propionate S_{pro}, amino acids and sugar S_{AS}, and fatty acids S_{FA}, equation (8.19).

$$S_s = -(S_{ac} + S_{pro} + S_{AS} + S_{FA}) \tag{8.19}$$

Dissolved oxygen and nitrates will be assigned zero values, equation (8.20). They are not expected from the anaerobic digester.

$$S_o = S_{no} = 0 \tag{8.20}$$

Biodegradable nitrogen will be estimated as a fraction of the amino acids, equation (8.21). Note that amino acids are lumped together with sugars in one state variable in the Siegrist ADM.

$$S_{nd} = -i_{S\,AS} \cdot S_{AS} \tag{8.21}$$

where $i_{S\,AS}$ is the mass of nitrogen per mass of S_{AS}.

Alkalinity is estimated as moles of bicarbonates, equation (8.22).

$$S_{alk} = -S_{HCO3} \tag{8.22}$$

8.2.2.2 Particulate components

Inert particulates will pass through, equation (8.23).

$$X_i = -X_{IN} \tag{8.23}$$

Heterotrophs are estimated as a fraction of the fermenters, equation (8.24).

$$X_{bh} = -f_{H\,AS} \cdot X_{AS} \tag{8.24}$$

where $f_{H\,AS}$ is the fraction of fermenting biomass that are heterotrophic aerobes.

Particulate products arising from biomass decay are estimated as the remaining fraction of the anaerobic biomass, equation (8.25). The remaining anaerobic biomass will decay under aerobic conditions.

$$X_p = -f_{P\,An} \cdot (X_{AS} + X_{FA} + X_{pro} + X_{AC} + X_{H2}) \tag{8.25}$$

where $f_{P\,An}$ is the fraction of anaerobic biomass that leads to inert particulate matter.

Slowly biodegradable substrate X_s is estimated from the corresponding $X_{S(SIEG)}$ in addition to the remaining fraction of biomass, equation (8.26).

$$X_S = -X_{S(SIEG)} - (1-(f_{P\,An} + f_{H\,AS})) \cdot X_{AS} - (1-f_{P\,An}) \cdot (X_{FA} + X_{pro} + X_{AC} + X_{H2}) \quad (8.26)$$

Autotrophs are assigned a zero value, equation (8.27). Nitrifiers are not expected in the digester outflow.

$$X_{ba} = 0 \quad (8.27)$$

Particulate nitrogen should be estimated to keep the nitrogen mass balance between incoming Siegrist ADM fractions and outgoing ASM1 fractions. X_{nd} is estimated from equation (8.28). X_{nd} is calculated in the outflux and therefore it should be negative. If $X_{nd} > 0$ the fraction parameters in the transformer need to be changed.

$$X_{nd} = -i_{X_S\,(SIEG)} \cdot X_{S(SIEG)} - i_{X_{IN}} \cdot X_{IN} - i_{X\,An} \cdot (X_{AS} + X_{FA} + X_{pro} + X_{AC} + X_{H2}) + i_{X_P} \cdot (X_I + X_P) + i_{X\,B} \cdot (X_{bh} + X_{ba}) \quad (8.28)$$

where $i_{X\,*}$ are the mass of nitrogen per mass of COD contents of the corresponding components.

8.3 Practical simplifications

The same transformers could easily be adjusted for other models. As an approximation for practical use, the transformers can be simplified by only assuming the transfer of particulates from the aerobic model to the anaerobic model. Indeed, particulates (sludge) are the main input from the aerobic plant to the anaerobic plant. For example, if the first transformer needs to be adjusted for ADM1 (IWA, 2002), the model has disintegration and hydrolysis steps and, therefore, the simplification assuming only the particulates input to the digester will reduce the number of fraction parameters in the first transformer. With a fair approximation, most of the other inputs could be set to zeroes, whereas hydrolysis fractions are considered within the model itself. However, for a more accurate calculation, maintaining the continuity of COD and nitrogen, the same approach presented in this chapter can be extended and applied for ADM1. Extended and more detailed approaches for transformations between ASM1 and ADM1 will be applied and compared in chapter 9.

8.4 Application

The Benchmark Simulation Model No.1 was developed for evaluation of activated sludge system performance (Spanjers et al., 1998; Copp, 2002). BSM1 represents a large municipal treatment plant of 100,000 P.E. and an average influent flow of 18446 m^3 day^{-1}. For the detailed description of the standard benchmark reference is made to (Copp, 2002). In this chapter, BSM1 is extended with sludge thickening, digestion and drying to allow the study of a treatment plant including its sludge digestion. The proposed extended benchmark is shown in Figure 8.3.

The underflow from the final clarifier with a solid concentration of about 1% is fed to a thickener. The thickener is modelled as a point settler with an underflow of 45 m^3day^{-1} that gives an underflow solid concentration of about 6%. The first transformer converts the sludge flow from ASM1 to Siegrist ADM components. The sludge digester is designed with a liquid volume of 1400 m^3 and a gas volume of 100 m^3. The second transformer is applied to convert from Siegrist ADM to ASM1 components.

The transformed outflow from the digester is fed to a sludge-drying unit. The sludge drying is modelled as an ideal separator that acts as mechanical drying. The dryer was configured to increase the solids concentration to about 16-18%. The overflow from the thickener and the liquor from the drying units are returned back to the inlet of the activated sludge plant. With this configuration, the sludge volume is reduced in the digester by conversion to biogas and the sludge is further concentrated by the drying unit. Therefore, the extended benchmark plant presents a typical configuration of the sludge handling facilities.

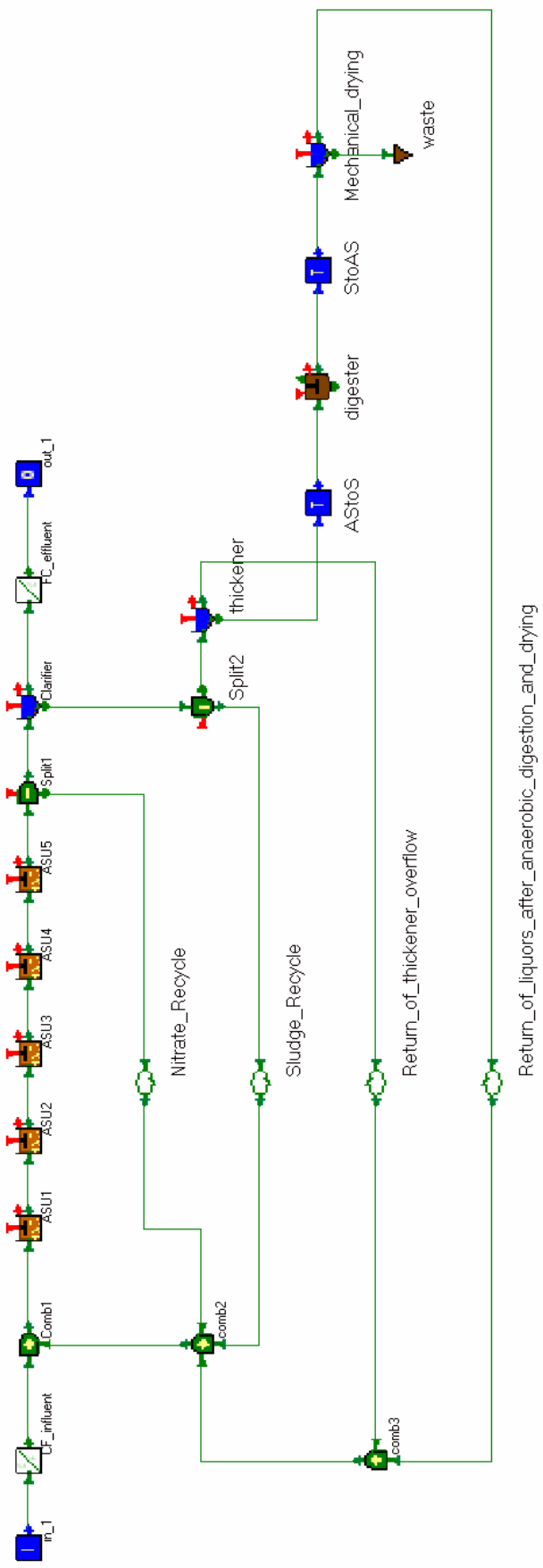

Figure 8.3 Extended benchmark plant

8.5 Simulation Results

First, the plant was run for 1000 days on the standard steady state flow to initialize the state variables. Then the standard dynamic dry weather flow was simulated. The dynamic results are evaluated in terms of biogas production, solids reduction and the effect of return flows from the digester to the ammonia and nitrate concentration in the plant effluent. It can be seen in Figure 8.4 that the amount of gas produced in terms of CO_2 and CH_4 is close to what is expected in common practice.

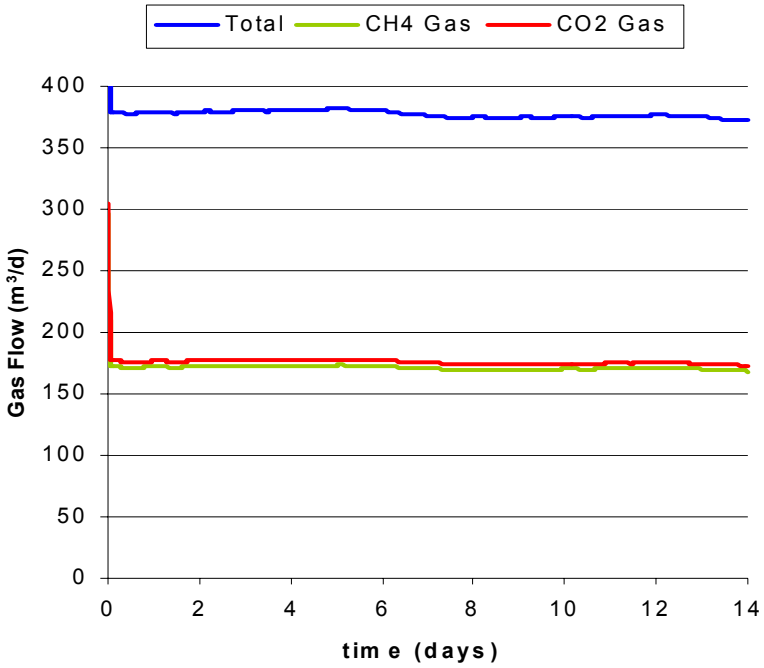

Figure 8.4 Total gas production (digestor)

The amount of CH_4 produced is considerable but the CH_4/CO_2 ratio is a bit low, 50%, compared to what is optimally expected from the sludge digester, 60-65% CH_4/CO_2. The Siegrist el. (1995) ADM over predicts the CO_2 flow since it considers immediate stripping of the produced gases and doesn't consider the gas transfer into the liquid. Reference is made to the gas flow modelling simplification described for the Siegrist et al. (1995) ADM in chapter 3. CO_2 is more soluble compared to CH_4 and therefore a considerable portion of the produced CO_2 will dissolve in the liquid and not appear in the gas flow.

Figure 8.5 shows the fluxes of digester influent and effluent total Volatile Suspended Solids, VSS. The total volatile suspended solids flux is reduced to about half due to the conversion to biogas in the digester. Comparing the trend of the influent and effluent VSS, the dynamics of the influent is eliminated in the outflow. The high solids residence time, about 20 days, in the digester causes the smoothing of the dynamics that occur at relatively short time, e.g. diurnal dynamics.

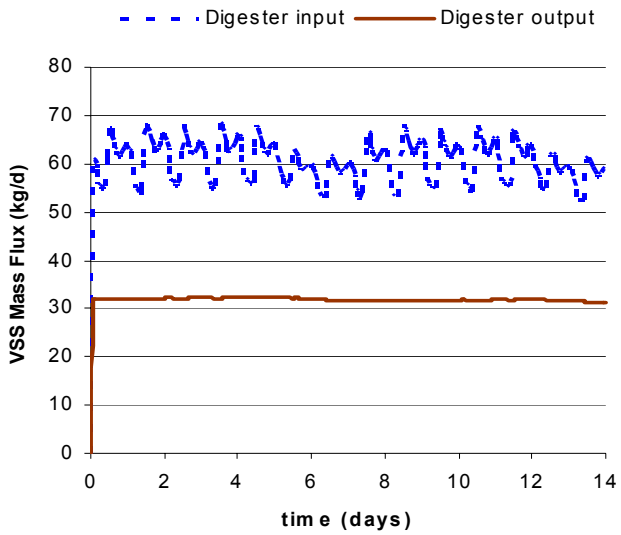

Figure 8.5 Digester influent and effluent total volatile suspended solids

Figure 8.6 shows the nitrate concentration in the activated sludge plant effluent. The figure compares the nitrate concentration results with and without the sludge digester recycle flows. The system with sludge digester has an improved operation because the recycled readily biodegradable substrates (VFA) are enhancing denitrification and therefore a reduction of the nitrate concentration is observed in the final plant effluent.

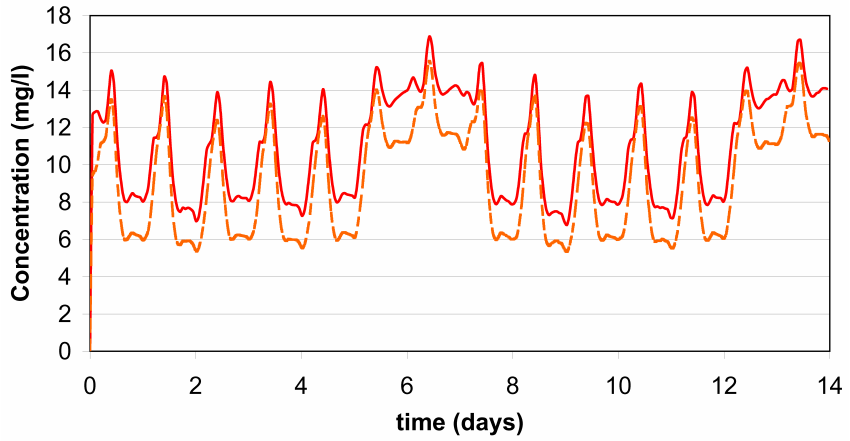

Figure 8.6 Nitrate effluent from the treatment plant with (– – –) and without (———) the sludge digestion loop

Figure 8.7 shows the ammonia concentration in the activated sludge plant effluent. The figure compares the ammonia concentration results with and without the sludge digester return liquors. Including the digester loop, ammonia is slightly higher as it is produced in the digester and therefore increases the ammonia loads to the activated sludge system to levels that are higher than the nitrification capacity allows to remove. However, a separate treatment of sludge return liquors could be added, for instance by incorporating a SHARON reactor (Hellinga et al, 1999; van Dongen et al, 2001; Van Hulle, 2005; van

Kempen et al., 2001; Volcke et al., 2003) between the digester and the activated sludge system.

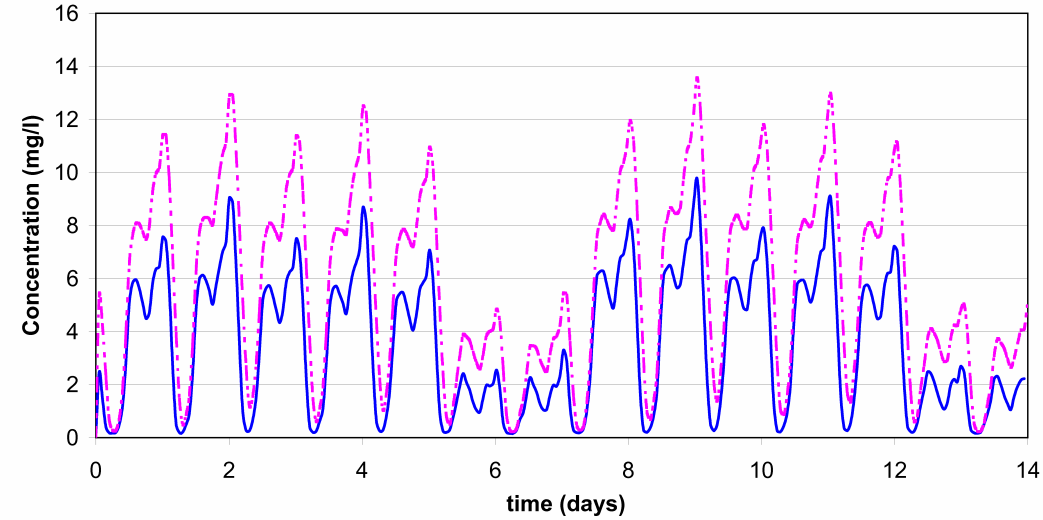

Figure 8.7 Ammonia effluent from the treatment plant with (— . . —) and without (——) the sludge digestion loop

8.6 Conclusions

The approach of connecting digesters by transformers successfully facilitated the inclusion of the anaerobic digestion model and sludge treatment train in a plant-wide modelling application. The extended benchmark example could be used for the evaluation of the performance of the sludge digester and its impact on the activated sludge process. The methane production rates could be simulated and therefore the economic value of using methane for energy production can be evaluated. The reduction of sludge volumes can be estimated from the simulated volatile suspended solids and therefore the sludge handling and disposal can be planned efficiently. Impacts of the digester on the overall plant performance could be evaluated. Thus, improvement of denitrification due to the recycle of VFA from the digester can be simulated and therefore the denitrification capacity of the plant can be optimised. The increase of the ammonia loads due to recycled digester overflows can be simulated and therefore the necessary increase of the plant nitrification capacity can be studied. The inclusion of a new process such as SHARON to treat the digester overflows can now be evaluated in an easy way too. Because of the flexibility introduced in the approach, connecting other flows with characteristics more specific to the anaerobic model state variables is now possible and therefore more general strategies of anaerobic digestion can be evaluated. The option of central sludge treatment from several plants can be studied as well. Connecting other wastewaters, e.g. from industry, to the treatment plant digester rather than connecting them to the inflow of the activated sludge system can be studied too.

Chapter 9

Comparison of transformation methods: application to ASM1 and ADM1

Abstract

In view of the growing importance of integrated and plant-wide modelling of wastewater treatment plants, this work reviews, applies and compares two transforming/interfacing methods by connecting anaerobic and aerobic models. The two methods are systematic approaches to transform state variables of one model to another and vice versa. The theory of the first method was presented before (Vanrolleghem et al., 2005) as a general approach for interfacing any two models presented by Petersen matrices. The present work is the first application and therefore validation of this general method. The theory of the second method was specifically developed for connecting ASM1 and ADM1, both standard IWA models. As an illustration, in this work a specific simulation example is presented in which the COST/IWA activated sludge benchmark plant is extended by sludge treatment and digestion facilities.

CHAPTER 9

9.1 Introduction

Integrated modelling of wastewater systems comprising the collection network (sewer system), the treatment plant and the receiving water has been growing and advancing since the late 90's (Butler and Schütze, 2005; Meirlaen et al., 2001). Therefore, general interfacing methods are needed to build standard transformers and connect different models of the wastewater systems. The treatment plant processes too should be dealt with in an integrated manner. Plant-wide modelling including anaerobic sludge digestion which is closely integrated to the activated sludge system has been proposed (Jeppsson et al., 2004). The flexible approach of using transformers and the example of the extended benchmark implemented in Chapter 8 will be used in this Chapter to compare two interfacing methods. The example is applied here to interface ADM1 to ASM1 as shown schematically in Figure 9.1. The schematic figure shows the flexibility introduced by transformers so that other loads are fed to the digester, for instance, with externally supplied truck loads of organic waste.

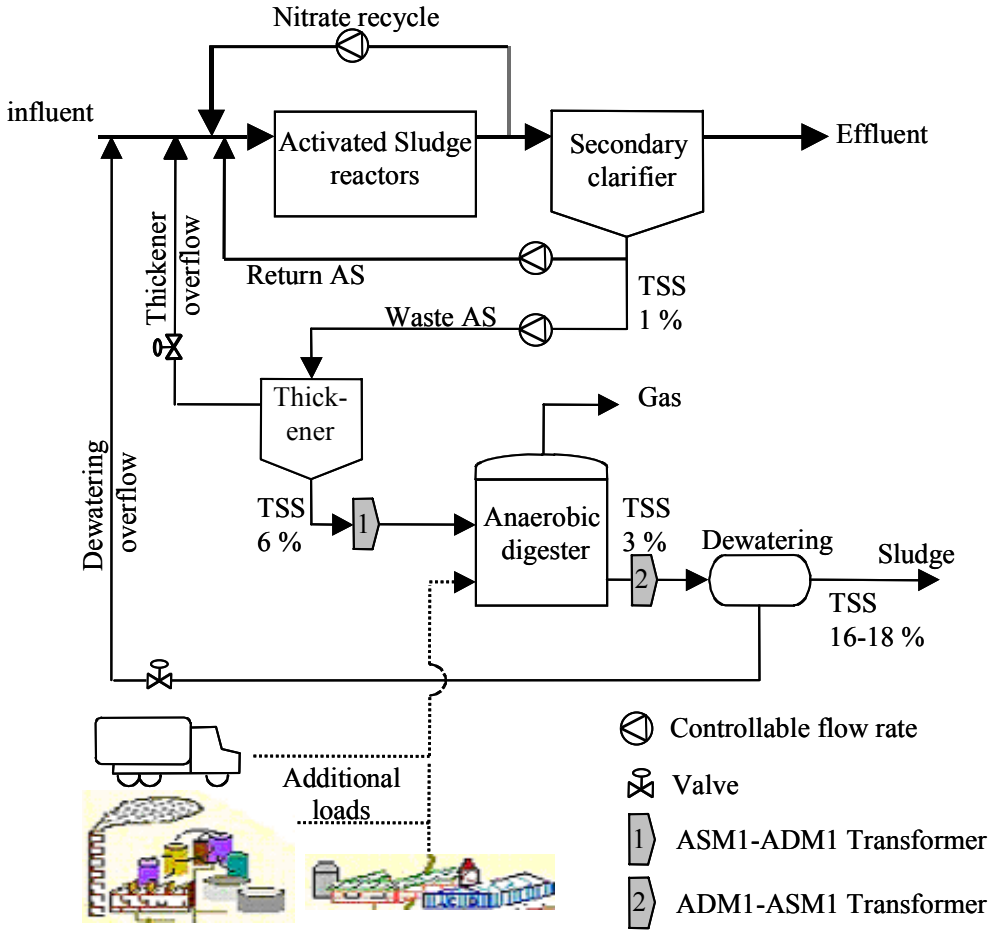

Figure 9.1 Extended benchmark plant with sludge treatment including the anaerobic digester, adapted from (Jeppsson et al., 2004).

The considered models are ASM1 (Henze et al., 2000) as description of the activated sludge process and ADM1 (Batstone et al., 2002) for the digester. Two transformers are built for each of the two interfacing methods that are compared and implemented in this study. The activated sludge plant is considered as a pre-treatment that concentrates the pollutants in the form of thickened secondary sludge to the digester; for this an ASM1-ADM1 transformer is needed. The activated sludge plant is also considered as post-treatment of the return liquors originating from sludge digestion and drying; for this, an ADM1-ASM1 transformer is needed.

9.2 Interfacing methods

Two methods are implemented in this work to interface the anaerobic model ADM1 to the activated sludge model ASM1 and vice versa. The first method is the general Continuity-Based Interfacing Method (CBIM) for models of wastewater systems described by Petersen matrices (Vanrolleghem et al., 2005). Since it is the first time the CBIM is applied and validated, the CBIM itself and its results will be illustrated in detail. The second method was specifically developed for ASM1-ADM1-ASM1 interfacing. It operates by Maximising some components with respect to the total COD and Nitrogen contents. In this chapter the method is further referred as MCN. The complete theory of MCN is described in detail in (Copp et al., 2003) but no examples or results are given there. Therefore, the MCN will be introduced briefly in the case study section and results of its application will be presented. It will be also compared with the general CBIM method.

9.2.1 CBIM transformer

A CBIM transformer is built in 4 main steps:

Step 1: Elemental mass fractions and charge density

The fundamental formulation of elemental mass fractions is based on the hypothesis that the mass of each component in a model is made up of constant mass fractions of the elements C, H, O, N and P according to Reichert et al. (2001). Note that no other elements are considered here (e.g. S, K, …), but an extension would be straight forward. Furthermore, each component may have an associated charge per unit of mass (De Gracia et al., 2004; Reichert et al., 2001). The elemental mass fractions **($\alpha_{C,k}$, $\alpha_{H,k}$, $\alpha_{O,k}$, $\alpha_{N,k}$, $\alpha_{P,k}$)** for a generic model component X_k are defined as the mass of elements: C, H, O, N or P per unit of mass of this component (X_k). The calculation of these mass fractions is immediate for all those model components that have a known composition formula. A proper estimation must be carried out for the elemental mass fractions of the components that do

not have a known composition. According to the hypothesis above, the sum of all elemental mass fractions of each component X_k must be unity, equation (9.1).

$$\alpha_{C,k} + \alpha_{H,k} + \alpha_{O,k} + \alpha_{N,k} + \alpha_{P,k} = 1 \tag{9.1}$$

The charge density (α_{Chk}) for a generic model component X_k is defined as the electric charge associated to its unit of mass. For each component X_k, it is calculated as the quotient of its molecular charge and its molecular weight. Normally, not all the components X_k can be defined by a molecular formula, i.e. their molecular weight is unknown. However, once the elemental mass fractions and the charge density have been assigned, one unit of mass of any model component X_k can be expressed with a general formula, equation (9.2).

$$\left[C_{(\alpha_{C,k}/12)} H_{(\alpha_{H,k})} O_{(\alpha_{O,k}/16)} N_{(\alpha_{N,k}/14)} P_{(\alpha_{P,k}/31)} \right]^{\alpha_{Ch,k}} \tag{9.2}$$

Step 2: Composition matrix

A composition matrix can be defined as in Table 9-1. For a model component $\boldsymbol{X_k}$ that has an elemental mass fraction α_k of certain element (mass unit of element / mass unit of model component), a composition matrix element i_k (mass unit of element / stoichiometric unit of model component) can be defined from equation (9.3).

$$i_k = \alpha_k \cdot m_k \tag{9.3}$$

where m_k is the mass of the component per stoichiometric unit. For all model components, corresponding composition matrix elements ($i_{ThoD,k}$, $i_{C,k}$, $i_{N,k}$, $i_{O,k}$, $i_{H,k}$, $i_{P,k}$) are evaluated in unit of mass per stoichiometric unit. As the models to be interfaced can express their components in different units, a certain unit of mass is chosen in common for all composition matrix elements except for charge. As a result, the unit conversions between both models are considered during transformation. In the presented case study, the composition matrix elements have been expressed as grams of C, H, N, O, P and charge per stoichiometric unit. The charge of the ionised portion of the component, $i_{e,k}$ is calculated as positive or negative charge unit per stoichiometric unit of component. The composition matrix elements are easily calculated when the stoichiometric formulas of the components are well-known. However, for the components with unknown stoichiometric formulas and measured in COD units, a relationship between the mass fractions and COD must be established to calculate the corresponding composition matrix elements. Once the elemental mass fraction and charge density have been defined for these model components,

their Theoretical Oxygen Demand (***ThOD***) can be calculated. ***ThOD*** has been introduced to characterise organic as well as inorganic compounds (Gujer et al., 1999).

Step 3: Transformation matrix

The CBIM aims to construct a set of algebraic transformation equations on the basis of a Petersen matrix description of the two models to be interfaced. In this methodology, the matrix description is somewhat different from the original models' Petersen matrices. The new matrix has the components of the two models to be interfaced, sorted into two panes: *P* components of the "origin" model and *Q* components of the "destination" model (see Table 9-1). A set of transformation (conversions) are left to the CBIM user to be defined based on expert knowledge concerning the two model systems. Yet, before starting to generate the algebraic transformation equations, the elemental mass fractions of the models' components need to be defined. The mass fractions of all the components are determined and subsequently the composition matrix elements are defined.

Table 9-1 Matrix description of interface between Petersen matrix based models, adapted from (Vanrolleghem et al., 2004)

Petersen matrix section Model 1 ("origin")						**Petersen matrix section Model 2 ("destination")**				
j ↓ k →	X_1	X_2	…	X_P		X_{P+1}	X_{P+2}	…	X_{P+Q}	Rate
Conv. 1	$\nu_{1,1}$	$\nu_{1,2}$	…	$\nu_{1,P}$		$\nu_{1,P+1}$	$\nu_{1,P+2}$	…	$\nu_{1,P+Q}$	ρ_1
:	:	:	:	:		:	:	:	:	:
Conv. n	$\nu_{n,1}$	$\nu_{n,2}$	…	$\nu_{n,P}$		$\nu_{n,P+1}$	$\nu_{n,P+2}$	…	$\nu_{n,P+Q}$	ρ_n
Composition matrix section Model 1						**Composition matrix section Model 2**				
ThOD	$i_{ThOD,1}$	$i_{ThOD,2}$	…	$i_{ThOD,P}$		$i_{ThOD,P+1}$	$i_{ThOD,P+2}$	…	$i_{ThOD,P+Q}$	
C	$i_{C,1}$	$i_{C,2}$	…	$i_{C,P}$		$i_{C,P+1}$	$i_{C,P+2}$	…	$i_{C,P+Q}$	
N	$i_{N,1}$	$i_{N,2}$	…	$i_{N,P}$		$i_{N,P+1}$	$i_{N,P+2}$	…	$i_{N,P+Q}$	
H	:	:	:	:		:	:	:	:	
O	:	:	:	:		:	:	:	:	
P	:	:	:	:		:	:	:	:	
charge	$i_{e,1}$	$i_{e,2}$	…	$i_{e,P}$		$i_{e,P+1}$	$i_{e,P+2}$	…	$i_{e,P+Q}$	

Next is to define the conversion processes from the origin to the destination components. All proposed conversions must guarantee the continuity of C, H, O, N, P and charge. For this purpose a set of components taken either from the origin or the destination model should act as source-sink. These components are also called compensation terms (Benedetti et al., 2004) and are needed to accomplish the next equations that are written for each conversion *j*:

$$\sum_k \nu_{j,k} i_{j,Comp} = 0 \quad _{with\ Comp=Thod,C,N,H,O,e} \tag{9.4}$$

Equation (9.4) generates a set of algebraic equations as constraints on the stoichiometry terms $\nu_{j,k}$ to achieve the mass and charge conservation of a conversion *j*. If the number of non-zero $\nu_{j,k}$ is less than the number of rows in the composition matrix, the set of equations will be over-determined. The approach in this situation is to add other "source-sink" components in order to have a single solution of the equations that maintains the continuity. For other conversions, the number of non-zero $\nu_{j,k}$ may be larger than the number of rows in the composition matrix and the solution of the linear equation to calculate the stoichiometric parameters is under-determined.

Guiding Transformation Principles (GTPs) that will lead to a feasible solution of the linear system of equations produced by equation (9.4) (stoichiometry calculation) are as follows:

- Try different choices of source-sink components.
- Some reactions conversions can be split some other can be combined.
- More knowledge (assumptions) can be incorporated in the conversions, e.g. fractions of "origin" components to "destination" components.

For calculating the stoichiometric parameters, the GTPs are applied to guide the user to select proper conversions. These principles are also to be applied in two other steps when setting up the transformation algebraic equations.

The introduction of the sourcing components turns the problem of defining the stoichiometry from an algebraic solution of linear equations to a minimisation problem. In general, the value of $\nu_{j,k}$ related to the "sourcing" components should be kept to a minimum, e.g. just to compensate for the difference in the elemental composition between origin and destination components. One component, in the presented case study it is only Oxygen, can be chosen to be minimised by tuning the other $\nu_{j,k}$ in each conversion reaction to maintain the continuity within an acceptable tolerance.

A constraint needs to be added on the sign of some stoichiometric parameters. First, an exception is that the sign of a stoichiometric parameter related to the sourcing components is allowed to be positive or negative. Second, for conversions that are assumed to happen immediately in the "origin" model only, e.g. oxygen and nitrate depletion and immediate hydrolysis of slowly degradable substrate, the sign of the corresponding

stoichiometric parameters should be assigned logically to maintain the conversion direction. Third, the sign of the remaining stoichiometry is such that the "origin" stoichiometry is negative while the destination stoichiometry is positive to maintain the conversion in the right direction.

A spreadsheet can be used to easily evaluate the stoichiometry. Minimisation can be done using the spreadsheet. Also, the evaluation of the stoichiometry can be automated by building the transformer in a simulation platform and implementing a simple constrained minimisation algorithm.

Step 4: Transformation equations

Once the stoichiometric parameters have been defined, a set of algebraic equations is generated, equation (9.5), to determine the unknown conversion rates of all conversion reactions ρ_j by using the influxes of the transformer that are coming from the "Origin" model.

$$\sum_{j=1}^{n} \nu_{j,k} \rho_j = Influx_k \qquad for\ k=1,P \tag{9.5}$$

Transformer outfluxes can then be calculated as function of the calculated conversion rates according equation (9.6)

$$Outflux_k = \sum_{j=1}^{n} \nu_{j,k} \rho_j \qquad for\ k=P+1,P+Q \tag{9.6}$$

Two conditions need to be fulfilled to make the solution of equation (9.5) for values of ρ_j feasible and practical. First, to make it feasible, the number of suggested conversions should not exceed the number of the "origin model" components. The use of fraction parameters can help in combining conversions and therefore reduce their total number. Reducing the number of conversions solves the problem of an under determined solution of linear equations needed to calculate the conversion rates. This is the second step in which the GTPs can be applied to help in designing the right conversions. Second, to make the solution of equation (9.5) practical, all rates should lead to obligatory negative outfluxes, i.e. the transformation should be carried out in the right direction. This can be tested by applying a practical range of influxes and check the sign of the outfluxes. If some outfluxes are not negative, the conversions should be modified. This is the third step in which the GTPs can be applied to guide the user to find the right conversion reactions and maintain the transformation in the right direction.

9.2.2 Case study

In this section, the CBIM is applied to build ASM1-ADM1 and ADM1-ASM1 transformers. A brief description is also provided for implementing the alternative methodology to build the transformers, MCN of Copp et al. (2003). A plant-wide model is used to compare both CBIM and MCN methods in the results section.

9.2.2.1 CBIM ASM1-ADM1 transformer

Step 1: Elemental mass fractions and charge density

A list of mass fractions suggested for ASM1 and ADM1 is given in Table 9-2 and Table 9-3, respectively. The mass fractions of the models' components are estimated according their stoichiometric formulae. For components that do not have stoichiometric formulae, some assumptions are made as indicated in Table 9-2 and Table 9-3.

For example, empirical formula $C_5H_7O_2N$ is used to represent biomass, as in the ASM series (Henze et al. 1987) and as suggested in the IWA ADM1 report (Batstone et al., 2002) but adjusted with addition of a phosphorous fraction. Note, however, that phosphorous is not considered in the original models. A 3% phosphorous mass fraction has been considered for the biomass to ensure a complete implementation of the elemental mass balances.

Table 9-2 Elemental mass fractions and charge density of ASM1 components

	components	S_s	S_{no3}	S_I	X_S	X_{BH}	X_{BA}	X_I	X_P	S_{nh4+}	S_{ND}	X_{ND}	S_{alk}	S_{n2}	S_O
mass fractions	α_C (gC/gComponent) [a]	0.62		0.65	0.62	0.51	0.51	0.56	0.51				0.20		
	α_N (gN/gComponent)		0.23			0.12[d]	0.12[d]	0.09[e]	0.12[d]	0.78	1.00	1.00		1.00	
	α_O (gO/gComponent)	0.28[b]	0.77	0.28[b]	0.28[b]	0.28[d]	0.28[d]	0.28[e]	0.28[d]				0.79		1.00
	α_H (gH/gComponent)	0.08[b]		0.07[b]	0.08[b]	0.06[d]	0.06[d]	0.06[e]	0.06[d]	0.22			0.02		
	α_P (gP/gComponent)	0.02[c]			0.02[c]	0.03[c]	0.03[c]	0.01[c]	0.03[c]						
	α_Ch (Ch/gComponent)		-0.02							0.06			-0.02		-1.00

a: calculated as the remaining mass fraction after the assignment of other elements fractions.
b: taken from RWQM1 (Reichert et al., 2001).
c: assumed phosphorous content
d: biomass stoichiometric formula (Batstone et al., 2002; Henze et al., 1987)
e: similar to ADM1

Table 9-3 Elemental mass fractions and charge density of ADM1 components

	components	S_l	S_{su}	S_{aa}	S_{fa}	S_{va}	S_{bu}	S_{pro}	S_{ac}	S_{h2}	S_{ch4}	X_l	X_c	X_{ch}	X_{pr}	X_{li}	$X_{su\cdots h2}$	S_{in}[f]	S_{ic}[g]
mass fractions	α_C (gC/gComponent)	0.56[b]	0.40	0.47[b]	0.75	0.59	0.55	0.49	0.41		0.75	0.56[b]	0.57[b]	0.40	0.47[b]	0.76	0.51[a]		0.20
	α_N (gN/gComponent)	0.09[b]		0.15[b]								0.09[b]	0.06[b]		0.15[b]		0.12[d]	0.78	
	α_O (gO/gComponent)	0.28[e]	0.53	0.28[b]	0.12	0.32	0.37	0.44	0.54			0.28[e]	0.28[e,d]	0.53	0.28	0.11	0.28[d]		0.79
	α_H (gH/gComponent)	0.06[a]	0.07	0.10[a,b]	0.13	0.09	0.08	0.07	0.05	1.00	0.25	0.06[a]	0.09[a]	0.06	0.10	0.12	0.06[d]	0.22	0.02
	α_P (gP/gComponent)	0.01[c]										0.01[c]	0.01[c]	0.01[c]		0.01[c]	0.03[c]		
	α_Ch (Ch/gComponent)					-0.01	-0.01	-0.01	-0.02									0.06	-0.02

a: calculated as the remaining mass fraction after the assignment of other elements fractions.
b: satisfy ADM1 fraction parameters
c: assumed phosphorous content
d: biomass stoichiometric formula (Batstone et al., 2002; Henze et al., 1987)
e: similar to ASM1
f: $S_{in} = NH_4^+$
g: $S_{ic} = HCO_3^-$

Note that model parameters should agree with the applied assumptions. For the example, the fractions of nitrogen, hydrogen and oxygen are maintained similar to the empirical formula so that they agree with the nitrogen content given in ASM1. Accordingly, the biomass carbon and nitrogen fractions in ADM1 should be 0.0305 kmole C/kg COD and 0.0061 kmole N/kg COD.

In another example, the carbon and nitrogen fractions are considered first to agree with the ADM1 parameters, i.e. the fractions of X_c leading to carbohydrates, proteins, lipids and inerts. Consequently, the oxygen mass fraction is assumed similar to biomass (secondary sludge), but a lower phosphorous fraction of 1% is assumed (release of phosphorous under anaerobic conditions). It is also assumed that the pH will be in the optimum range of both processes, e.g. pH from 7 to 8. Hence, alkalinity and inorganic carbon will be mainly bicarbonate, inorganic nitrogen is mainly ammonium and VFA's are mainly in the ionised form. The charge density for those components is calculated accordingly.

In addition to the elemental mass fractions of the components of both models, three source-sink components are needed. Their mass fractions are defined in Table 9-4. Also, a component S_{n2} is considered for stripping of nitrogen when S_{no3} is nitrified.

Table 9-4 Elemental mass fractions and charge density of the additional sourcing components

	components	S_{ip}	S_{H+}	S_{H2O}
mass fractions	α_C (gC/gComponent)			
	α_N (gN/gComponent)			
	α_O (gO/gComponent)	0.67		0.89
	α_H (gH/gComponent)	0.01	1.00	0.11
	α_P (gP/gComponent)	0.32		
	α_Ch (Ch/gComponent)	-0.02	1.00	

Step 2: Composition matrix

The mass fractions α are calculated as g element/g component. The composition matrices i of both models are calculated by multiplying the elemental mass fractions and charge density by the number of grams in each component's stoichiometric unit. The units of the composition matrix are g element/stoichiometric unit. Therefore, differences in stoichiometric units between components of both models are reflected in the composition matrices and unit conversions need to be considered during transformation. Composition matrices are given as the bottom panes of the transformation matrices Table 9-5 and Table 9-6.

Step 3: Transformation matrix

The Petersen matrix suggested in Table 1 is built and presented Table 9-5 and Table 9-6. From the "origin" model ASM1 S_o is taken as a "sourcing sink" component for Oxygen. Accordingly, $\nu_{j,14}$ was kept minimal during the calculation of the other stoichiometric parameters. On the other side, two sourcing components S_{ic} and S_{in} are taken from the "destination" model ADM1 as sourcing components for carbon and nitrogen. Three other components S_{ip}, S_{H+} and S_{H2O} (inorganic phosphorus, protons and water) are introduced to the destination matrix. These components are used as source-sink for phosphorous, charge and hydrogen respectively. If these components and the corresponding continuity of phosphorus, charge and hydrogen are eliminated, the other stoichiometry values and the COD, C and O continuity will remain unaffected. However, these components are still mentioned in both transformers' matrices for the sake of completeness of the method illustration. They could be used in future for interfacing extended models but their stoichiometry will not be considered in the present implementation and simulation.

The number of suggested conversions is 12. In reaction 1 and 3, S_{nh4+} and S_{alk} are assigned directly to the sourcing components S_{in} and S_{ic}. The conversions 4, 5 and 6 are held internally in the "origin" model pan assuming the immediate hydrolysis of X_{ND} to S_{ND} and the depletion of S_o and S_{no3-}. The depletion is accompanied with formation of X_{bh} and a minimal increase of S_{ic} and a decrease of S_{in}.

Conversion 2 represents transformations of S_{ND} and S_s to S_{su}, S_{aa} and S_{fa}. Note that this is the most complex conversion. For $\nu_{2,1}$= -1 (under S_s) the assumed COD fractions to S_{su} and S_{fa} are 0.3 and 0.2 respectively. So, the $\nu_{2,16}$ (under S_{su}) and $\nu_{2,18}$ (under S_{fa}) are then calculated straightforwardly. The $\nu_{2,17}$ (under S_{aa}) has been assigned a formula to close the nitrogen balance of this conversion. The $\nu_{j,10}$ is assigned a value of -1 (under S_{ND}). The $\nu_{2,4}$ (under X_s) is then determined by minimising $\nu_{2,14}$ (under S_o), i.e. by closing the COD

balance properly. The main reason for the complexity of this conversion is the simultaneous transformation of S_{ND} and S_s with the instantaneous hydrolysis of X_s. Efforts have been made to split this conversion into two independent conversions, one for each component, but it was not feasible because the conversion of S_{ND} alone to S_{aa} will need a big sourcing of COD for which the S_s influxes are normally not sufficient. It would lead to a reverse outflux, i.e. immediate COD consumption from the digester. Of course, this is not acceptable. That is why conversion 8 that was originally meant for the direct conversion of S_s has been eliminated and combined with conversion 2. Further needs of COD can now be provided from X_s, in two steps. The first compensates the COD deficiency in the transformation to S_{aa}. The second step will be described in the next section as part of the calculation of the conversion rates. The design of conversion 2 highlights the insight required when designing the conversion reactions.

Understanding conversion 2 makes the rest of the conversions straightforward and self-explanatory from the matrix. Some points should be noted, however. In conversion 7, $\nu_{7,10}$ was calculated from the nitrogen balance. $\nu_{7,15}$ was determined by minimising $\nu_{7,14}$, i.e. by closing the COD balance without oxygen leaks. In conversions 9 and 10 a 10% fraction of the inerts in ASM1 was assumed to be anaerobically biodegradable. A 10% fraction of the aerobic heterotrophic biomass is considered capable of sugar fermentation. These fractions are examples of the degrees of freedom that one can add to reflect some actual phenomena occurring in the system. However, with such assumptions, the continuity should still be carefully checked to prevent any leaks of mass.

Table 9-5 ASM1-ADM1 transformer: "origin" model pan

		K	1	2	3	4	5	6	7	8	9	10	11	12	13	14
		components	S_s	S_{no3}	S_I	X_S	X_{BH}	X_{BA}	X_I	X_P	S_{nh4+}	S_{ND}	X_{ND}	S_{alk}	S_{n2}	S_O
	J	Conversions	(gCOD m^{-3})	(gN m^{-3})	(gCOD m^{-3})	(gCOD m^{-3})	(gCOD m^{-3})	(gCOD m^{-3})	(gCOD m^{-3})	(gCOD m^{-3})	(gN m^{-3})	(gN m^{-3})	(gN m^{-3})	(molHCO$_3^-$ m^{-3})	(gN m^{-3})	(-gCOD m^{-3})
	1	S_{nh4+}_S_{in}									-1					3.331E-16
	2	S_{ND},S_s_S_{aa},S_{fa},S_{su}	-1			-11.32222						-1				-2.22E-15
	3	S_{alk}_S_{ic}												-1		
	4	Hydrolysis X_{ND}										1	-1			
	5	O_2 depletion	-1.492537				1									-0.492537
	6	NO_3 depletion	-1.492537	-0.172216			1								0.1722158	-0.000492
	7	S_i_S_I			-1							-0.052754				-1E-06
	9	X_P_X_I								-1						1.318E-16
	10	X_L_X_I							-1							-4.86E-17
	11	X_s_X_c				-1										-2.78E-16
	12	X_{bh}_X_c,X_{su}					-1									-8.33E-17
	13	X_{ba}_X_c						-1								-8.33E-17
composition matrix		i_ThOD (gThOD/stoich.unit)	1.000	-4.571	1.00	1.000	1.00	1.00	1.00	1.00		-1.714	-1.714		-1.714	-1.000
		i_C (gC/stoich.unit)	0.305		0.32	0.305	0.37	0.37	0.36	0.37				12.000		
		i_N (gN/stoich.unit)		1.000			0.09	0.09	0.06	0.09	1.00	1.000	1.000		1.000	
		i_O (gO/stoich.unit)	0.137	3.429	0.14	0.137	0.20	0.20	0.18	0.20				48.000		1.000
		i_H (gH/stoich.unit)	0.039		0.03	0.039	0.04	0.04	0.04	0.04	0.29			1.000		
		i_P (gP/stoich.unit)	0.009			0.009	0.02	0.02	0.01	0.02						
		i_Ch (Ch/stoich.unit)		-0.0714286							0.07			-1.000		

Table 9-6 ASM1-ADM1 transformer: "destination" model pan

J	Conversions	15 S_I	16 S_{su}	17 S_{aa}	18 S_{fa}	19 S_{va}	20 S_{bu}	21 S_{pro}	22 S_{ac}	23 S_{h2}	24 S_{ch4}	25 X_I	26 X_c	27 X_{ch}	28 X_{pr}	29 X_{li}
	components	($kgCOD\ m^{-3}$)	($kgCOD\ m^{-3}$)	($kgCOD\ m^{-3}$)	($kgCOD\ m^{-3}$)	($kgCOD\ m^{-3}$)	($kgCOD\ m^{-3}$)	($kgCOD\ m^{-3}$)	($kgCOD\ m^{-3}$)	($kgCOD\ m^{-3}$)	($kgCOD\ m^{-3}$)	($kgCOD\ m^{-3}$)	($kgCOD\ m^{-3}$)	($kgCOD\ m^{-3}$)	($kgCOD\ m^{-3}$)	($kgCOD\ m^{-3}$)
1	S_{nh4+}_S_{in}															
2	S_{ND},S_s_S_{aa},S_{fa},S_{su}		0.0003	0.0101079	0.0002											
3	S_{alk}_S_{ic}															
4	Hydrolysis X_{ND}															
5	O_2 depletion															
6	NO_3 depletion															
7	S_i_S_I	0.0009096														
9	X_P_X_I											0.0009	0.0001			
10	X_i_X_I											0.0009	0.0001			
11	X_s_X_c												0.001			
12	X_{bh}_X_c,X_{su}												0.0009			
13	X_{ba}_X_c												0.001			
composition matrix	i_ThOD (gThOD/stoich.unit)	1000	1000	1000	1000	1000	1000	1000	1000	1000	1000	1000	1000	1000	1000	1000
composition matrix	i_C (gC/stoich.unit)	360.883797	375	309.987437	256.849315	288.5	300	321.4	375		187.5	360.883797	309.539613	388.6	310	263
composition matrix	i_N (gN/stoich.unit)	57.9991817		98.9321608								57.9991817	30.9539613		98.93	
composition matrix	i_O (gO/stoich.unit)	180.441899	500	184.673367	41.0958904	153.8	200	285.7	500			180.441899	151.511495	514.9	184.7	38.07
composition matrix	i_H (gH/stoich.unit)	38.6661211	62.5	65.9547739	44.5205479	43.27	43.75	44.64	46.88	125	62.5	38.6661211	46.7024679	58.29	65.95	41.53
composition matrix	i_P (gP/stoich.unit)	6.44435352										6.44435352	4.34441562	9.715		3.461
composition matrix	i_Ch (Ch/stoich.unit)					-4.81	-6.25	-8.93	-15.6							

J	Conversions	30 X_{su}	31 X_{aa}	32 X_{fa}	33 X_{c4}	34 X_{pro}	35 X_{ac}	36 X_{h2}	37 S_{an}	38 S_{cat}	39 S_{in}	40 S_{ic}	41 S_{ip}	42 S_{H+}	43 S_{H2O}
	components	($kgCOD\ m^{-3}$)	($kgCOD\ m^{-3}$)	($kgCOD\ m^{-3}$)	($kgCOD\ m^{-3}$)	($kgCOD\ m^{-3}$)	($kgCOD\ m^{-3}$)	($kgCOD\ m^{-3}$)	($kmole\ m^{-3}$)	($kmole\ m^{-3}$)	($kmoleN\ m^{-3}$)	($kmoleC\ m^{-3}$)	($kmoleP\ m^{-3}$)	($kmole\ m^{-3}$)	kmole
1	S_{nh4+}_S_{in}										7.143E-05			-1.39E-20	-2.08E-20
2	S_{ND},S_s_S_{aa},S_{fa},S_{su}											3.806E-05	3.468E-06	4.5E-05	-0.000149
3	S_{alk}_S_{ic}											0.001			
4	Hydrolysis X_{ND}														
5	O_2 depletion										-6.16E-06	7.368E-06	-2.64E-07	1.3E-05	9.961E-06
6	NO_3 depletion										-6.16E-06	7.368E-06	-2.64E-07	6.951E-07	1.611E-05
7	S_i_S_I											-4.5E-07	-1.86E-07	-8.22E-07	5.285E-07
9	X_P_X_I										2.206E-06	8.775E-07	4.861E-07	-3.57E-07	-3.11E-06
10	X_i_X_I										1.932E-07	4.279E-07	6.666E-09	2.48E-07	-1.13E-06
11	X_s_X_c										-2.21E-06	-4.08E-07	1.436E-07	2.09E-06	-2.48E-07
12	X_{bh}_X_c,X_{su}	0.0001									3.55E-06	4.255E-06	4.915E-07	1.688E-06	-1.19E-05
13	X_{ba}_X_c										3.945E-06	4.728E-06	5.461E-07	1.875E-06	-1.33E-05
composition matrix	i_ThOD (gThOD/stoich.unit)	1000	1000	1000	1000	1000	1000	1000							
composition matrix	i_C (gC/stoich.unit)	366.27907	366.3	366.3	366.3	366.3	366.3	366.3				12000			
composition matrix	i_N (gN/stoich.unit)	86.1833105	86.18	86.18	86.18	86.18	86.18	86.18			14000				
composition matrix	i_O (gO/stoich.unit)	201.094391	201.1	201.1	201.1	201.1	201.1	201.1				48000	64000		16000
composition matrix	i_H (gH/stoich.unit)	43.0916553	43.09	43.09	43.09	43.09	43.09	43.09			4000	1000	1000	1000	2000
composition matrix	i_P (gP/stoich.unit)	21.5458276	21.55	21.55	21.55	21.55	21.55	21.55					31500		
composition matrix	i_Ch (Ch/stoich.unit)										1000	-1000	-2000	1000	

Step 4: Transformation equations

Once all $\nu_{j,k}$ have been evaluated, a set of algebraic equations is generated to evaluate the reaction rates ρ_i using equation (9.5). During simulation, these equations are evaluated at every time step as functions of the influxes, i.e. incoming fluxes of components of the "origin" model. According table A1, the equations are as follows:

$$\rho_1 = \text{influx}_9 / \nu_{1,9} \tag{9.7}$$

$$\rho_2 = (\text{influx}_{10} - \nu_{4,10} \cdot \rho_4 - \nu_{7,10} \cdot \rho_7) / \nu_{2,10} \tag{9.8}$$

$$\rho_3 = \text{influx}_{12} / \nu_{3,12} \tag{9.9}$$

$$\rho_4 = \text{influx}_{11} / \nu_{4,11} \tag{9.10}$$

$$\rho_5 = (\text{influx}_{14} - \nu_{6,14} \cdot \rho_6 - \nu_{7,14} \cdot \rho_7) / \nu_{5,14} \tag{9.11}$$

$$\rho_6 = \text{influx}_2 / \nu_{6,2} \tag{9.12}$$

$$\rho_7 = \text{influx}_3 / \nu_{7,3} \tag{9.13}$$

$$\rho_9 = \text{influx}_8 / \nu_{9,8} \tag{9.14}$$

$$\rho_{10} = \text{influx}_7 / \nu_{10,7} \tag{9.15}$$

$$\rho_{11} = (\text{influx}_4 - \nu_{2,4} \cdot \rho_2) / \nu_{11,4} \tag{9.16}$$

$$\rho_{12} = (\text{influx}_5 - \nu_{5,5} \cdot \rho_5 - \nu_{6,5} \cdot \rho_6) / \nu_{12,14} \tag{9.17}$$

$$\rho_{13} = \text{influx}_6 / \nu_{13,6} \tag{9.18}$$

The equations (9.7) to (9.18) calculate the conversion rates in terms of the influxes. The influx of S_s is not used since conversion 8 is cancelled for the above stated reasons. Instead of estimating ρ_8, equation (9.19) is used to determine the theoretical S_s influx required to satisfy the COD required for conversions 2, 5 and 6. As a second step for sourcing a COD deficiency, e.g. to accomplish O_2 and NO_3 depletion. The difference between the theoretically needed and actual influx of S_s is deducted from the X_s influx. If the influx of X_s is not sufficient for the removal of O_2 and NO_3, an update to the plant design is probably needed to avoid O_2 and NO_3 effects on the digester.

$$\text{influx}_{1,\text{theoretical}} = \nu_{2,1} \cdot \rho_2 + \nu_{5,1} \cdot \rho_5 + \nu_{6,1} \cdot \rho_6 \tag{9.19}$$

Note that in equation (9.11) for the evaluation of ρ_5 some terms were ignored since the stoichiometry values were too small (< 1E-15); the Oxygen sourcing was kept to a minimum for all other conversions.

Last calculate the outfluxes using equation (9.6) and check that all outfluxes are oriented outward.

9.2.2.2 CBIM ADM1-ASM1 transformer

For the reverse transformation, the elemental mass fractions and charge density are of course the same as defined for the first transformer. Also, the composition matrix is the same but its two panes are switched according to the new direction of transformation, as shown in Table 9-7 and Table 9-8. Accordingly, *Step 1* and *2* are similar to the first transformer. Note that the sourcing components are replaced as illustrated below.

Step 3: Transformation matrix

The Petersen matrix suggested in Table 9-7 and Table 9-8. In a similar way to the previous transformer, source-sink components are designated. From the "destination" model, ASM1 S_o, S_{alk} and S_{nh4+} are chosen as source-sink components for Oxygen, carbon and nitrogen respectively. Also, the three other source-sink components S_{ip}, S_{H+} and S_{H2O} (inorganic phosphorus, protons and water) are introduced to the destination matrix.

The number of suggested conversions is 22. The evaluation of the stoichiometry for this transformer is straightforward since ADM1 is based on more specific components that are likely to be assigned directly to ASM1 lumped components. In conversion 1, ADM1 S_i is assigned to ASM1 S_i on the basis of the ThOD continuity and to ASM1 S_{nd} on the basis of the nitrogen balance. ADM1 soluble components 2 to 8 are converted by conversions 2 to 8. They are converted to *Ss* on the basis of the ThOD continuity and only ADM1 S_{aa} produced ASM1 S_{nd} on the basis of the nitrogen continuity. In a similar way, the transformations of the particulate components are defined. In conversion 9, ADM1 X_i is mapped to ASM1 X_i. ADM1 particulate components 12 to 22 are transformed by conversions 10 to 20. In these conversions the transformations to ASM1 X_{nd} are evaluated on the basis of nitrogen continuity. Transformations to ASM1 X_S are calculated by minimising $\nu_{j,43}$ (stoichiometry under S_O). In the remaining two conversions S_{in} and S_{ic} are mapped to ASM1 S_{nh4+} and S_{alk}, respectively. Note that in both transformers, gas components are not considered in the transformations because they are assumed to be stripped to the gas phase and transformations are only considered for components in the liquid phase.

Table 9-7 ADM1-ASM1 transformer: "origin" model pan

j	Conversions / components (K →)	1	2	3	4	5	6	7	8	9	10	11	12	13	14	15	16	17	18	19	20	21	22	23	24	25	26
		S_I	S_{su}	S_{aa}	S_{fa}	S_{va}	S_{bu}	S_{pro}	S_{ac}	S_{h2}	S_{ch4}	X_I	X_c	X_{ch}	X_{pr}	X_{li}	X_{su}	X_{aa}	X_{fa}	X_{c4}	X_{pro}	X_{ac}	X_{h2}	S_{an}	S_{cat}	S_{in}	S_{ic}
		(kgCOD m^{-3})	(kgCOD m^{-3})	(kgCOD m^{-3})	(kgCOD m^{-3})	(kgCOD m^{-3})	(kgCOD m^{-3})	(kgCOD m^{-3})	(kgCOD m^{-3})	(kgCOD m^{-3})	(kgCOD m^{-3})	(kgCOD m^{-3})	(kgCOD m^{-3})	(kgCOD m^{-3})	(kgCOD m^{-3})	(kgCOD m^{-3})	(kgCOD m^{-3})	(kgCOD m^{-3})	(kgCOD m^{-3})	(kgCOD m^{-3})	(kgCOD m^{-3})	(kgCOD m^{-3})	(kgCOD m^{-3})	(kmole m^{-3})	(kmole m^{-3})	(kmoleN m^{-3})	(kmoleC m^{-3})
1	**S_{I}_S_I,S_{ND}**	-1																									
2	**S_{su}_S_S**		-1																								
3	**S_{aa}_S_{ND},S_S**			-1																							
4	**S_{fa}_S_S**				-1																						
5	**S_{va}_S_S**					-1																					
6	**S_{bu}_S_S**						-1																				
7	**S_{pro}_S_S**							-1																			
8	**S_{ac}_S_S**								-1																		
9	**X_{I}_X_I**											-1															
10	**X_c_X_S**												-1														
11	**X_{ch}_X_S**													-1													
12	**X_{pr}_X_S**														-1												
13	**X_{li}_X_S**															-1											
14	**X_{su}_X_S**																-1										
15	**X_{aa}_X_S**																	-1									
16	**X_{fa}_X_S**																		-1								
17	**X_{c4}_X_S**																			-1							
18	**X_{pro}_X_S**																				-1						
19	**X_{ac}_X_S**																					-1					
20	**X_{h2}_X_S**																						-1				
21	**Sin_S_{nh4+}**																									-1	
22	**S_{ic}_S_{alk}**																										-1
composition matrix	i_ThOD (gThOD/stoich.unit)	#####	1000	1000	1000	1000	1000	1000	1000	1000	1000	1000	1000	1000	1000	1000	1000	1000	1000	1000	1000	1000	1000				
	i_C (gC/stoich.unit)	360.9	375	310	256.8	288.5	300	321.4	375		187.5	360.9	309.5	388.6	310	263	366.3	366.3	366.3	366.3	366.3	366.3	366.3				12000
	i_N (gN/stoich.unit)	58.0		98.93								58	30.95		98.93		86.18	86.18	86.18	86.18	86.18	86.18	86.18			14000	
	i_O (gO/stoich.unit)	180.4	500	184.7	41.1	153.8	200	285.7	500			180.4	151.5	514.9	184.7	38.07	201.1	201.1	201.1	201.1	201.1	201.1	201.1				48000
	i_H (gH/stoich.unit)	38.7	62.5	65.95	44.52	43.27	43.75	44.64	46.88	125	62.5	38.67	46.7	58.29	65.95	41.53	43.09	43.09	43.09	43.09	43.09	43.09	43.09			4000	1000
	i_P (gP/stoich.unit)	6.4										6.444	4.344	9.715		3.461	21.55	21.55	21.55	21.55	21.55	21.55	21.55				
	i_Ch (Ch/stoich.unit)					-4.81	-6.25	-8.93	-15.6																	1000	-1000

Table 9-8 ADM1-ASM1 transformer: "destination" model pan

	K	27	28	29	30	31	32	33	34	35	36	37	38	39	40	41	42	43
	components	S_s	S_{NH3}	S_I	X_S	X_{BH}	X_{BA}	X_I	X_P	S_{ND}	X_{ND}	S_{N2}	S_{NH4+}	S_{alk}	$S_{Ib\ (HPO4+)}$	S_{H+}	S_{H2O}	S_O
		(gCOD m^{-3})	(gN m^{-3})	(gCOD m^{-3})	(gCOD m^{-3})	(gCOD m^{-3})	(gCOD m^{-3})	(gCOD m^{-3})	(gCOD m^{-3})	(gN m^{-3})	(gN m^{-3})	(gN m^{-3})	(gN m^{-3})	(molHCO$_3^-$ m^{-3})	(gP m^{-3})	(gH m^{-3})	(gH m^{-3})	(-gCOD m^{-3})
j Conversions																		
1 S_I_S_I,S_{ND}				1099.4272						57.999182				0.4946903	6.4443535	0.9038556	-1.162124	3.02E-13
2 S_{su}_S_S		1000												5.8628133	-8.866533	5.2998588	12.429708	3.268E-13
3 S_{aa}_S_{ND},S_S		1169.598								98.932161				-3.860516	-10.37028	-4.518947	28.827963	1.99E-13
4 S_{fa}_S_S		1000												-3.983077	-8.866533	-4.546032	14.142037	-8.53E-14
5 S_{va}_S_S		1000												-1.348725	-8.866533	-6.719372	12.429708	5.684E-14
6 S_{bu}_S_S		1000												-0.387187	-8.866533	-7.200141	12.429708	5.684E-14
7 S_{pro}_S_S		1000												1.3985276	-8.866533	-8.092998	12.429708	1.137E-13
8 S_{ac}_S_S		1000												5.8628133	-8.866533	-10.32514	12.429708	1.99E-13
9 X_I_X_I								1000										
10 X_C_X_S					1053.0639						30.953961			-0.939363	-4.992611	-1.256354	7.7880562	7.105E-15
11 X_{ch}_X_S					1000									6.9952343	0.8481932	7.0490878	5.0280122	4.974E-14
12 X_{pr}_X_S					1169.598						98.932161			-3.860516	-10.37028	-4.518947	28.827963	-2.84E-14
13 X_{li}_X_S					1000									-3.467723	-5.405565	-3.810933	9.7927805	3.126E-13
14 X_{su}_X_S					1147.7428						86.183311			1.3852946	11.369328	2.1071567	-5.740731	8.527E-14
15 X_{aa}_X_S					1147.7428						86.183311			1.3852946	11.369328	2.1071567	-5.740731	8.527E-14
16 X_{fa}_X_S					1147.7428						86.183311			1.3852946	11.369328	2.1071567	-5.740731	8.527E-14
17 X_{c4}_X_S					1147.7428						86.183311			1.3852946	11.369328	2.1071567	-5.740731	8.527E-14
18 X_{pro}_X_S					1147.7428						86.183311			1.3852946	11.369328	2.1071567	-5.740731	8.527E-14
19 X_{ac}_X_S					1147.7428						86.183311			1.3852946	11.369328	2.1071567	-5.740731	8.527E-14
20 X_{h2}_X_S					1147.7428						86.183311			1.3852946	11.369328	2.1071567	-5.740731	8.527E-14
21 Sin_S_{nh4+}													14000					
22 S_{ic}_S_{alk}														1000				
composition matrix	i_ThOD (gThOD/stoich.unit)	1.000	-4.571	1.000	1.000	1.000	1.000	1.000	1.000	-1.714	-1.714	-1.714						-1.000
	i_C (gC/stoich.unit)	0.305		0.323	0.305	0.366	0.366	0.361	0.366					12.000				
	i_N (gN/stoich.unit)		1.000			0.086	0.086	0.058	0.086	1.000	1.000	1.000	1.000					
	i_O (gO/stoich.unit)	0.137	3.429	0.139	0.137	0.201	0.201	0.180	0.201					48.000	2.032		8.000	1.000
	i_H (gH/stoich.unit)	0.039		0.035	0.039	0.043	0.043	0.039	0.043				0.286	1.000	0.032	1.000	1.000	
	i_P (gP/stoich.unit)	0.009			0.009	0.022	0.022	0.006	0.022						1.000			
	i_Ch (Ch/stoich.unit)		-0.07										0.071	-1.000	-0.063	1.000		

Step 4: Transformation equations

Setting up the transformation conversions is also straightforward because of the detailed structure of ADM1 compared to ASM1. In the "origin" model pan Table 9-7 the stoichiometry is a diagonal matrix and therefore each conversion rate is presented explicitly as a function of the influx of one component of the "origin" model components, equation (9.20).

$$\rho_j = \text{influx}_k / \nu_{j,k} \tag{9.20}$$

Last, the outfluxes are calculated using equation (9.6).

9.2.3 MCN transformers

Copp et al. (2003) developed ad hoc transformers to connect ASM1 and ADM1. Their transformation concept is twofold. First, the total COD and TKN are determined for the components of the "origin" model and then distributed to the other model components. Second, the distribution is done step-wisely with the aim to maximise certain components in a predefined order. The distribution is done so that the COD continuity is maintained. If there is remaining TKN, it is mainly assigned to ammonia that is a component in both models.

For the transformation from ASM1 to ADM1, the COD of all ASM1 soluble components is summed and subsequently reduced to compensate for ASM1 nitrate and oxygen concentrations that need to be removed before entering ADM1. The reduction is done in sequence to ASM1 components S_S, X_S, X_{bh} and X_{ba}. Based on the ASM1 S_{nd}, ADM1 S_{aa} is maximised as far as the soluble COD allows. ASM1 S_i is mapped to ADM1 S_i. If there is soluble COD left from the assignment to ADM1 S_{aa} and S_i, the remaining is assigned to sugars, ADM1 S_{su}. In a similar way, starting from ASM1 particulate COD and X_{nd}, ADM1 X_c is maximised first and X_i is mapped according to the available ASM1 X_{nd}. If there is COD remaining after assignment of ASM1 X_{nd}, it will be assigned to X_{ch} and X_{li} according to predefined fractions. In the assignment of ASM1 TKN, if the ASM1 COD is insufficiently to source the assignments, the remaining nitrogen is added to the inorganic nitrogen pool of ADM1, i.e S_{in}.

For the transformation ADM1-ASM1, a similar procedure is followed with the goal to maximise X_s, S_s, S_i and X_i with respect to the available COD and maximise S_{nh}, X_{nd} and S_{nd} with respect to nitrogen.

In a last step of both of the above transformations, direct assignment is done between S_{nh} and S_{in}. Direct mapping is also done between S_{alk} and S_{ic}. In ADM1, S_{cat} is considered equal to S_{ic} and S_{an} is considered equal to S_{in}.

9.2.4 Plant-wide modelling

All modelling and simulation were performed in the WEST software (Hemmis nv, Kortrijk, Belgium) – (Vanhooren et al., 2003). An extended benchmark plant is implemented according to the configuration of Figure 9.1. The added units are dimensioned to achieve the average Total Suspended Solids (TSS) indicated on the figure. The plant is extended for receiving additional loads to the digester. However, during the comparison of the transformation methods, no external flows were assigned. Two similar configurations were built: one is using the CBIM transformers and the other is using the MCN transformers. The 14 day dynamic influent of BSM1 is simulated by both configurations starting from initial conditions obtained with a 1000 days constant influent load.

9.3 Results and discussions

The simulation results are discussed in two parts. In the first part, using the practical plant-wide example, the CBIM transformers are designed and the standard MCN transformers are applied. The first part aims to study the practical issues related to the use of the CBIM transformers and presents the ad hoc assumptions implemented in the first CBIM transformer to produce additional fluxes of S_{fa}, S_{su} and X_{su}. The second part of the results discusses the main differences between the two transformer types by using identical inputs and without additional fluxes of the S_{fa}, S_{su} and X_{su} as originally designed for the MCN.

9.3.1 Plant-wide simulation

In this section, the designed CBIM and MCN transformers are simulated with the plant-wide model. The dynamic simulation results are shown and discussed at 5 locations in the treatment system presented in Figure 9.1 (components before and after the two transformers and the digester pH and biogas flow).

9.3.1.1 Inflow to ASM1-ADM1 transformers

Although the model initialisation is done separately for each transformation method and there is recycle after the sludge dewatering, the input concentrations from the thickener to the ASM1-ADM1 transformer are identical using either methods. For example, ammonia and alkalinity were expected to be the most different when comparing both methods but the influent to the first transformer is almost the same as shown in Figure 9.2. Therefore,

using any of the transformation methods has the same effect on the 14 days simulation of the activated sludge plant final effluent.

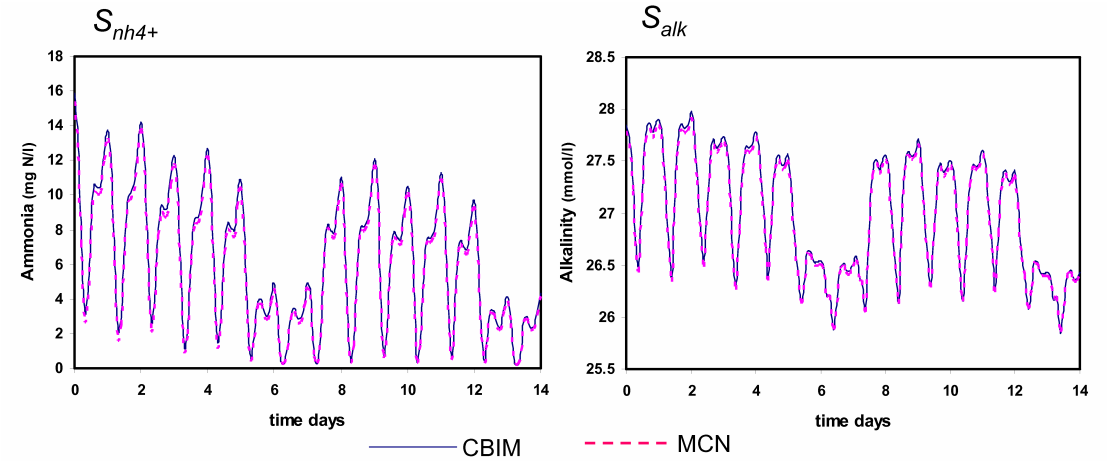

Figure 9.2 Ammonia and alkalinity concentrations in the influents to ASM1-ADM1 transformers

9.3.1.2 Outflow from ASM1-ADM1 transformers

The effluent from the transformers is different due to the differences between the two methods and their assumptions. Figure 9.3 shows the main differences in effluent concentrations from the ASM1-ADM1 transformers. The S_{in} from the CBIM transformer is slightly higher than the MCN. However, when all components are considered the nitrogen balance is closed with both methods, i.e. the difference in S_{in} is compensated by the nitrogen content of other components. The CBIM S_{ic} is much higher compared to the MCN one. CBIM achieves the carbon balance using S_{ic} as a source-sink component for carbon while MCN is not considering the carbon balance and its S_{ic} is only mapped from ASM1 S_{alk}.

Although MCN aims to maximise S_{aa}, MCN doesn't produce S_{aa} and only produces S_i as soluble substrate. Thus, MCN produces slightly higher S_i compared to CBIM. S_{aa} is produced by CBIM. Also, sugars and fatty acids are produced (results not shown). The MCN COD source required for S_{aa} is S_S only. Normally in the effluent of activated sludge plant, S_S is very low compared to the COD required to deplete the effluent oxygen and nitrate and, therefore, no COD is left to produce S_{aa} as originally proposed in the MCN. In CBIM, both S_S and X_s are used to source the conversion to S_{aa}, S_{su} and S_{fa}. Also, the COD deficiency for the depletion of oxygen and nitrate is balanced by utilising from the X_S influx. The use of X_S to source COD for the transformation to S_{aa}, S_{su} and S_{fa} can be supported by the fact that a fraction of X_S (aerobically: slowly biodegradable substrate) is quickly hydrolysed to easily biodegradable substrates when confronted with the anaerobic enzymes.

For particulates, MCN produces only X_i and X_c while CBIM produces X_{su} too. Both methods result in the same X_i (results not shown). X_{su} is produced only by the CBIM approach since it is assumed that a part of the heterotrophic biomass is capable of fermenting. The assigned value to X_{su} is reflected as a difference between the X_c values estimated by both methods.

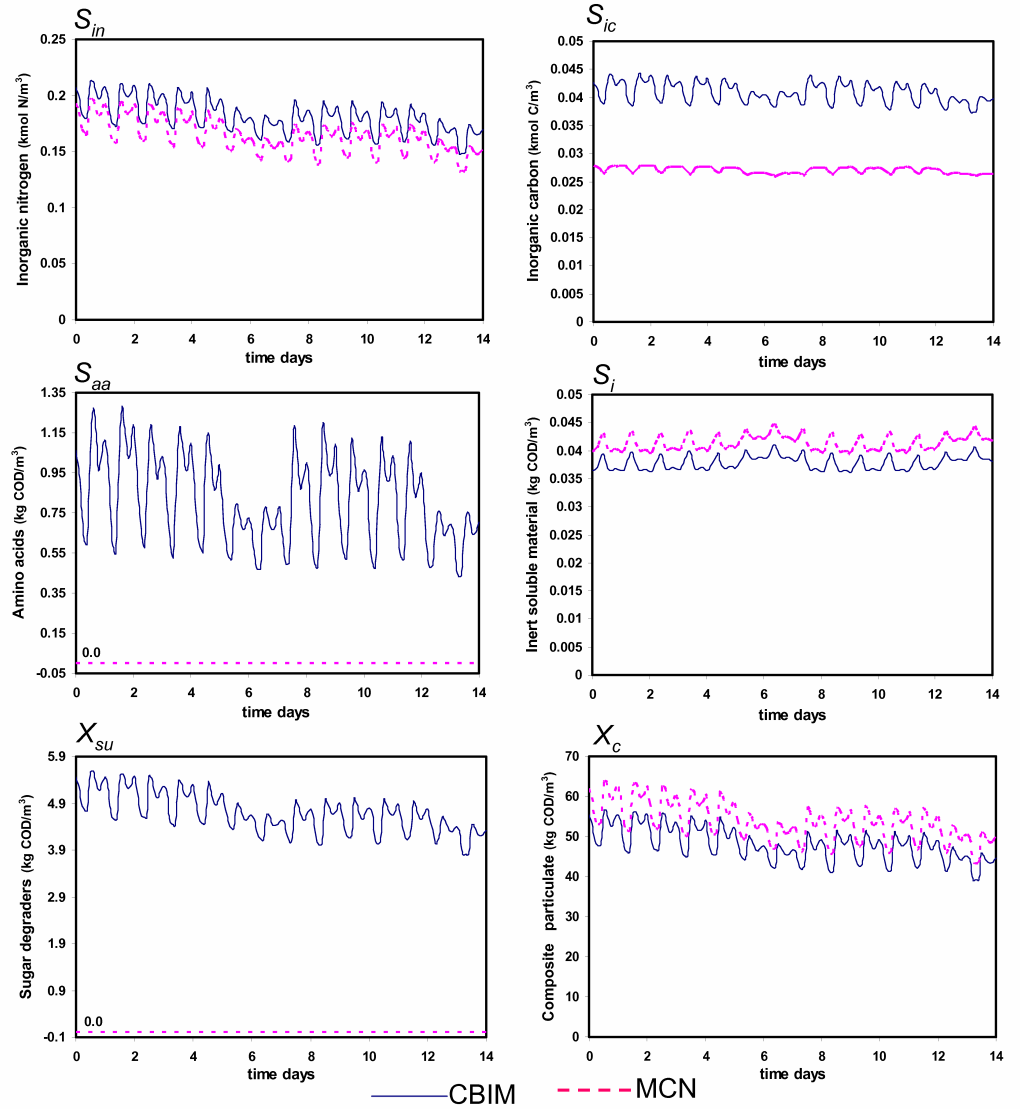

Figure 9.3 Comparison of effluent concentrations from the ASM1-ADM1 transformers using the CBIM and the MCN methods

9.3.1.3 Inflow to ADM1-ASM1 transformers

Concentrations at this location are equal to the concentrations in the ideally mixed digester. Noticeable differences between both methods are shown in Figure 9.4. In the case of CBIM, S_{in} and S_{ic} are higher since they were also higher in the digester influent. The dynamics of soluble substrates, e.g. S_{aa} and S_{bu}, are more pronounced when using the CBIM because of the distribution of the soluble substrates in the digester influent.

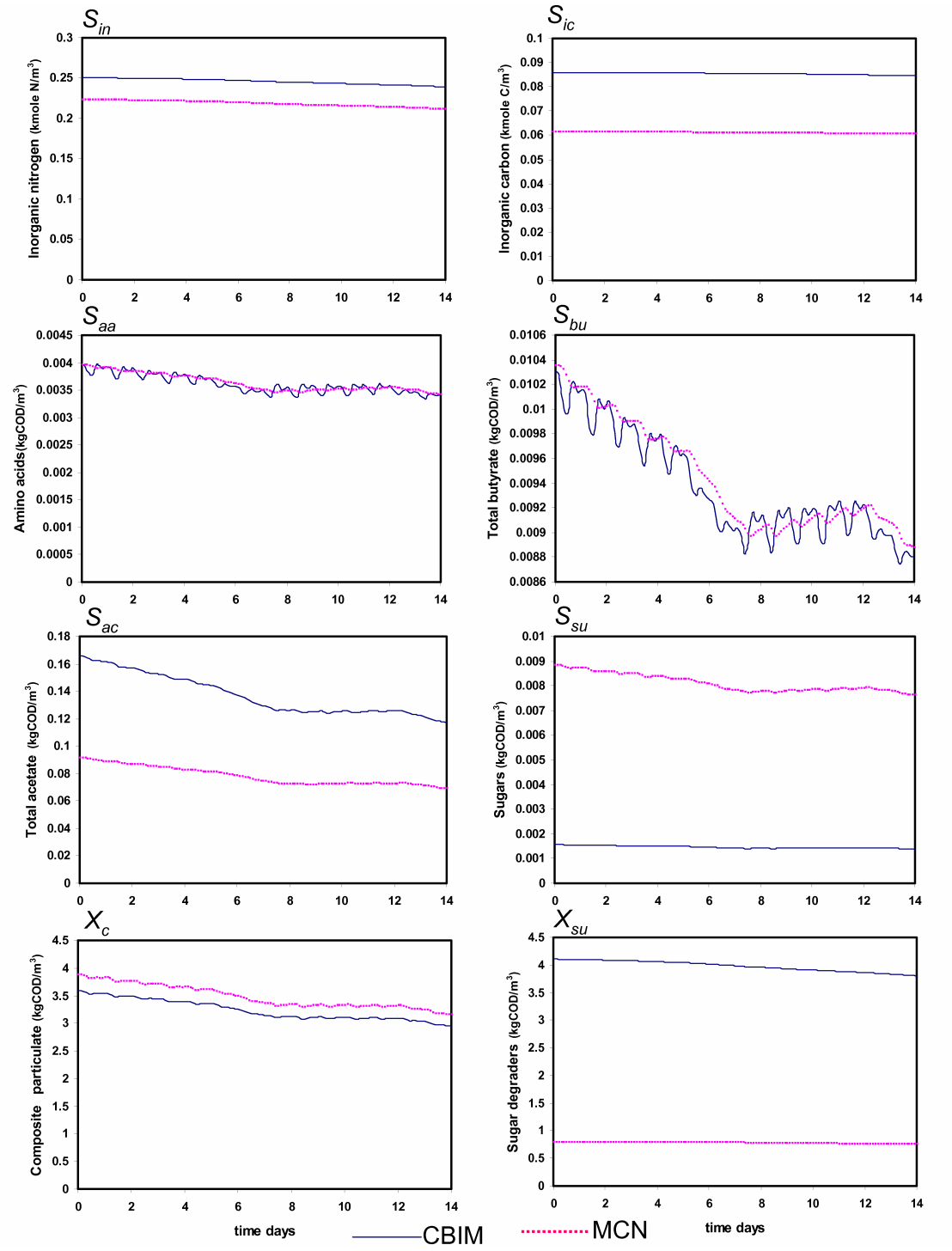

Figure 9.4 Comparison of influent concentrations to the ADM1-ASM1 transformers using the CBIM and the MCN methods

In CBIM, S_{ac} is higher and S_{su} is lower than in MCN since CBIM estimated the sugar fermenters input to the digester. Also, the fermenters influent results in a lower X_c and a higher X_{su} value by the CBIM approach. This is due to the conversion of some X_{bh} into X_{su}.

The conversion S_s to S_{su} in the CBIM ASM1-ADM1 transformer will support the rapid growth of X_{su} in the anaerobic digester.

9.3.1.4 Outflow from ADM1-ASM1 transformers

Results at this location are shown in Figure 9.5.

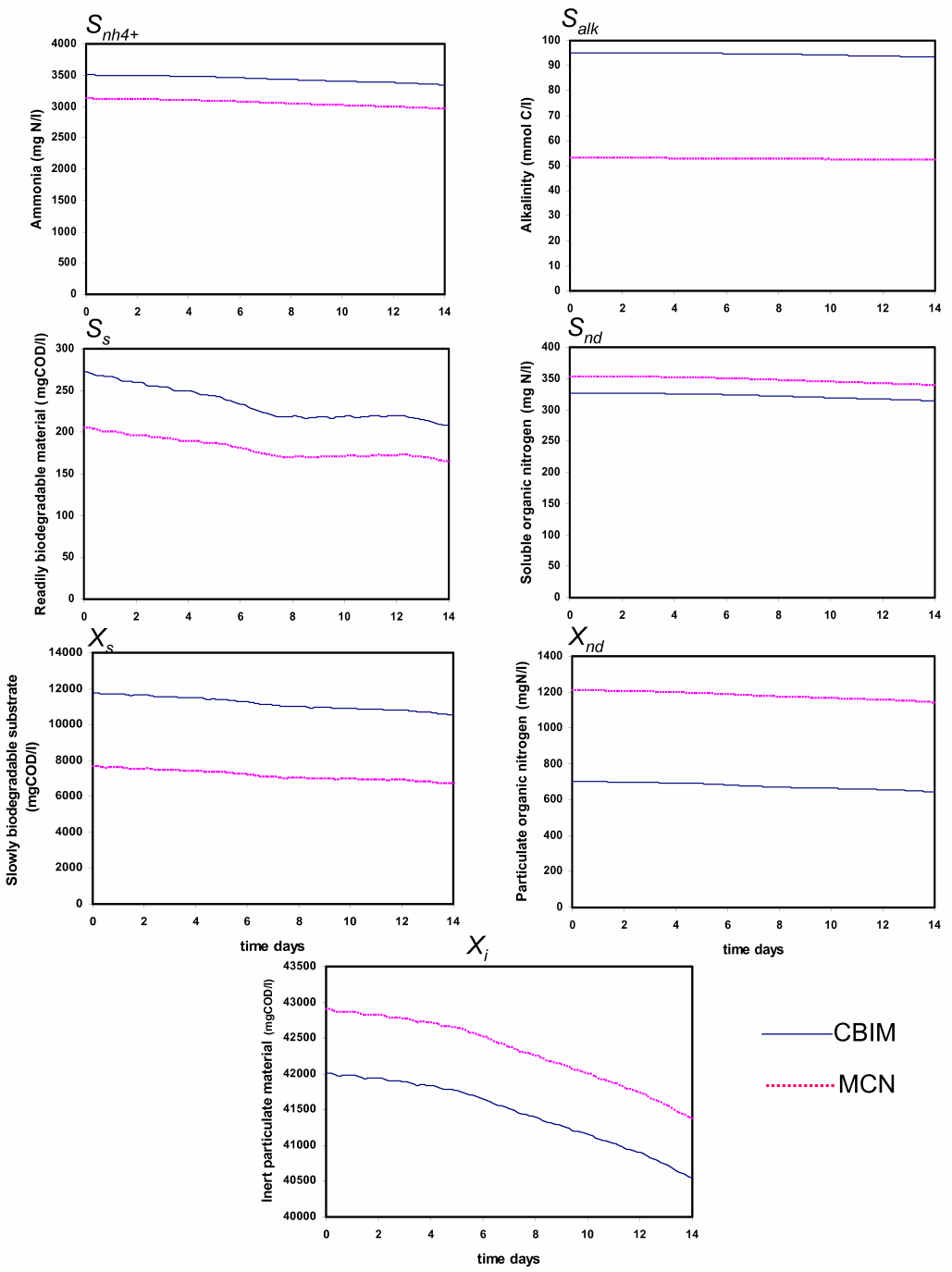

Figure 9.5 Comparison of effluent concentrations from the ADM1-ASM1 transformers using the CBIM and the MCN methods

S_{nh4+} and S_{alk} are calculated to be higher when using the CBIM transformer. Alkalinity is higher due to the conservation of carbon. The slight difference in ammonia is due to the compensation needed for other components in terms of the nitrogen balance. For instance, the non-nitrogen components of ASM1 S_s and X_s are calculated to be higher when CBIM transformation is used. On the other side, the nitrogen components of ASM1 S_{ND} and X_{ND} are estimated higher by the MCN transformer. For all model components the nitrogen continuity is maintained by both methods. X_s is estimated higher by CBIM since with the CBIM the X_{su} in the digester effluent is higher and X_s sums all anaerobic particulates. This is counteracted by the X_i results. In other words, MCN leads to a more stabilised sludge from the digester. However, the difference in X_i is only about 2% of its total concentration. Note that X_i is the largest particulate product from the digester and it is the most significant component in terms of stabilised sludge.

9.3.1.5 Digester biogas flow and pH

As shown in Figure 9.6, both transformation methods lead to almost the same pH in the digester and the same gas output from the digester. Also, the difference in gas composition is very small (data not shown).

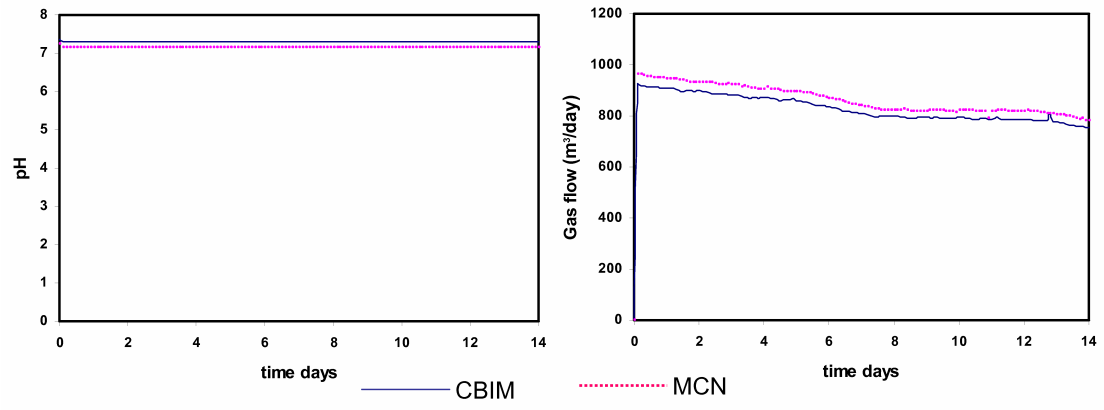

Figure 9.6 pH in and gas flow from the digester

9.3.2 Main differences between transformer types

In order to compare the two transformers on a completely equal basis, another simulation study was performed with the following settings for the two transformer approaches. Similar to the MCN ASM1-ADM1 transformer, the ASM1-ADM1 CBIM transformer was updated to have zero fractions from S_s to S_{su} and S_{fa} and a zero fraction from X_{bh} to X_{su}. Accordingly, some values of stoichiometric parameters are changed in Table 9-5 and Table 9-6 to maintain the continuity of the elemental mass and COD. The values of $\nu_{2,4}$, $\nu_{2,16}$, $\nu_{2,18}$, $\nu_{2,4o}$, $\nu_{12,26}$, $\nu_{12,30}$, $\nu_{12,39}$ and $\nu_{12,40}$ are changed to -10.822, 0, 0, 3.9E-05, 0.001, 3.94E-

06 and 4.73E-06, respectively. Transformation to S_{aa} was maintained in both the MCN and CBIM ASM1-ADM1 transformers.

Three configurations were created from the plant-wide example Figure 9.1 to compare the transformer types using identical inputs. Figure 9.7 shows the arrangement of the transformers in the three configurations. Three changes were necessary. First, the recycle from the dewatering unit was cancelled to prevent propagation of the differences in the transformer outputs back into their inputs. Hence, The three configurations in Figure 9.7 have exactly the same influent of thickened secondary sludge. Second, simulations of the three configurations were started from the same initial conditions. Third, when comparing the ADM1-ASM1 transformers (configuration 2 and 3) the ASM1-ADM1 transformer was of the MCN type. The results from the three configurations confirm the main differences of the transformer types and agree with the detected differences using the plant-wide model.

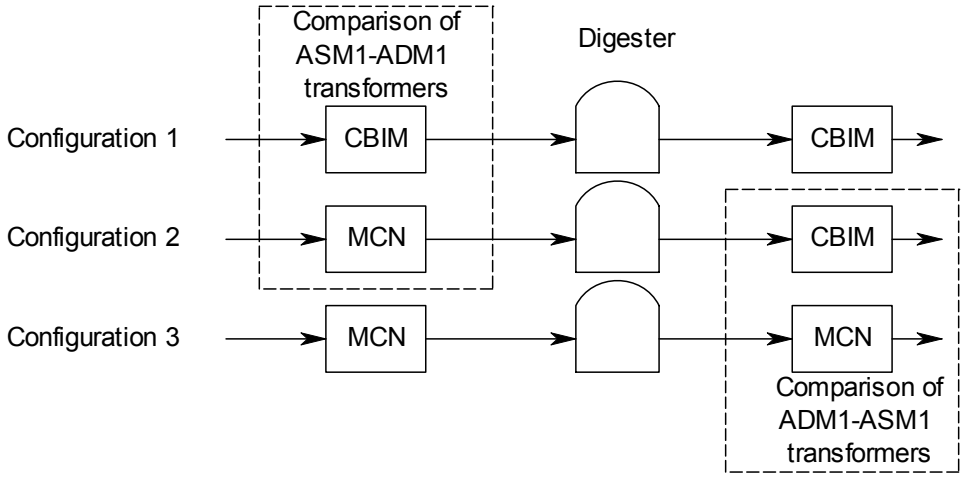

Figure 9.7 Transformers arrangements for their comparisons using identical inputs

Two main differences were detected in the outflow of the two types of ASM1-ADM1 transformers (by comparing configuration 1 and 2). First, the CBIM transformer produces more S_{ic} than the MCN transformer. The CBIM transformers maintain the continuity of carbon through all transformations, whereas the MCN transformers only consider the continuity of COD and nitrogen. Second, the CBIM transformer produces S_{aa} where as the MCN transformer does not. However, it should be noted that the input sludge in this case is secondary sludge only and in case of transforming primary sludge, the S_s will be sufficient to source the required COD for the MCN transformer so as to produce the required amino acids. The transformation to S_{aa} induced more dynamics of VFAs of the digester outflow in configuration 1 than in configuration 2. Indeed, the uptake of S_{aa} in the ADM1 model yields all types of VFAs.

Comparing ADM1-ASM1 transformers by using configurations 2 and 3, the main difference was found in the produced S_{alk}. Again, the CBIM transformer maintains the continuity of carbon and, therefore, produces more S_{alk} compared to the MCN transformer. An appropriate estimate of bicarbonate alkalinity (S_{ic} and S_{alk}) by maintaining the carbon balance is important since alkalinity is important in both models. Alkalinity is connecting heterotrophic and autotrophic processes in the ASM1 model whereas it is important for pH simulation in the ADM1 model that is connected to all substrate uptake processes through inhibition terms.

The eliminated ad hoc assumptions and fraction parameters from the ASM1-ADM1 CBIM transformer helped the fair comparison with the MCN transformer. However, the selection of these fractions can lead to significant differences in the related digester output components, e.g. S_{su} and X_{su} (Figure 9.4). Therefore, it is recommended to also include these fractions in the MCN transformers with the advantage that they can be estimated from real measurements, whereas in the CBIM transformer they need to be determined first by wastewater characterisation and need then to be considered in the transformation matrix to update the continuity check.

9.4 Conclusions

Two methods recently proposed to interface ASM1 and ADM1 models in a case study of plant-wide model of treatment works. Both lead to similar results in terms of the plant-wide output. Both interfacing methods also lead to almost the same output of the activated sludge plant, biogas from the digester and sludge production. However, with the additional flexibility of the CBIM approach, the transformation of "origin" components can be distributed over a larger number of components on the "destination" side. This will lead to better simulations of dynamics which are needed for better parameter estimation, control strategy benchmarking and implementation of advanced treatment processes, e.g. for high rate nitrogen removal. The CBIM approach is general and it can be applied to any model conversion and it, therefore, allows to incorporate more knowledge about the process, e.g. the amino acids and sugar fermenters estimation in the influent to the digester.

The CBIM interface is relatively complex and is more meant for model developers to define consistent interfaces between any combination of Petersen-based models. The MCN interface is possibly easier to understand and makes it possible to create a reasonable interface between ASM1-ADM1 and extend it for particular needs. An example of this extension is due to the aim of the MCN approach to maximise the conversion from the soluble organic nitrogen and COD to amino acids. This maximisation is possible when

implementing the MCN transformer for primary sludge treatment. In case of secondary sludge treatment, however, the MCN transformer should be extended to allow the conversion to amino acids, i.e. by utilising part of the ASM1 slowly biodegradable substrate. The conversion to amino acids is important in order to represent deserved VFA dynamics. Also, other fraction parameters can be added to the MCN for better simulation of the digester components. These parameters can be estimated from measurements in the digester.

An important advantage of the CBIM approach is maintaining the continuity of all elements and the COD. For instance, the CBIM transformers maintained the continuity of carbon when interfacing ASM1 and ADM1 whereas the MCN approach didn't consider the carbon balance. The carbon balance is important in the presented case study since alkalinity is connected to the main processes considered by both models

For both applied methods, the transformation from ADM1 to ASM1 is easier to set up compared to the one from ASM1 to ADM1. This is due to the fact that ADM1 is based on a more detailed and more specific set of components. Application of the CBIM approach needs a careful design of the conversion reactions requiring deep insight in the two models to be connected. However, there are three Guiding Transformation Principles (GTPs) to help the user to refine the conversion reactions. The GTPs are suggested to solve the under-determination problems found in the definition of the transformer stoichiometry and conversions. Also, the GTPs are useful to update the designed conversions and guarantee that transformation occurs in the right direction.

The introduction of the source-sink components is necessary since, so far in the field of wastewater treatment, the developed models do not consider all elemental balances. Therefore, the CBIM transformation approach provides a good opportunity to close this gap in terms of integrated modelling.

The general steps for applying the CBIM transformation are:

1. to define the mass fractions of all the components from both models;
2. to design the composition matrix;
3. to design the transformation matrix assigning the right source-sink components;
4. to obtain outfluxes by means of a set of algebraic equations.

Part III

Monitoring

Chapter 10

General review of monitoring equipment and titrimetric analysis

Abstract

In this chapter, the commercial availability of anaerobic digestion monitoring equipment is reviewed. The cost of sensors and analysers and practical information for their application are quoted. It is found that titrimetric analysers are not commercially available. Therefore, focus is turned towards titrimetric analysis. The concepts of titration and buffer capacity are introduced. Applications of titration in various fields are reviewed. In anaerobic digestion, titrimetric determination of VFA is found to be applied for a long time, but only in research or for off-line analysis. Many interpretation methodologies have been developed for the titrimetric determination of VFA. It is found that titrimetric determination of VFA is more cost efficient than alternative methods and it has acceptable accuracy.

Three titrimetric analysers are reviewed. Two of them were developed in previous research but never became commercially available. A third one is developed in parallel to this research and is now commercially available for on-line implementation. The principles, device descriptions, operation and calculation methods for the three analysers are reviewed. Further developments to be described in the next chapters are highlighted.

CHAPTER 10

10.1 Introduction

The anaerobic process appears to be an efficient and economic process for wastewater treatment at different scales of applications. It is based on a complex ecosystem of anaerobic bacterial species that degrade organic matter. It presents very interesting advantages compared to the traditional aerobic treatment: high capacity to degrade difficult substrates at high concentrations, very low sludge production, low energy requirements and a possibility for energy recovery through methane combustion. Generally, the control of wastewater treatment plants relies on four building blocks: a proper process model, on-line sensors and analysers, adequate control strategies and actuators that implement the controller output.

Therefore, it is an important objective to develop instrumentation and control equipment to make the wastewater treatment processes and particularly the anaerobic process more reliable and usable at different application scales. The primary step towards this objective is the development of robust sensors and analysers. The state of the art of equipment for on-line monitoring of wastewater treatment and anaerobic digestion can be found in (Vanrolleghem, 1995; Vanrolleghem and Lee, 2003). These articles review the applied measuring principles, and ongoing research and development of sensors and analysers. This chapter briefly reviews commercial availability of anaerobic digestion monitoring equipment.

Titrimetric analysis is the most cost-efficient and informative means to collect information about the anaerobic process operation. Therefore, in this chapter focus will be turned to titrimetric analysis and its applications. The concept of titration is introduced through a simple example. The buffer capacity concept is presented to highlight the effect of the buffering capacity of individual components on the measuring principle. The literature on the application of titration techniques in wastewater treatment is reviewed. Finally, the titrimetric analysers used throughout this research are reviewed in detail.

10.2 Availability of on-line sensors

Data of commercially available sensors were collected from major sensor manufacturing companies and a review was made for operation ranges, accuracies and average prices. The review results are presented in Table 10-1. It should be noted that it is not practical nor cost efficient to have all the listed sensors at every anaerobic digestion plant. Indeed, a selection of these sensors at an anaerobic digestion depends on the process design, reactor configuration and control strategy. The whole installation should be practical and economic. Hence, the collected practical information and average prices will be useful to

assess the sensor selection. Despite the importance of the VFA measurement for on-line monitoring of anaerobic digestion, on-line VFA analysers are not commercially available, yet. The most economic method for VFA measurement with relevant accuracy for on-line control appears to be titration. Titrimetric analysers are available for alkalinity measurement and have already been applied to activated sludge processes. Therefore, in the following sections focus will be turned on the titrimetric analysis and applications.

Table 10-1 Practical information of commercially available sensors and analysers for on-line monitoring of anaerobic digestion

Measurement	Type / (analyser method)	Average price (€)	Practical information		
			range	electrical output	accuracy
Temperature	sensor	120	-50 , 600°C	4-20 mA	+/- 0.7°C
Pressure	sensor	450	0-2,5 bar; 0-600 bar	4-20mA	0,25 or 0,5%
Liquid Level	meter	700	liquids up to 5m	12-36 V DC, 90-127 VAC, 180-250 VAC	3 mm
Liquid flow	meter	2000	up to 80 m^3/h	pulse output	0,50%
Gas flow	meter	4000	0-500 Nl/min	4-20 mA	
pH	electrode	300	0-14 (0-11)		
	transmitter	600	-2 to 16	0/4-20 mA	0,75%
Conductivity	sensor	450	10µS/cm to 20mS/cm		
	transmitter	600	Variable 0-2000 mS/cm	0/4-20 mA	0,75%
COD	(Standard)	30000	0-1500 mg/l O_2	4-20 mA	2%
TOC	(combustion)	25000	0-10,000 ppm	0-10 VDC; 4-20 mA	3%
	(UV/Persulfate)	25000	0-10,000 ppm	0-10 VDC; 4-20 mA	2%
	(Ozone Promoted)	25000	0-5,000 ppm	0-10 VDC; 4-20 mA	3%
	(Ultra pure)	25000	4-10,000 ppm	0-10 VDC; 4-20 mA	2%
Turbidity/Suspended Solids	sensor	1700	Up to 40,000 ppm		1%
	(analyzer)	2200	varies	4-20 mA	1%
Gaseous products	H_2 sensor	340	0-4%		
	O_2 sensor	130	0-25%		
	H_2S sensor	220	0-50ppm		
	CO_2 sensor	800			5%
	transmitter	600		4-20mA	
	H_2S (IR-UV)	17500	0-1 ppm		1%
	CH_4 and CO_2 (IR)	800	CH_4:20-100vol% CO_2:10-50vol%		
Ammonia	colorimetric	14000	0-10 mg/l	4-20 mA	2% or 0.015 mg/l
	ISE	15000	0-20000 mg/l		1%

IR: Infra red
UV: Ultraviolet
ISE: Ion Selective Electrode
DC: Direct current
AC: Alternating current

10.3 Titration and buffer capacity

10.3.1 Titration concept

Titration is performed by adding small amounts of a strong base to a weak acid solution, or by adding small amounts of a strong acid to a weak base solution, and measuring the pH after each addition. Consequently, a titration curve can be obtained by plotting the amount of base/acid added versus the change in pH. An example of a titration curve for 1 liter of a 0.01 M acetic acid (HAc) solution is presented in Figure 10.1. The curve has an S-shape, which suggests that the pH does not change at a constant rate with the addition of strong base.

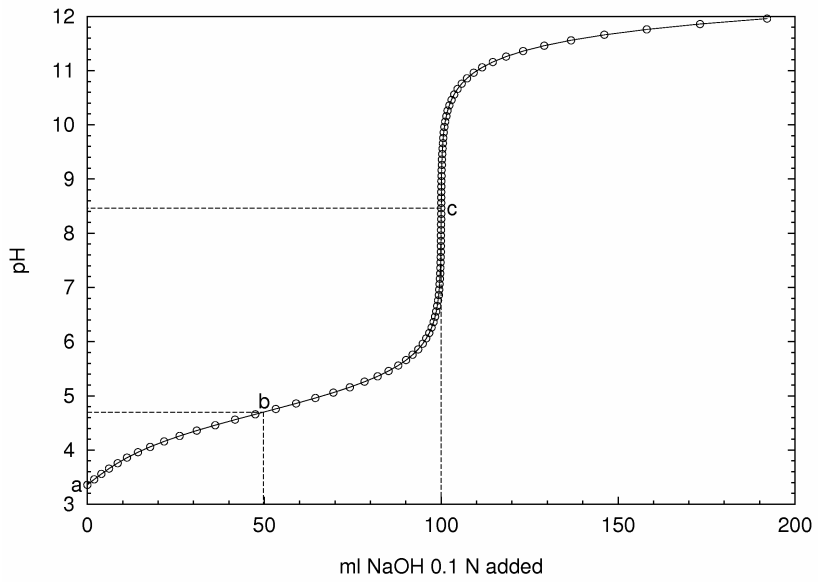

Figure 10.1 Titration curve for 1 litre of a 0.01 M acetic acid solution (Benefield, 1982).

Points a, b and c are normally used to describe the major chemical events happening during a titration experiment. Also they can be used to explain the development of the S-shape of the curve. This will be discussed in the following paragraphs.

Point a: This point represents the equilibrium pH established in a 0.01 *M* acetic acid solution. At this point no base has been added. Furthermore, the concentration of the ionized form is much smaller than the unionized form (in this sample 4 % A^- against 96 % HA), so that the unionized acid concentration can be considered almost equal to the initial concentration.

Point b: This point represents the pH established when the concentration of unionized acid equals the concentration of the ionized acid; i.e. $[HA]=[A^-]$. At point b, acetate shows the highest resistance to pH change, i.e. the highest buffering capacity.

Point c: This point represents the pH established when the concentration of ionized acid approaches the initial acid concentration, thus $\lfloor A^- \rfloor \cong 0.01M$. Theoretically, at high pH values there always remains a very small fraction of unionized acid [HA]. The pH at point c is the equivalence-point for a 0.01 M acetate salt solution. Further addition of a strong base past point c will result in a continued increase in pH. The limiting pH is set by the pH of the titrant.

In the titration example, Figure 10.1, only 1 monoprotic buffer system in an aqueous solution is considered. A titration curve can also be obtained by adding small amounts of strong base to a solution, containing more than 1 buffer system, including poly-protic buffers. An example of such more complex titration curves is shown in Figure 10.2. The difference with the previous example is that the points a, *b* and *c* cannot be distinguished for the individual buffers on the graph, because of its complexity.

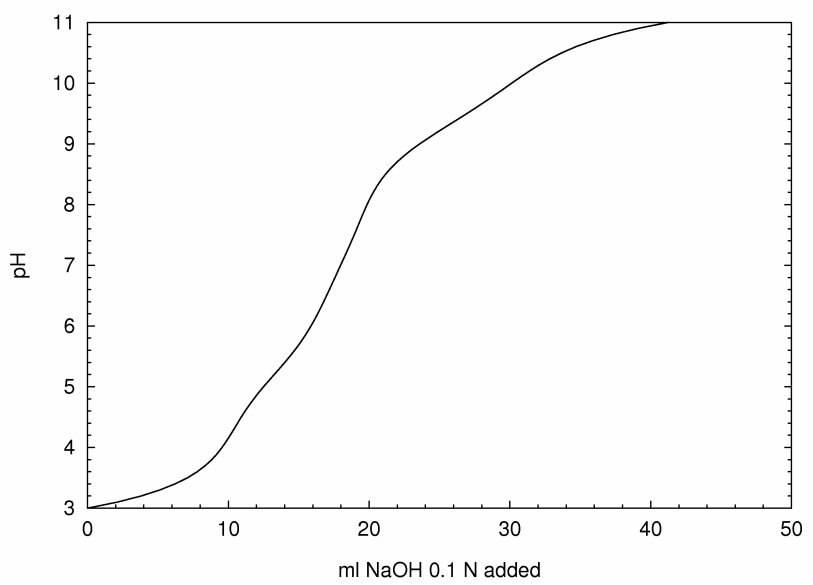

Figure 10.2 Titration curve for 1 litre of a more complex aqueous system containing 5 mgCO_2 l^{-1}, 7 mg o-PO_4-P l^{-1}, 15 mgNH_4^+-N l^{-1} and 0.6 meq l^{-1} of an unspecified soap (Van Vooren, 2000).

10.3.2 Buffer capacity curve (BC)

The slope of a titration curve (pH versus added base/acid) is related to the tendency of the solution at any point in the titration curve to change the pH upon addition of base or acid. The buffer capacity (BC) at any point of the titration is inversely proportional to the slope of the titration curve at that point and may be defined as :

$$\beta = \frac{dC_b}{dpH} = -\frac{dC_a}{dpH} \qquad (10.1)$$

β : buffer capacity (BC) ($eql^{-1}pH^{-1}$)
dC_b, dC_a: differential quantity of strong base or acid added (eql^{-1})
dpH: differential change in pH due to addition of dC

β is always positive. A graphical representation of β as a function of pH may be obtained by plotting the inverse of the slope of the titration curve versus pH. The BC curve corresponding with the titration curve in Figure 10.1 is shown in Figure 10.3. The point with the highest buffer capacity, excluding the water buffer is point b, the top of the buffer capacity profile. Also, points a and c are indicated and the three points are more distinguishable than in Figure 10.1. With more complex BC curves these important points are still distinguishable as can be seen in Figure 10.4.

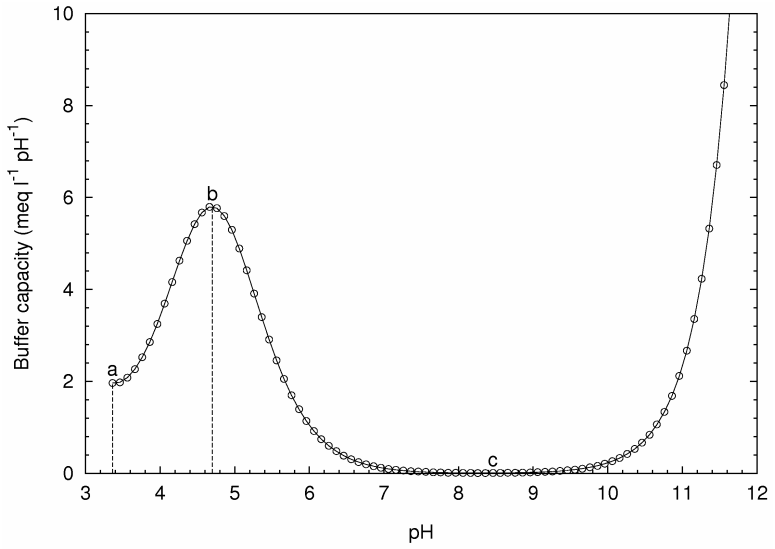

Figure 10.3 Buffer capacity curve for a 0.01 M acetic acid solution

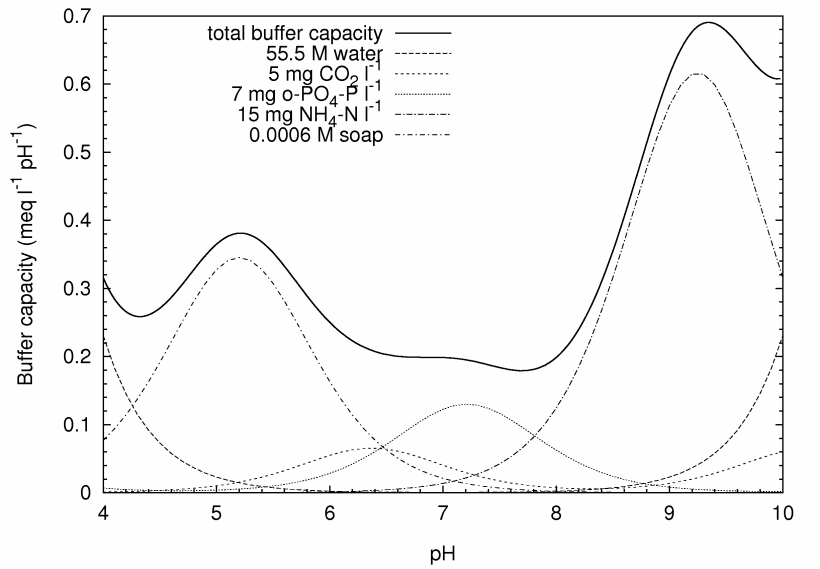

Figure 10.4 Buffer capacity curve for 1 litre of a more complex aqueous system containing 5 mgCO_2 l^{-1}, 7 mg o-PO_4-P l^{-1}, 15 mgNH_4^+-N l^{-1} and 0.6 meq l^{-1} of an unspecified soap (Van Vooren, 2000).

10.4 Titration applications

In this section, the role of titration among other measurement methods in identifying alkalinity and VFA, the most important measurements in anaerobic digestion, is highlighted. In addition, the most recent applications and studies of titration for on-line measurement are listed. The review will cover biological processes in general and anaerobic treatment in particular.

10.4.1 Standard measurement of alkalinity

In most literature since the seventies, the standard method for measuring alkalinity is titration (American Society for Testing and Materials, 1999; Sawyer et al., 1994; Skougstad et al., 1979; Winter and Midgett 1969). When alkalinity is entirely due to the carbonate or bicarbonate content (i.e. the major buffering system in the anaerobic digestion), total alkalinity is determined by the equivalent acid added to the sample from pH 8.3 to about 4.5 (Sawyer et al., 1994). The first point corresponds to the equivalence point for the conversion of carbonate ion to the bicarbonate ion. The second, end-point, corresponds to the equivalence point for the conversion of bicarbonate ion to carbonic acid. The second point cannot, however, be accurately specified. It depends on the initial concentration of bicarbonate and it is influenced by the stripping of the carbonic acid in the form of carbon dioxide during the titration experiment. Therefore, it is generally recommended that the actual pH of the stoichiometric end-point be taken as the corresponding inflection point that is determined by continuous potentiometric titration (Sawyer et al., 1994). This is essential when other buffers than bicarbonate are also contributing to the total alkalinity.

10.4.2 Standard measurement of VFA

According to Buchauer (1998), the most common methods for measuring VFA are listed below. For application in WWTP, the titration methods are preferred.

- *Steam distillation* (DeutscheEinheitsverfahren, 1971): requires certain specialized equipment plus experience, and it is time-consuming.

- *Colorimetric method* according to Montgomery et al. (1962): A simple procedure, which is said to be of poor accuracy at low VFA concentrations and which is rather sensitive towards residual color (Moosbrugger et al., 1993).

• *Chromatographic methods* (HPLC, GC): Require high investment in technical equipment which is not commonly available at a WWTP.

• *Titrimetric methods:* Mostly very simple procedures, which can be conducted with a minimum of time and effort. According to Buchauer (1998), there are many simple titration procedures developed for VFA determination and it is found that methods of Kapp (1984) and Moosbrugger et al. (1992; 1993) are the most worthy for a closer study and comparison. Indeed, these two methods are examples of the two approximate titrimetric method classes according the classification that will be illustrated in chapter 12.

According to Buchauer (1998), both Kapp (1984) and Moosbrugger et al. (1992; 1993) titration procedures are considered equivalent in terms of their accuracy to determine VFA concentrations. However, this conclusion was concerning influents to aerobic wastewater treatment processes and it would no longer hold for anaerobic processes where VFA concentrations are much higher. Handling of both methods is rather simple but requires carefulness. It seems advantageous that the Kapp method does not need a base addition and enables VFA calculation by simple explicit equations. The method of Moosbrugger et al. (1992; 1993) is superior if not only VFA but other buffers are required too. Hence, information about other buffers are required for the latter method.

In chapter 12, the Kapp method will be introduced for a titrimetric setup but with modification in order to also determine the bicarbonate concentration (Bouvier et al., 2002). The main objective of the implementation was to be simple and robust, even if that was at the expense of some precision.

Actually, according to (Buchauer, 1998), the Kapp method was originally developed for the control of mesophilic sludge digesters. It was founded on a principle suggested by McGhee (1968). The basic idea is that the acid required to titrate a sample from pH 5.0 to pH 4.0 can be considered proportional to the content of VFA present in the sample. This applies because between pH 5.0 and pH 4.0 there is usually no weak acid/base subsystem apart from the acetate subsystem that strongly effects acid consumption. Moreover, the pKa values of acetic acid, propionic acid, butyric acid and valeric acid are all close to 4.75. Thus, they show very similar buffering characteristics and can indeed be lumped together as one parameter. The only additional buffer considered in the VFA calculation procedure of Kapp (1984) is the carbonate subsystem of HCO_3^- / CO_2 which has a pKa of approximately 6.3. Other buffer systems are assumed negligible. Kapp (1984) argues that the ammonia subsystem (NH_3 /NH_4^+) whose pKa is 8.95, is far from the pH range under discussion. Similarly $H_2PO_4^-$ /HPO_4^{2-} (pKa of 7.2) influences the alkalinity only to a

minimal extent. Of course, this argument is only correct if the concentrations of the latter two buffering systems are low enough to ignore their influence on the accuracy.

10.4.3 Anaerobic digestion

Indirect measurement of VFA by mixing the anaerobic digestion effluent with denitrifying organisms in excess of nitrate was suggested in (Rozzi et al., 1997). The suggested method relies on the relation between NO_3 reduction and the VFA available as easily biodegradable substrate. Also, titration by acid addition to compensate for the resulting proton consumption was suggested to measure the denitrified NO_3.

Titration is also applied as a basis for a Methanogenic Activity and Inhibition Analyzer, MAIA (Rozzi et al., 2001). Simply by neutralizing the alkalinity produced by acetoclastic methanogens by acid titration, the activity of the acetoclastic methanogens can be calculated as a function of the titrant flow rate.

Feitkenhauer et al. (2002) used titration for on-line measurement of VFA in anaerobic digestion of synthetic textile wastewater. In this work it was found that a concentration of NaCl in the range of 2.5 to 150 g/l has no effect on the measurement accuracy and the deviation from the standard measurement, using gas chromatography, was ±1%.

Bouvier et al. (2002) introduced a cheap titrimetric sensor for the measurements of total and partial alkalinity and the estimation of bicarbonate and volatile fatty acids concentrations in anaerobic digestion processes. The sensor has been tested on-line by monitoring a 1 m^3 upflow fixed bed reactor treating raw industrial wine vinasses for almost 5 years. An implementation of a model-based adaptive linearizing controller (or fuzzy controller) utilizing the VFA and alkalinity measurements proved to result in good performance of the reactor (Bernard et al., 2001).

Some titrimetric developments originally intended for application to aerobic and anoxic systems were later extended to also yield useful information regarding anaerobic systems. For instance, the DENICON titration biosensor was originally developed to measure denitrification activity and nitrate concentration (Massone et al., 1996[a]). However, it has been further tested to measure the readily biodegradable BOD or COD in the influent of anaerobic digesters that is fed on variable and highly concentrated wastewater (Rozzi et al., 1998), e.g. winery effluents, distillery slops…etc. This titration biosensor is a pH-stat reactor applying denitrification as a biological reaction where the acid consumption correlates satisfactorily to the readily biodegradable COD content of the sample.

10.4.4 Water quality management

In water quality management and for monitoring of wastewater treatment plant effluents, an automatic buffer capacity based sensor (Van Vooren et al., 1996) was used to determine ammonia and orthophosphate concentrations. This sensor is based on titration and is connected to a data interpretation unit.

In natural treatment good results have been shown by Van Vooren et al. (1999) for monitoring of algal wastewater treatment using the automatic buffer capacity based sensor.

In natural resources the same sensor was applied to determine the nutrient contents, phosphorus and nitrogen, in manure-destructed samples (Van Vooren, 2000)

The data interpretation unit of the automatic buffer capacity based sensor was further developed to automatically and in a stepwise manner build buffer capacity models for each particular titrated sample, and to quantify the individual buffer systems that constitute the total buffer capacity (Van Vooren et al., 2001). An automatic and robust model building algorithm was developed and applied to many titration curves of effluent and river water samples. The application of automatically built buffer capacity models mostly resulted in similar or better estimations of ammonium and ortho-phosphate in the samples compared to the previous application. The automatic modelling approach is also advantageous for alarm generating purposes because unexpected buffers are easily detected.

To generalize the use of the sensor, advanced interpretation of the titration curves has been developed (Van de Steene et al., 2002). The interpretation is based on an accurate technique for buffer capacity model selection and will be described in detail in section 10.5. Also, the buffer capacity interpretation is upgraded and tested for anaerobic digestion monitoring in the next chapters 11 and 12.

10.4.5 Aerobic and Anoxic Treatment

Rozzi et al. (1999) applied titration in combination with a respirometric sensor to measure the autotrophic bacteria degradation rates in treating different textile wastes. This application has been extended (Ficara et al., 2000) by using alkaline titration but in combination with respirometry that uses H_2O_2 as oxygen supply.

Other techniques using titration have been evaluated to yield useful information for nitrification process control (Gernaey et al., 1998; Bogaert et al., 1997; Massone et al., 1996[b]; Ramadori et al., 1980). For example, Gernaey et al. (1998) used both a simple slope extrapolation method and a model-based non-linear extrapolation method to interpret

the titration curves of samples taken from activated sludge treatment plant for ammonia determination. Determined concentrations of ammonia were as accurate as obtained with an automatic ammonia analyzer. Also, interpretation yielded important information about the process kinetics.

Titration was combined with respirometry to monitor nitrification (Gernaey et al., 2001) as well as to estimate model parameters (Petersen et al., 2000). For instance, Gernaey et al. (2001) maintained a constant pH in an activated sludge sample in the respirometric chamber by addition of acid/base. Thus, as an alternative to complete titration, the cumulative acid/base addition to maintain constant pH served as a complementary information source to respirometry. Assessments by Petersen et al. (2001) demonstrated that titrimetric data lead to more accurate and faster identification of activated sludge process kinetics.

In monitoring the denitrification process (Devisscher, 1998; Massone et al., 1996[b], Petersen et al., 2002; Sin and Vanrolleghem, 2004), titration yielded good results and made its monitoring possible. To cite an example, Petersen et al., (2002) monitored denitrification by combining pH-stat titrimetric measurements with an ion-selective nitrate electrode that monitored the nitrate uptake rate in presence of excess carbon source. The methodology was significantly improved by Sin and Vanrolleghem (2004) combining the pH-stat titrimetric measurement with a more robust nitrate biosensor that has a linear signal and can measure low concentrations of nitrate.

10.4.6 Summary

In conclusion, as for many other aspects, the application and assessment of titration methods appears to advance faster in aerobic processes/systems than in anaerobic ones. In the aerobic as well as the anoxic processes (e.g. nitrification and denitrification), the interest in titration is focusing more on application of the pH-stat principle since the accumulative base/acid addition to balance proton production/consumption can be directly related to the process kinetics. For water quality management titration is performed to cover the full range of buffering systems. Thus, detection and quantification of different components such as phosphorus and ammonia as well as some pesticides/detergents are possible. For more accuracy of the measurement, the buffer due to the carbonate system should be removed by stripping as CO_2. Similarly, the carbonate system should be removed to accurately measure ammonia in algal water treatment and to determine nutrients (i.e ammonia and phosphorus) when recycling of natural resources is concerned.

In anaerobic systems though, there are three degrees of complexity (problems) to consider when using titration methods. First, it is not beneficial to perform titration based on the pH-stat principle since the process consists of a combination of parallel and consecutive processes where it is not easy to relate proton consumption/production to an overall anaerobic activity. Second, the alkalinity due to the carbonate system plays an important role in the process stability and it should be considered explicitly during the titration. Third, intermediate products of the anaerobic process (i.e VFAs) are considered as alkalinity species. Thus, an interference of measuring the carbonate alkalinity and VFA is expected. However, both of them are necessary measurements for the anaerobic process. The first problem asks for the extension of the titration over a certain pH range while the second and the third problem complicate the calculation methods and affect their accuracy, especially at high concentrations.

10.5 Titrimetric analysers

Three analysers were used for further development of on-line titrimetric monitoring throughout this research. The BIOMATH titration setup was developed at Department of Applied Mathematics, Biometrics and Process Control, Ghent University, Belgium (Van Vooren, 2000; Van De Steene et al., 2002). The INRA titration analyser was developed at the Laboratoire de Biotechnologie de l'Environnement, Institut National de la Recherche Agronomique, LBE-INRA, Narbonne, France (Bouvier et al., 2002). Finally, the AnaSense® on-line titrimetric analyser was developed at AppliTek NV, Nazareth, Belgium (De Neve et al., 2004).

10.5.1 BIOMATH titration setup

10.5.1.1 Principle of the device

The elementary measurement used in this setup is pH measurement. From the successive measurements of pH as function of stepwise acid or base addition (with known concentration) to the sample, a titration curve is constructed. From the measured titration curve (typically around 30 to 50 points), the buffer capacity in each point is calculated as the derivative of the amount of base/acid needed in (meq l^{-1}) for a pH increase/decrease of one pH unit.

The obtained buffer capacity (meq l^{-1} pH^{-1}) in function of the pH is called the buffer capacity curve. The pH(s) at which a certain component gives its maximum buffer capacity is (are) called the pKa(s) of that component(s). For samples containing several pH buffering components, the buffer capacity curve consists of the sum of the buffer capacities of each individual component. From the buffer capacity curve, estimates of the different

buffering components can be computed using a mathematical model. The principle of the analyser is illustrated in Figure 10.5.

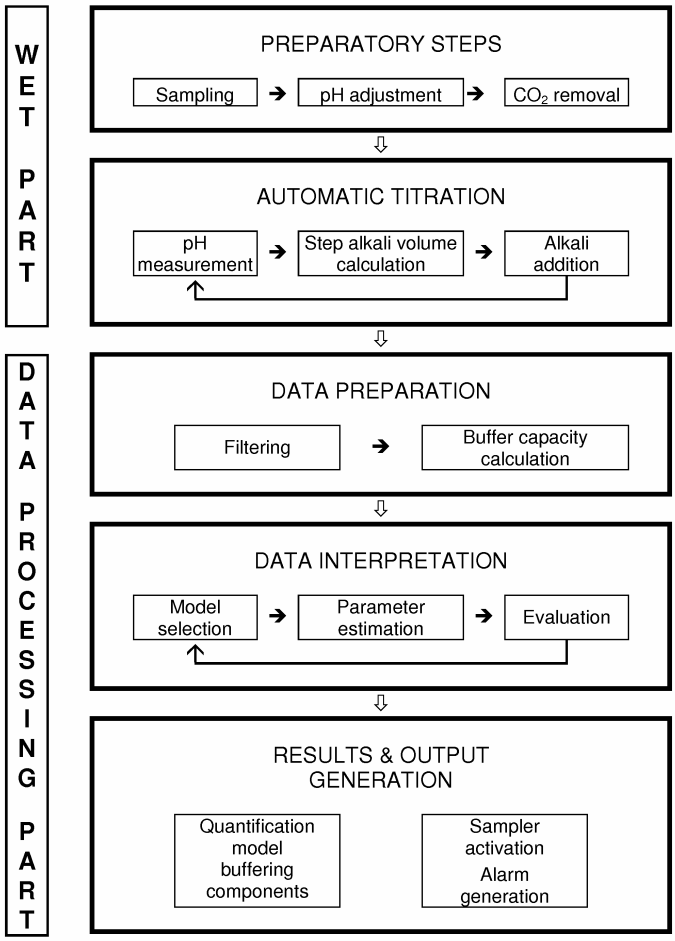

Figure 10.5 Principle of the buffer capacity analyzer

In the wet part, the first step is the sampling (originally 100 - 200 ml, for on-line implementation the sample volume is reduced to 10 - 20 ml) and a pH adjustment to pH 3, followed by a short aeration of 5 minutes to strip the dissolved CO_2 (this was for the cases where measurement of carbonate alkalinity is not needed). Alternatively, when carbonate alkalinity is important, the step of CO_2 stripping is canceled. In the second step a dynamic titration is performed between pH 3 and pH 11.

The data processing part is performed in a computer connected to the titration apparatus. First, if necessary, the titration data are filtered (smoothened, outliers removed). Second, the buffer capacity in each point of the titration curve is calculated as the derivative of the amount of base/acid needed for a pH increase/decrease of one pH unit. The next step is the mathematical model selection followed by parameter estimation.

The candidate models differ in the number of buffering components they would include. In the parameter estimation step, the concentrations and eventually corresponding pKa values for the buffering components defined in the model, are obtained. Eventually, a different model can be selected if the fit is not satisfying. The used mathematical models describe the chemical equilibria taking place in the reaction vessel during titration. Models could be built using different equilibria of chemical reactions. Then concentrations are worked out mathematically. In the final output of the sensor, a list of buffering components is given. If certain preset values are exceeded an alarm is given. The time for 1 complete run is approximately 30 minutes.

10.5.1.2 Device description

The titration procedure is carried out by combining the following components: Metrohm® sample changer 730, Metrohm® Titrino 716, and PC, illustrated in Figure 10.6. They are described below.

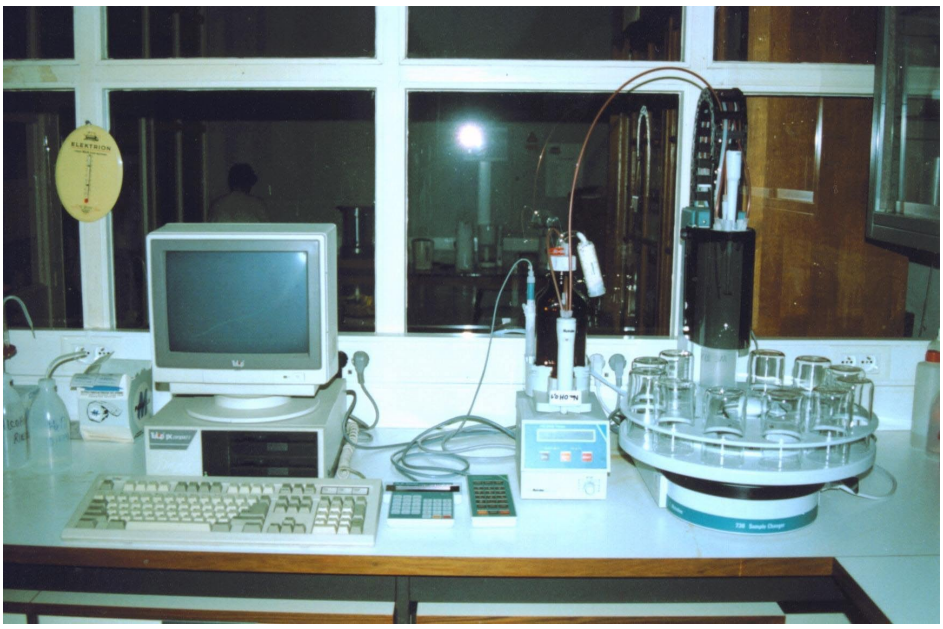

Figure 10.6 Experimental setup: PC on the left side, sample changer with samples in the glass pots on the right side, and Titrino 716 between PC and sample changer

10.5.1.2.1 Automatic titrator (Titrino 716)

The Titrino 716 is connected to the sample changer and PC for data collection. This device has exchangeable units with 0.1 N NaOH or 0.1 HCl (for on-line implementation to anaerobic digestion, a higher titrant normality up to 0.5N is used). Titration of the samples with strong base or strong acid is automatically done by these units. The volume of titrant

(strong base or acid) that is added each step into the sample to be titrated is based on the slope of the titration curve.

10.5.1.2.2 PC data capture

The recorded data are saved in the computer for further data analysis. A preliminary data check or plotting of the raw data could also be done with this unit. This PC data collection system is connected on-line to the other setup components.

10.5.1.2.3 Sample changer 730

The sample changer is an automatic device for which the number of samples, the method of sample handling, and other options can be programmed and automatically run. The maximum number of samples to be programmed at one time is 12 (similar to the available positions in the sampler). However, more samples can be titrated consequently by replacing empty pots with new samples. The pH electrode calibration can also be controlled by this device. When it is not in use, the electrode is kept in 3 M KCl solution at position 12.

Other functions of the sample changer include aeration and rinsing of the pots. Aeration of samples is done using a magnetic stirrer. Aeration is required when measuring alkalinity is not essential and to remove CO_2 that can be absorbed from the atmosphere or is already present in the sample. Two containers of distilled water are also connected to the system for rinsing; when one is in use the other one is kept as a reserve.

10.5.1.2.4 Setup operation

The samples to be titrated are placed in series of sample positions on the sample changer. The number of samples and type of titration method are programmed with the sample changer. Then, the titration method of the Titrino (up titration or down titration) is also programmed. Before the titration system starts, the level of water for rinsing, and the level of titrant (NaOH or HCl) should be checked to be sufficient for the programmed samples. When all components are ready, the titration procedure is started with the start button of the sample changer. The titration system automatically stops when all programmed samples are titrated.

10.5.1.2.5 Data analysis

The raw data taken from the data collection PC are split into a number of files corresponding to the titrated samples by using the “split software”. The concentration of

the components is then estimated with the simulation software "bomb" (Van De Steene et al., 2002). This programme performs the data processing part as shown in Figure 10.5 using a general model that is based on:

1. Dissociation reactions of buffering components, e.g. carbon, phosphorous, ammonia, acetate and the water buffers; Table 10-2 section (A)

2. Mass balance of each buffer component, e.g. Table 10-2 section (B)

3. Charge balance of all ion forms in the solution, e.g. Table 10-2 section (C).

Table 10-2 Example of the general buffer capacity model basis

(A) Example dissociation reaction	pKa =(-Log *K*)
$H_2CO_3 \overset{K}{\longleftrightarrow} HCO_3^- + H^+$	6.37
$HCO_3^- \overset{K}{\longleftrightarrow} CO_3^{2-} + H^+$	10.25
$H_3PO_4 \overset{K}{\longleftrightarrow} H_2PO_4^- + H^+$	2.12
$H_2PO_4^- \overset{K}{\longleftrightarrow} HPO_4^{2-} + H^+$	7.21
$HPO_4^{2-} \overset{K}{\longleftrightarrow} PO_4^{3-} + H^+$	12.67
$NH_4^+ \overset{K}{\longleftrightarrow} NH_3 + H^+$	9.25
$HAc \overset{K}{\longleftrightarrow} Ac^- + H^+$	4.75
$H_2O \overset{K}{\longleftrightarrow} OH^- + H^+$	15.744

(B) Example mass balances
$C_{carbon} = H_2CO_3 + HCO_3^- + CO_3^{2-}$
$C_{phosphate} = H_3PO_4 + H_2PO_4^- + HPO_4^{2-} + PO_4^{3-}$
$C_{ammonium} = NH_4^+ + NH_3$
$C_A = HA + A^-$
$C_{water} = 55.5 + (OH^-)$

(C) Example general charge balance

Negatively charged ions	Positively charged ions
HCO_3^-, $2CO_3^{2-}$, $H_2PO_4^{2-}$, $3PO_4^{3-}$, OH^-, A^-	Na^+, H^+, NH_4^+

Programme parameters are defined in a text according a foreseen application and properties of expected buffer components. According the defined set of parameters the programme performs model optimisation and model selection. Model optimisation and model selection procedures are performed using the general buffer capacity model,

described later in chapter 11. The model is generally defined for mono-, di- and tri-protic buffers.

The model and the programme parameters are defined in a separate text file that consists of 6 parts. The 6 parts are shown in Boxes 10-1 to 10-6. Parameters have to be redefined after a change in titration experiment settings, and so are the model optimisation and selection settings, and the buffer constituents. For on-line implementation of the software, automatic initialisation modules are implemented as a software layer around the "bomb" software, as presented in chapter 11. Part 6 is changed as shown in BOX 10-7 to allow the automation and minimise the required redefinition of parameters. The text file is built to be self-explanatory. It is written with comments (starting with "#") that are not inputs to the programme but useful to guide the user when parameter changes are needed. However, a brief explanation is given in the following listing of the parts.

In part 1, BOX 10-1, the volume of the sample to be titrated is expressed in liters.

BOX 10-1

```
#======================================================================
# Installation related parameters
#
0.100  # volume titration vessel (l)
```

In part 2, BOX 10-2, the actual normality of the titrant (i.e. NaOH for up-titration or HCl for down-titration) is stated with other experimental data related parameters.

BOX 10-2

```
#======================================================================
     # Experimental data related parameters
0.1  # calculation factor ml -> meq for the raw titration data
1    # buffer capacity calculation algorithm (0: linear, 1: parabolic)
5    # window width for the calculation of the buffer capacity (ODD !)
1    # Ionic strength correction: Activity coefficient for H+
```

In part 3, BOX 10-3, general settings for simulation and optimization are defined with three options: simulation, optimisation and buffer capacity calculation. Simulation and optimisation are selected by specifying the number 0 and 1 respectively. In the model selection section, the minimum and maximum simulation pH interval must be defined. Minimum and maximum trials of the optimiser are chosen to either stop the algorithm if it starts running unsuccessfully giving Not-A-Number "NaN" values or cannot achieve a better model fit. The higher the maximum number of trials, the better the results will be but also the slower they will be obtained. A typical value of 0.1 is chosen as a simulation step and a linear basic model is selected.

BOX 10-3

```
#=========================================================================
        # General settings for simulation and optimization
1       # 0: simulate, 1: optimize, 2: only buffer capacity calculation
0       # optimization routine (0: PRAXIS, 1: not available)
2.5     # minimum of the pH simulation interval ( van 3.5 )
11.0    # maximum of the pH simulation interval
.1      # pH simulation step
1       # model to be used (0: not available, 1: linear model)
0       # info from optimizer (0: to screen, 1: to file)
5       # minimum correctly ended trials for optimizer
30      # maximum allowed trials for optimizer (if Nan values are #returned!)
```

Part 4, BOX 10-4, is for the optimization control parameters. The praxis-oriented parameters are specified. It is specifically to be noted that the maximum number of function calls refers to the maximum number of buffer capacity simulations that will be done to find the best fit.

BOX 10-4

```
# Optimization control parameters
0       # controls the quantity of iteration info (0: none, 1, 2, 3: most)
1.0e-8  # tolerance for precision of optimum
10      # number of times tolerance criterion should be fulfilled to stop
0.01    # steplength
1       # scaling parameter (1: no scaling)
1       # illconditioned (0: no, 1: yes)
1000    # max number of function calls for optimization
1       # confidence information calculation (0: no, 1: yes)
```

In part 5, the automatic model building is turned on/off and the corresponding parameters are to be defined as illustrated in the following BOX 10-5.

BOX 10-5

```
# Automatic model building parameters
0       # Automatic model building (0: off, 1: on)
1       # How to stop model building (0: add all B-buffers, 1: model #selection)
6       # Selection criterion: 1..7: AIC, AICc, SIC, FPE, Run-test, F-    # test,
        SSE
0.0001  # Alpha for Run-test and F-test
0.005   # Boundary touch condition: touch if distance from boundary < x * # range
2       # Symmetrical narrowing factor for blind buffers ; 1 no narrowing
3       # Maximum number of tuning cycles within 1 model building cycle
0.2     # Minimum width for pKa-interval of BLIND-buffers
1.5     # Initial and maximum width for pKa-interval of BLIND-buffers
```

In part 6, BOX 10-6, model parameters of buffer components are defined. There are seven columns to be defined: Name (NAME), initial value (INITIAL), minimum value (MIN), maximum value (MAX), molecular weight (MOLW), blind (B-), and optimization (OPT).

BOX 10-6

```
# Model descriptions for simulation, optimization and model extension

# NAME--------->  INITIAL     MIN      MAX    MOLW  B-   OPT # comments
PKA_WATER         15.744     15.62     15.82   0     0     0  # water
PKA1_CARBON        6.37        6.3      6.5    0     0     1  # carbonate
PKA2_CARBON       10.25        9.5     10.5    0     0     1  # carbonate
PKA_PHENOL         9.92        9.7     10.2    0     0     0  # phenol
PKA1_PHOS          2.15        2.1      2.2    0     0     1  # phosphate
PKA2_PHOS          7.21        6.5      7.8    0     0     1  # phosphate
PKA3_PHOS         12.35       11.5     12.5    0     0     1  # phosphate
PKA_AMMON          9.25        9.2      9.50   0     0     1  # ammonium
PKA_SOAP           5.5         4.0      6.0    0     0     0  # soap
PKA_SULPHATE       1.99        1.98     2.0    0     0     0  # sulphate
PKA_TOTALFA        4.75        3.7      6      0     0     1  # monoprotic
PKA_BLANK3          0          0        0      0     0     0  # monoprotic
PKA1_BLANK4         0          0        0      0     0     0  # diprotic
PKA2_BLANK4         0          0        0      0     0     0  # diprotic
PKA1_BLANK5         0          0        0      0     0     0  # diprotic
PKA2_BLANK5         0          0        0      0     0     0  # diprotic
PKA1_BLANK6         0          0        0      0     0     0  # triprotic
PKA2_BLANK6         0          0        0      0     0     0  # triprotic
PKA3_BLANK6         0          0        0      0     0     0  # triprotic
PKA_BLIND1          6          2       11      0     1     0  # blind 1
PKA_BLIND2          8          2       11      0     2     0  # blind 2
PKA_BLIND3          7          2       11      0     3     0  # blind 3
PKA_BLIND4          7          2       11      0     4     0  # blind 4
PKA_BLIND5          7          2       11      0     5     0  # blind 5
PKA_BLIND6          7          2       11      0     6     0  # blind 6
PKA_BLIND7          7          2       11      0     0     0  # blind 7
PKA_BLIND8          7          2       11      0     0     0  # blind 8
CONC_WATER         55.5        0        0      0     0     0  # water! in mol/l
CONC_CARBON         0.001      0        0.1    0     0     1  # carbonate
CONC_PHENOL         0.001      0        0.1    0     0     1  # phenol
CONC_PHOS           0.001      0      200     31     0     1  # phosphate
CONC_AMMON          0.001      0      600     14     0     1  # ammonium
CONC_SOAP           0.000      0        0      0     0     0  # soap
CONC_SULPHATE       0.0        0        0      0     0     0  # sulphate
CONC_TOTALFA      140         50      262     60     0     1  # monoprotic
CONC_BLANK3         0.0        0        0      0     0     0  # monoprotic
CONC_BLANK4         0.0        0        0      0     0     0  # diprotic
CONC_BLANK5         0.0        0        0      0     0     0  # diprotic
CONC_BLANK6         0.0        0        0      0     0     0  # triprotic
CONC_BLIND1         0.0        0        0.02   0     1     0  # monoprotic
CONC_BLIND2         0.0        0        0.01   0     2     0  # monoprotic
CONC_BLIND3         0.0        0        0.005  0     3     0  # monoprotic
CONC_BLIND4         0.0        0        0.005  0     4     0  # monoprotic
CONC_BLIND5         0.0        0        0.005  0     5     0  # monoprotic
CONC_BLIND6         0.0        0        0.005  0     6     0  # monoprotic
CONC_BLIND7         0.0        0        0.005  0     0     0  # monoprotic
CONC_BLIND8         0.0        0        0.005  0     0     0  # monoprotic
```

Under column NAME, there are two parameter categories: pKa value and concentration. The concentration of the components can be expressed in mg l^{-1} or mol l^{-1}. Milligram per liter is obtained when the molecular weight of a component is specified in the MOLW column; if not results are considered in mol l^{-1} form. In column OPT, the parameters that need to be optimized are indicated by writing 1. By writing zero they are used as such. The same procedure is applied to incorporate an unknown buffer in the model. The unknown parameters can be defined as blank 1 or blank 2 …etc. depending on how many buffers

are required in the model. The use of blanks could optionally be used in order to obtain the best model fit. Besides, the range of concentration and pKa values can be set variable or fixed by filling 1 or 0 in the column OPT. The pKa ranges should not overlap. Overlap introduces a high correlation among the parameters and troubles the optimisation. Part 6 was updated to allow automatic initialisation, as described in chapter 11, for the on-line implementation and the detection of more interfering buffers. The updated part is listed in BOX 10-7.

BOX 10-7

```
# Updated Model descriptions for simulation, optimization and model extension
#index NAME--------> INITIAL    ini_MIN    MIN   ini_MAX    MAX   MOLW B-    OPT   r_index
0      PKA_WATER     15.744     15.62      15.62 15.82      15.82 0    0     0     27
1      PKA1_CARBON   6.361      5.3        6.0   6.9        6.6   0    0     0     28
2      PKA2_CARBON   10.329     9.9        10.1  10.5       10.4  0    0     0     28
3      PKA1_PHOS     2.148      1.398      1.398 3.00       3.0   0    0     0     29
4      PKA2_PHOS     7.25       6.7        7.2   8.0        7.4   0    0     0     29
5      PKA3_PHOS     12.342     11.5       11.5  13.092     13.0  0    0     0     29
6      PKA_AMMON     9.252      8.5        8.9   9.8        9.5   0    0     0     30
7      PKA_PHENOL    9.968      9.968      9.968 9.968      9.968 0    0     0     31
8      PKA_SULPHIDE  6.992      6.992      6.992 6.992      6.992 0    0     0     32
9      PKA_VFA       4.75       4.006      4.5   5.4        5.0   0    0     0     33
10     PKA_LACTIC    3.863      3.1        3.5   4.5        4.2   0    0     0     34
11     PKA_BLANK3    0          0          0     0          0     0    0     0     35
12     PKA1_BLANK4   0          0          0     0          0     0    0     0     36
13     PKA2_BLANK4   0          0          0     0          0     0    0     0     36
14     PKA1_BLANK5   0          0          0     0          0     0    0     0     37
15     PKA2_BLANK5   0          0          0     0          0     0    0     0     37
16     PKA1_BLANK6   0          0          0     0          0     0    0     0     38
17     PKA2_BLANK6   0          0          0     0          0     0    0     0     38
18     PKA3_BLANK6   0          0          0     0          0     0    0     0     38
19     PKA_BLIND1    6          2          2     11         11    0    1     0     39
20     PKA_BLIND2    8          2          2     11         11    0    2     0     40
21     PKA_BLIND3    7          2          2     11         11    0    3     0     41
22     PKA_BLIND4    7          2          2     11         11    0    4     0     42
23     PKA_BLIND5    7          2          2     11         11    0    5     0     43
24     PKA_BLIND6    7          2          2     11         11    0    6     0     44
25     PKA_BLIND7    7          2          2     11         11    0    0     0     45
26     PKA_BLIND8    7          2          2     11         11    0    0     0     46
27     CONC_WATER    55.5       0          0     0          0     0    0     0     0
28     CONC_CARBON   0.0        0          0     0          0     0    0     0     0
29     CONC_PHOS     0.0        0          0     0          0     0    0     0     0
30     CONC_AMMON    0.0        0          0     0          0     0    0     0     0
31     CONC_PHENOL   0.0        0          0     0          0     0    0     0     0
32     CONC_SULPHIDE 0.0        0          0     0          0     0    0     0     0
33     CONC_VFA      0.0        0          0     0          0     0    0     0     0
34     CONC_LACTIC   0.0        0          0     0          0     0    0     0     0
35     CONC_BLANK3   0.0        0          0     0          0     0    0     0     0
36     CONC_BLANK4   0.0        0          0     0          0     0    0     0     0
37     CONC_BLANK5   0.0        0          0     0          0     0    0     0     0
38     CONC_BLANK6   0.0        0          0     0          0     0    0     0     0
39     CONC_BLIND1   0.0        0          0     0.02       0.02  0    1     0     0
40     CONC_BLIND2   0.0        0          0     0.01       0.01  0    2     0     0
41     CONC_BLIND3   0.0        0          0     0.005      0.005 0    3     0     0
42     CONC_BLIND4   0.0        0          0     0.005      0.005 0    4     0     0
43     CONC_BLIND5   0.0        0          0     0.005      0.005 0    5     0     0
44     CONC_BLIND6   0.0        0          0     0.005      0.005 0    6     0     0
45     CONC_BLIND7   0.0        0          0     0.005      0.005 0    0     0     0
46     CONC_BLIND8   0.0        0          0     0.005      0.005 0    0     0     0
```

Four columns are added. Two columns are added for indexing the parameters to allow the programme extension to interactively update the parameters according the measured titration data. The other two columns are to define initialisation minimum and maximum pKa values. The initialisation range defines the possible overlap of adjacent buffers without affecting the optimisation. In fact, the other minimum and maximum values will be used for the optimisation without overlap. With such extension, the 6 parts of the parameters file need to be defined only once for an on-line installation and no further

updates are needed from the user. However, for each common application, e.g. anaerobic digestion, a list of possible buffers and their initialisation ranges need to be tuned in order to achieve the most accurate results. The Titrimetric Analyser Simulator TAS presented in chapter 4 is a very useful tool to automatically define the initialisation ranges using off-line simulations.

10.5.2 INRA titrimetric sensor

10.5.2.1 Principle of the device

For robustness, the analyser uses approximate methods for alkalinity (bicarbonate) and VFA measurements. In order to decide on the most appropriate approach for the INRA objectives (i.e., precision as high as possible while maintenance efforts remain as low as possible), a careful comparison was performed between the different approximate methods:

a) The Kapp method with Total Alkalinity (TA) and VFA corresponding to acid added from pH 5 to pH 4 (Kapp, 1992),

b) The Anderson method with pH 5.1 and pH 3.5 as reference values (Anderson and Yang, 1992),

c) Calculation from measurements of TA and PA at pH 5.75,

d) The Moosburger method using added volumes of acid between pH 6.7 and 5.9 and between pH 5.7 and 4.3.

It was experimentally noted that the Kapp method has the lowest residual standard deviation while being the most robust facing clogging of the pH meter. It was thus decided to use the Kapp method for the INRA analyser but with modification to also determine the bicarbonate concentration. The methods' basis are presented in more detail in chapter 12.

10.5.2.2 Device description

In order to reduce cost, a self-made titrimetric sensor was developed, Figure 10.7. This sensor is made of a pH electrode (Heito, France) in a titration vessel (internal diameter of 2 cm and height of 12 cm). The cell cleaning, the sample introduction and acid addition are performed by two 10-ml syringes, twelve valves and two step-by-step bipolar motors (48 steps/tour) connected to an electronic device made of two 8255 components and managed by a 66 MHz PC486 computer. A pump is also managed to ensure air replacement in the cell and good mixing of the sample and the acid. The overall operation of the titrimetric sensor is managed by simple software. Five containers of water, acid, base and buffer

solutions of pH 7 and pH 4 are connected to the analyser for rinsing, titration, initial pH adjustment and pH-probe calibration, respectively.

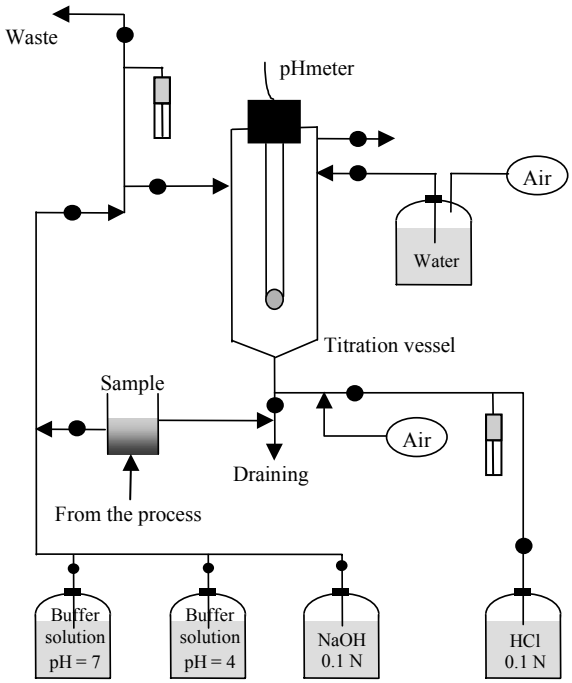

Figure 10.7 Schematic view of INRA titrimetric sensor

10.5.2.3 Setup operation

During the titration, 2 ml of sample is introduced under gravity in the vessel and pH is recorded during the titration of the sample by adding HCl acid (0.1N) from the syringe (1 rotation of the motor introduces 5 µl of acid) from an initial pH to 5.75 and then pH 3. In fact, it would have been enough to perform titration only until pH 4 since the calculations only require this value, but 3 is a good compromise to avoid influence of noise from the pH meter.

The time between introduction of the sample and ending of the calculation after titration is less than 3 minutes. In addition, the computer allows the titrimetric sensor to be fully autonomous since it manages the sample taking, the titration operation and the calculation of total and partial alkalinity together with VFA and bicarbonate concentrations. Automatic calibration of the pH meter is also performed using the buffering solutions of pH 4 and pH 7. Last but not least, calibration of the overall titrimetric sensor is automatically performed by using a NaOH 0.1N (100 meq/l) sample instead of a sample from the anaerobic digestion process.

10.5.3 AnaSense® on-line titrimetric analyser

The AnaSense® (De Neve et al., 2004) has been developed at "AppliTek NV, Nazareth, Belgium" in the context of the EU project "TELEMonitoring and Advanced teleControl of high yield wastewater treatment" (TELEMAC), IST-2000-28156. The know-how of INRA and BIOMATH as project partners and the present research supported the development of this analyser as the first commercially available on-line titrimetric analyser.

10.5.3.1 Principle of the device

The analyser uses approximate interpretation methods for bicarbonate and VFA as built-in methods of the analyser's industrial computer. It also produces detailed titration curves that can be transferred to a PC, through RS232 or by using a floppy drive, for advanced interpretation, such as by using the buffer capacity method (illustrated above for the BIOMATH titration setup and automated as in chapter 11). Two approximate methods are implemented. The first approximate method is the INRA-method that is implemented as described above for the INRA analyser and will be described in more detail in chapter 12. The second approximate method is newly developed by AppliTek and is based on the assumption of McGhee (1968) that the VFA concentration is related to the amount of acid added between pH 5 and 4. Therefore, the latter method strips the bicarbonate and hydrogen sulphide from the anaerobic samples (without any signficant stripping of the VFA) at a pH higher than 5 using air. Afterwards the VFA can be directly measured by a down-titration from pH 5 to 4.

The monotonic equivalence-point titration (MET) and the slope-based titration algorithms (Van Vooren, 2000) are implemented in the analyser. Titration can also be done by a mixed configuration of both algorithms. The whole pH range is divided in several intervals which can be defined via the software and the industrial PC of the analyser. In every interval a choice can be made between the two algorithms. Also, the time between two dosing steps and the waiting time between intervals can be defined in the software.

10.5.3.2 Device description

Figure 10.8 shows the developed analyser used for the on-line tests on the anaerobic digester. It consists of two parts, an upper data processing compartment with an industrial PC (touch screen) and a lower wet analysis compartment.

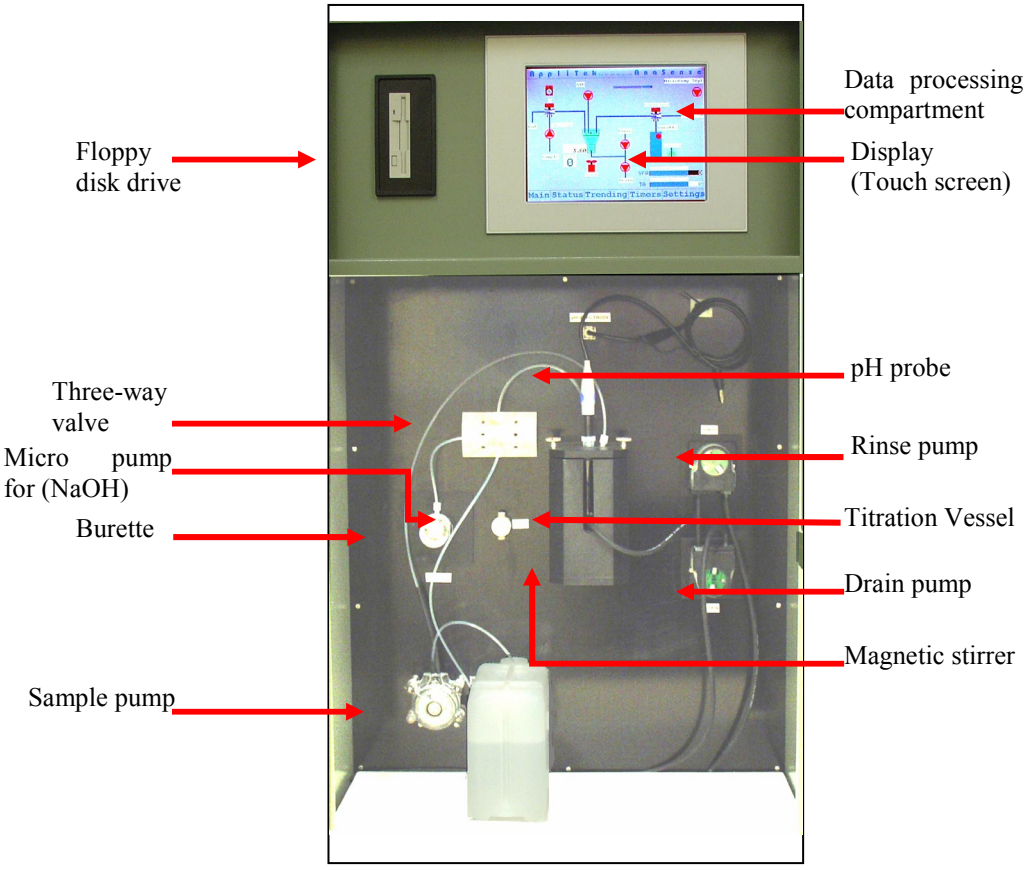

Figure 10.8 Front view of the of the AnaSense® analyser

The figure shows the analysis compartment and all the components used to perform the analysis. Effluent from the reactor is collected in an overflow vessel in order to refresh the sample continuously. A paper filter can be used to remove the big particles (like sludge). Filtration of the samples is usually not needed for the analysis, but sometimes it is necessary to prevent the sample tubing from clogging. For each analysis a sample volume of 10 *ml* is injected via a sample pump into the titration vessel. The sample mixing during titration is applied using a magnetic stirrer. Also, mixing with air can be provided by a membrane pump that can be mounted on the analyser. The dosing of the titrant (HCl 0.5 N) is performed by a burette with a minimum dosing step of 1 μl. Sometimes the pH of the reactor drops below pH 6 or VFA concentrations of an acidified influent need to be measured. In these cases it is necessary to adjust the initial pH by dosing NaOH. This is done by means of a micro-pump. The flow of the titrant and the sample into the titration vessel is regulated by a three-way valve. After each analysis the sample and rinsing water is drained with the drain pump. Rinse water is pumped by the rinsing pump.

10.5.3.3 Analyser operation

The analysis procedure takes 10 minutes and is performed according the following steps:

1. Emptying titration vessel.
2. Renewing the sample in the tubings.
3. Rinsing titration vessel with sample and then draining.
4. Dosing sample volume into titration vessel.
5. Stabilisation of the pH – probe.
6. Perform the titration with stepwise addition of acid.
7. Emptying titration vessel and rinsing with water.

The analyser and the titration itself are controlled by an industrial PC connected with a PLC. The control settings are adjustable from the computer touch screen. In the next chapters, the on-line implementation of the titrimetric analysis will be discussed.

10.6 Conclusions

The commercial availability of anaerobic digestion on-line monitoring equipment was reviewed. The result of this review is that most of the sensors and analysers of potential use in anaerobic digestion monitoring are commercially available, except for titrimetric analysers. The first one became commercially available for on-line implementation is developed parallel to and with support of this research.

The concept of titration is very simple, relying on a stepwise pH and volumetric measurements. According the reviewed literature, the titrimetric measurements are useful and applied to a wide spectrum of environmental and wastewater treatment applications. Most of the applications are, however, off-line. Some on-line applications are in ongoing research using prototype analysers and no evidence was found of full scale on-line applications.

Many titrimetric methods have been developed for measuring alkalinity and VFA in anaerobic digestion system. Most of these methods are simple and robust, but approximate. A more advanced method using advanced modelling techniques to interpret the buffer capacity curve is found accurate and useful to determine other buffers in addition to alkalinity and VFA. Therefore, three titrimetric analysers that use both approximate and advanced methods were described. Two are prototypes that have been developed in previous research and one is developed parallel to this PhD study for full-scale application. The analysers' principles, components and interpretation methods are illustrated in detail to support and clarify the further developments and applications that are introduced in the next chapters.

Chapter 11

Automatic initialisation for on-line Buffer Capacity Software (BCS)

Abstract

In this chapter, an automatic initialisation procedure has been developed as an extension to the software sensor Buffer capacity Optimal Model Builder (BOMB) that is used to determine the concentrations of buffers from a titration experiment. The extension has been integrated as a software layer around BOMB. The resulting Buffer Capacity Software (BCS) increased the robustness of the software sensor for on-line application and increased its ability to detect and quantify accurately a wide range of buffer combinations. A Titrimetric Analyser Simulator (TAS) was developed and used to test the BCS reliability in measuring buffer systems in an anaerobic digester that is operated under high dynamics and with very fast transition between different buffer combinations. The BCS has been tested and is now working with off- and on-line titrimetric analysers.

CHAPTER 11

11.1 Introduction

Buffer components are weak acids and bases that don't dissociate completely to their ions in aqueous solutions. Water itself is a buffer component that partially dissociates into H^+ and OH^-. Dissociated and undissociated species of buffer components will be held in equilibrium that tends to shift to release any stress exerted by the introduction of other buffer components, strong acids, strong bases or other external factors, e.g. temperature. Therefore, buffer components have a great influence on the chemical properties of a solution. Buffer components play an essential role in many, if not all, biological systems either due to their availability as substrate or due to their toxic effect to a living species. Therefore, quantification of buffer components is deemed to be very important for chemical, physical and biological process engineering.

Among other analytical techniques, titrimetric techniques are the most direct methods to quantify buffer components in aqueous solutions since they are directly related to their chemical equilibrium properties. Other techniques such as ion chromatography that can measure most of the buffers and gas chromatography that can measure volatile buffers, e.g. Volatile Fatty Acids (VFA), provide accurate results compared to titrimetric techniques. Furthermore, titrimetric techniques are far more economic, especially when considered for on-line applications.

Therefore, detailed titration data and advanced interpretation techniques are desirable to improve the accuracy of the titrimetric techniques and extend them for the determination of a wide range of buffer components. Detailed titration data can now be obtained on-line because of the present advances in instrumentation technology.

In the field of environmental engineering, water quality and wastewater treatment, determination of different combinations of buffer components is of significant importance. In such systems buffer components are subject to dynamics and transitions from one combination of buffers to another. Therefore, the developed measurement methods should be reliable to be applied to these varieties of applications and robust to cope with the rapid dynamics and transitions. In anaerobic digestion applications, as an example, many dynamics and transitions are observed. Bicarbonate and VFA are important buffers to monitor the process dynamics. Accumulation of VFA is important indicator of a digester overload. During overload, lactate will also start to build up in the reactor (Bjornsson et al., 2001). Phosphorous is released in the digester from polyphosphate hydrolysis and degradation of organic solids. Consequently, its quantification is important to assess recycling of digester overflows to a biological phosphorous removal plant (Wild et al.,

1997) or to study mineral precipitation problems in the pipe network and the sludge drying equipment of the treatment plant (van Rensburg et al., 2003). In certain anaerobic digestion applications, toxicant buffers exist in the influent wastewater at high concentrations and therefore their quantification is important. Ammonia is toxic to aceticlastic methanogenesis (Batstone et al., 2002). Except for their high ammonia concentration, different types of waste are suitable for anaerobic digestion such as piggery waste, poultry and cattle manure, and abattoir wastes (Ahn et al., 2004; Atuanya and Aigbirior, 2002; Borja et al.,1996; Wang and Banks, 2003). Cyanide and phenol are also toxic buffers that occur in many industrial applications. In many crop processing activities such as the production of starch from cassava, cyanide is produced and therefore is present in the produced wastewaters. They contain anaerobically degradable substrates but cyanide is inhibitory to methanogenesis (Gijzen et al., 2000). Therefore, a titrimetric sensor that is capable of quantifying different combinations of these buffers will be useful for the monitoring of the anaerobic digestion process.

A classification of the interpretation techniques for the titrimetric monitoring of the anaerobic digestion process (see Chapter 12) has shown that nonlinear fitting of buffer models is an advanced technique to improve the accuracy of the titrimetric measurement. A Buffer capacity based multipurpose hard- and software sensor for environmental applications was developed (Van Vooren, 2001). The software sensor fits a general buffer capacity model to a buffer capacity curve that is evaluated from a detailed titration experiment and estimates the characteristics of buffer components, e.g. concentrations and pKa values. The interpretation method depends on prior information about the buffer components to define and initialise the buffer capacity model. To deal with the expected limitation of prior information concerning the buffer systems in any application, the method was extended by model selection techniques (Van De Steene et al., 2002). The model selection starts with the optimisation of an initial model that is defined and initialised on the basis of the available information of buffer components in a certain system. Step-wisely, the model selection detects possible extensions to the initial model by other buffers that are introduced to the system and give new information on the most possible extension, e.g. pKa values of the new buffers. Both optimisation and model selection are built in the software sensor BOMB.

This chapter presents an extension to BOMB. From the raw titration data, the extension automatically defines and initialises the most probable model and as such increases the robustness of the software sensor for a wide range of on-line applications. The extension has been programmed in a software layer and integrated to BOMB. The result is a Buffer Capacity Software (BCS) that can work off/on-line with many titrimetric analysers. In this

chapter, BCS has been tested and validated with lab and on-line titrimetric analysers. Also, BCS has been tested using a Titrimetric Analyser Simulator (TAS). The test with TAS is designed to assess the linearity and robustness of BCS in measuring a wide range of buffer components under rapid transition conditions that may occur in anaerobic digestion applications.

11.2 Methods

11.2.1 General model

A general buffer capacity model was derived in (Van Vooren et al., 2001):

$$\beta = 2.303[H^+].\left(\begin{array}{l} 1+\sum_{i=1}^{l} C_i \left(K_a \frac{1}{([H^+]+K_a)^2} \right)_i + \sum_{j=1}^{m} C_j \left(K_{a1} \frac{[H^+]^2+4K_{a2}[H^+]+K_{a1}K_{a2}}{([H^+]^2+K_{a1}[H^+]+K_{a1}K_{a2})^2} \right)_j \\ \\ +\sum_{k=1}^{n} C_k \left(K_{a1} \frac{\begin{array}{r}[H^+]^4+4K_{a2}[H^+]^3+(K_{a1}+9K_{a3})K_{a2}[H^+]^2 \\ +(4[H^+]+K_{a2})K_{a1}K_{a2}K_{a3}\end{array}}{([H^+]^3+K_{a1}[H^+]^2+K_{a1}K_{a2}[H^+]+K_{a1}K_{a2}K_{a3})^2} \right)_k \end{array}\right) \quad (11.1)$$

where β: buffer capacity (eq $l^{-1}pH^{-1}$)

$[H^+]$: hydrogen ion concentration (mol l^{-1})

$C_{i,\ j,\ k}$: concentration of respectively a monoprotic, diprotic and triprotic weak acid (mol l^{-1})

K_a: acidity constant

The measurement principle is to successively measure pH as function of stepwise acid or base addition. In this way the titration curve is built. From this measured titration curve (typically around 30 to 50 points), the buffer capacity at each pH point is calculated as the derivative of the amount of base or acid needed to change the pH by one unit (meql $^{-1}$ pH^{-1}), equation (11.2), and a buffer capacity curve is produced. Based on the initialisation procedure developed below in this chapter, a buffer capacity model is defined using the general form of equation (11.1) and a model optimisation is initialised. The concentrations and pKa values are estimated by fitting the model to the buffer capacity curve.

The method was extended with an automatic model building procedure based on model selection techniques (Van De Steene et al., 2002). The model selection will act as a second barrier to alarm the user on the rare occasion that the initialisation procedure fails to

initialise other existing buffers. If the model selection detects such other buffers, it will provide an estimate of its pKa values and concentrations that will be useful to adapt the parameters of the initialisation procedure.

11.2.2 Monoprotic model initialisation

This procedure can be defined in three main steps. The first step is the generation of a smooth and uniform buffer capacity curve (BC) from the raw titration data. The titration experiment is a step wise addition of acid or base to the sample. At each step pH is measured so that data points are recorded as pairs of the pH and the volume of acid added. Knowing the experimental parameters, acid normality and sample volume, the buffer capacity is evaluated at each point using equation (11.2). With a reasonable number of calculated buffer capacity points, a smooth BC is obtained by parabolic interpolation at a 0.1 pH step. To this end, the BC is constructed and distributed at regular pH intervals between the experiment's minimum pH (TCmin) and maximum pH (TCmax).

$$\beta = -\frac{\Delta C_a}{\Delta pH} \quad \text{where } C_a \text{ is the acid concentration} \qquad (11.2)$$

The BC is $n \times 2$ array in (11.3)

$$\begin{matrix} BC_{j,1} = pH_j = (TC_{\min}, TC_{\min} + 0.1, \cdots, TC_{\max}) \\ BC_{j,2} = \beta_j \end{matrix}, \; j = (0,1,2,\cdots,n-1) \qquad (11.3)$$

The second step is a successive detection and subtraction of buffer components that possess the maximum buffer capacity after a previous subtraction. This step starts with the subtraction of the water buffer that usually have the maximum buffering capacity but at the extreme ends of the pH axis. In general the water buffer is the most dominant buffer at pH < 2.5 and at pH >10.5. For simplicity, only in this initialisation step, a buffer capacity model is assumed in which all buffers are considered monoprotic.

$$\beta_j = 2.303\left[H^+\right]\left(1 + C_w K_w^\dagger \frac{1}{\left(\left[H^+\right] + K_w^\dagger\right)^2} + \sum_i^m C_i K_i \frac{1}{\left(\left[H^+\right] + K_i\right)^2}\right)$$

$$\text{where: } \begin{matrix} [H^+] = 10^{-pH_j} = h_j(pH), \\ i = (1,2,\cdots,m) \end{matrix} \qquad (11.4)$$

It is assumed that m buffers exist in the sample. Each buffer has a concentration C_i and acidity constant K_i. In addition, the water buffer B_w exists with concentration $C_w = 55.5$ mol/l and $K_w^\dagger$ is function of the water acidity constant (11.5)

$$K_w^{\dagger} = \frac{K_w}{C_w} \tag{11.5}$$

Subtracting the water buffer and hydrogen ion effect from the raw BC results in another curve ($BC_{j,step,0}$), as in (11.6).

$$\forall j : BC_{j,step,0} = BC_{j,2} - B_{w,j} \tag{11.6}$$

If plotted against $\forall j : pH_j$, maxima of $BC_{j,step,0}$ curve are clear and the corresponding pH points are the $pK_{a,i}$ of buffering systems, provided that all buffer systems are distant enough (minimum overlap of adjacent buffers). Finding the maximum value of $BC_{step,0}$ at point j, the maximum concentration limit of the maximum buffering component can be determined and its pKa will be pH_j as defined in (11.7) and its maximum concentration value is calculated from (11.8).

$$\exists i, j : BC_{j,step,0} = \max\left(BC_{j,step,0}\right) \rightarrow \{pK_{a,i}, C_{i,\max}\} \tag{11.7}$$

for $\left(H_j^+ = K_i\right)$

$$C_{i,\max} = \frac{1}{2.303} \cdot BC_{j,step,0} \cdot \frac{\left(H_j^+ + K_i\right)^2}{H_j^+ \cdot K_i} = \frac{4}{2.303} \cdot BC_{j,step,0} \tag{11.8}$$

Equation (11.6) is applied again to subtract the buffer determined by (11.7) and (11.8) allowing to determine $BC_{step,l}$ and a new buffer. The steps involving equations (11.6) to (11.8) will be repeated till the maximum concentrations and pKa's are determined for all buffers. From equation (11.4) each buffer $B_i[j] = b(H_i^+, K_i, C_i)$. Therefore, the repetition of steps can be generalised in (11.9) for $l = (0) \cup (i)$.

$$\begin{aligned} &\forall l, j : BC_{j,step,l+1} = BC_{j,step,l} - B_{j,l+1} \\ &\forall l \exists i, j : BC_{j,step,l} = \max(BC_{step,l}) \rightarrow \left\{pK_{a,i}, C_{i,\max}\right\} \\ &C_{i,\max} = \frac{4}{2.303} \cdot BC_{j,step,0} \end{aligned} \tag{11.9}$$

Searching for buffers is stopped when the last buffering capacity value is less than a predetermined value. In the implementation this value is fixed to 10% of the highest buffer capacity value detected. Knowing the pKa values allows to identify the buffers present in the system. Therefore, at the end of this second step the model to be optimised is defined. However, for the optimisation buffer concentrations, range and initial value need to be defined. At this point, only the maximum limit for the concentration is known.

The third step defines the minimum possible BC and concentration of each detected buffer component B_i by looping over the other detected buffers ($r = 1 : m, r \neq i$) and subtracting

the maximum BC that can be introduced by these other existing buffers at the pKa point under consideration. This procedure is formulated in (11.10) assuming *m* detected monoprotic buffers.

$$B_{i,\min} = \frac{2.303}{4} \cdot C_{i,\max} - \sum_{r=1, r\neq i}^{m} 2.303\left[H_i^+\right]\left(1 + \frac{C_{r,\max} K_{a,r}}{\left(\left[H_i^+\right] + K_{a,r}\right)^2}\right) \qquad (11.10)$$

From this, a set of buffer objects is defined (11.11) so that a model can be defined. In addition, the concentration range of each buffer has been defined so that concentrations can be estimated by a minimisation algorithm, that aims at fitting the BC model to the BC data.

Buffers: $B_i = \{B_1, B_2, \cdots, B_m\}$ Buffer characteristics: $\forall i : B_i = \{pk_{a,i}, C_{i,\max}, C_{i,\min}\}$ (11.11)

It was found that $C_{i,\max}, C_{i,\min}$ are usually close to the actual concentration. This is useful for most of the minimisation algorithms to quickly find a global minimum and therefore the correct concentration. However, this narrow range can trouble some minimisation algorithms. For example, setting a narrow range can trouble the Praxis minimisation algorithm (Brent, 1973) that is used by the BOMB software. Therefore, it is decided to use the detected minimum concentration $C_{i,\min}$ as the initial value for the optimisation and extending the minimum bound to a significantly smaller value, i.e. allowing more freedom to the optimisation from the lower concentration end. This approach works well for the definition of the most probable model if the buffers are distant enough so that each buffer is present as a clear peak in the BC, see Figure 11.2.

However, if the buffers are not distant enough, adjacent buffers will overlap and form one peak, for instance as shown in Figure 11.3. One pKa value will be evaluated between their true pKa values. Since the detected peak doesn't correspond to one buffer, the subtraction of the monoprotic buffer model at the evaluated pKa will result in large residuals on both sides. The residual peaks will be erroneously detected by the above procedure as more buffers. Therefore, in case of overlap (interference), the initialisation procedure should be extended with some logic based rules for the accurate detection of interfering buffers.

11.2.3 Logic based rules

The logic in this extension of the initialisation is threefold. First, for the system that is intended for application (e.g. anaerobic digestion), a set of all possible buffers should be defined.

Second, for each pKa of the possible buffers, two acceptable ranges are defined. For initialisation purposes, a wide range for each pKa is assumed and overlap is allowed for any two adjacent buffers. It should be stressed that areas of overlap are not allowed for more than two buffers. Otherwise, a high correlation may make the optimisation fail. Another range is determined for the parameter estimation and is used to deal with the expected variation of external factors, e.g. temperature and ionic strength. These optimisation ranges shouldn't overlap as this is an essential requirement to guarantee the convergence of the optimisation algorithm. For example, for lactate (pKa = 3.86) and VFA (pKa = 4.75), their wide initialisation ranges could be 3.4-4.4 and 4.2-5.3 respectively. For pKa parameter estimation of lactate and VFA, reasonable ranges for optimisation are 3.6-4.2 and 4.4-5, respectively. It should be noted that some buffer components are diprotic or triprotic. Therefore, the corresponding pKa and pKa ranges should be defined twice or three times, respectively. But at the same time, their concentration is only defined once. For a number q of pKa definitions for possible buffers, the suggested characteristics are defined in (11.12).

$$B_p = \{B_{p,1}, B_{p,2}, \cdots, B_{p,s}\}$$

where

$$B_{p,s} = \{pK_{a,p,s}, pK_{a,s,\max}, pK_{a,s,\min}, pK_{a,s,in\_\max}, pK_{a,s,in\_\min}, C_{p,s.ini}, C_{p,s,\min}, C_{p,s,\max}\} \qquad (11.12)$$

with $s = 1:q$

The characteristics of possible buffers are defined on the basis of optimisation and interference:

- $pK_{a,p,s}$: the initial value for the optimisation pKa evaluated at standard conditions
- $pK_{a,s,\max}$, $pK_{a,s,\min}$: the maximum and minimum pKa values allowing a possible shift from standard conditions; overlap of adjacent ranges is not allowed.
- $pK_{a,s,in\_\max}$, $pK_{a,s,in\_\min}$: logical initialisation range for the detection of interference; overlap of adjacent ranges is allowed.
- $C_{p,s,ini}, C_{p,s,\min}, C_{p,s,\max}$: are respectively the initial, minimum and maximum concentrations of a buffer to initialise the optimisation of its concentration.

Last, the detected buffers B_i, determined in the monoprotic model-based initialisation, will be used in view of the initialisation of the pKa values of possible buffers. The result is a definition of the initial model for optimisation and an initialisation of their concentration. If B_i is generated by two interfering buffers, it will initialise two buffers B_p among the listed possible buffers using the switch $pK_{a\_hits,s}$. This switch has a default value of 0 and it changes to 1 on the first time that the detected buffer corresponds to one of these particular

two buffers B_p. This switch helps to test the hypothesis that only one of the two buffers is actually present. Also, it helps to adjust the maximum concentration bound of the different B_p's to the highest detected value. Initialised buffers will be defined for optimisation, $opt(B_{p,s})$. Therefore, if the buffer's $pK_{a,i}$ is within the initialisation range of a B_p buffer $(pK_{a,s,in\_\min} < pK_{a,i} < pK_{a,s,in\_\max})$, the logic procedure can be simplified in two situations, Equation (11.13). In the first situation ($pK_{a\_hits,s} = 0$), the buffers that will be optimised and their concentration ranges are defined. In the second situation ($pK_{a\_hits,s} = 1$), the concentration bounds are adjusted.

$$pK_{a\_hits,s}\begin{cases} = 0 \Rightarrow \begin{cases} opt(B_{p,s}) \\ C_{p,s,ini} = C_{i,\min} \\ C_{p,s,\min} = C_{i,\min} \\ C_{p,s,\max} = C_{i,\max} \end{cases} & \text{with:} \\ = 1 \Rightarrow \begin{cases} (C_{p,s,\max} < C_{i,\max}) \xrightarrow{Change} C_{p,s,\max} = C_{i,\max} \\ C_{p,s,ini} = 0 \\ C_{p,s,\min} = 0 \end{cases} & i = 1:m \quad (11.13) \\ & s = 1:q \end{cases}$$

Further rules need to be defined depending on the implementation and the software into which the initialisation procedure is to be integrated. For example, some rules are needed to define the settings of the optimisation algorithm, estimate the ionic strength of the titrated samples when using BOMB, …etc.. For the present implementation, the interference detection has been integrated with the monoprotic model-based initialisation procedure, programmed in C++ , supplemented with other interface modules and combined as a software layer around the BOMB software.

11.2.4 On-line implementation

Figure 11.1 shows the flow chart of BCS. After a titration experiment is done by a titrimetric analyser the titration curve is logged into a computer. The user starts the BCS and chooses the run mode: off-line or on-line, according to the analyser to which BCS is connected. For each instance of the internal loop, BCS manages different procedures for calculation, result output and logging the information, necessary to assess the quality of the titration experiment. All calculation procedures and modules are managed by the integration module. The calculation modules and procedures comprise the initialisation module, the BCS parameters procedure, the interference detection module and the Buffer capacity Optimal Model Builder (BOMB) procedure. The BCS parameters procedure reads the parameters needed for other modules and procedures from a standard initialisation file. The initialisation and interference detection modules work interactively with the BCS

parameters procedure to update its objects according the information abstracted from the titration data and the defined logic rules. The appropriate initial model, parameters and data are then passed to BOMB.

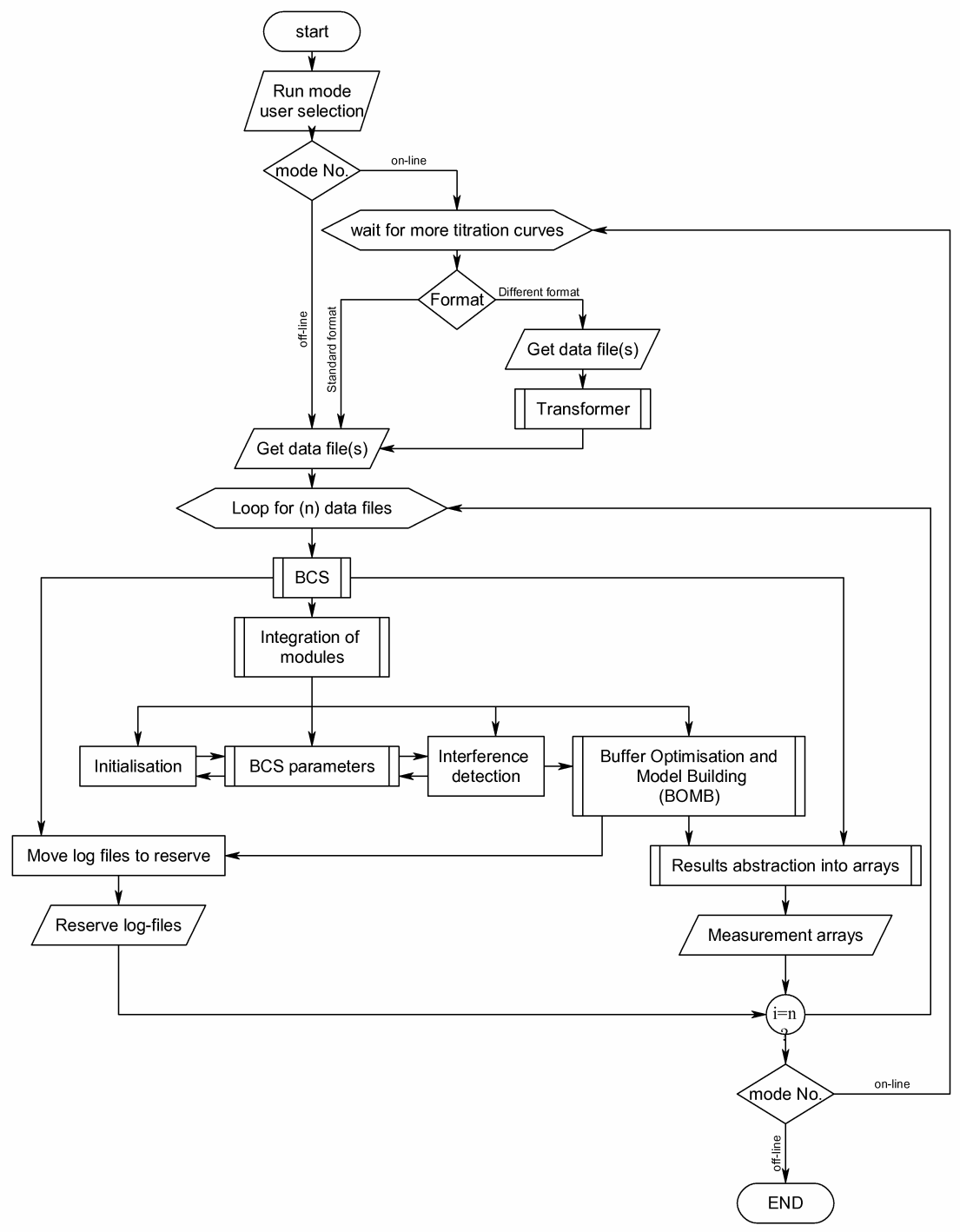

Figure 11.1 Flow chart of the Buffer Capacity Software (BCS)

BOMB optimises the initialised model to fit the buffer capacity data that is calculated from the titration experiment. As a check point BOMB applies advanced model selection techniques to evaluate the optimisation results of the initial model and propose a model

extension if deemed useful to get a better fit. The optimisation results and quality parameters of the titration curve are stored in log files. The results are stored in separate arrays for each buffer concentration and pKa values so that each measurement can be dealt with as an on-line mono-sensor output that is useful for data validation, e.g. detection of outliers, shifts, drift…etc.

11.2.5 Validation methods

Validation has been performed in three ways. First, a titrimetric analyser simulator was built using the WEST modelling software (HEMMIS N.V., Kortrijk, Belgium). The simulator generates ideal titration curves for any buffer combination defined in the simulator parameters and using the sampled input concentration. In the present work external factors such as temperature and ionic strength were not considered. The BCS, with the initialisation software layer, is then used to analyse the virtual titration curves and its results were compared to the simulator parameters and inputs.

Second, titration experiments were done with various combinations of buffer standard solutions. A Metrohm® lab titrimetric analyser was used for the titration experiments. These lab titration experiments were designed to test the detection of the most interfering buffers.

Third, BCS was tested with titration data collected from the on-line titrimetric analyser AnaSense® (AppliTek, Nazareth, Belgium). The analyser was installed on-line at a lab-scale UASB reactor which was fed with synthetic wastewater made of wine and starch (COD of the influent is varying between 5000 and 10000 mg/l). The temperature of the reactor was 37°C and pH was stabilized around 7.2. The BCS results are then compared with the bicarbonate and VFA measurement provided by the on-line analyser using two other methods to interpret the raw titration curves (De Neve et al., 2004). The analyser measurement method 1 was developed by INRA (Institut National de la Recherche Agronomique, Narbonne, France) and is based on the Kapp method for VFA measurement, extended for bicarbonate measurement (Bouvier et al., 2002). The analyser method 2 was developed by AppliTek (Nazareth, Belgium), based on the Method of McGhee (1968). Bicarbonate is stripped in the form of CO2 from the anaerobic samples at a pH below 5 using compressed air. Due to the stripping of CO2 the pH will tend to rise. The quantity of acid added till pH 5 can be related to the bicarbonate alkalinity. Afterwards, the VFA can be directly measured by a down-titration since it is directly related to the volume of acid added between pH 5 and pH 4 (McGhee, 1968).

11.3 Results and discussions

11.3.1 Simulated titration curves

Ideal titration curves were produced by the Titrimetric Analyser Simulator (TAS) and then used to test the initialisation and optimisation procedure. It can be seen in Figure 11.2 that, as expected, a perfect fit could be reached. Figure 11.2 (a) shows the BC of 0.1 M VFA and 0.1 M carbon system mixture. In this combination, 3 peaks are very clear for VFA, bicarbonate and carbonate at pH points that correspond to their approximate pKa values. The carbon system is a diprotic buffer and therefore produces two peaks. Table 11-1 shows the detected buffer characteristics using the monoprotic model based approach, the initialised model and the optimisation results.

Table 11-1 Initialisation and optimisation results of 0.1 M VFA and 0.1 M carbon mixture

	Detected buffer characteristics			Buffer model initialisation		
Buffer: No./component	0	1	2	VFA	carbonate	bicarbonate
$pKa_{detected/initial}$	4.9	10.3	6.4	4.75	10.33	6.361
pKa_{min}	-	-	-	4.1	10.1	5.6
pKa_{max}	-	-	-	5.5	10.9	6.6
Maximum BC (mmol/l/pH)	62.78	56.69	61.62	-	-	-
Maximum concentration (mol/l)	0.109	0.098	0.107	0.109	0.107	
Minimum BC (mmol/l/pH)	55.45	56.66	54.13	-	-	-
Minimum concentration (mol/l)	0.096	0.098	0.094	0.00096	0.00094	
Initial concentration	-	-	-	0.096	0.094	
	Optimisation results:		pKa	4.745	10.36	6.344
			pKa STD	0.001	0.001	0.000
			concentration	0.099	0.10	
			Conc. STD	0.00086	0.00060	

The detected pKa values were used to define the components of the buffer model. For the optimisation of the pKa values, they were initialised to their standard value. Their optimisation ranges (minimum and maximum values) were set to predefined values to accommodate possible shifts due to external factors such as temperature and ionic strength of the solution. The detected buffer characteristics are from the monoprotic model based initialisation approach. The detected minimum and maximum concentration are very close to the real concentration. The detected minimum concentrations were used as initial values for the optimisation problem. The minimum bounds were set to 1% of the initial value and the maximum bounds were maintained as detected. The carbon system was detected by

both its species, i.e. bicarbonate and carbonate. Automatically, the initialisation program recognised that the carbon system is diprotic and thus the concentration parameters were assigned only once, for both of them. The maximum bound was chosen as the largest of the two, while the minimum and initial concentrations were chosen as the lowest from the detected values of bicarbonate and carbonate. With this accurate and concise initialisation, the minimisation algorithm reached a global minimum quickly and gave accurate results. Figure 11.2 (b) shows the BC of a VFA and phosphorous mixture. For this mixture, 2 peaks will be very clear for VFA and phosphorous at pH points that correspond to their approximate pKa values.

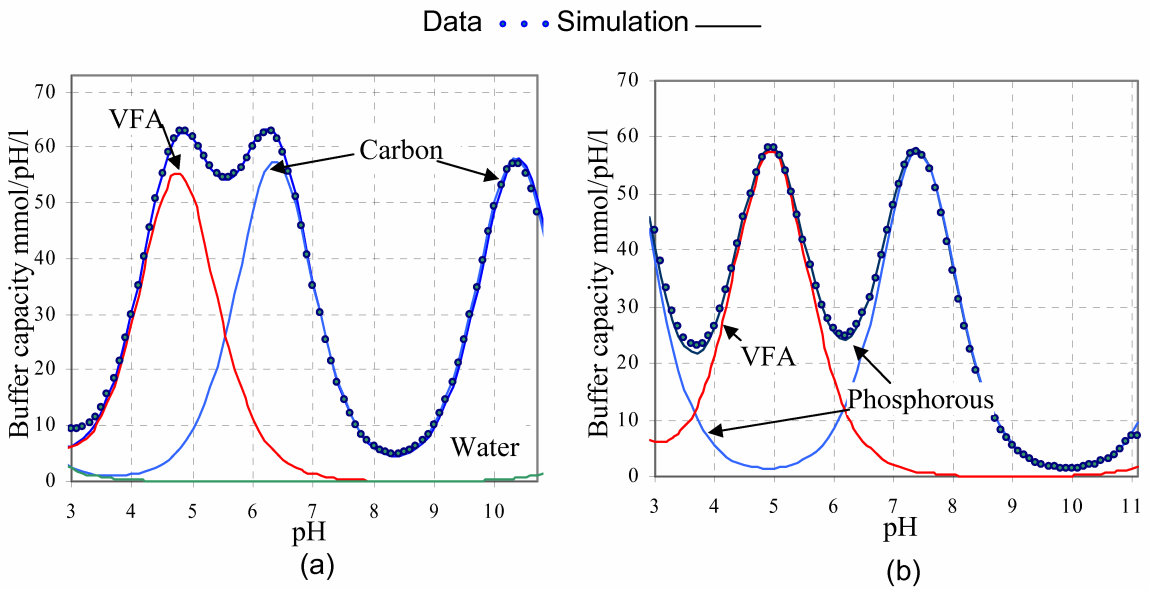

Figure 11.2 Examples of sufficiently distant buffers to be initialised by the monoprotic model approach. (a) 0.1M VFA and 0.1M carbon. (b) 0.1M VFA and 0.1M phosphorous.

Despite the fact that phosphorous is triprotic and hence has 3 pKa values, only the middle one will be clear because the other two, at 2.15 and 12.35, cannot be seen in the BC because they will be in the range of high interference by the water buffer. The initialisation and optimisation results for this example are listed in Table 11-2. These results lead to a similar interpretation as described for Table 11-1 except that the phosphorous concentration was directly initialised according to the only detected middle peak (pKa_2).

Table 11-2 Initialisation and optimisation results of 0.1 M VFA and 0.1 M phosphorous mixture

	Detected buffer characteristics		Buffer model initialisation	
Buffer: No./component	0	1	VFA	phosphorous
$pKa_{detected/initial}$	4.8	7.2	4.75	7.206
pKa_{min}	-	-	4.1	7.1
pKa_{max}	-	-	5.5	8.0
Maximum BC (mmol/l/pH)	58.02	57.56	-	-
Maximum concentration (mol/l)	0.101	0.010	0.101	0.010
Minimum BC (mmol/l/pH)	55.54	56.63	-	-
Minimum concentration (mol/l)	0.096	0.098	0.00096	0.00098
Initial concentration	-	-	0.096	0.098
Optimisation results:		pKa	4.75	7.20
		pKa STD	0.000	0.000
		concentration	0.10	0.10
		Conc. STD	0.00048	0.00044

Figure 11.3 shows 2 examples of buffer interferences. The accurate initialisation leads to accurate optimisation results as shown in Table 11-3. Also, it can be seen from Figure 11.3 that a perfect fit could be reached. Figure 11.3 (a) shows the BC of a mixture of 0.05 M VFA, 0.1 M sulphide and 0.05 M carbon system. In this combination, 3 peaks are clear. The peaks of VFA and carbonate are clear at their approximate pKa Values. Sulphide interferes with bicarbonate and both are shown as one peak between their pKa values. Table 11-3 shows the detected buffer characteristics using the monoprotic model-based approach, the initialised model and the optimisation results.

In addition to the steps illustrated for the buffer combinations that are presented in Table 11-1 and Table 11-2, the logic based rules are implemented to deal with the interference between bicarbonate and sulphide. The pKa of the detected buffer 0 hits the initialisation ranges defined for both sulphide and bicarbonate and therefore both buffers were activated for optimisation. The pKa values are initialised with standard condition values. The pKa optimisation ranges are set to the predefined values. The detected maximum concentration of buffer 0 is used as the upper bound of both the sulphide and carbon system concentration. Initial and minimum values are set to very small values (to numerically approximate zero). This initialisation of concentrations corresponds with asking the optimiser two questions:

- Is the detected area of interference due to both interfering buffers or only due to one of them?

- How much are the concentrations, provided that it shouldn't exceed the specified maximum concentration?

Then, the optimiser gives its answer in the light of the best fit of this peak of interference and within the constraints of the specified pKa optimisation ranges. It can be seen from the optimisation results in Table 11-3 that accurate concentration results of all buffers can be reached.

Table 11-3 Initialisation and optimisation results of 0.05 M VFA, 0.1 M sulphide and 0.05 M carbon mixture (logic based rules are applied)

	Detected buffer characteristics			Buffer model initialisation			
Buffer: No./component	0	1	2	VFA	sulphide	carbonate	bicarbonate
$pKa_{detected/initial}$	6.8	4.8	10.3	4.75	6.9	10.33	6.36
pKa_{min}	-	-	-	4.3	6.7	10.1	5.6
pKa_{max}	-	-	-	5	7	10.9	6.6
Maximum BC (mmol/l/pH)	77.62	32.86	28.47	-	-	-	-
Maximum concentration (mol/l)	0.135	0.057	0.045	0.057	0.135	0.135	
Minimum BC (mmol/l/pH)	76.30	29.82	28.37	-	-	-	-
Minimum concentration (mol/l)	0.132	0.052	0.0493	0.00052	1e-05	1e-05	
Initial concentration	-	-	-	0.052	1.1e-05	1.1e-05	
Optimisation results:			pKa	4.747	6.987	10.35	6.36
			pKa STD	0.013	0.006	0.012	0.000
			concentration	0.050	0.10	0.050	
			Conc. STD	0.00066	0.00099	0.00054	

Figure 11.3 (b) shows the BC of a mixture of 0.05 M VFA, 0.05 carbon and 0.1M ammonia and Table 11-4 shows the detected buffer characteristics. In this combination, 2 peaks for VFA and bicarbonate are very clear at pH points that correspond to their approximate pKa values. Ammonia and carbonate appear as one peak. Despite this interference, they were detected by the monoprotic model-based approach and therefore concise concentration ranges could be defined for optimisation. The reasons for this good result are that the approach applies successive subtraction of buffers and the approximate 1 pH unit difference between the ammonia pKa and carbonate pKa allows their detection in the monoprotic model-based approach.

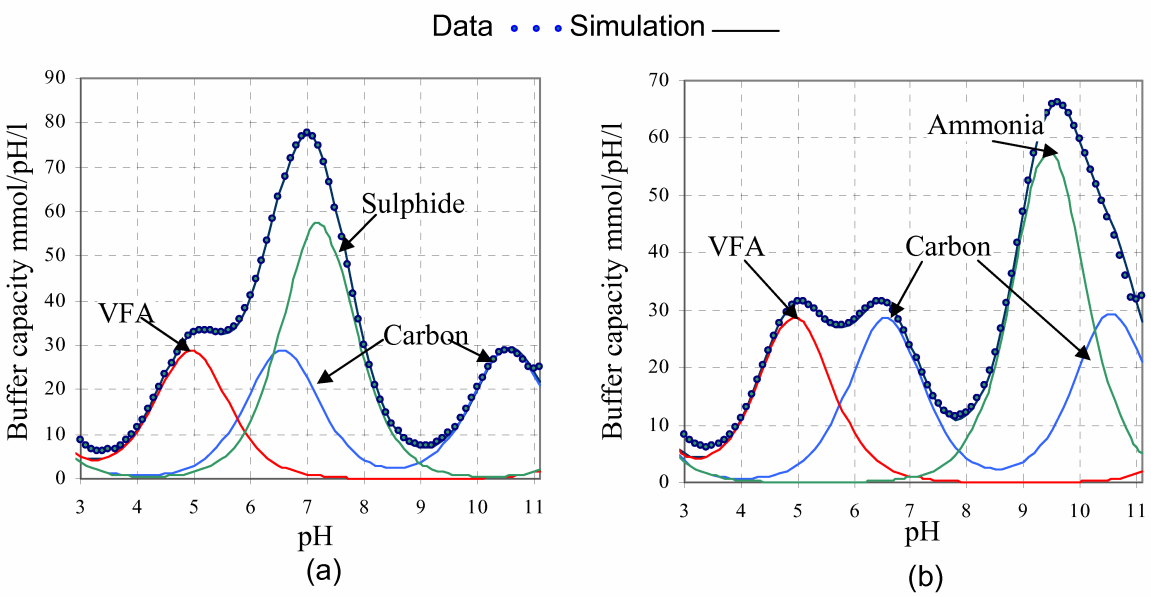

Figure 11.3 Examples of mixtures with interfering buffers that can accurately be initialised by integrating the monoprotic model approach and the logic based approach. (a) 0.05M VFA, 0.05M carbon and 0.1 sulphide. (b) 0.05M VFA, 0.05M carbon and 0.1 ammonia.

Table 11-4 Initialisation and optimisation results of 0.05 M VFA, 0.1 M ammonia and 0.05 M carbon mixture

	Detected buffer characteristics				Buffer model initialisation			
Buffer: No./component	0	1	2	3	VFA	ammonia	carbonate	bicarbonate
pKa detected/initial	9.4	6.3	4.7	10.5	4.75	9.252	10.33	6.361
pKamin	-	-	-	-	4.3	8.5	10.1	5.6
pKamax	-	-	-	-	5	9.7	10.9	6.6
Maximum BC (mmol/l/pH)	66.23	31.65	30.75	38.72	-	-	-	-
Maximum concentration (mol/l)	0.115	0.055	0.053	0.067	0.053	0.115	0.067	
Minimum BC (mmol/l/pH)	55.57	28.49	27.72	20.65	-	-	-	-
Minimum concentration (mol/l)	0.096	0.050	0.048	0.036	0.00050	0.00096	0.00036	
Initial concentration	-		-	-	0.0481	0.096	0.0359	
Optimisation results: pKa					4.748	9.267	10.4	6.357
pKa STD					0.014	0.007	0.024	0.000
concentration					0.050	0.101	0.050	
Conc. STD					0.00066	0.00104	0.00062	

11.3.2 Robustness during fast transitions

Based on simulations, the usefulness of BCS and the developed initialisation procedure for monitoring of anaerobic digestion is illustrated. Also, the BCS with the initialisation modules is tested for the automatic detection of rapidly changing buffer combinations. The test is performed on the hypothetical change of buffer concentrations that is shown by the

solid lines in Figure 11.4. The change of buffers was designed to imitate different scenarios that would be relevant in the practice of monitoring the anaerobic digestion process under rapid transitions of operating conditions. Indeed, these dynamics would be very severe to an anaerobic digester but the idea is to test BCS and the initialisation procedure on such hypothetical extreme case. The dynamics were designed as a combination of triangular waves of different buffer concentrations. Two peaks of amplitude 0.105 M VFA with a minimum of 0.005 M VFA are accompanied with similar but inverse waves of carbon. This imitates the dynamics in a digester during overloads: Bicarbonate alkalinity is consumed during VFA accumulation. Then the alkalinity is recovered when the VFA concentration drops. The first peak of VFA is accompanied with a peak of lactate that is expected to accumulate during overload too. The second VFA peak is accompanied with a peak of ammonia that is toxic to methanogenesis and therefore would cause such VFA accumulation. Between the two peaks of VFA, a peak of phosphorous is introduced to imitate a case of phosphorous release, VFA uptake and alkalinity increase that would happen in a digester fed by sludge from a biological phosphorous removal plant. Along the first 10 time units hydrogen sulphide is added as a source of toxicity to the anaerobic digestion process during the feed with a high sulphate concentration. Also, at the last 10 time units phenol is added as a source of toxicity that may be expected in some types of wastewaters.

The evolution was simulated in WEST with the TAS running simulations of titration experiments at the regular sampling rate. At each sampling point an ideal titration curve is simulated for the corresponding buffer combination. All titration curves are subsequently evaluated by BCS with the same pKa optimisation and initialisation ranges $pK_{a,p,s}$, $pK_{a,s,\max}$, $pK_{a,s,\min}$, $pK_{a,s,in\_\max}$, $pK_{a,s,in\_\min}$. Automatically BCS activates the proper model for optimisation at each sampling point. Other initialisation parameters $C_{p,s.ini}$, $C_{p,s,\min}$, $C_{p,s,\max}$ were determined automatically by the monoprotic model-based approach and the logic based rules extension. It can be seen from Figure 11.4 that the BCS measurements correlate well with the simulated dynamics of the different buffer combinations.

Figure 11.5 shows the results that were obtained when using BOMB under the designed dynamics without BCS initialisation or human interaction to improve its initial model. It was found that it was not possible to run BOMB with all buffers defined for optimisation. The initial model was then defined for BOMB such as to optimise the two main buffers (the carbon system and the VFA). Except for a few sampling points that correspond to the lactate interference, the model selection performed by BOMB was not powerful enough to extend the initial model with blind buffers for this particular set of complicated

interferences. However, the concentrations for bicarbonate (carbon system) and VFA determined by BOMB still show a reasonable correlation with the simulated dynamics of the two components. Visually, it is clear, however, that the initialisation by BCS gives better results. This will be evaluated statistically below.

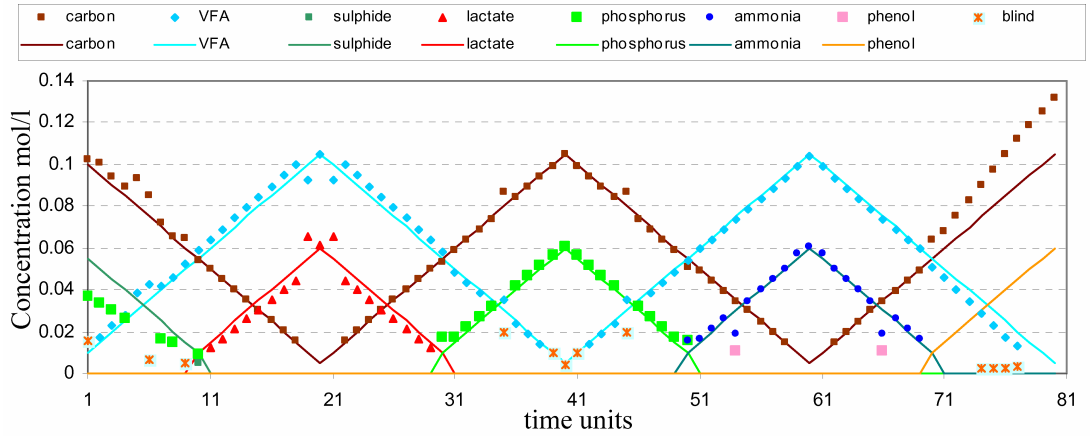

Figure 11.4. Robustness test of BCS under fast transitions of buffer combinations. Lines are simulated buffer concentrations and symbols are BCS estimated concentrations.

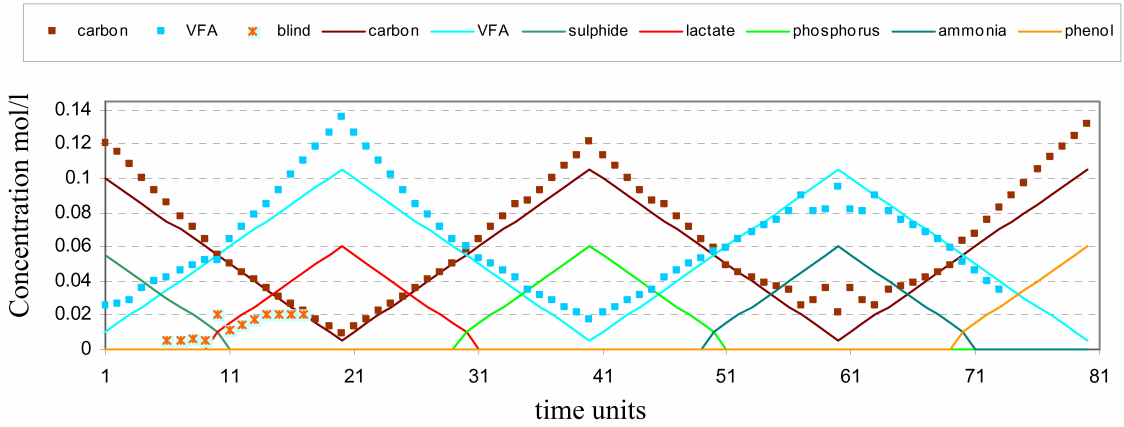

Figure 11.5 Possible results from BOMB under fast transitions of buffer combinations. Lines are simulated buffer concentrations and symbols are BOMB estimated concentrations.

To reflect the extent of the linear relationship between the expected concentrations and the BCS and BOMB measurements, the Pearson product moment correlation coefficient, r, was calculated for each buffer component:

$$r = \frac{n \cdot (\sum XY) - (\sum X) \cdot (\sum Y)}{\sqrt{\left[n \cdot \sum X^2 - (\sum X)^2\right] \cdot \left[n \cdot \sum Y^2 - (\sum Y)^2\right]}} \qquad (11.14)$$

X: is the independent value (the expected measurement).

Y: is the dependent value (the observed measurement).

Table 11-5 shows the r values for each buffer except phenol, since phenol could not be detected when present in combination with carbonate (see below). The high linearity of the BCS data can be deduced from the high r values. Sulphide has the lowest value since it was confused with phosphorous and calculated as such. However, from investigating the optimised pKa values, it can be observed that they are usually equal to the lower bound of the optimisation range of the pKa of phosphorous. Indeed, three buffers at the same peak cannot be accurately measured, even if the three can be automatically initialised. The high correlation will trouble the minimisation algorithm (i.e. Praxis will be trapped in a local minimum) and the three interfering components will not be estimated accurately. The pKa of sulphide at 7 is close to that of phosphorous at 7.2 and doesn't allow that both are initialised besides bicarbonate at pKa of 6.35. Therefore, it is up to the user to decide which component exists. In another situation, if both sulphide and phosphorous need to be determined, an additional titration experiment needs to be performed for the same sample. The additional experiment should be performed by first stripping of CO_2 and H_2S at low pH. This way phosphorous could be determined accurately. Then a second experiment is performed without stripping and phosphorous is fixed in the model building to the value detected from the first experiment. Then the bicarbonate and sulphide can be estimated. However, handling of nested titration experiments is out of the scope of the present approach of automatic initialisation. Similarly, phenol could not be detected because of interference of its pKa of 9.97 to the carbonate pKa of 10.35 and the high interference of the water buffer at pH > 10.5. Also, in this situation, an additional titration experiment with CO_2 stripping would be required.

Table 11-5 Pearson correlation coefficient of BCS linearity with the real concentrations in case of ideal titration curves.

buffer	carbon	VFA	sulphide*	lactate	phosphorous	ammonia
r (BCS)	0.982828	0.99038	0.901139	0.984847	0.943402	0.991353
r (BOMB)	0.981025	0.945581	-	-	-	-

* was detected as phosphorous due the high interference of three buffers (bicarbonate, sulphide and phosphorous)

It can be seen from Figure 11.4 that some outliers appear. Also, drift and shift can be seen upon the introduction of some buffers that cannot be initialised due their interferences with other buffers. Examples, shown in Figure 11.4, are H_2S and phenol as discussed above. Therefore, on-line mono-sensor validation procedures to detect outliers, drift and shift can be applied to ensure that improper data are not passed on to an automatic control system (Olsson and Newell, 1999). It will be shown later in the on-line validation section that such procedures are also useful to filter out other bias that is due to anomalies in the titration experiments.

11.3.3 Validation with standards

The initialisation procedure and BCS were further validated by titrating standard solutions with known buffer concentrations. The experiments with standards aim to test combinations of important interfering buffers that are expected in anaerobic digestion.

The main buffer components in anaerobic digestion are Bicarbonate and VFA. The most interfering buffer with VFA is lactate that can be considered as an indicator of digester overloads (see Chapter 12). Figure 11.6 (a) gives an overview of the obtained BCS measurements of VFA and lactate mixtures. The results cover a wide range of VFA/lactate ratios. The linearity of the results was tested with equation (11.14). For VFA, r is 0.99 and for lactate r is 0.995.

Phosphorous can be considered as the buffer that is most interfering with bicarbonate. Figure 11.6 (b) shows the linearity of the BCS measurements of bicarbonate and phosphorous mixtures. Again, linearity was tested. For bicarbonate r is 0.998 and for phosphorous r is 0.996.

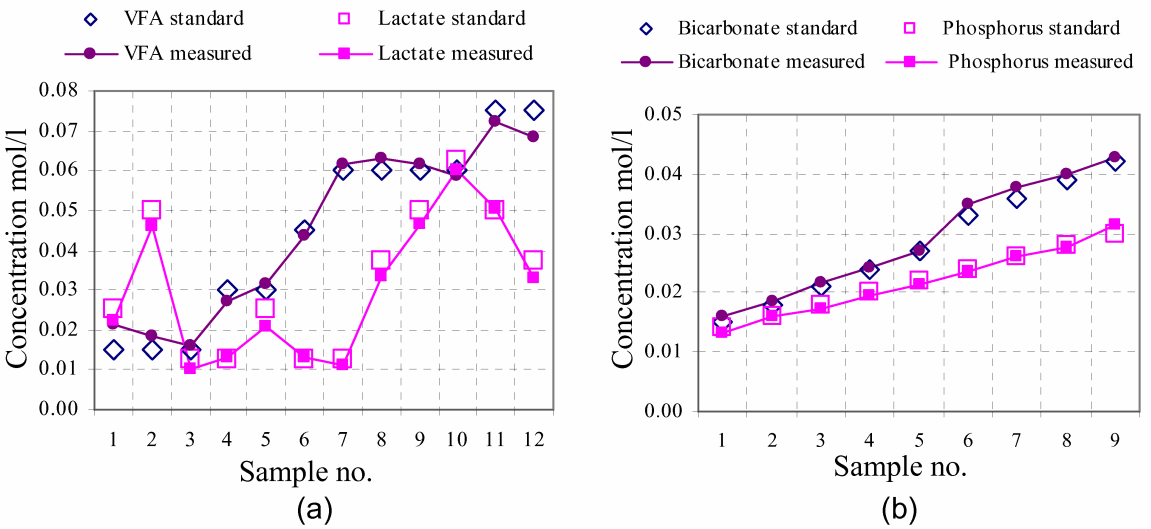

Figure 11.6. Validation of BCS with standard solutions. (a) VFA and lactate (b) bicarbonate and phosphorous

When performing actual titration, the actual pKa values may differ from their standard values because the titration is not performed under standard conditions. Also, a shift in the pH measurement (due to drift in the electrode) will change the detected pKa value. Such shifts will not affect the detected results as long as the shifts are within the pKa initialisation ranges. Indeed, the pKa-value will be estimated so as to fit optimally to the measured BC data. Figure 11.7 (a) shows the measured and simulated BC curves of sample 3 in Figure 11.6 (a). VFA and lactate buffers could be initialised and accurately measured although there was a shift from the standard pKa values. Similarly, in Figure 11.7 (b), the

bicarbonate and phosphorous values could be initialised and accurately estimated despite the shift in pKa values. Figure 11.7 (b) shows the measured and the simulated BC curves of sample 5 in Figure 11.6 (b).

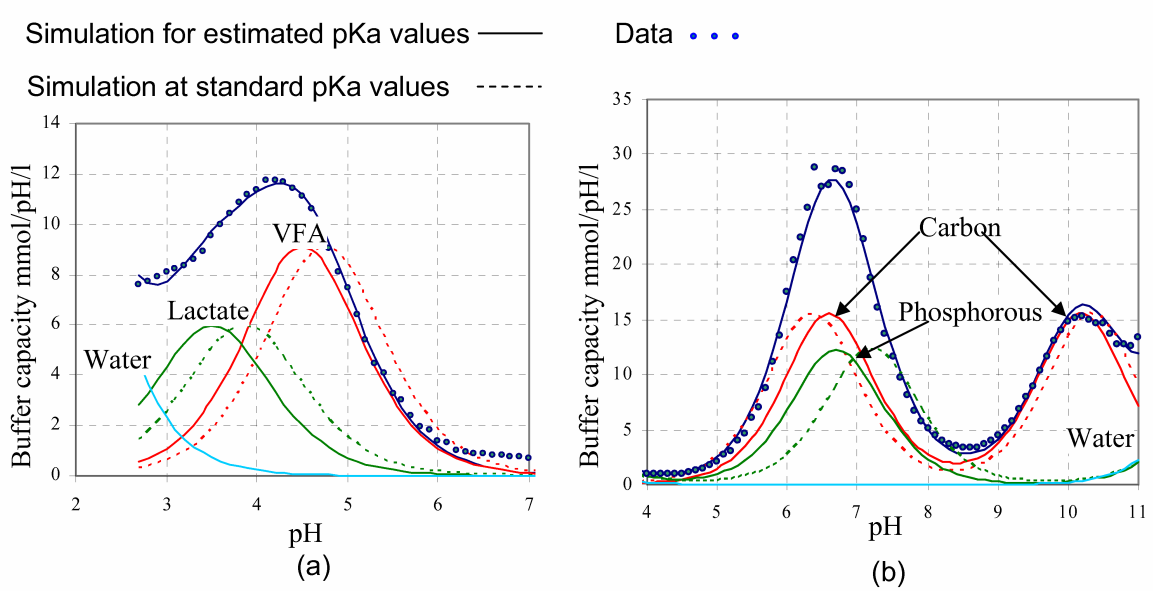

Figure 11.7. BC results for measuring standard solutions while having pKa shifts. (a) VFA and lactate (b) carbon and phosphorous.

11.3.4 On-line validation

The Titrimetric analyser, AnaSense® (AppliTek, Nazareth, Belgium) was installed on-line at an UASB reactor (De Neve et al., 2004) to monitor bicarbonate and VFA concentrations. The AnaSense® performed the titration experiments on-line, starting from the pH of the reactor (maintained around 7) and titrating down to pH 3.5 with step acid addition every 8 seconds. Titration data were collected from the titrimetric analyser during three periods (382-395 h, 401-418 h and 427-433 h). The BCS analysed the collected titration data and results are shown in Figure 11.8 (a) for bicarbonate and (b) for VFA. The results are compared with the results of the interpretation methods 1 and 2 that are built-in in the analyser (De Nave et. al., 2004). Similar results of the BCS and the analyser are obtained for bicarbonate, Figure 11.8 (a). Figure 11.8 (b) shows the VFA results of the three methods compared to the GC results. The three methods follow the same dynamics and correspond to the GC.

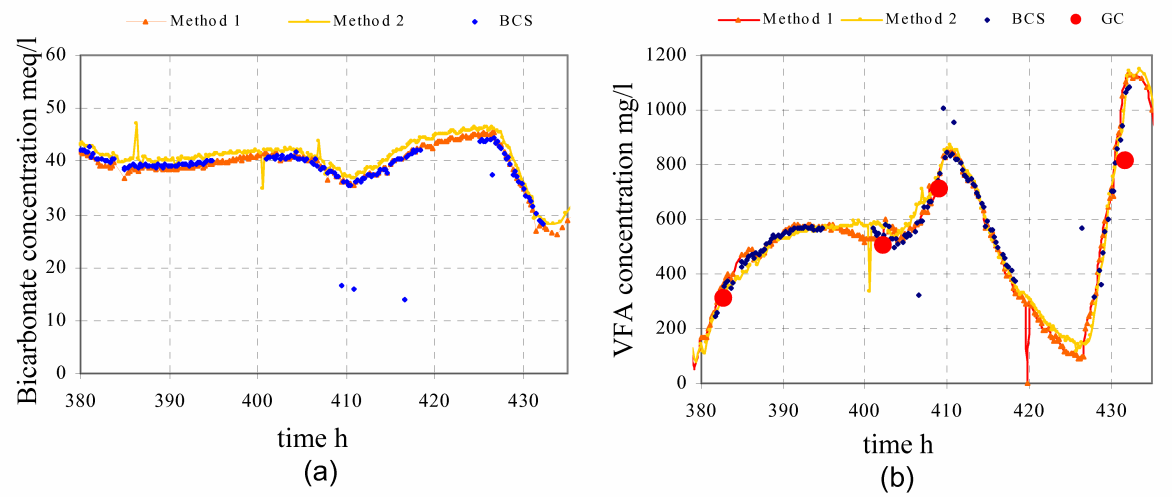

Figure 11.8. On-line validation analysis results using AnaSense® built-in methods 1and 2, BCS and Gas Chromatography (GC)

11.4 Conclusions

The initialisation procedure presented in this chapter is able to extract useful information from simple titration experiments. The required information concerns the likely buffers to be present in the titrated sample and their expected concentration range. This information is shown to be sufficient to initialise an optimisation procedure that allows to accurately determine the buffer concentrations.

The procedure doesn't require frequent interaction with the user to study prior analyses results or information about the system to update the optimisation model. The model is defined and initialised automatically and therefore the robustness for on-line application increases.

The initialization procedure has been implemented in a software layer and integrated to a buffer capacity software sensor, Buffer capacity Optimal Model Builder (BOMB), that applies modelling and optimisation techniques to analyse buffer systems observed in titration data. The resulting Buffer Capacity Software (BCS) was tested in three ways: a titrimetric simulator, a lab-analyser and an on-line analyser. BCS showed its potential to accurately measure a wide range of buffer components and combinations. It also has a high measuring quality, even under fast transitions between different buffer combinations. For biological processes such as anaerobic digestion that require continuous and on-line monitoring of buffering substrates or toxic compounds, BCS is a good solution.

Chapter 12

Extended applications of titrimetric monitoring and evaluation of BCS results

Abstract

This chapter illustrates different titrimetric monitoring applications and compares BCS results with other titrimetric and standard methods. The advanced interpretation techniques implemented in BCS can be used to quantify almost any buffering system while other approximate methods are used to determine bicarbonate and VFA only. An anaerobic fixed bed reactor was overloaded with the aim to assess the accuracy of titrimetric analysers and methods under highly dynamic variations of bicarbonate and VFA as well as lactate as an overload indicator. The BCS was also tested for titrimetric monitoring of a fully autotrophic nitrogen removal processes (combined SHARON-Anammox process) that is used as post-treatment of anaerobic digestion effluent. The titrimetric results are compared with classic colorimetric results in the light of the on-line application of BCS for process control. Third, an experiment was performed at an industrial scale digester to test BCS, an approximate titration method and the on-line titrimetric analyzer AnaSense®. In the presence of di- and trivalent cations (calcium and iron ions) and precipitation, a complex mixture of buffer components is dosed to the anaerobic digester effluent. Ten conditions were designed purposefully to test the titrimetric analyser and methods with a wide range of buffer concentrations in a digester effluent. On-line measurements of VFA, bicarbonate, ammonia, phosphorus and lactic acid are compared with standard measurements. Results are interpreted in the light of control applications to anaerobic digestion under these extreme conditions.

CHAPTER 12

12.1 Introduction

It is generally accepted that alkalinity is very important to assess the anaerobic digestion stability. The main alkalinity components in a digester are bicarbonate and VFAs which are consumed and produced through the anaerobic process steps. Bicarbonate buffers the system in the optimum pH range for the process to run efficiently. VFAs buffer the system at low pH that is inhibitory to the anaerobic biomass. Bicarbonate is maintained by CO_2 production in the digester. COD overloads or introduction of toxicities to a digester leads to accumulation of VFA, a drop in alkalinity and deterioration of the process.

Titrimetric methods are found to be the most cost-effective analysis for VFA and alkalinity with acceptable accuracy (Buchauer, 1998; Vanrolleghem and Lee, 2003). Therefore, many titrimetric methods were developed to determine VFA and alkalinity to study and control also overload conditions and evaluate the impact of toxicities. Lactate can be measured by titration and, hence, can be used as a direct indicator of overloads as will be shown in this chapter. Due to the large number of titrimetric methods developed so far, their common basis will be illustrated in this chapter. They will be classified into general categories according their interpretation methods. The factors influencing their accuracy will be highlighted through the comparison of two titrimetric sensors for monitoring a digester under overload conditions.

A number of sensors were developed for determining alkalinity (bicarbonate) and VFA (Bouvier et al., 2002; Di Pinto et al., 1990; Guwy et al., 1994; Hawkes et al., 1994; Rozzi et al., 1997). In this chapter, a new titrimetric analyser AnaSense®, illustrated in chapter 10, recently developed within the frame of the TELEMAC project (Bernard, 2005) and commercially available (De Neve and Lievens, 2004), is tested at industrial scale. The produced titration curves are analysed by the BCS for the determination of an extended list of buffers. An experiment to validate the AnaSense® for implementation in a difficult industrial environment was designed at the brewery wastewater treatment plant of Estrella Galicia Hijos de Rivera S.A., in A Coruña (Spain). The main results of the experiment are presented in terms of the titrimetric determination of different compounds by the BCS compared to the standard methods implemented by the analyser.

The SHARON-Anammox process (van Dongen *et al.*, 2001) can significantly reduce the pressure on nitrogen removal in the main wastewater treatment plant (WWTP) by separately treating the sludge digester effluent (typically 1gN /l) before this stream is recycled to the entrance of the WWTP. The process relies on partial nitrification of ammonia to nitrite in the SHARON process and subsequent conversion of the resulting

50/50 mixture of NH_3/NO_2 to nitrogen gas. Up to now the methods used for the off-line measurement of the relevant components, ammonia and nitrite (e.g. spectrophotometry and ion chromatography) are time-consuming, expensive and difficult to automate, especially in view of the concentration ranges typical for the SHARON reactor (1gN /l). In this chapter, therefore, the results of using the BCS for the monitoring of the combined SHARON-Anammox process is presented to illustrate the extended appliction of BCS to monitor both the anaerobic digester and the process treating its effluent.

12.2 Titrimetric method classification

All titrimetric methods use the same basis taken from equilibrium chemistry. From the equilibrium of a buffering system (weak acid / weak base), mass balances and the water dissociation reaction, the buffer ions can be defined in terms of their total concentration. Examples for acetate (monoprotic) and bicarbonate (diprotic buffers) are given in equations (12.1) and (12.2):

$$Ac^- = \frac{K_{ac}}{H^+ + K_{ac}} \cdot Ac_T = f_{Ac^-}(K_{ac}, H^+) \cdot Ac_T \qquad (12.1)$$

$$HCO_3^- = \frac{1}{1 + \frac{K_{C2}}{H^+} + \frac{H^+}{K_{C1}}} \cdot C_T = f_{HCO_3^-}(K_{C1}, K_{C2}, H^+) \cdot C_T \qquad (12.2)$$

Similarly, ions from triprotic buffers can be presented as functions of their total concentration. After addition of a titrant (e.g. a strong acid) to a sample the concentration of acid in the sample will be C_a and the concentration of H^+ will shift to maintain the charge balance in equation (12.3).

$$C_a = H^+ + Z - \sum_{i=1}^{n} z_i \cdot f_{A_i}(\{K_{A_i, p=1 \to z_i}\}, H^+) \cdot A_{i_T} - \frac{K_w}{H^+} \qquad (12.3)$$

Z is the total alkalinity and z_i is the ion charge. Equation (12.3) forms the general basis of titrimetric methods and the only difference between the methods will be in the further mathematical manipulation and algebraic solution algorithms.

From a mathematical point of view the titrimetric methods can be classified into 3 categories, explained below.

Solution of linear algebraic equations. Examples of methods that fit under this category are the method according to (Moosbrugger et al., 1992; 1993) and its extended version by (Lahav et al., 2002). Presenting the equation (12.3) in terms of mass, leads to equation (12.4):

$$V_a \cdot N_a = (V_a + V_s) \cdot H^+ + V_s \cdot \left(Z - \sum_{i=1}^{n} z_i \cdot f_{A_i}(\{K_{A_i, p=1 \to z_i}\}, H^+) \cdot A_{i_T} \right) - (V_a + V_s) \cdot \frac{K_w}{H^+} \tag{12.4}$$

At each point with a recorded added acid volume and pH, an equation linear in total concentrations can be produced. Assuming values of the expected acidity constants, $n+1$ data points are needed to determine the concentration of n buffers and the total alkalinity. More titration points can be used to introduce additional equations and in this way estimate the error in the results. These errors are mainly due to the assumptions made on the acidity constants. Iteration over all equations can then be used to reduce the error. To avoid singularity of the produced set of equations, it is necessary to carefully locate the data points. For feasible and accurate interpretation of the titration curve, the considered buffers should have sufficiently different pKa-values and the data points should be distributed evenly around the pKa values.

Linear regression. A good example of this approach is the method of (Kapp, 1984; 1992). The method uses the regression model in (12.5).

$$VFA = a \cdot (V_{a,pH_4} - V_{a,pH_3}) - b \cdot (V_{a,pH_2} - V_{a,pH_1}) + c \tag{12.5}$$

The volume of the acid that causes the change of the pH between two points around the pKa of VFA (e.g. pH_3= 5 to pH_4= 4) is assumed to correspond to VFA concentration. A similar assumption can be made for bicarbonate with a proper choice of pH_1 and pH_2. Using the Kapp method, the a, b and c parameters in equation (12.5) are experimentally evaluated by titrating samples of known concentrations. For certain applications and using proper configurations of the titration experiment, the added acid volumes and the known concentrations are used to fit the regression model of equation (12.5). Accordingly, the parameters a, b and c are estimated. The equation is then used to estimate concentrations of samples with unknown composition taken from the same application and titrated using the same titration experiment configuration (with volumes estimated at the same pH points.

In fact, using symbolic manipulation of the equations, equation (12.5) can be derived directly from equation (12.4). The derivation was made using the Matlab symbolic toolbox (see appendix 4) assuming that the carbon system is mainly due to the bicarbonate buffer, and it was found that:

$$a = f_1(\mathrm{K_{ac}}, \mathrm{K_{HCO_3}}, \mathrm{N_a}, \mathrm{V_s}, \mathrm{pH_1}, \mathrm{pH_2}, \mathrm{pH_3}, \mathrm{pH_4}) \quad (12.6)$$

$$b = f_2(\mathrm{K_{ac}}, \mathrm{K_{HCO_3}}, \mathrm{N_a}, \mathrm{V_s}, \mathrm{pH_1}, \mathrm{pH_2}, \mathrm{pH_3}, \mathrm{pH_4}) \quad (12.7)$$

$$c = f_3(\mathrm{K_{ac}}, \mathrm{K_{HCO_3}}, \mathrm{Z}, \mathrm{N_a}, \mathrm{V_s}, \mathrm{pH_1}, \mathrm{pH_2}, \mathrm{pH_3}, \mathrm{pH_4}) \quad (12.8)$$

From equations (12.6), (12.7) and (12.8) it can be seen that defining the regression model corresponds in fact in defining 3 combinations of acidity constants and total alkalinity, Z. The values of the regression model constants *a*, *b* and *c* are dependent on the experiment parameters (volume of sample, V_s and normality of titrant, N_a), acidity constants and the choice of the pH points. An equation similar to equation (12.5) can be produced to determine bicarbonate, equation (12.9).

$$bicarbonate = a_1 \cdot (V_{a,pH_2} - V_{a,pH_1}) - b_1 \cdot (V_{a,pH_4} - V_{a,pH_3}) + c_1 \quad (12.9)$$

where a_1, b_1 and c_1 are regression parameters that are also determined experimentally by titrating samples with known bicarbonate concentrations. Note that a_1, b_1 and c_1 are also functions in the same arguments corresponding to equations (12.6), (12.7) and (12.8), respectively.

Nonlinear fitting. The model presented by equation (12.3) can be directly fitted to the titration data to estimate its parameters, i.e. both the unknown total buffer concentrations A_{i_T} and the acidity constants K_{A_i}. However, for better practical identifiability of these model parameters, a general buffer capacity (BC) model can be obtained by the derivative of equation (12.3) with respect to pH. The general BC model can be referred to in chapter 11. The model can be presented in a simplified form as equation (12.10).

$$\beta = -\frac{dCa}{dpH} = 2.303H^+\left(\frac{1}{\gamma H^+} + \sum_{i=1}^{n} g_{A_i}(\{K_{A_i,p=1\to k_i}\}, H^+)\cdot A_{i_T}\right) \quad (12.10)$$

In addition to the easy to understand physical meaning of buffer capacity, deriving equation (12.3) into equation (12.10) leads to another advantage. The dynamics of the titration experiment are more pronounced and, hence, a better practical identifiability of the acidity constants as well as the total buffer concentrations is achieved. The dynamics are more distinct since the g_{Ai} functions in equation (12.10) will be of higher order in H^+ and the acidity constants K_{Ai} compared to f_{Ai} in equation (12.3). Since more parameters (indeed, they also include the acidity constants that are nonlinear in the model) are estimated in this

advanced interpretation method, more measurement points are required from the titration. Note that the buffer capacity model is still linear in the concentration A_{i_T}.

12.3 Monitoring digester overloads

The anaerobic digestion consists of an interplay of biological activities. With simplification they are, in order, acidogenesis, acetogenesis and methanogenesis. Both CO_2 and VFA are produced first, in addition to H_2, by acidogenesis and acetogenesis. Successively, methanogenesis occurs in two ways. Acetotrophic methanogenesis utilises VFA in the form of acetate only and produces methane and CO_2. Hydrogenotrophic methanogenesis utilises CO_2 and H_2 for the production of CH_4. The bottleneck here is that methanogenic bacteria are more delicate compared to acidogenesis and acetogenesis. Therefore, during toxic events they are more easily inhibited and during organic overload they cannot catch up with the previous steps. Consequently, VFA starts to accumulate while CO_2 is continuously stripped to the gas phase, pH decreases, biological activities are inhibited and the digester stops functioning. An additional effect is the mutual relation between both forms of methanogenesis. For instance, if the hydrogenotrophic form is inhibited, H_2 will start to build up to a level that inhibits acetogenesis and therefore less acetate becomes available for the other form. VFA's as well as lactate will start to build up in the reactor (Bjornsson et al., 2001).

12.3.1 Experiment

An experiment was designed so that an anaerobic fixed bed reactor treating vinasses is overloaded in two steps. The experiment was performed at the pilot plant "Laboratoire de Biotechnologie de l'Environnement, Institut National de la Recherche Agronomique, LBE-INRA, Narbonne, France" (Steyer et al., 2002). The plant is shown in Figure 12.1. The plant has a 1 m^3 anaerobic fixed bed reactor that is fully instrumented and controlled. The fixed bed configuration prevents the washout of the biomass during the experiment. Full control of the reactor guarantees the accurate application of the designed protocol of the overload experiment. The reactor overload protocol is designed to be achieved by controlling the feed flow and the dilution tank shown in Figure 12.1. Figure 12.2 shows the designed COD load to the reactor that is achieved by increasing the flow rate to 5 times the normal flow and later doubling the influent concentration. Parallel off-line analyses were performed to determine VFA using gas chromatography GC and alkalinity using the standard end-point method.

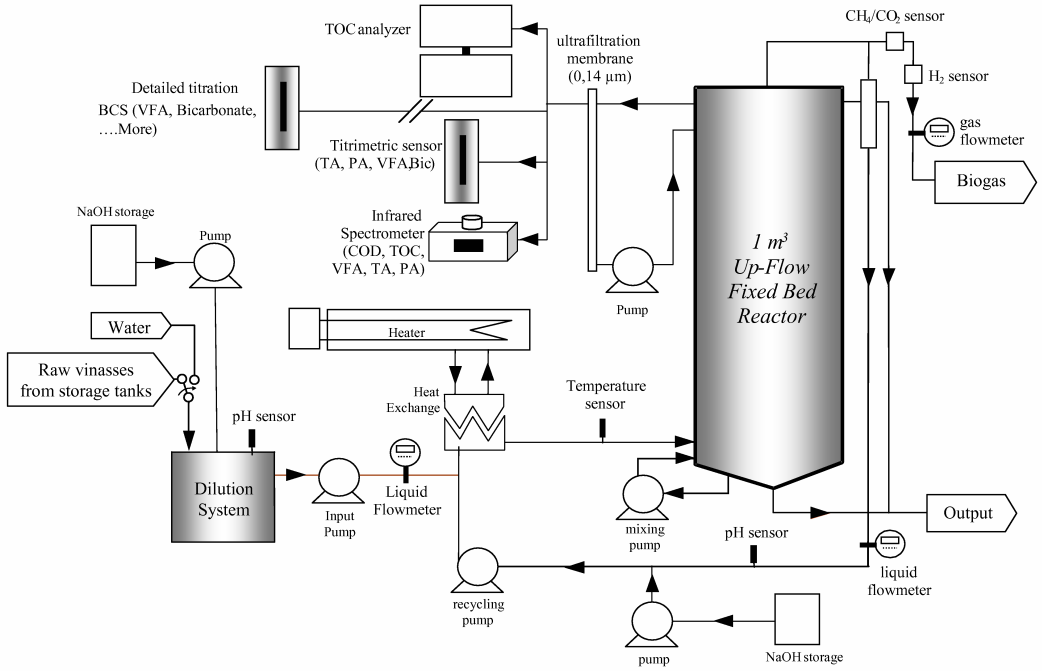

Figure 12.1 INRA anaerobic digestion pilot plant, the reactor, the dilution systems and tested titrimetric sensors are indicted in gray (adapted from Steyer et al., 2002)

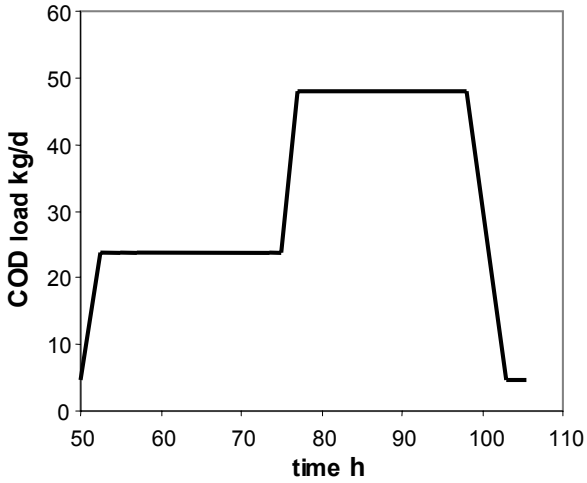

Figure 12.2 Designed experiment protocol

12.3.2 Titrimetric monitoring equipment

The INRA titrimetric sensor and the BIOMATH titration setup, illustrated in chapter 10, were used for continuous titrimetric monitoring of the reactor during the experiment. The Titrimetric Sensor, TS, (Bouvier et al., 2002) is designed to use the approximate interpretation methods belonging to the first two categories, e.g. (Kapp, 1984; 1992; Moosbrugger *et al.*1992). Samples were titrated slowly using the BIOMATH titration setup to run the Buffer Capacity Software (BCS) that is developed for determination of the

existing buffer combinations, as illustrated in chapter 11. BCS is using the interpretation method of the third category, in addition to automatic model building (Van De Steene et al., 2002) and automatic initialisation modules (see chapter 11). The automatic initialisation module determines the most probable initial buffer model and estimates bounds on its parameters for robust optimisation. The automatic model building of BCS starts with calibrating the initial model. The residuals (differences between model and data) are analysed and used to suggest a candidate model extension, if needed, i.e. adding an additional buffer with unknown pKa and concentration. Then another fitting cycle is performed with the extended model, the residuals are analysed, a new extension is defined, and so on, until one of the stopping criteria is reached. The stopping criteria are based on a set of model selection techniques, which determine the optimum BC model and, therefore, pKa's and concentrations of the significant buffers. Also, based on the fitting results standard deviations for each of the pKa and concentration values are estimated.

The TS is automated to run titrations in 3 minutes to capture all the experiment dynamics. The BCS is running a 30 minutes titration to obtain a more detailed titration curve and therefore leads to a lower sampling frequency. Titration was performed by addition of 0.1N hydrochloric acid starting from the pH of the reactor (around pH 7) to a pH 3.5 for TS and to pH 2.5 for BCS. The accuracy of BCS and TS and their methods are compared on an extended range of concentrations produced by the overload experiment.

12.3.3 Results and discussions

Figure 12.3 shows the buffer capacity profile measured during the experiment.

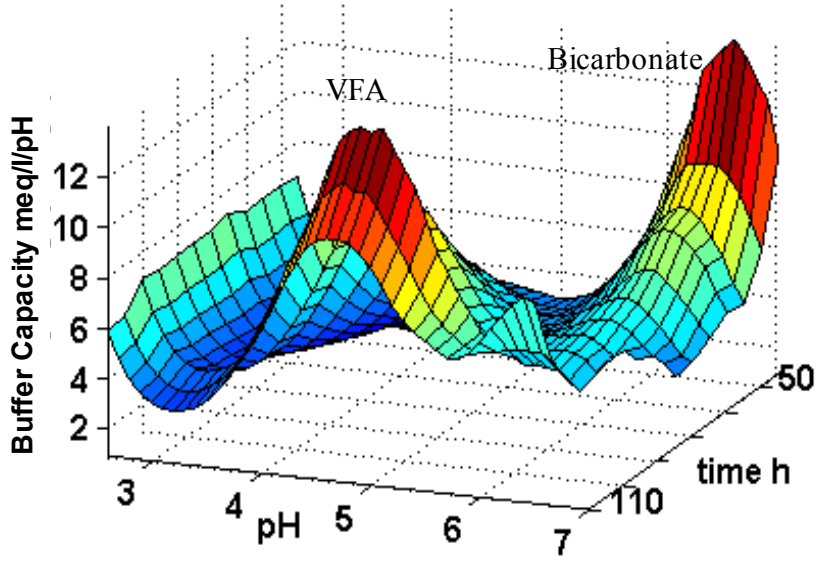

Figure 12.3 Buffers evolution from bicarbonate alkalinity to VFA during overload

As the overload proceeds, as shown in Figure 12.3, the main buffer in the system shifts from the bicarbonate (pKa ≈ 6.35) to the VFA (pKa ≈ 4.75) buffer plus small concentrations of the lactate buffer (pKa ≈ 3.86). Clearly, the observed shift in the buffering systems is useful information to detect an overload and the accumulation of VFAs. Indeed, the experiment dynamics provided good conditions to test the sensors over a wide range of variation of the two main buffers. It can be noticed from Figure 12.3 that the initial pH of the titrated sample is very close to pH 7. The reactor pH was kept around this point by continuous addition of NaOH to the influent wastewater. In such situation pH measurements cannot be used as indicator for the overload (Almeida *et al.,* 2001) but the amount of base added can.

Figure 12.4 shows VFA results from the TS and the BCS compared to the GC, and the lactate concentration detected by the BCS. BCS was only tested until 105h. No lactate was detected after the release of the overload at 100h. The sampling points for BCS were less frequent than TS but they covered all the GC sampling points. Also, it should be noted that the TS was not calibrated before the experiment.

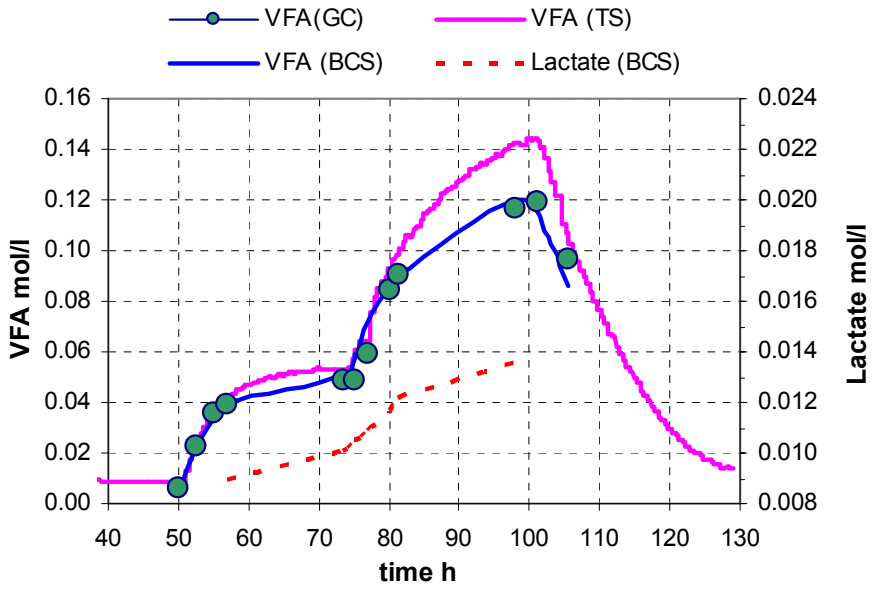

Figure 12.4 VFA and lactate measurement

For VFA (BCS), the correlation coefficient with GC is r = 0.977. For TS r = 0.758 but r = 0.995 for VFA < 0.05 mol/l ≈3000 mg/l. The total ionic strength increased due to the higher concentrations and the extra addition of cations (i.e. NaOH) to the reactor. Accordingly, the acidity constants will shift from the original values that were valid during the calibration of the regression model used in the Kapp method. Indeed, the regression model constants are functions of the acidity constants, see equations (12.6), (12.7), (12.8). However, extending the calibration range to cover the wide concentration range of this

experiment would have achieved better results with the TS since the experimental determination of the regression constants will compensate most of the shift effects. Therefore, the shift effects would be worse if a method of the first category, e.g. Moosbrugger et al. (1992; 1993), is used without correcting the acidity constants. For a method of the third category (e.g. BCS) the accuracy will not be affected since the acidity constants are optimised. A temperature change will also shift the acidity constants and affect the accuracy of the estimated concentrations if the acidity constants are not estimated at the same time. Finally, a drift in the pH probe used in the titration analyser will also not affect the results of the BCS approach. Whereas, it will affect the other interpretation methods but to less extent if using a regression model that is calibrated on an extended range of concentrations.

Figure 12.5 shows the bicarbonate concentration from both TS and BCS compared to the partial alkalinity obtained from the TS and manual end-point analysis. During the overload from 50h to 100h, it can be seen that the partial alkalinity and bicarbonate are decreasing, indicating the overload condition. At 100h the operating conditions were brought to normal and therefore a rapid increase of bicarbonate and decrease of VFA occurred. This rapid recovery is related to the design of the reactor, i.e. a fixed bed reactor. In other reactor configurations recovery would be much slower. Partial alkalinity is determined at an end-point of 5.75 and therefore, it almost avoids the VFA buffer. Bicarbonate from the TS is determined by a regression model similar to that determined for VFA.

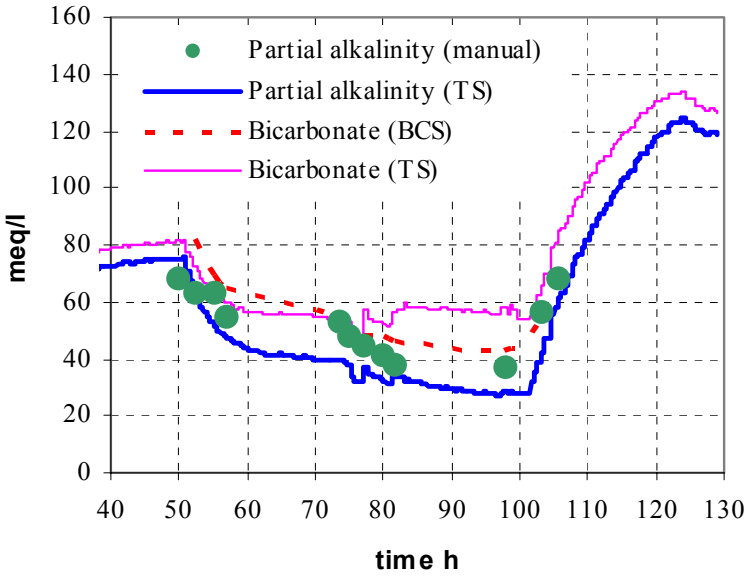

Figure 12.5 Bicarbonate and partial alkalinity measurement results

Outside the overload period, the partial alkalinity and bicarbonate measurements are very close and nicely correlated. During the overload, however, the gap between these measurements increases as the overload proceeds. The shift of the acidity constants

increases the influence of the accumulated VFA on the bicarbonate measurement. Recalibration of the regression model for the bicarbonate determination is required for better accuracy during this period. The bicarbonate measurement from the BCS is not influenced by VFA since the acidity constants are optimised for each titration experiment. The BCS bicarbonate measurement correlates nicely to the partial alkalinity and it is expected to have better accuracy.

In addition to these common factors of shifting the acidity constants, other buffers can affect the accuracy if they are not considered in the calculation procedure or the initial model. For instance, during the overload to the digester lactate may be formed in addition to the increase of VFA and can therefore be a good indicator of the overload and an additional component for advanced understanding of the process behaviour. However, it is not considered in the regression model of the Kapp method and it is therefore quantified by TS as extra VFA. On the other hand, if lactate is considered in the calculation procedure or initial model and it is not present in the titrated sample, it is likely that some of the VFA will be reported as lactate. Indeed, the lactate pKa is relatively close to the pKa of VFA and it may therefore be highly correlated with it. Therefore, in addition to model optimisation, the advanced techniques of initialisation and model selection implemented in the BCS will be necessary for the accurate detection of such interfering buffers. For instance, Figure 12.6 shows a BCS analysis of a sample in which lactic acid is introduced. The simulated BC curve has two peaks at pH 6.35 and 4.3, corresponding to the inflection points in the titration curve.

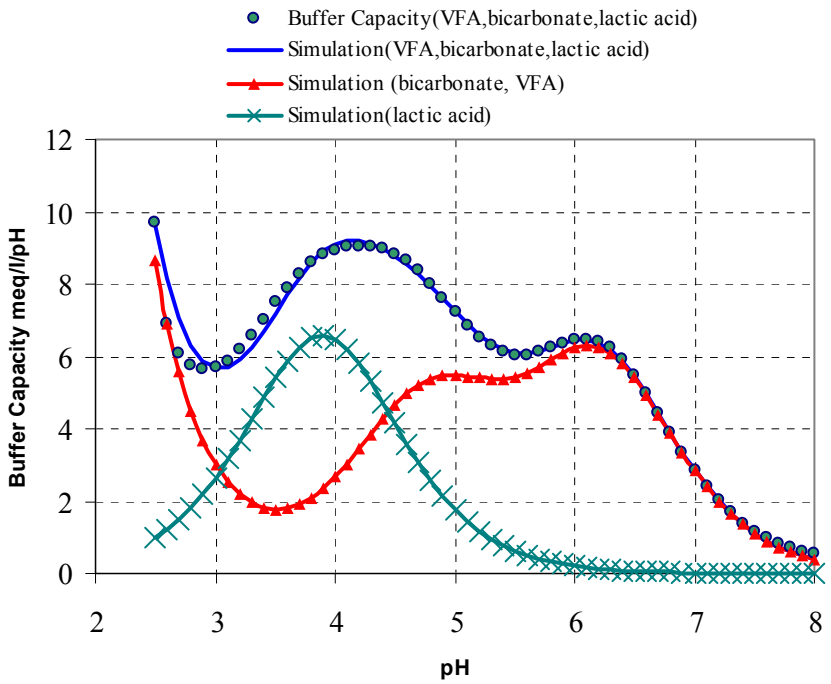

Figure 12.6 BCS analysis of a simulated bicarbonate, VFA and lactate mixture

Direct interpretation of the overall titration curves would lead to the misinterpretation that VFA were present but that a considerable shift of the pKa to pH 4.3 had occurred (either due to a pH-probe drift or salt content). The initialisation module for the BCS, however, will recognise that this peak is due to two (albeit highly correlated) adjacent buffers. Therefore, it initialises the monoprotic model of lactic acid as well as the bicarbonate and VFA models. Bicarbonate, VFA and lactic acid are then combined in one model that is fitted to the data. The combined model is then tested for possible extension for any further enhancement in fitting the data. In this case, no extension was needed. The optimised and combined model is selected as the final model. The corresponding pKa's and concentrations of the buffering components are accurately estimated.

The lactate concentration detected by the BCS during the overload experiment was usually less than one tenth of the VFA concentration. BCS was tested over a wider range and different ratios of VFA and lactate, as illustrated in chapter 11. From the same titration experiment, the BCS can also find, next to VFA and alkalinity, other buffers which are important in anaerobic digestion (e.g. ammonia, phenol, phosphorus, hydrogen sulphide...etc.).

12.4 Monitoring complex digester effluent

So far, the BIOMATH titrimetric setup was used to produce titration curves for BCS interpretation. The titration algorithms of the BIOMATH setup were designed to produce the needed highly accurate titration data that suit the detailed buffer capacity interpretation. In practice and with on-line analysers, however, some difficulties might reduce the quality of the titration data.

Therefore, two objectives are stated for the application presented in this section. The first objective is to use BCS for the interpretation of the titration data produced by the AnaSense® on-line titrimetric analyser at industrial scale. The second objective is to test the BCS, simpler titrimetric methods and the AnaSense® with its interpretation method in the presence of possible complicating factors that might occur at industrial plants.

12.4.1 Application

Figure 12.7 shows the Estrella Galicia wastewater treatment plant where the experiments were performed. The plant consists of homogenisation tank, a pre-acidification reactor and an expanded granular sludge blanket reactor with internal recirculation of 120 m^3/h (EGSB-IC). The EGSB-IC reactor has a volume of 800 m^3 volume, a height of 26 m and a

diameter of 6.5 m. It is treating a mean influent flow rate of 80 m^3/h with an influent COD of 3000 to 4000 mg/l, achieving a COD removal efficiency of 85 to 90%.

Different complications for titrimetric methods and analysers are considered in this industrial application. The chosen industrial plant applies calcium and ferrous ions to enhance the performance of its process units. Such cations lead to precipitation during the titration experiments. Precipitation is not considered in the implemented titrimetric methods. Precipitation might also cause blocking of the tubing of the titrimetric analyser and affect its performance, e.g. reduce the accuracy of the sampling volume.

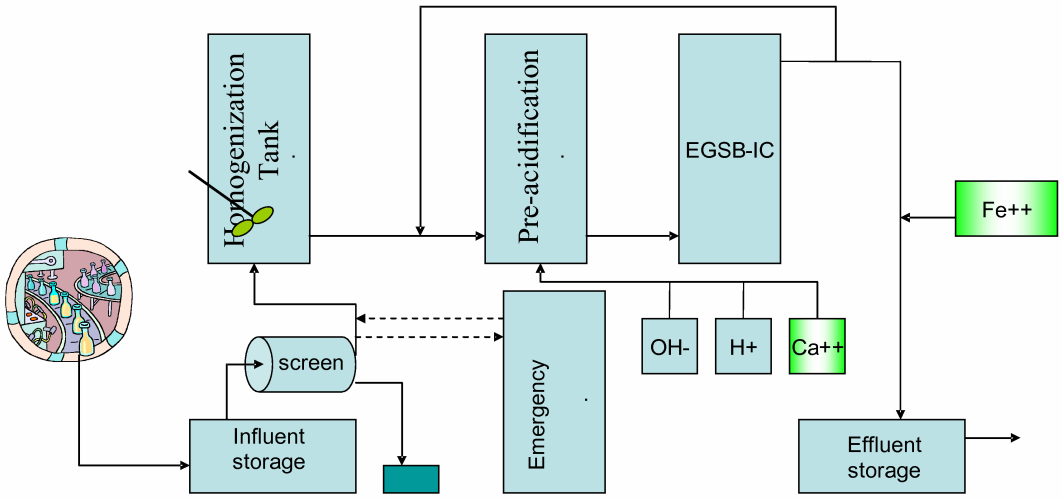

Figure 12.7 Scheme of the wastewater treatment plant at the Brewery Estrella Galicia.

12.4.2 Experiment design

Other complexities are implemented by dosing a complex mixture of standard buffer solutions to the plant effluent before the sampling point. The titrimetric analyser simulator (TAS), presented in chapter 4, was used to design 10 step changes of the buffer mixtures to be added so that an interesting profile of buffer changes during a digester overload is simulated. The mixture components are bicarbonate, VFA, lactate, phosphorous and ammonia. The TAS was used to simulate the titration curve at every step change in the buffer mixture to check that complete titration experiments can be achieved without exceeding the maximum total amount of titrant imposed by the AnaSense® operation. This maximum limit could be maintained and, by trial and error, the amount of buffers was maximised at each step according the overload profile, Figure 12.8. The simulated titration

curves for each mixture were then analysed by BCS and the interpretation results are also shown in Figure 12.8.

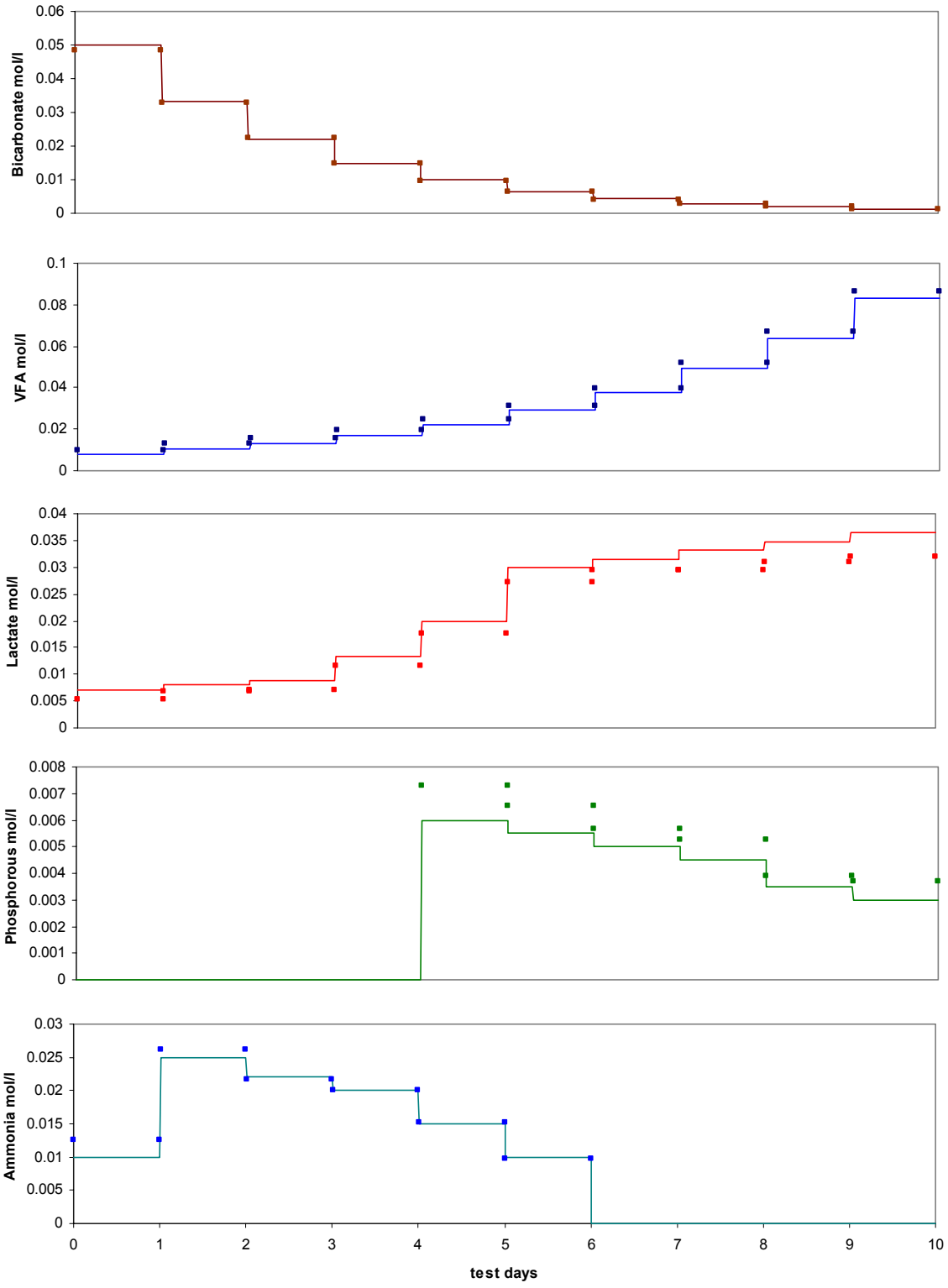

Figure 12.8 Protocol of buffer mixtures addition to the digester effluent, Simulated by TAS ____; evaluated by BCS ■

Analysing the simulated titration curves, accurate results are expected for bicarbonate, VFA, and ammonia. Less accuracy can be foreseen for BCS results of lactate and phosphorus due to their high correlation with VFA and bicarbonate, respectively. However, it can be concluded that the trends can be nicely determined.

The standard solutions were pumped continuously at 0.24 l/h into the sampling stream flow of 2.88 l/h and before the AnaSense® sampling point, as shown in Figure 12.9. The dilution ratio of the standard solution to the mixing container was 13. The standard buffer's solutions were prepared daily at 13 times the designed protocol concentrations and each condition of the protocol is applied for one day. However, concentrations are expected to deviate to a small extent from the designed protocol due to the existing concentrations in the digester effluent and the dynamics in the mixing container. The small deviations will not violate the protocol design objectives of creating an overload profile and maintaining the maximum concentrations within the analyser limit of total titrant volume.

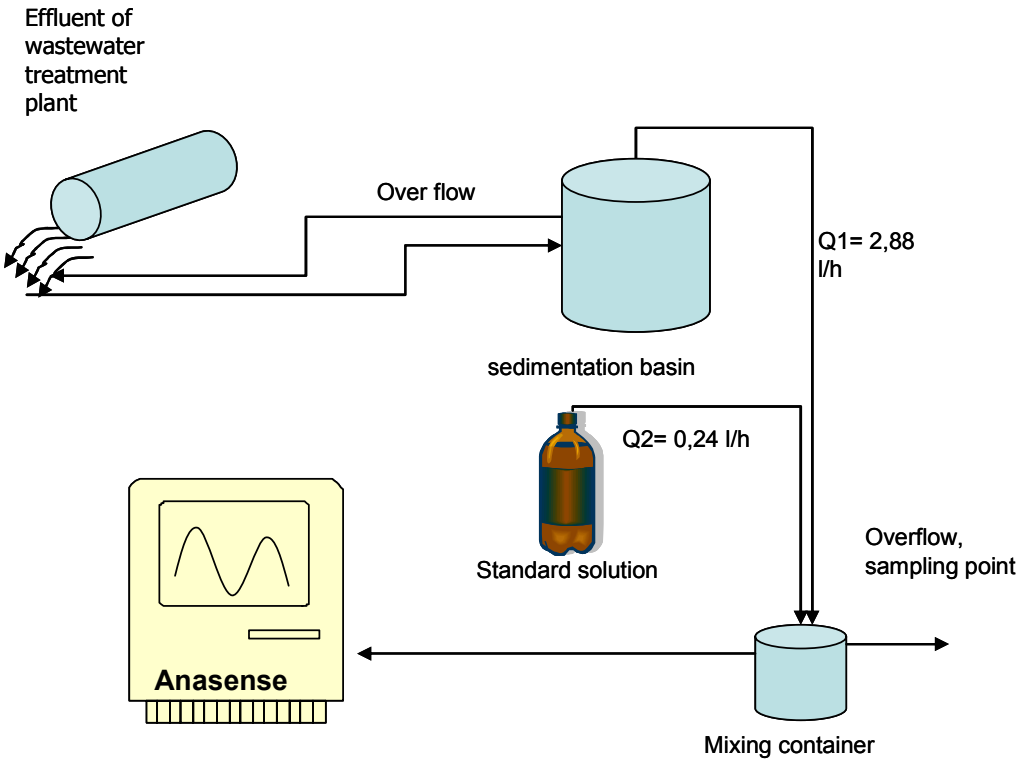

Figure 12.9 Application of the additional buffer mixture to complicate the titrimetric analysis of the sampled effluent

12.4.3 Titrimetric methods and reference chemical analysis

The designed experiment was performed and was monitored on-line using the titrimetric methods. Each step of the designed buffer profile was applied for one day and a daily sample (i.e. one reference sample for each condition) was collected for reference analysis.

Reference analyses were performed in the laboratory of the Chemical Engineering Department, School of Engineering, University of Santiago de Compostela (USC), Spain. The applied measurement methods are as follows:

Titrimetric methods: Two methods were applied with the AnaSense® titration data:

1. *Built-in method* (INRA): As illustrated in chapter 10, the AnaSense® has two built-in methods: with CO_2 stripping and without CO_2 stripping. Only the built-in method without stripping was used. It is the same method applied by the INRA titrimetric sensor, chapter 10, i.e. using the Kapp method with a modification to determine bicarbonate. According the classification in section 12.3, it is an approximate method that uses linear regression for the determination of VFA, equation (12.5), and a similar equation for the determination of bicarbonate.

2. *BCS* (Biomath 1 and Biomath 2): As illustrated in chapter 10, the BIOMATH titrimetric setup uses the buffer capacity for the titrimetric data analysis. According the classification in section 12.3, the buffer capacity interpretation is an advanced method that uses nonlinear fitting of the buffer capacity model, equation (12.10). The method is upgraded to BCS by integrating the automatic initialisation module, illustrated in chapter 11, for on-line implementation, as here in the present application with AnaSense®. AnaSense® ran titrations without and with initial pH adjustment to pH 11 for BCS interpretation (the corresponding results were called Biomath 1 and 2, respectively).

Volatile Fatty Acids (VFA) and bicarbonate: Three sets of data (INRA, Biomath1 and Biomath 2) were generated on-line by the analyser. The reference VFA concentration was determined by Gas Chromatography (GC) using a Hewlett Packard 5690 chromatograph, with a FID detector and pivalic acid as internal standard. The reference bicarbonate measurements were determined as total inorganic carbon (TIC), using an automatic analyzer, Shimadzu TOC-5000, with a NDIR detector.

Ammonium nitrogen: the TAN was determined on-line from titration data obtained after pH adjustment to pH 11 (Biomath 2). The reference ammonium nitrogen concentration was determined by an automatic TKN analyzer, DOHRMANN DN 1900.

Lactic acid: The concentration of the lactic acid was determined on-line without and with initial pH adjustment to pH 11 (Biomath 1 and Biomath 2 respectively). Reference lactic acid concentrations were computed from a TOC balance, considering the sample TOC and

the TOC of the added VFA. The difference was assigned to lactic acid. TOC was determined by an automatic analyzer, Shimadzu TOC 5000, with a NDIR detector.

Phosphorous: The orthophosphate concentration was determined on-line without and with initial pH adjustment (Biomath 1 and Biomath 2 respectively). The reference phosphate concentration was determined with a capillary electrophoresis analyzer for ion species, CIA WATERS.

12.4.4 Results and discussion

12.4.4.1 Analyzer performance

Two main problems were reported during the operation of the analyser and caused some noise and inaccuracy of the titration data (see Figure 10.8 of the analyser). The first problem was precipitation and subsequent obstruction of the drainage line. Although the sampled effluent contained little solids (about 200 mg/l), the high cation (Ca^{++} and Fe^{++}) concentrations effected precipitation and obstructed the drain line from the titration vessel. As a side effect of the drainage problem, left over from a previous sample or rinsing water influenced the sample volume and the true concentration. The other problem that was discovered concerned inaccurate records of titrant volume. Observation of air bubbles in the burette was reported during the analyser operation. This leads to some inaccuracy in the recorded titrant volume. As a result, at some titration steps a constant pH was recorded as injected air was recorded as an added titrant volume. However, the present experiment was the first industrial trial of the AnaSense® and the detected fouling can be easily avoided by minor adjustments to the analyser as explained hereafter.

The BCS method requires accurate titration and buffer capacity curves. To eliminate noise from the titration experiment, the buffer capacity curve is evaluated by using a moving window and parabolic regression. The regression is made by a symmetric window to avoid phase shifts and therefore window width should be an odd number. The minimum window width is three. For good titration, the optimum for BCS was found to be five titration curve data points. Figure 12.10 shows buffer capacity curves that are built for one sample using different window widths. The sample is taken under the mixture number 7 of the protocol defined in Figure 12.8. The sample contains carbon, VFA, lactate, and phosphorous buffers. It is clear from Figure 12.10 that considerable noise exists for points below pH 7. The noise is clear using a window width of three (w3) and cannot be removed using a window width of five (w5). Using larger window widths the noise could be removed but with considerable loss of information in the buffer capacity curve. The noise shown in Figure 12.10 can be caused by either precipitation or inaccurate titrant volume recording.

The outlier at pH 5.65 and the irregularity of the shown buffer capacity curves at lower pH could be due to dissolution of precipitates with acid addition. Precipitates could be of ferric phosphate and also calcium lactate since ferrous and calcium ions are present in the effluent; phosphate and lactate are indeed dosed before the sampling point. Raising the initial pH of the sample to pH 11 is expected to increase precipitation, while acid addition during down titration will effect dissolution of precipitates. However, precipitation is not considered in the interpretation methods. The outlier at pH 5.65 can also be caused by an air bubble that is recorded as an added acid volume. Consequently, a higher buffer capacity is erroneously calculated at this particular point.

Such problems and noise on the titration curves significantly affect the accuracy of the interpretation methods in the present application. However, in future applications they could be easily avoided by some changes in the analyser's operation or accessories. For instance, an acid dose from the burette while rinsing after a previous titration will help in two ways. It will help to continuously remove any air bubbles from the burette before the start of a new titration. The injected acid in the rinsing water will help in removing the precipitates after each titration experiment. A further upgrade of the analyser accessories, e.g. by changing the drainage pump to a better type or installation of a pre-filtration system, will certainly improve the analyser performance.

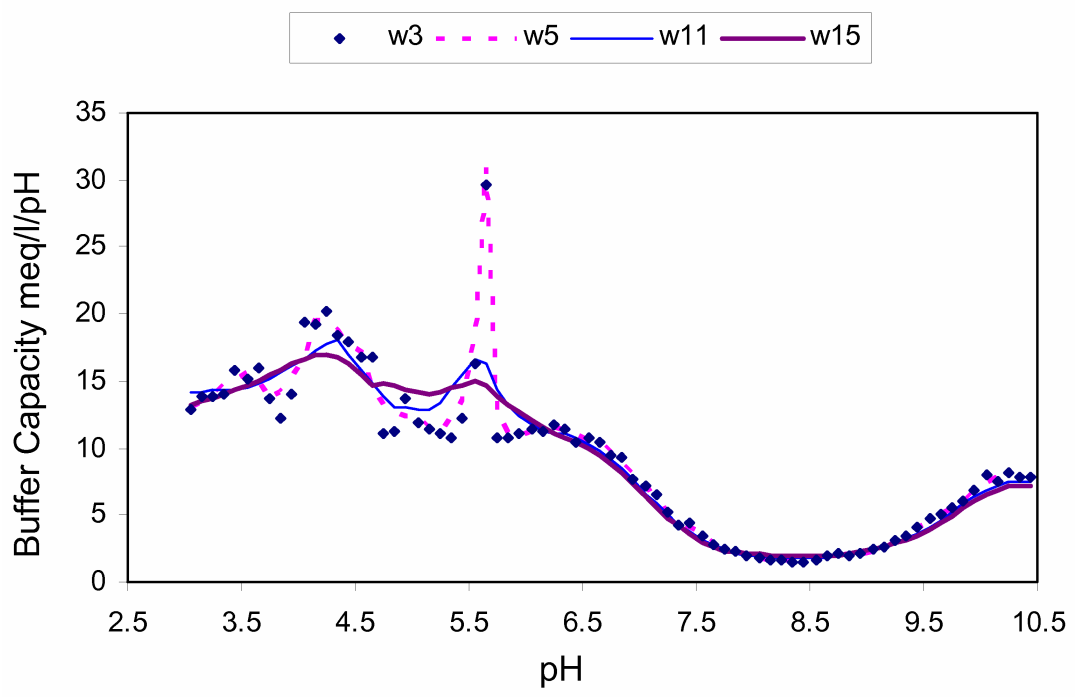

Figure 12.10 Buffer capacity evaluation with different parabolic regression window widths and elimination of titration noise

12.4.4.2 Results of simulated overload

An overload was simulated, following the protocol presented in Figure 12.8. The effluent was used as a matrix and known amounts of acetic acid, lactic acid, ammonium, phosphate and bicarbonate were added in the 10 different conditions. Condition number 1 was repeated at the end of the experimentation to check for consistency and stability of the measurements; it will be called condition 11. At each condition, the applied concentrations deviated from the designed protocol concentrations because of the first three factors listed below. Therefore, the on-line titrimetric measurements will be compared with the daily reference measurements. Some constraints at the industrial plant however limited the number of samples for reference analysis to one sample per day.

In the following, the daily average of the on-line measurements is compared with the daily reference measurement. The on-line measurement standard deviation throughout each day is also presented to interpret the measurement error. However, it should be noted that different factors are contributing to the standard deviation values such as:

1. Dynamics of the digester effluent concentrations,
2. Dynamics in the mixing container before the sampling point,
3. Precipitation dynamics,
4. Noise in the titration data,
5. As well as deviations (errors) of the interpretation methods.

Also, the linearity of the on-line titrimetric measurements is tested by linear regression of their daily average with the daily reference measurement. However, it should be noted that the standard deviation is not constant along all days (i.e. during the application of the implemented protocol conditions). In other words, even though the errors are not normally distributed $N(0, \sigma)$ which is a requirement for an accurate linear regression, the linear regression is made for the interpretation of the reproducibility of the results along the extended range of concentrations. It is generally noted that the standard deviation (error) is smaller at lower concentrations than at higher concentrations. Therefore, the regression is made considering 0 intercepts. Indeed, only drift in the measurement is expected with an increase of the concentration due to the increase of the ionic strength of the titrated solutions and therefore, such effect will be reflected by the slope of the regression line. A shift is not expected in the measurement methods since titrations were made with the same calibrated pH electrode and using the same configuration, i.e. temperature, sample volume,

titrant normality…etc. Therefore, the intercept is ignored in the following interpretations. R^2 is evaluated to reflect the noise in each measurement as it is influenced by the error in the measurement and the dynamic changes throughout each day.

Bicarbonate measurement: Table 12-1 lists the reference measurement and the daily average of the on-line titrimetric results for bicarbonate at each overload condition.

Table 12-1 Mean of the bicarbonate concentration (meq/l) for each condition

Condition	Reference	INRA	Biomath 1	Biomath 2 (with initial pH adjust to pH 11)
1	49.7	46.1	42.1	30.4
2	33.8	36.7	30.1	36.4
3	24.6	24.5	28.7	29.1
4	20.0	18.6	25.8	25.0
5	20.3	21.2	24.3	26.5
6	15.6	7.7	18.8	18.4
7	14.4	7.0	18.6	16.9
8	10.0	2.9	17.2	14.5
9	5.9	0.0	15.0	12.8
10	7.4	1.2	19.2	16.2
11	45.5	49.8	53.2	50.0

Figure 12.11 shows the bicarbonate results. In the left pane, the trend of the measurements is followed well. Accurate on-line measurements are in the range of 20 to 30 meq/l, conditions 2 to 5. The BCS results with and without pH adjustment (Biomath2 and Biomath1) are similar at all conditions except for condition 1. Although the same mixtures are applied at conditions 1 and 11, the reference measurements are quite different. The dynamics in the effluent bicarbonate caused this difference. The on-line measurement is underpredicting at condition 1 and overpredicting at condition 11. Titration noise due to precipitation/dissolution at such elevated concentrations is expected and could be the cause of the deviations. The presence of calcium ions causes precipitation of calcium carbonate, especially after initial pH adjustment to pH 11. This coincides with the Biomath 2 method largely underpredicting at condition 1. At low concentrations (conditions 6 to 10) the INRA results are slightly underpredicting while the Biomath1 and 2 methods are slightly overpredicting. Possible reasons of these differences at low concentrations are that the regression model of the INRA method was calibrated using a higher range of concentrations and the interference of added phosphorus may affect the BCS interpretation at these conditions.

A similar interpretation applies to the linear regression in the right pane of Figure 12.11. The slope is 0.96, 1.06 and 0.99 for the INRA, Biomath 1 and Biomath 2 methods, respectively. Generally, low drift is shown for the three measurement sets. R^2 is 0.92, 0.65

and 0.48 for the INRA, Biomath 1 and Biomath 2, respectively. The INRA bicarbonate measurement is less influenced by the titration noise and therefore is more robust under the present experimental conditions.

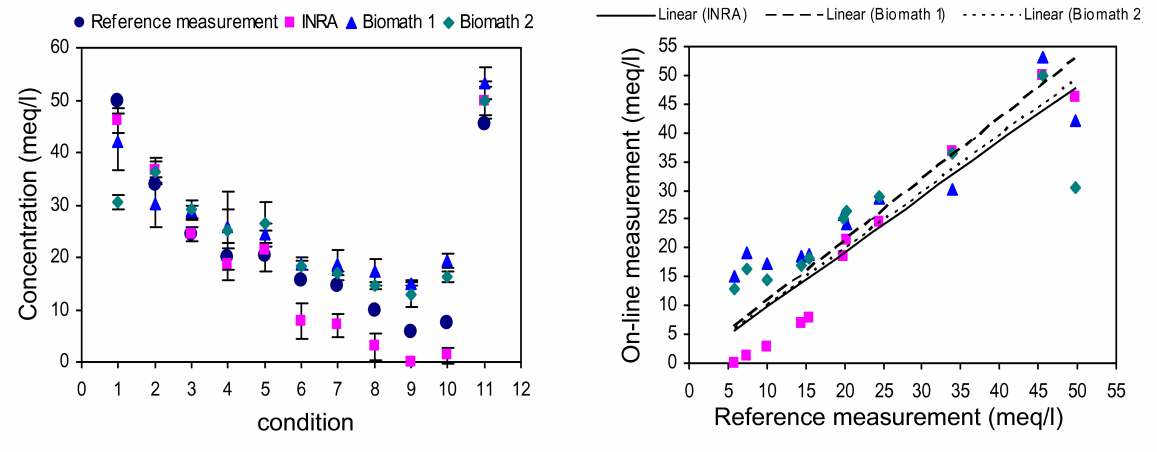

Figure 12.11 Comparison of the on-line titrimetric bicarbonate measurement, (left) concentrations at each condition of the applied experiment protocol, (right) the linear regression of the different titrimetric results

VFA measurements: Table 12-2 lists the VFA gas chromatography reference measurements and the daily average of the on-line titrimetric VFA results at each overload condition.

Table 12-2 Average on-line VFA concentrations for each condition compared to the gas chromatography reference concentration (VFA expressed as mg/l assuming VFA is only acetate)

Condition	Sampled Reference measurement	Analyser measurements for each method at each condition (average over 10h)		
		INRA	Biomath 1	Biomath 2 (with initial pH adjustment to pH 11)
1	448	627	287	520
2	602	581	468	495
3	830	938	722	541
4	1,166	1,324	932	639
5	1,079	1,549	1,031	1,449
6	1,775	2,057	1,106	1,132
7	2,473	2,472	1,602	1,526
8	2,790	3,167	2,194	2,250
9	3,690	3,808	2,517	2,694
10	4,263	4,923	3,492	3,119
11	833	661	516	500

Figure 12.12 shows the average VFA results at each condition, reference measurement using gas chromatography and the linear regression of the titrimetric methods. In general, the trend of the VFA increase is well detected. The INRA VFA results are slightly

overpredicting while BCS results (Biomath1 and Biomath2) are underpredicting. From the linear regression in the right pane of Figure 12.12, the slope is 1.1, 0.75 and 0.73 for INRA, Biomath1 and Biomath2, respectively. The drift in the on-line results is probably due to the interference of lactate whose addition was increasing with an increase of the added acetate. The INRA method uses the regression equation (12.5) for VFA evaluation, considering the volume of acid added between pH 5 and 4. Lactate will increase this amount of acid and cause the slight overprediction. BCS could automatically initialise the buffer capacity model and consider both VFA and lactate. However, the optimisation underestimates the VFA and overestimates the lactate content, Figure 12.13. The reason is the high correlation of lactate and VFA that couldn't be accurately resolved due to the irregularity of the measured buffer capacity curve, Figure 12.10. BCS uses the buffer capacity curve to estimate more accurate bounds on the concentration to enhance the estimation of the concentration of the interfering (correlated) buffers. From the regression, the R^2 is 0.98, 0.97 and 0.92 for INRA, Biomath1 and Biomath2, respectively. The low noise and lower standard deviation compared to the bicarbonate can be explained by three factors. The very low VFA in the digester effluent reduced the dynamic change of VFA during the day. The reference measurement by gas chromatography is accurate. The titrimetric methods are robust in determining VFA concentrations.

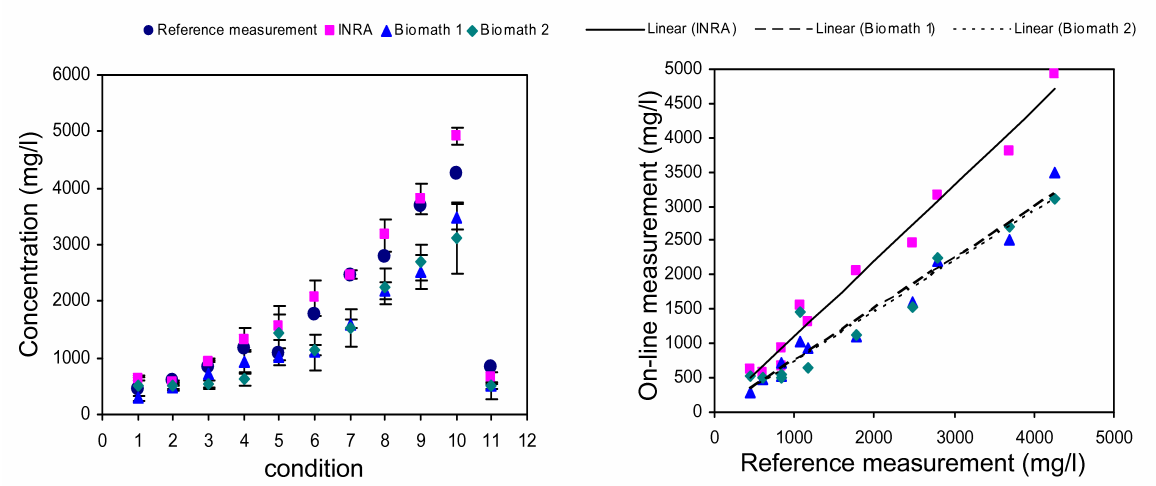

Figure 12.12 Comparison of the on-line titrimetric VFA measurement, (left) concentrations at each condition of the applied experiment protocol, (right) the linear regression of the different titrimetric results

Lactate measurements: Figure 12.13 shows the lactate results measured by BCS, estimated lactate concentrations from the TOC balance (reference measurement) and the applied protocol values. The on-line titrimetric concentration results are accurate at small concentrations, e.g. conditions 1 to 3. During the next conditions, the average of the on-line measurements is always higher but has the same trend when compared with the

estimated lactate concentrations. This can be explained by the previously mentioned correlation with VFA. However, the standard deviation is high at these conditions and indicates the presence of some dynamics during the day or noise. Also, the applied protocol concentrations of lactate are higher than estimated from TOC and the average on-line measurements are in between. Indeed, calcium ions that are present in the sample may form calcium lactate that has limited solubility. Partial precipitation may have occurred, especially when high concentrations of lactate are applied. During titration, adding acid enhances the solubility again and some lactate buffer is recovered in the measurement. This explains the large drift indicated by the slope of the regression lines in the right pane of the figure. The slopes are 1.42 and 1.55 for Biomath1 and Biomath2, respectively. The drift is larger with Biomath2 since precipitation is increased with the addition of base to adjust the pH. Precipitation-dissolution reactions usually create noise to the titration curve. This is confirmed by the large standard deviation values and low R^2 values, 0.77 and 0.7 for Biomath1 and Biomath2, respectively.

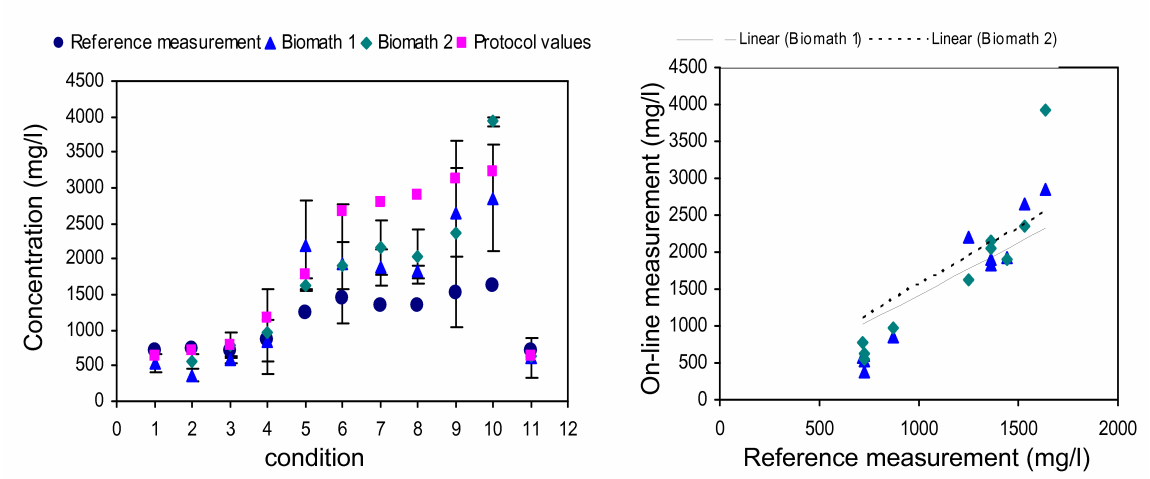

Figure 12.13 Comparison of the on-line titrimetric lactate measurement, (left) concentrations at each condition of the applied experiment protocol, (right) the linear regression of the different titrimetric results

Ammonia measurements: Figure 12.14 shows the on-line titrimetric results for ammonia, in comparison with TKN reference measurements using an automatic analyser. The ammonia concentration is determined only with the Biomath 2 method since pH adjustment is required to start titration from above the ammonia pKa of 9.25. The trend of ammonia is well determined on-line. Large standard deviations at conditions 4 and 5 indicate some daily dynamics and noise that occurred during those two days. For the conditions 7 and 10 the reference TKN results show small values while a zero concentration is determined on-line for ammonia. Indeed, the ammonia concentration is zero during these conditions since

there was no ammonia addition according the applied protocol (Figure 12.8). The drift in the measurement is very small, and the slope is 0.98. However, the noise is high and R^2 is 0.72. Some dynamics and titration noise were cleary present.

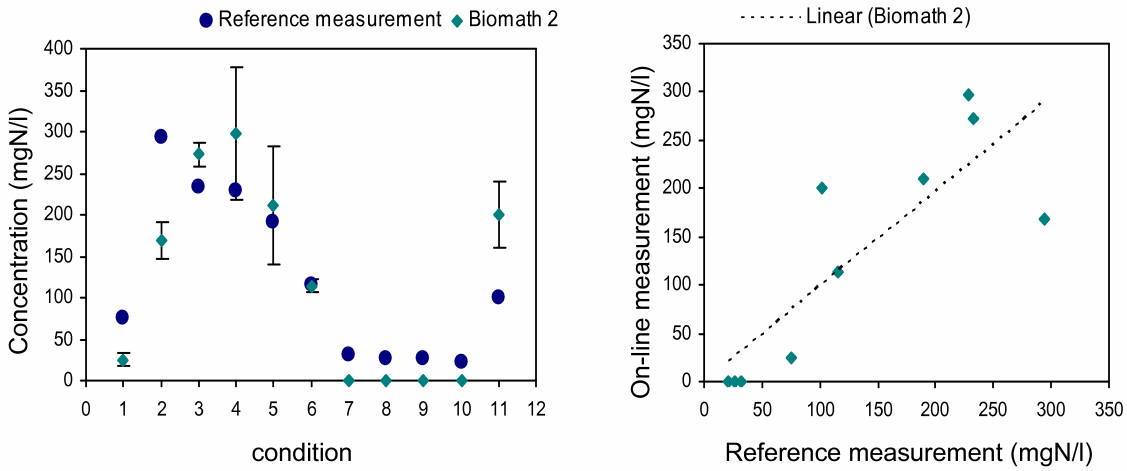

Figure 12.14 Comparison of the on-line titrimetric ammonia measurement, (left) concentrations at each condition of the applied experiment protocol, (right) the linear regression of the on-line titrimetric results

Phosphorus detection: Measurement of orthophosphate was not possible since iron was dosed to the plant effluent to enhance the solids separation and for the removal of sulphides. The presence of ferric ions in the samples caused precipitation of the phosphorus that was added in conditions 4 to 10. Especially, when the sample pH is raised to 11 (Biomath 2) the phosphorus precipitation is increased and therefore the detected concentrations are not comparable to the reference measurements. However, it is a positive result that the method could detect the phosphorus presence in the system under these conditions.

12.5 Monitoring digesters' post treatment

In the sludge treatment of a wastewater treatment plant (WWTP) the digested sludge is allowed to decant and then dried, e.g. mechanically. The supernatant from the decanting and drying processes is very high in Total Ammonia Nitrogen (TAN) content and it is very harmful if disposed to the environment. Recycling the high TAN stream (≈1g/l) to the upstream of a WWTP is therefore obvious, but it will require a significant increase of the activated sludge nitrogen removal capacity through the traditional nitrification and denitrification pathways. Therefore, the recently developed SHARON-Anammox process (van Dongen et al., 2001) can be used as a post treatment of digester return liquors to significantly reduce the TAN loads.

The application of the post process requires continuous monitoring of TAN and total nitrite TNO_2. Indeed, the highly loaded nitrogen stream from the digester is first partially oxidized in a SHARON reactor which works at a solids retention time (SRT) of 1 to 1.5 days and a temperature between 30°C and 40°C. As such, ammonium oxidizers are maintained in the reactor while nitrite oxidizers are washed out and further nitrification of TNO_2 to nitrate is prevented (van Dongen et al., 2001). The SHARON reactor can produce an almost 1:1 total ammonium to total nitrite (TAN:TNO_2) ratio depending on the total ammonium to total inorganic carbon (TAN:TIC) ratio in the influent of the SHARON reactor (Van Hulle et al., 2003). The effluent of the SHARON reactor is then sent to the Anammox reactor where the remainder of the TAN is oxidized anoxically with TNO_2 as electron acceptor (Jetten et al., 1999).

Both ammonia and nitrite are buffering components and, therefore, can be measured titrimetrically. In this context, the BCS was tested for continuous monitoring of ammonia and nitrite, eventually among other buffers in both reactors.

12.5.1 Experiment and application

First, a series of titration experiments was performed with standard solutions to test the accuracy of ammonia and nitrite measurement using the BCS and to determine the optimum titrant normality. Second, BCS was applied for continuous monitoring of SHARON and Anammox lab-scale reactors. The SHARON reactor is a 2 litre continuously stirred tank reactor (CSTR) without biomass retention. A detailed description of the SHARON setup can be found in (Van Hulle et al., 2003). The Anammox reactor is a 2 L Sequencing Batch Reactor (SBR) described in detail in (Wyffels, 2004). The first reactor is fed with a synthetic waste that contains 1000 mg/l TAN and a similar molar concentration of Total Inorganic Carbon (TIC). The designed TAN concentration and TAN:TIC ratio are similar to what can be expected in the effluent of a digester under normal operating conditions. The effluent of the SHARON reactor was stored and then used to batch feed the Anammox reactor after adjustment of TAN and TNO_2 concentrations to a designed equal value, 400 mgN /l each. The equal value of TAN and TNO_2 concentrations is applied to imitate the practical and optimum operation of the SHARON-Anammox process.

12.5.2 Results and discussion

12.5.2.1 Titration with standard solutions

For simplicity, the buffer capacity model, given in chapter 11, considers a constant volume of the titrated sample. It doesn't consider the step change of the sample volume due to step addition of titrant volume. Therefore, the total titrant volume added to the sample should

be smaller than the sample volume. Generally, the titrant concentration should increase with the increase of the buffer concentrations in the titrated sample. On the other hand, at low total concentration of buffers, the titrant concentration should be decreased so that the titration can be performed with sufficient titration steps to achieve an accurate interpretation of the titration data. To find a reasonable titrant normality, different concentrations of ammonia and nitrite were titrated using different base (NaOH) normalities. Figure 12.15 shows the BCS results for titrated ammonia concentrations using different base normalities. Accurate results are achieved for ammonia concentrations from 100 to 4000 mg/l, provided that for concentrations above 1000 mg N/l the titrant is 0.5 mol/l. The BCS interpretation results correlate very well with the tested standard concentrations. The Pearson product moment correlation coefficient, *r*, is 0.9999. Hence, in the mentioned concentration range the effect of titrant concentration can be ignored for ammonium titration.

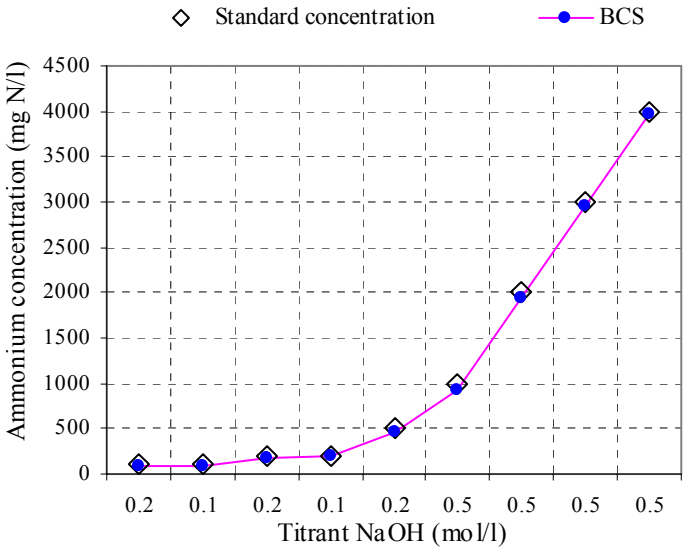

Figure 12.15 BCS measurements of ammonia standards using different titrant base concentrations

A similar test was done with titration of different nitrite concentrations, Figure 12.16. A titrant concentration of 0.5 mol/l was used for concentrations above 1000 mg N/l. Nitrite concentrations from 50 to 2000 mg N/l were tested. The Pearson r is 0.995, but the accuracy decreased at high concentrations and titrant normality.

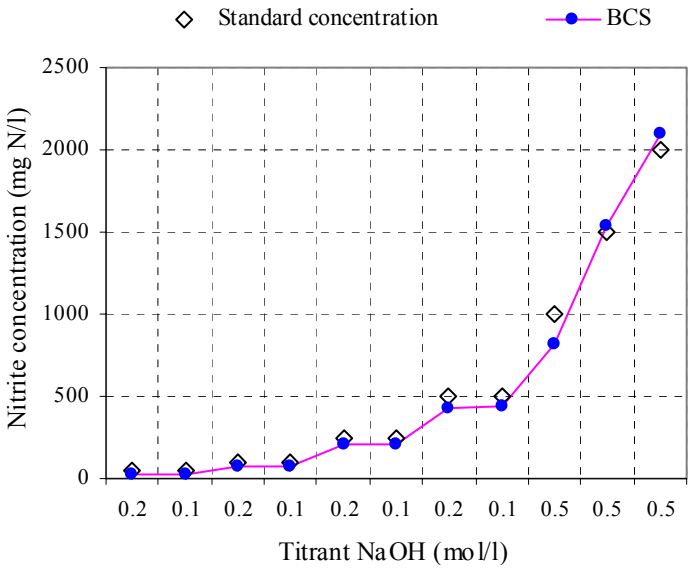

Figure 12.16 BCS measurements of nitrite standards using different titrant base concentrations

Since lower concentration than 50 mg N/l need to be measurable too, it was decided that a NaOH titrant concentration of 0.05 mol/l can be used for a measuring range from 10 to 1000 mg N/l for both ammonium and nitrite.

12.5.2.2 Monitoring the SHARON reactor

Figure 12.17 shows the colorimetric and titrimetric measurements made for TAN and TNO_2 concentrations in the SHARON reactor.

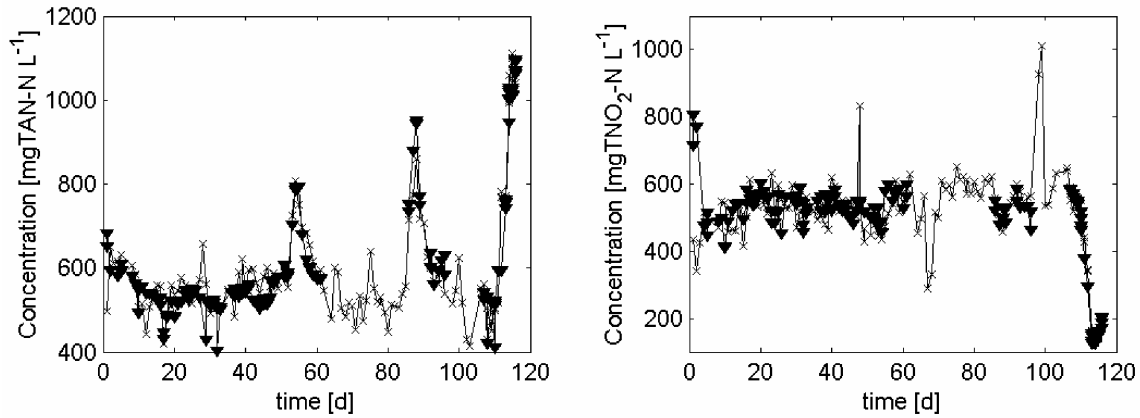

Figure 12.17 Top: Comparison between colorimetric (×) and titrimetric measurements (▼) for TAN concentrations (left) and TNO_2 (right) in the SHARON reactor

Samples from the SHARON reactor were taken daily and analysed once with the colorimetric method and twice with the titrimetric method. For practical reasons one of the two samples analysed with the titrimetric set-up was diluted twice and a 50 ml sample was used. For the other sample only a 35 ml volume was used. Three times, around day 55, day 95 and day 110, a disturbance occurred in the reactor causing the TAN concentration to

increase and the TNO_2 concentration to decrease. With both methods this disturbance could be detected. During the rest of the studied period, the reactor operated stably. For TAN, the concentrations determined with both methods are very similar. The TNO_2 concentrations determined with both methods also follow the same trend, but here the colorimetric results show somewhat more scattering. This high variability may be due to the high dilution (100 times) that needs to be applied for determining the TNO_2 concentrations with the colorimetric method. As such, small errors during sample handling are amplified in the final result. BCS was also applied to study a period of unstable reactor operation. During this period, TAN and TNO_2 concentrations fluctuated between 150 and 1000 mg N/l. Figure 12.18 shows the q-q plot and shows the agreement of the colorimetric and titrimetric analysis performed during the instability period.

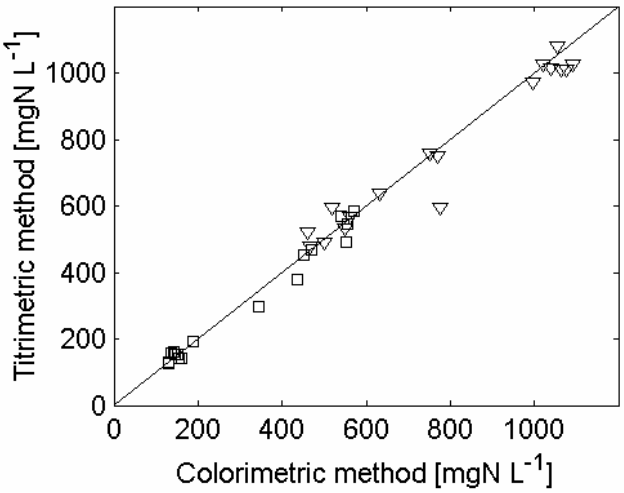

Figure 12.18 q-q plot of TAN (▽) and TNO_2 (□) for comparing concentrations measured with the colorimetric and titrimetric methods during the instability period of the SHARON reactor

Furthermore, a statistical paired t-test was performed using 17 samples that were analysed twice with each method during the instability period. The hypothesis that the titrimetric analysis with BCS offers an alternative to colorimetric methods for measuring the TAN and TNO_2 is tested. The t-values calculated for a paired t-test (Weiss, 2002) were 1.027 and 1.065 (n=17) for TAN and TNO_2 respectively. As the tabulated t-value for the 95 % confidence interval is 2.12 ($t_{16,\ 0.975}$) the hypothesis can not be rejected with 95% confidence and it can therefore be concluded that titrimetric analysis is a valid alternative for colorimetric analysis.

The average pKa values of TAN and TNO_2 determined with the BCS software for these 17 samples was 9.42 +/- 0.05 and 2.85 +/- 0.06 respectively. This indicates that a shift in pKa values occurred in comparison to the values mentioned by Stumm and Morgan (1996) possibly caused by temperature and salinity effects. The BCS software, however, easily dealt with these shifts as it allows some freedom around the default values.

In addition to cost-effective TAN and TNO_2 measurements, the titrimetric measurement also allows the determination of orthophosphate that was present in the effluent of the SHARON reactor. However, this only works on condition that the concentration is sufficiently high compared to TAN and TNO_2. From day 1 until day 26 the concentration of phosphorous in the influent was 228 mgP/l, after day 26 the phosphate concentration was reduced 20 times in view of the possible toxic effects of phosphorous on the Anammox biomass (van de Graaf et al., 1996). On average, the phosphorous concentration determined before day 26 was 244±35 $mgPO_4^{3-}$/l. This concentration is somewhat higher than the one present in the influent, possibly because of the concentrating effect of the evaporation that occurs in the SHARON reactor (Van Hulle et al., 2003). After day 26 phosphorous could no longer be detected in the effluent because the concentration was too low compared to the TNO_2 and the TAN concentrations. Typical buffer capacity curves of the period before and after the phosphorous reduction are depicted in Figure 12.19.

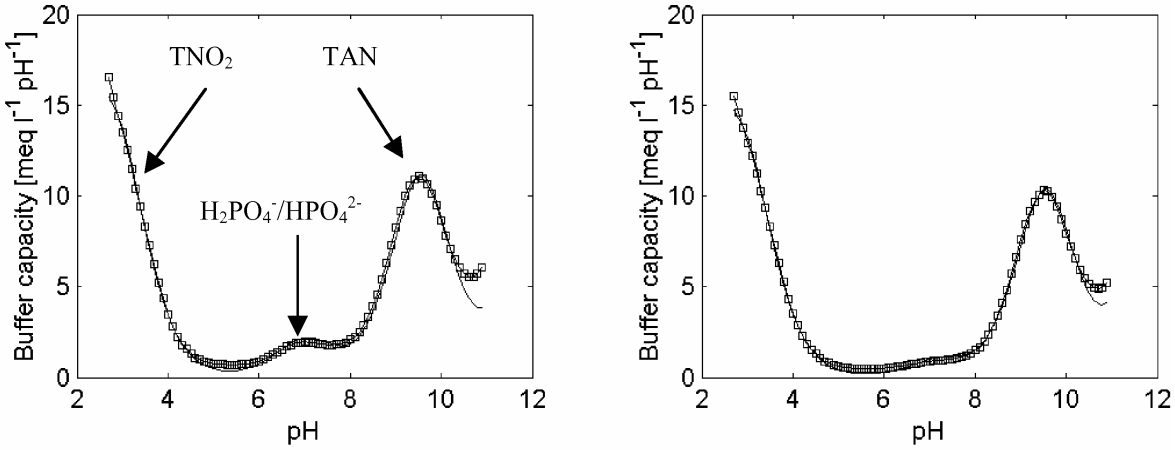

Figure 12.19 Typical buffer capacity curves for the period with 228 mgP /l phosphorous in the influent (left) and the period with 11 mgP /l phosphorous in the influent (right).

12.5.2.3 Monitoring the Anammox reactor

Samples from the Anammox reactor were also taken on a daily basis and analysed once with the colorimetric method and twice with the titrimetric method. A 50 ml sample without dilution was applied for the titrimetric method. Unfortunately, the Anammox reactor operation was not stable at the time of the study. Possible reasons for this are phosphorous and TNO_2 inhibition. Also, the presence of oxygen can inhibit the Anammox process, but the reactor was regularly purged with nitrogen gas and no oxygen was detected in the reactor. Figure 12.20 compares colorimetric and titrimetric measurements for TAN concentrations in the Anammox reactor. It can be seen that both analytical methods give approximately the same result, ever though the measured TAN concentration fluctuates considerably. Because of the unstable operation it was not possible to perform a more elaborated comparison as was the case with the SHARON reactor.

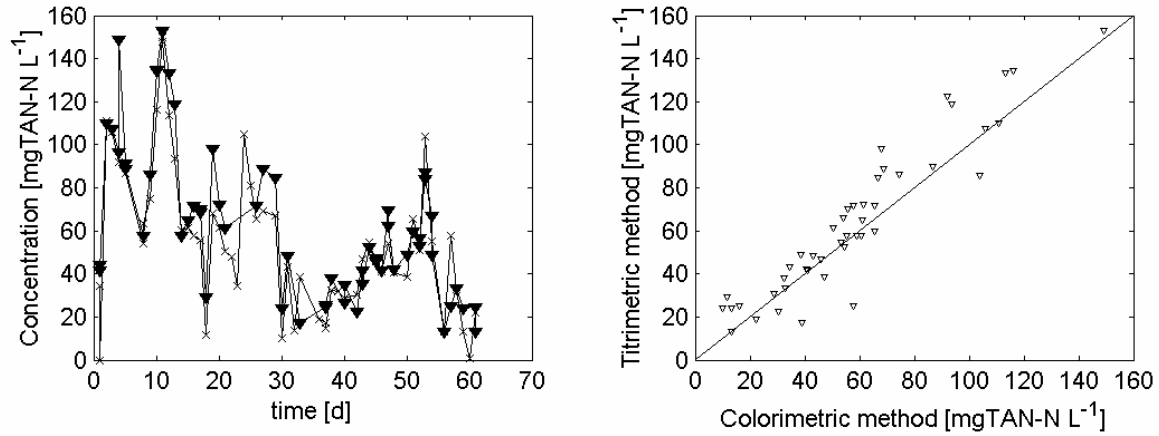

Figure 12.20 Comparison between colorimetric and titrimetric measurements for TAN concentrations in the SHARON reactor (left) and corresponding q-q plot (right)

While trying to determine all components by one titration of the Anammox samples, it became clear that the measured TNO_2 concentrations were different from the colorimetric measurements. TNO_2 concentrations determined with titration were overestimated up to two times compared to the colorimetric method. Possible interferences with other components (e.g. phosphorous or bicarbonate) may have led to the unidentifiability of low TNO_2 concentrations in the Anammox sample. An additional titration experiment could be configured to avoid the interference and enhance the TNO_2 measurements. A different titrant concentration can be used and/or bicarbonate could be stripped first. Figure 12.21 shows the buffer capacity curve and the simulation of the constituting buffers: ammonia, carbon, nitrite and water. The interference to the nitrite buffer is mainly from the water buffer and to a lower extent from bicarbonate.

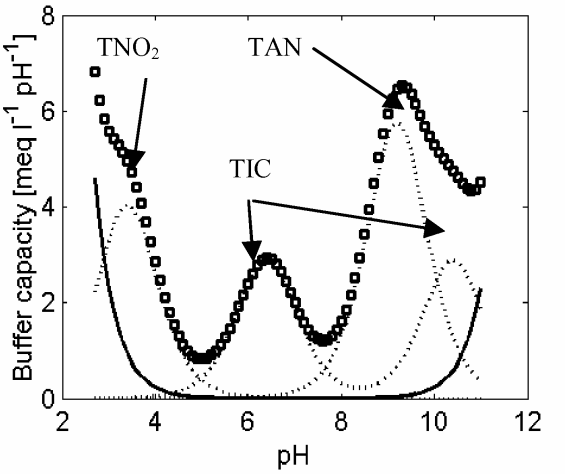

Figure 12.21 Contribution of individual components (...) (in casu TNO_2, TIC and TAN) and the water buffer (-) to the buffer capacity curve (□). The height of each peak is proportional to the concentration, while the position is depending on the pKa value(s) of the component.

In the implemented buffer capacity model the water concentration in the sample is assumed constant, ignoring the added volumes of the titrant. A higher titrant concentration

will guarantee this assumption to hold, but less titration points will be produced. Therefore, the additional titration experiment can be configured to use the limited titration data points for the detection of nitrite only. A likely configuration is first to adjust the pH of the sample to pH 4.5 and strip the bicarbonate alkalinity in the form of CO_2 by vigorous mixing. Then, a down titration is performed using acid with lower normality till the pH is less than 2.5.

In view of the inhibition of Anammox at elevated TNO_2 concentrations, the TNO_2 concentration in the Anammox reactor should be monitored closely either by such additional titration experiment or by an alternative method. In view of control systems design, however, this additional measurement is not necessary. The preferred control strategy would be to install the on-line titrimetric sensor in between the SHARON and Anammox reactor. Control actions would then be applied in feedback mode to the SHARON process to achieve an effluent that suits the Anammox process (Volcke et al., 2003). An excess of TAN compared to TNO_2 will safeguard the Anammox reactor for TNO_2 inhibition.

12.6 Conclusions

Three case studies were performed to evaluate the Buffer Capacity Software (BCS) and Titrimetric analysers. The first case study was applied to a Fixed Bed Reactor (FBR) digester during overload conditions. The INRA titrimetric sensor and the Biomath titrimetric setup using the approximate method based on linear regression and the advanced method of BCS, respectively, were compared. Both analysers and their methods showed acceptable accuracy for VFA and bicarbonate alkalinity analysis for a wide range of operating conditions. They could nicely follow the digester overload dynamics of bicarbonate consumption and VFA accumulation. Therefore, each of the analysers can be applied for feedback control of such overload conditions. Added values of the BCS are the accurate results at high concentrations and estimation of other interfering buffers that may occur in the samples, e.g. lactate in this case study. The better accuracy of the BCS method is related to the simultaneous estimation of acidity constants with concentrations. However, for determination of this larger set of parameters, a detailed titration curve and therefore good titration hardware is needed.

The second case study was designed to evaluate the performance of the on-line titrimetric analyser AnaSense® using a built-in and the BCS interpretation method. The aim was to an monitor industrial scale digester with many added complicating factors. In the presence of calcium and iron ions, the analyser needs some improvements so as to increase its

robustness. The approximate linear regression method (INRA method) was the most simple and efficient for determining VFA and bicarbonate. The BCS method determined ammonium and lactic acid concentrations in addition to bicarbonate and VFA. However, the BCS was influenced by the titration noise and the presence of multivalent cations. Phosphorus was also detected by BCS but the determined phosphorus concentrations were not comparable to the reference measurements due to the presence of precipitate inducing ferric ions dosed to the plant effluent. Due to constraints at the industrial plant, the number of collected samples for a detailed reference analysis was limited. Therefore, the obtained linear regression of the measurements cannot be considered accurate for the assessment of the analyser nor the methods' linearity and accuracy, but it can be seen as a reasonable interpretation of the reproducibility of the results in the context of control applications.

The third case study evaluated the BCS for titrimetric monitoring of the SHARON-Anammox process that is used as post-treatment of digester effluent and removal of high ammonia concentrations. The BCS accurately measured a wide range of Total Ammonia Nitrogen (TAN) and Total Nitrite Nitrogen (TNO_2) concentrations. This information is necessary to control both processes. Moreover, from the same titration experiments, the BCS measured other buffers existing in the samples such as phosphorus that is considered toxic to the Anammox bacteria. Generally, the titrimetric measurements were comparable to the parallel colorimetric method using a standard lab-methods. While monitoring the lab-scale SHARON reactor, the TNO_2 concentrations determined with the colorimetric device varied considerably. The BCS avoids the errors induced by the high dilution that is required by the colorimetric method. For the Anammox reactor only the TAN concentrations obtained with both methods agreed, while the TNO_2 concentrations were overestimated with the titrimetric measurement due to the low concentration of TNO_2 in the Anammox effluent. Optimum titration experiment and titrant normality should be determined for accurate TNO_2 measurements. However, measurement of the low TNO_2 concentration from the Anammox process effluent is not needed in the light of a control strategy of the combined SHARON-Anammox process. A titrimetric analyser placed in-between the two process reactors will suffice to control the TAN:TNO_2 ratio of the SHARON reactor effluent in the optimum range for the Anammox reactor influent.

Summarising, the BCS was tested with different titrimetric analysers, compared with other measurement methods and showed a high capability for on-line titrimetric monitoring of anaerobic digestion and its advanced post-treatment processes.

Conclusions and perspectives

Chapter 13

General conclusions and perspectives

CHAPTER 13

13.1 Developed modelling and monitoring tools

The objectives of this research to implement and apply anaerobic digestion models, plant-wide models and on-line titrimetric monitoring were achieved by the following key outcomes of this research:

- Implementation and validation of the IWA Anaerobic Digestion Model no.1 ADM1 on three simulation platforms.

- Development of a conceptual approach for ADM1 application to simulate process dynamics using a concise set of measurements.

- Extension of the ADM1 implementation with cyanide hydrolysis, inhibition and product degradation pathways, and modelling the population shift of the aceticlastic methanogens to explain the acclimatisation of anaerobic digestion to such irreversible toxicity exposure.

- Application of ADM1 as a virtual plant to generate data that is subsequently used to validate and calibrate anaerobic digestion control models, test and implement optimal experiment design tools, and design and setup anaerobic digestion monitoring systems.

- Implementation and validation of the simplified anaerobic digestion control model AM2 and its application as part of a general protocol to base the design of a monitoring system.

- Implementation of the Siegrist anaerobic digestion model as part of a plant-wide model and application of the transformers' concept to interface activated sludge and anaerobic digestion models so as to increase the potential of modelling anaerobic digestion applications.

- Development of ASM1-ADM1-ASM1 transformers using the general Continuity-Based Interfacing Method (CBIM) and compare it to the ADM1-ASM1 specific transformation that operates by Maximising some components with respect to the total COD and Nitrogen contents, the MCN method. Both methods are used to integrate ADM1 in plant-wide models.

- Development and implementation of a general procedure to calculate total equivalents of the ions of a mixture of buffer components in a solution, calculate the cation concentrations in flows of known buffer composition and pH, simulate

pH with any model that implements chemical equilibrium reactions, and build a titrimetric analyser simulator, TAS.

- Supporting the development of the first commercial on-line titrimetric analyser for anaerobic digestion applications.

- Development and implementation of the automatic initialisation procedure of the Buffer Capacity Software (BCS) for on-line titrimetric monitoring of unknown buffer solutions and validation of BCS on lab, pilot and industrial anaerobic digestion applications.

These research outcomes were complementary to each other in different ways. With the validated ADM1 implementation, it was possible to study cyanide hydrolysis and degradation, and hence extend the ADM1 model with the suitable kinetics to model such irreversible toxicity. In the validation experiment of the extended model, the general-pH procedure helped to calculate the influent cation concentration and the simulation of pH in presence of more buffer components than was possible in the original model, i.e. phosphorous and cyanide. The implementation of an external pH calculation procedure with ADM1 improved the simulation speed and therefore helped the implementation of ADM1 in plant-wide models.

Due to the detailed structure of ADM1 it was possible to apply the model to represent a virtual plant that could then generate measurement signals to test and apply an optimal experimental design (OED) procedure to design the monitoring system and enhance the confidence in a simpler control model AM2.

A change was made to ADM1 to describe the SRT in proportion to the HRT. It uses a parameter with known bound for high rate anaerobic reactors, therefore leading to a better parameter identifiability. Accordingly, it was possible to model UASB reactors treating cyanide-contaminated wastewaters. Similarly, this introduced parameter can be used to model CSTR configurations and detect the washout of biomass from the reactor.

The titrimetric simulator TAS helped to test the BCS. Also, the TAS was used to design a protocol to test both the BCS and the titrimetric analyser at an industrial scale digester with different applied complicating practical circumstances.

13.2 Findings with the developed modelling tools

13.2.1 Key updates of ADM1

Key updates were necessary to have a successful implementation of the standard IWA ADM1:

- The model inorganic carbon and nitrogen components need to be used to close the carbon and nitrogen balance over all reactions to guarantee continuity of mass.
- It is necessary to state the implemented inhibition terms more clearly since they were loosely specified in the model report.
- For pH-simulation with ADM1, some updates are necessary to the chemical reaction rates that are described in the model report as a Differential Equation implementation (DE). For the Differential and Algebraic Equation (DAE) implementation of the model, the algebraic equations for the calculation of the pH equilibrium should be solved externally to solve the models with simple DE solvers and obtain improved simulation speed.
- For modelling high rate reactors the SRT needs to be modelled higher than and in proportion to the HRT by considering the particulate fraction in the reactor effluent.
- To have a successful implementation of multiphase models in WEST, updates are necessary to the WEST standard model declarations as presented for ADM1.

13.2.2 pH and gas transfer modelling

There are possible simplifications of pH and gas transfer modelling in anaerobic reactors as presented by the two simpler models, Siegrist et al. (1995) and AM2 Bernard et al. (2002), compared to ADM1. It should be noted that these simplifications are valid only if the assumptions of both models are acceptable for the modelling application. If the assumptions are not valid at certain applications, more extended models should be used, e.g. ADM1 Batstone et al. (2002) and the extended model Siegrist et al. (2002). More specifically, the gas transfer simplification in the Siegrist et al. (1995) model is valid for reactors with continuous gas flow through the liquid compartment of the anaerobic reactor to strip the gas components. The pH simulation of the Siegrist et al. (1995) model is valid with waste water of enough bicarbonate alkalinity in the treated wastewaters to buffer the anaerobic reactor contents. The AM2 simulation is only accurate if the considered acetogenesis and methanogenesis steps are the main steps in the anaerobic reactor, i.e. the influent wastewater to the anaerobic reactor is low in organic particulates and is to a large extent acidified.

The general formulas for ion concentrations as function of their total buffer concentrations are systematically evolving with the buffer types and ion order. Therefore, it was possible to implement them in a general form that is then implemented in the calculation of total equivalents and cation concentrations, and for the simulations of pH and titration experiments. Implementing the pH calculation using this general form can consider all buffer components without reducing the simulation speed. Therefore, no assumptions are needed to simplify the pH calculations and the main reason of model stiffness is eliminated. An additional benefit is that the proposed methodology of pH calculation is general. Therefore, it is applicable to other pH-dependent models. Also, it can be used as a basis for titration algorithms and to simulate titration experiments.

13.2.3 Extension of ADM1 to model irreversible toxicity

The implemented approach of using two aceticlastic biomass populations with different cyanide tolerances helped in resolving the contradiction of the observed reversible effect of cyanide to the anaerobic process with the literature statement that cyanide is an irreversible toxicant. Therefore, the extended model can be used to study the feasibility of anaerobic treatment of wastewaters contaminated with irreversible toxicants such as cyanide. The use of two biomass populations is especially important if selection of cyanide-tolerant biomass is not likely to occur completely. This is expected to happen if the acclimatisation is insufficient and/or the applied cyanide load is low, e.g. less than 5mgCN/l. Sensitivity analysis has shown that yield and the decay parameters of the cyanide-tolerant aceticlastic methanogens are the most important parameters. The sensitivity analysis supports the importance of modelling the population shift and shows that the parameters are practically identifiable from experimental data.

The modelled hydrolytic pathway for cyanide degradation as function of the proposed cyanide-tolerant aceticlastic methanogens concentration helps to accurately simulate the cyanide dynamics. The introduction of the cyanide inhibition term in the acetate uptake kinetics helped to predict the acetate accumulation during the cyanide overload, even after the accumulation of the tolerant acetoclastic methanogens had occurred. It is experimentally shown that if the sludge is acclimatised sufficiently long to cyanide loads above 5 mg CN/l, a single population of aceticlastic methanogens would suffice to adequately model the cyanide effects, provided that the inhibition term is applied to the acetate uptake. After a reasonable acclimatisation period to cyanide, the biogas followed the influent COD dynamics and could be accurately simulated.

13.2.4 Applying ADM1 with a concise set of measurements

Information about the wastewater composition and knowledge of the upstream industrial processes are successfully applied with a concise set of practical measurements to run accurate model simulations. A detailed characterisation of the influent wastewater could be performed allowing to produce good simulation results using the IWA ADM1 and a default set of parameters. In addition to the general information about the wastewater composition, the detailed model structure enables the use of some in-reactor measurements to estimate the influent substrate fractions and total alkalinity. However, in the presence of toxicities, e.g. due to the reduction of influent sulphates, a model extension is necessary to describe the applied toxicity and enhance simulations results.

The ADM1 model could be extended to adequately predict the process dynamics in the presence of the cyanide irreversible toxicity. The model simulated three UASB reactors treating cassava wastewater that is cyanide-contaminated. The known composition of cassava wastewater and a few daily measurements in the influent to the reactors were sufficient to achieve an appropriate influent characterisation for ADM1. Also, the general pH calculation procedure was useful to estimate the cation concentration in the influent and to extend the ADM1 model with the introduced buffer components to obtain the right pH simulation. Daily measurements from one reactor were used for initial calibration of the model. The model was validated with measurements from the other two reactors.

13.2.5 Model-based design of a monitoring system

A validated control model (AM2) implementation and an iterative Optimal Experimental Design (OED) were successful as basis for a simple protocol to design and setup the monitoring system of an anaerobic digester. The protocol was validated using a virtual case study. The virtual case study was the first application in the scientific community that uses a reference model (ADM1) as a data generator to evaluate methodologies and validate other simple models. The virtual data are calculated in the most common measurement units, are generated with predefined noise levels and measurement intervals, and are evaluated as function of the ADM1 state variables and parameters. The protocol to design a monitoring system is based on OED methodology that was applied to anaerobic digestion for the first time. It is found to be useful to determine the need for additional sensors, the type of measurement equipment, measurement frequencies and an optimal influent profile that excites the system sufficiently to allow good model calibration. Accordingly, the precision of the AM2 control model increased, i.e. a better parameter estimation quality is achieved. Therefore, the protocol can be used to design an efficient monitoring system that will allow to successfully manage and control anaerobic digestion plants.

13.2.6 Plant-wide modelling

The methodology of connecting an anaerobic digestion model with other process model by transformers is successful and facilitates the inclusion of the anaerobic digestion model and sludge treatment stream in a plant-wide modelling application. Accordingly, it is possible to evaluate the performance of the sludge digester and its impact on the activated sludge process. The methane production rates can be simulated and therefore the economic value of using methane for energy production can be evaluated. The reduction of sludge volumes can be estimated and therefore the sludge handling and disposal can be planned efficiently. Impacts of the digester on the overall plant performance can be evaluated. It is found by simulation that denitrification can be improved, thanks to the recycle of VFA from the digester. The increase of the ammonia loads due to the recycled digester overflows can be simulated as well.

It was found in the plant-wide application of ASM1 and ADM1 models that the global plant output by using the **C**ontinuity-**B**ased **I**nterfacing **M**ethod (CBIM) is comparable to the output obtained by the interfacing method that aims at **M**aximising some components with respect to the total **C**OD and **N**itrogen contents (MCN). Both interfacing methods lead to almost the same output of the activated sludge plant, biogas from the digester and sludge production. However, with the additional flexibility of the CBIM approach, the transformation of "origin" components could be distributed over a larger number of components on the "destination" side of the interface. This wider distribution leads to better simulation of digester dynamics that is quite useful for accurate parameter estimation, control strategy benchmarking and implementation of advanced treatment processes, e.g. for high rate nitrogen removal.

The CBIM approach is general and it can be applied to any couple of models to be interfaced and it, therefore, allows to incorporate more knowledge about the process. For instance, in the provided plant-wide example using CBIM, amino acids were estimated in the digester influent knowing that part of the protein will be hydrolysed during sludge thickening. Also, sugar fermenters were estimated in the digester influent knowing that part of the heterotrophs in the activated sludge are capable of fermenting. On the other hand, even though the MCN approach aims to maximise the conversion from the soluble organic nitrogen and COD to amino acids, the method does not achieve the conversion to amino acids from the waste activated sludge due to the low soluble COD content.

For both applied methods, the transformation from ADM1 to ASM1 is easier to set up compared to the one from ASM1 to ADM1. This is due to the fact that ADM1 is based on

a more detailed and more specific set of components. Application of the CBIM approach needs a careful design of the conversion at the interface, requiring deep insight in the two models to be connected. However, there are three Guiding Transformation Principles (GTP) to help the user to refine the conversions. The GTP help to solve the under-determination problems found in the definition of the transformer stoichiometry and conversions. Also, the GTP are useful to update the designed conversions and guarantee that transformation occurs in the right direction.

The introduction of the sourcing components as implemented in CBIM is necessary since, so far in the field of wastewater treatment, the developed models do not consider all elemental balances. Therefore, the CBIM approach provides a good opportunity to close this gap in terms of integrated modelling.

13.3 Findings with the developed monitoring tools

13.3.1 On-line titrimetric monitoring

According the reviewed literature, most of the sensors and analysers of potential use in anaerobic digestion monitoring are commercially available except titrimetric analysers. The first commercial on-line titrimetric analyser was developed parallel to and with support of this research. The titrimetric measurements are useful and applied to a wide spectrum of environmental and wastewater treatment applications. Most of the applications are, however, off-line. Some on-line applications are in on-going research using prototype analysers but no evidence of full-scale on-line applications was found.

Generally, the titrimetric methods can be classified into three categories according their mathematical solution of the estimation problem. Two approximate method categories determine the concentrations of the buffers present by linear solution of algebraic equations or linear regression. These two categories comprise many titrimetric methods that apply different titration algorithms, i.e. using different numbers of titration end-points at different pH-values, typically 3 or 5 points. They are mainly developed for measuring alkalinity and VFA in anaerobic digestion. Most of these methods are simple and robust but approximate. The third category comprises advanced methods that use nonlinear fitting of a model to many titration points. The most dominant method is using nonlinear fitting to the buffer capacity curve that is produced from a slow titration, i.e. having a large number of titration points, approximately 50 points. This method was implemented in a software sensor (Buffer capacity Optimal Model Builder, BOMB) that uses advanced optimisation and model selection techniques. Also, through this research, BOMB is upgraded to the

Buffer Capacity Software (BCS) by an automatic initialisation module that has increased the robustness of the on-line determination of a wide range of buffer mixtures.

The automatic initialisation procedure implemented in BCS is able to extract useful information from simple titration experiments. The information concerns the likely buffers to be present in the titrated sample and their expected concentration range. This information is shown to be sufficient to initialise the optimisation procedure and accurately determine the buffer concentrations. The BCS integrates the initialisation procedure and BOMB and, therefore, does not require frequent interaction with the user to study prior analysis results or information about the system to update the optimisation or the model selection parameters. The model is defined and initialised automatically for each titrated sample and therefore the robustness for on-line application increases.

BCS was tested in three ways using a titrimetric simulator, a lab-analyser and an on-line analyser. BCS showed its potential to accurately measure a wide range of buffer mixtures. It also has a high measuring quality, even under fast transitions between different buffer combinations. For biological processes such as anaerobic digestion that require continuous and on-line monitoring of buffering substrates or toxic compounds, BCS is considered to be a good solution.

13.3.2 Monitoring digester overloads

A case study in which a digester overload was monitored titrimetrically, it was demonstrated that the monitoring was successful with both a prototype sensor and a titrimetric setup that use the approximate method of linear regression and the advanced method of BCS, respectively. Both analysers and their methods show acceptable accuracy for VFA and alkalinity analysis for a large range of operating conditions of the digester and, therefore, can be used in closed loop control schemes. The added value of the BCS was the more accurate results at high concentrations and the estimation of other interfering buffers, e.g. lactate in this case. The better accuracy was due to the simultaneous estimation of acidity constants that is possible with BCS. The acidity constants tend to shift due to several factors, e.g. temperature and ionic strength or pH meter drift. In the approximate methods the acidity constants are either assumed to previously known values, e.g. the values at standard conditions or they are estimated via fitting a regression model under defined calibration conditions. To maintain a high accuracy level with the approximate method, determination of the acidity constants or recalibration of the regression model is essential in case of major changes in the operation conditions.

In overload situations, VFAs of higher molecular weight than acetate tend to accumulate. Also, lactate formation is expected. As it interferes, lactate will decrease the accuracy of VFA determination by the approximate methods. In situations other than treatment of vinasses, buffer components other than bicarbonate and VFA are likely to exist. These additional buffers are also interfering with bicarbonate and VFA (e.g. phosphorus, H_2S and other weak acids) and they should be quantified and considered in the calculation procedure of the approximate methods. This may call for other techniques for measuring these components. Thus, since BCS can cope with these additional buffers, it can be considered to be a good monitoring tool for anaerobic digestion not only during normal operating conditions but also during overload and exposure to buffering interferences. However, for determination of this larger set of buffers, a detailed titration curve and therefore good titration hardware is needed.

13.3.3 Monitoring digester post-treatment

In a second case study BCS was evaluated for the titrimetric monitoring of advanced post treatment processes (in the study a SHARON-Anammox process) treating digester effluent liquors. The study clearly demonstrated that it was possible to monitor Total Ammonia Nitrogen (TAN) and Total Nitrite Nitrogen (TNO_2). The optimal titrant concentration was determined to be 0.05 M based on measurements of standard solutions within the typical concentration range. The titrimetric measurements were comparable to colorimetric measurements using a standard device. Comparing measurements of both titrimetric and colorimetric methods for samples taken from a lab-scale SHARON reactor, TAN and TNO_2 were determined similarly by both methods but the TNO_2 concentrations determined with the colorimetric device were more noisy due to the large dilution required by the colorimetric method. A statistical test showed that both methods could not be distinguished from each other at 95% confidence level. Next to TAN and TNO_2, phosphate could also be detected as an additional measurement in the SHARON reactor.

For the Anammox reactor only the TAN concentrations obtained with both methods agreed, while the TNO_2 concentrations were overestimated with the titrimetric measurement due to the low concentration of TNO_2 in the effluent and possible interferences by other components. Basically, the titrimetric set-up gives the possibility to replace part of the analyses work by a cheaper and easy to automate method that requires no dilution and hence is less sensitive to errors. More accurate titrimetric measurement of TNO_2 in the Anammox reactor can be foreseen by an additional and differently configured titration experiment. However, this additional experiment is not needed in the light of a control strategy of the combined SHARON-Anammox process. A titrimetric analyser

placed in between the two process reactors will suffice to control the TAN:TNO_2 ratio of the SHARON reactor effluent in the optimum range for the Anammox reactor influent.

13.3.4 Challenges of on-line titrimetric monitoring

In a third case study, the BCS and the on-line titrimetric analyser AnaSense® were challenged for on-line monitoring of effluent from a full-scale digester with many artificially introduced factors. These complications included the introduction of multivalent cations, e.g. calcium and iron ions, and artificially added buffers of lactate, additional VFA, ammonia and phosphorous. They were found to generally reduce the accuracy of the titrimetric analyser and the titrimetric methods. The presence of calcium and iron ions effected precipitation of carbonate and phosphate. The precipitation affected the analyser operation due to blocking of its tubing. Also, precipitation affected the accuracy of the titrimetric methods since precipitation kinetics are not considered in the calculation methods. The approximate linear regression method was the most simple and efficient for determining VFA and bicarbonate since it also works with the fast titration algorithm and, therefore, avoids most of the precipitation/dissolution influence. The advanced BCS method was highly influenced by the titration noise and the presence of highly charged cations. However, BCS could detect all buffer components introduced to the system and reproduced most of the applied dynamics and trends as would be necessary for control applications. In addition to bicarbonate and VFA, BCS also determined ammonium and lactic acid concentrations. This can be very precious information concerning these key parameters in AD monitoring. Phosphorous was also detected by BCS but the determined phosphorous concentrations were not comparable to the reference measurements due to the presence of ferric ions dosed to the plant effluent and fast precipitation of phosphorus before the titrimetric analysis is complete.

In summary, BCS showed a high capability for on-line titrimetric monitoring of anaerobic digestion and its advanced post-treatment processes. BCS is applicable with lab and commercial on-line titrimetric analysers. BCS can measure different mixtures of buffer solutions accurately. The presence of precipitation affects the accuracy of BCS, especially for the determination of bicarbonate and phosphorus.

13.4 Perspectives for future research and applications

Three main directions are foreseen for research and applications of anaerobic digestion modelling and monitoring where the tools developed in this research can be further

implemented for optimisation and smooth operation of the process and wastewater treatment systems.

The first direction is optimisation of the anaerobic process and plant design. In this direction, the ADM1 implementation helps to better understand the process behaviour in treating different types of wastewaters. The model can be used to optimise the process to treat certain types of wastewater efficiently. For instance, in this research, the model was extended for anaerobic treatment of cyanide contaminated wastewater and, therefore, the extended model was used to optimise the process, e.g. determine the necessary acclimatisation period to start-up a new plant. Furthermore, the model implementation can be used to optimise a plant design. In this research the model could simulate a washout from a CSTR and higher SRT in UASB reactors. Accordingly, the model can be used to optimise the plant design to, for example, prevent biomass washout, improve the SRT and determine the optimum reactor volume. Also, the model can be used to determine optimum configurations of advanced reactor types, e.g. to determine the optimally phased compartments of a baffled anaerobic reactor to deal with a certain feed regime.

The second direction concerns the optimisation of anaerobic digestion applications in the context of an integrated wastewater treatment solution. A plant-wide model can be used to optimise anaerobic sludge digestion at conventional wastewater treatment plants. In this research, an extended benchmark plant implemented anaerobic digestion models to model sludge treatment in connection with activated sludge process models. The extended benchmark could predict digester and plant outputs, and the impact of recycled overflows from sludge treatment to the activated sludge units. Model connections were established using a flexible methodology of transformers so that more than one digester can be connected to the plant and loads from different sources can be connected to each digester. This flexibility enables the optimisation of central sludge treatment options. Also, the methodology enables the optimisation of decentralised wastewater solutions that can apply anaerobic digestion units near wastewater sources, e.g. industries and farms, and connect their overflows to other treatment systems, e.g. conventional wastewater treatment plants. Also, the transformation approaches implemented and compared in this research are illustrated in detail to enable their application not only to connect anaerobic digestion models to other models but also to connect different models in an integrated scheme.

The third direction focuses on the optimisation of anaerobic digestion and wastewater treatment plant operation. In this research, a Buffer Capacity Software (BCS) was developed to automate buffer estimation and determination of buffer concentrations in unknown buffer solutions. BCS is working with on-line titrimetric analysers and can

measure different buffer components in mixtures. Therefore, it can be used for titrimetric monitoring of anaerobic digestion and be a basis for control of the process. In a case study in this research, BCS was successful to monitor a digester under overload conditions measuring bicarbonate, VFA and lactate. It can monitor the fate of bicarbonate alkalinity, the VFA accumulation and the production of lactate under the overload conditions. Therefore, with one on-line analyser implementing BCS, three control loops can be implemented. More loops can be developed, e.g. for toxic conditions since, with the same analysis, BCS can determine toxicant buffers such as ammonia, cyanide, phenol …etc. Also, BCS was tested to monitor advanced digester post-treatment processes (SHARON-Anammox) measuring ammonia and nitrite. Therefore, the implementation of BCS can be extended to optimise and control the operation of other processes. The anaerobic digestion models and the Titrimetric Analyser Simulator (TAS) that were implemented and developed in this research can be used to evaluate BCS and the control schemes. Based on simulation, the economic value of the titrimetric measurements can be calculated and compared with the value of alternative sensors.

All in all, the availability of commercial titrimetric analysers (e.g. AnaSense®) and the BCS interpretation have a large application potential, in anaerobic digestion and beyond.

Appendices

Appendix 1 *ADM1-WEST implementation: Default set of parameters*

Parameter	Unit	Value	Definition
Stoichiometric parameters			
$f_{sI,xc}$	–	0.1	Yield of soluble inerts from disintegration of complex particulates
$f_{xI,xc}$	–	0.2	Yield of particulate inerts from disintegration of complex particulates
$f_{ch,xc}$	–	0.2	Yield of carbohydrates from disintegration of complex particulates
$f_{pr,xc}$	–	0.2	Yield of proteins from disintegration of complex particulates
$f_{li,xc}$	–	0.3	Yield of lipids from disintegration of complex particulates
N_{xc}	kmole N (kg COD) $^{-1}$	0.00221	Nitrogen content of particulate degradable COD
N_I	kmole N (kg COD) $^{-1}$	0.00414	Nitrogen content of soluble inert COD
		0.00414	Nitrogen content of particulate inert COD
N_{aa}	kmole N (kg COD) $^{-1}$	0.0071	Nitrogen content of amino acids
C_{xc}	kmole C (kg COD) $^{-1}$	0.0258	Carbon content of complex particulates
C_{sI}	kmole C (kg COD) $^{-1}$	0.03	Carbon content of soluble inert COD
C_{ch}	kmole C (kg COD) $^{-1}$	0.0313	Carbon content of carbohydrates
C_{pr}	kmole C (kg COD) $^{-1}$	0.03	Carbon content of proteins
C_{li}	kmole C (kg COD) $^{-1}$	0.022	Carbon content of lipids
C_{xI}	kmole C (kg COD) $^{-1}$	0.03	Carbon content of particulate inert COD
C_{su}	kmole C (kg COD) $^{-1}$	0.0313	Carbon content of sugars
C_{aa}	kmole C (kg COD) $^{-1}$	0.03	Carbon content of amino acids
$f_{fa,li}$	–	0.95	Yield of long chain fatty acids (as opposed to glycerol) from lipids
C_{fa}	kmole C (kg COD) $^{-1}$	0.0217	Carbon content of long chain fatty acids
$f_{h2,su}$	–	0.19	Yield of hydrogen from monosaccharide degradation
$f_{bu,su}$	–	0.13	Yield of butyrate from monosaccharide degradation
$f_{pro,su}$	–	0.27	Yield of propionate from monosaccharide degradation
$f_{ac,su}$	–	0.41	Yield of acetate from sugar degradation
N_{bac}	kmole N (kg COD) $^{-1}$	0.0062	Nitrogen content of biomass
C_{bu}	kmole C (kg COD) $^{-1}$	0.025	Carbon content of butyrate
C_{pro}	kmole C (kg COD) $^{-1}$	0.0268	Carbon content of propionate
C_{ac}	kmole C (kg COD) $^{-1}$	0.0313	Carbon content of acetate
C_{bac}	kmole C (kg COD) $^{-1}$	0.0313	Carbon content of biomass
Y_{su}	–	0.1	Yield of biomass on uptake of monosaccharides
$f_{h2,aa}$	–	0.06	Yield of hydrogen from amino acid degradation
$f_{va,aa}$	–	0.23	Yield of valerate from amino acid degradation
$f_{bu,aa}$	–	0.26	Yield of butyrate from amino acid degradation
$f_{pro,aa}$	–	0.05	Yield of propionate from amino acid degradation
$f_{ac,aa}$	–	0.4	Yield of acetate from amino acid degradation
C_{va}	kmole C (kg COD) $^{-1}$	0.024	Carbon content of valerate
Y_{aa}	–	0.08	Yield of biomass on uptake of amino acids
Y_{fa}	–	0.06	Yield of biomass on uptake of long chain fatty acids
Y_{c4}	–	0.06	Yield of biomass on uptake of valerate or butyrate
Y_{pro}	–	0.04	Yield of biomass on uptake of propionate

Parameter	Unit	Value	Definition
C_{ch4}	kmole C (kg COD) $^{-1}$	0.0156	Carbon content of methane
Y_{ac}	–	0.05	Yield of biomass on uptake of acetate
Y_{h2}	–	0.06	Yield of biomass on uptake of elemental hydrogen
Kinetic parameters			
k_{dis}	d^{-1}	0.5	Complex particulate disintegration first order rate constant
$k_{hyd,ch}$	d^{-1}	10	Carbohydrate hydrolysis first order rate constant
$k_{hyd,pr}$	d^{-1}	10	Protein hydrolysis first order rate constant
$k_{hyd,li}$	d^{-1}	10	Lipid hydrolysis first order rate constant
$K_{S,IN}$	M	0.0001	Inorganic nitrogen concentration at which growth ceases
$k_{m,su}$	d^{-1}	30	Maximum uptake rate for monosaccharide degrading organisms
$K_{S,su}$	kg COD m^{-3}	0.5	Half saturation constant for monosaccharide degradation
$pH_{UL,aa}$		5.5	pH level at which there is no inhibition…(for bacteria in general e.g. aa and fa degraders)
$pH_{LL,aa}$		4	pH level at which there is full inhibition …(for bacteria in general e.g. aa and fa degraders)
$k_{m,aa}$	d^{-1}	50	Maximum uptake rate amino acid degrading organisms
$K_{S,aa}$	kg COD m^{-3}	0.3	Half saturation constant for amino acid degradation
$k_{m,fa}$	d^{-1}	6	Maximum uptake rate for long chain fatty acid degrading organisms
$K_{S,fa}$	kg COD m^{-3}	0.4	Half saturation constant for long chain fatty acids degradation
$K_{Ih2,fa}$	kg COD m^{-3}	5E-6	Hydrogen inhibitory concentration for FA degrading organisms
$k_{m,c4}$	d^{-1}	20	Maximum uptake rate for C4 degrading organisms
$K_{S,c4}$	kg COD m^{-3}	0.2	Half saturation constant for butyrate and valerate degradation
$K_{Ih2,c4}$	kg COD m^{-3}	1E-5	Hydrogen inhibitory concentration for C4 degrading organisms
$k_{m,pro}$	d^{-1}	13	Maximum uptake rate for propionate degrading organisms
$K_{S,pro}$	kg COD m^{-3}	0.1	Half saturation constant for propionate degradation
$K_{Ih2,pro}$	kg COD m^{-3}	3.5E-6	Inhibitory hydrogen concentration for propionate degrading organisms
$k_{m,ac}$	d^{-1}	8	Maximum uptake rate for acetate degrading organisms
$K_{S,ac}$	kg COD m^{-3}	0.15	Half saturation constant for acetate degradation
$K_{I,nh3}$	M	0.0018	Inhibitory free ammonia concentration for acetate degrading organisms
$pH_{UL,ac}$		7	pH level at which there is no inhibition of acetate degrading organisms
$pH_{LL,ac}$		6	pH level at which there is full inhibition of acetate degradation
$k_{m,h2}$	d^{-1}	35	Maximum uptake rate for hydrogen degrading organisms
$K_{S,h2}$	kg COD m^{-3}	7E-6	Half saturation constant for uptake of hydrogen
$pH_{UL,h2}$		6	pH level at which there is no inhibition of hydrogen degrading organisms
$pH_{LL,h2}$		5	pH level at which there is full inhibition of hydrogen degrading organisms

Parameter	Unit	Value	Definition
$k_{dec,Xsu}$	d^{-1}	0.02	Decay rate for monosaccharide degrading organisms
$k_{dec,Xaa}$	d^{-1}	0.02	Decay rate for amino acid degrading organisms
$k_{dec,Xfa}$	d^{-1}	0.02	Decay rate for long chain fatty acid degrading organisms
$k_{dec,Xc4}$	d^{-1}	0.02	Decay rate for butyrate and valerate degrading organisms
$k_{dec,Xpro}$	d^{-1}	0.02	Decay rate for propionate degrading organisms
$k_{dec,Xac}$	d^{-1}	0.02	Decay rate for acetate degrading organisms
$k_{dec,Xh2}$	d^{-1}	0.02	Decay rate for hydrogen degrading organisms
Physiochemical parameters			
R	bar M^{-1} K^{-1}	0.08314	Gas law constant
T_{base}	K	--	" Not used " … i.e. operating temperature (T_{op}) is considered constant and parameter values should correspond to this operational temperature
T_{op}	K	308.15	Temperature
K_w	M	2.08E-14	Water acidity constant (temperature correction needed)
$K_{a,va}$	M	1.38E-5	Valerate acidity constant (temperature correction can be ignored)
$K_{a,bu}$	M	1.5E-5	Butyrate acidity constant (temperature correction can be ignored)
$K_{a,pro}$	M	1.32E-5	Propionate acidity constant (temperature correction can be ignored)
$K_{a,ac}$	M	1.74E-5	Acetate acidity constant (temperature correction can be ignored)
$K_{a,co2}$	M	4.94E-7	CO_2 acidity constant (temperature correction needed)
$K_{a,IN}$	M	1.11E-9	NH_4^+ acidity constant (temperature correction needed)
P_{atm}	Bar	1.013	Pressure of atmosphere
$p_{gas,h2o}$	Bar	0.0557	Partial pressure of water (Note: can be defined empirically)
k_La	d^{-1}	200	Gas liquid transfer coefficient (Note: dependent on the reactor type)
$K_{H,co2}$	M_{liq} bar^{-1}	0.0271	Henry's law constants for carbon dioxide
$K_{H,ch4}$	M_{liq} bar^{-1}	0.00116	Henry's law constants for methane
$K_{H,h2}$	M_{liq} bar^{-1}	0.000738	Henry's law constants for hydrogen
Physical parameters			
V_{liq}	m^3	varies	Volume of liquid in the reactor
V_{gas}	m^3	varies	Volume of the gas vessel
f_{xout}	–	1 (CSTR) 0 (FBR)	Fraction of the anaerobic particulate matter that leaves the reactor

Appendix 2 *Siegrist et al.(1995) ADM-WEST implementation: Default set of parameters*

Parameter	Unit	Value	Definition
b_{AC}	d^{-1}	0.1	Specific decay rate for acetoclastic methanogens.
b_{AS}	d^{-1}	1	Specific decay rate for amino acids and sugar fermenting bacteria
b_{FA}	d^{-1}	0.1	Specific decay rate for fatty acids oxidising anaerobic bacteria
b_{H2}	d^{-1}	0.4	Specific decay rate for hydrogenotrophic methanogens.
b_{PRO}	d^{-1}	0.1	Specific decay rate for propionate degrading organisms
f_{X_Out}	-	1 (CSTR) 0 (FBR)	Fraction of the anaerobic particulate matter that leaves the reactor
H_{CH4}	atm. $m^3.Mol^{-1}$	0.876	Henry coefficient for CH_4
H_{CO2}	atm.$m^3.Mol^{-1}$	0.04	Henry coefficient for CO_2
H_{H2}	atm.$m^3.Mol^{-1}$	1.334	Henry coefficient for H_2
$Q_{gas\_initial}$	$m^3.\ d^{-1}$	varies	Initial (minimum) value of total gas flow
k_{CO2}	d^{-1}	0.0045	Rate of carbon dioxide deprotolysis
k_{HCO3}	$d^{-1}.m^3.Mol^{-1}$	10	Rate of bicarbonate protolysis
$K_{I\_AC\_FA}$	$g.m^{-3}$	2000	Inhibitory acetate concentration for anaerobic fatty acids oxidation
$K_{I\_AC\_PRO}$	$g.m^{-3}$	1500	Inhibitory acetate concentration for propionate degrading organisms
$K_{I\_H2\_FA}$	$g.m^{-3}$	0.012	Inhibitory elemental hydrogen concentration for fatty acids anaerobic oxidation
$K_{I\_H2\_PRO}$	$g.m^{-3}$	0.0006	Inhibitory elemental hydrogen concentration for propionate degrading organisms
$K_{I\_H\_AC}$	$Mol.m^{-3}$	0.00063	Inhibitory proton concentration for acetoclastic methanogens
$K_{I\_H\_H2}$	$Mol.m^{-3}$	0.00063	Inhibitory proton concentration for hydrogenotrophic methanogens
$K_{I\_H\_PRO}$	$Mol.m^{-3}$	0.00063	Inhibitory proton concentration for propionate degrading organisms
k_R	gCOD/(gCOD.d)	0.25	Specific hydrolysis rate of biopolymers
K_{S_AC}	g COD m^{-3}	30	Half saturation constant for acetoclastic methanogenesis
K_{S_AS}	g COD m^{-3}	50	Half saturation constant for amino acids and sugar fermentation
K_{S_FA}	g COD m^{-3}	200	Half saturation constant for fatty acids anaerobic oxidation
K_{S_H2}	g COD m^{-3}	0.06	Half saturation constant for hydrogenotrophic methanogenesis
$K_{S\_H\_AC}$	$Mol.m^{-3}$	1E-5	Half saturation constant of proton concentration for acetoclastic methanogenesis
$K_{S\_H\_H2}$	$Mol.m^{-3}$	1E-5	Half saturation constant of proton concentration for hydrogenotrophic methanogenesis
$K_{S\_H\_PRO}$	$Mol.m^{-3}$	1E-5	Half saturation constant of proton concentration for propionate degrading organisms
K_{S_PRO}	g COD m^{-3}	15	Half saturation constant for propionate degrading organisms
mu_{AC}	d^{-1}	0.95	Maximum specific growth rate of acetoclastic methanogens
mu_{AS}	d^{-1}	5	Maximum specific growth rate of amino acids and sugar fermenting bacteria
mu_{FA}	d^{-1}	0.55	Maximum specific growth rate of anaerobic bacteria for fatty acids oxidation

Parameter	Unit	Value	Definition
mu_{H2}	d^{-1}	3.6	Maximum specific growth rate of hydrogenotrophic methanogens
mu_{PRO}	d^{-1}	0.8	Maximum specific growth rate of propionate degrading organisms
p	Pa	101325	Head pressure in the digester
Q_{Gas}	$m^3 . d^{-1}$	30	Gasflow for stripping
T	°C	35	Celsius temperature
R	$J M^{-1} K^{-1}$	8.31451	Gas law constant

Appendix 3 *Anaerobic digestion transformers-WEST implementation: Default set of parameters*

3.1 ASM1-Siegrist et al. (1995) ADM

Parameter	Unit	Value	Definition
f_{AC_S}	-	0.3	Fraction of S_S that is acetate (S_{AC})
f_{AS_H}	-	0.5	Fraction of X_{BH} (heterotrophs in ASM1) that are capable of fermenting
f_{AS_S}	-	0.1	Fraction of S_s that are amino acids and sugar (S_{AS})
f_{PRO_S}	-	0.1	Fraction of S_S that is propionate (S_{PRO})
f_{XSAn_A}	-	0.92	Fraction of X_{BA} (ASM1) that becomes biodegradable under anaerobic conditions
f_{XSAn_H}	-	0.08	Fraction of X_{BH} (ASM1) that becomes biodegradable under anaerobic conditions
f_{XSAn_I}	-	0.1	Fraction of X_I (ASM1) that becomes biodegradable under anaerobic conditions
f_{XSAn_P}	-	0.1	Fraction of X_P (ASM1) that becomes biodegradable in anaerobic conditions
i_{S_AS}	gN/gCOD	0.04	Mass of nitrogen per mass of COD in amino acids (S_{AS})
i_{X_An}	gN/gCOD	0.08	Mass of nitrogen per mass of COD in anaerobic biomass
i_{X_B}	gN/gCOD	0.086	Mass of nitrogen per mass of COD in biomass (ASM1)
i_{X_IN}	gN/gCOD	0.04	Mass of nitrogen per mass of COD in inert particulates
i_{X_P}	gN/gCOD	0.04	Mass of nitrogen per mass of COD in products formed (ASM1)
$i_{X\_S\_An}$	gN/gCOD	0.02	Mass of nitrogen per mass of COD in slowly biodegradable matter (X_{S_An})

3.2 Siegrist et al. (1995) ADM -ASM1

Parameter	Unit	Value	Definition
f_{H_AS}	-	0.5	Fraction of fermenting biomass that are heterotrophs
f_{P_An}	-	0.08	Fraction of anaerobic biomass that leads to inert matter
i_{S_AS}	gN/gCOD	0.04	Mass of nitrogen per mass of COD in amino acids (S_{AS})
i_{X_An}	gN/gCOD	0.08	Mass of nitrogen per mass of COD in anaerobic biomass
i_{X_B}	gN/gCOD	0.086	Mass of nitrogen per mass of COD in biomass (ASM1)
i_{X_IN}	gN/gCOD	0.04	Mass of nitrogen per mass of COD in inert particulates
i_{X_P}	gN/gCOD	0.04	Mass of nitrogen per mass of COD in products formed (ASM1)
$i_{X\_S\_An}$	gN/gCOD	0.02	Mass of nitrogen per mass of COD in slowly biodegradable matter (X_{S_An})

3.3 MCN transformer ASM1- ADM1

Parameter	Unit	Value	Definition
f_X_I	-	0.1	Fraction of X_I and X_p (ASM1) that becomes biodegradable under anaerobic conditions
i_X_B	gN/gCOD	0.086	Mass of nitrogen per mass of COD in biomass (ASM1)
i_X_e	gN/gCOD	0.04	Mass of nitrogen per mass of COD in products formed and inert particulates (ASM1)
f_ch_xc	dUnit/dUnit	0.2	Yield of carbohydrates from disintegration of complex particulates
f_li_xc	dUnit/dUnit	0.3	Yield of lipids from disintegration of complex particulates
N_aa	mole-N/g COD	0.007067	Nitrogen content of amino acids
N_SI	mole-N/g COD	0.004143	Nitrogen content of soluble inert
N_Xc	mole-N/g COD	0.002211	Nitrogen content of degradable particulates
N_XI	mole-N/g COD	0.004143	Nitrogen content of particulate inert COD

3.4 MCN transformer ADM1- ASM1

Parameter	Unit	Value	Definition
i_X_e	gN/gCOD	0.04	Mass of nitrogen per mass of COD in products formed and inert particulates(ASM1)
N_aa	mole-N/g COD	0.007067	Nitrogen content of amino acids
N_biom	mole-N/g COD	0.006156	Nitrogen content of biomass
N_SI	mole-N/g COD	0.004143	Nitrogen content of soluble inert
N_Xc	mole-N/g COD	0.002211	Nitrogen content of degradable particulates
N_XI	mole-N/g COD	0.004143	Nitrogen content of particulate inert COD

3.5 CBIM transformer ASM1- ADM1

Parameter	Unit	Value	Definition
f_Xbh_Xsu	-	0.1	Fraction of X_bh that are fermenters
f_X_I	-	0.1	Fraction of X_I and X_p (ASM1) that becomes biodegradable under anaerobic conditions
Y_H	-	0.67	Yield for heterotrophic biomass

3.6 CBIM transformer ADM1- ASM1

"No parameters are needed for this transformer"

Appendix 4 *Symbolic derivation of the Kapp titrimetric method*

Instead of the determination of the linear regression model parameters of the Kapp method experimentally, the following functions can be used to evaluate them mathematically for known experimental conditions (see chapter 12)

```
 VFA=a(V_pH4-V_pH3) + b(V_pH2-V_pH1) + c

 bicarbonate=a1(V_pH2-V_pH1) + b1(V_pH4-V_pH3) + c1

where:

- pHi's: are the  pH-end points defined for Kapp method
 during the down titration
- Hi's are the corresponding proton concentrations respectively.
- Na: acid normality
- Vs: the sample volume
- V_pHi: the acid volume added to reach pHi
- Z: total cation concentration = total alkalinity
- Khco: bicarbonate acidity constant
- Kac: acetate acidity constant

Notes: all concentrations are in moles/(volume unit),
    all volumes should have the same units,
    carbon system is considered as bicarbonate only,
    b and a1 are usually negative for the proper selection of pHi's.


 For VFA

 a=
 /         Vs Khco                  Vs Khco       \   / /
 |- --------------------- + ----------------------|  /  |
 \  (Na - H2) (H2 + Khco)   (Na - H1) (H1 + Khco)/ /   \

       /       Vs Kac                  Vs Kac       \
       |-------------------- - --------------------|
       \(Na - H2) (H2 + Kac)   (Na - H1) (H1 + Kac)/

       /         Vs Khco                  Vs Khco       \
       |- --------------------- + ----------------------| +
       \  (Na - H4) (H4 + Khco)   (Na - H3) (H3 + Khco)/

       /         Vs Khco                  Vs Khco       \
       |- --------------------- + ----------------------|
       \  (Na - H2) (H2 + Khco)   (Na - H1) (H1 + Khco)/

       /         Vs Kac                  Vs Kac       \\
       |- -------------------- + --------------------||
       \  (Na - H4) (H4 + Kac)   (Na - H3) (H3 + Kac)//
```

b=

$$
\left|\frac{Vs\ Khco}{(Na - H4)\ (H4 + Khco)} - \frac{Vs\ Khco}{(Na - H3)\ (H3 + Khco)}\right|\ \left|\frac{}{}\right|
$$

$$
\left|\frac{Vs\ Kac}{(Na - H2)\ (H2 + Kac)} - \frac{Vs\ Kac}{(Na - H1)\ (H1 + Kac)}\right|
$$

$$
\left|\frac{Vs\ Khco}{(Na - H4)\ (H4 + Khco)} + \frac{Vs\ Khco}{(Na - H3)\ (H3 + Khco)}\right| +
$$

$$
\left|\frac{Vs\ Khco}{(Na - H2)\ (H2 + Khco)} + \frac{Vs\ Khco}{(Na - H1)\ (H1 + Khco)}\right|
$$

$$
\left|\frac{Vs\ Kac}{(Na - H4)\ (H4 + Kac)} + \frac{Vs\ Kac}{(Na - H3)\ (H3 + Kac)}\right|\left|\frac{}{}\right|
$$

c=

$$
\left|\frac{Vs\ Khco}{(Na - H4)\ (H4 + Khco)} + \frac{Vs\ Khco}{(Na - H3)\ (H3 + Khco)}\right|
$$

$$
\left|\frac{Vs\ (H2 + Z)}{Na - H2} - \frac{Vs\ (H1 + Z)}{Na - H1}\right| - \left|\frac{Vs\ (H4 + Z)}{Na - H4} - \frac{Vs\ (H3 + Z)}{Na - H3}\right|
$$

$$
\left|\frac{Vs\ Khco}{(Na - H2)\ (H2 + Khco)} + \frac{Vs\ Khco}{(Na - H1)\ (H1 + Khco)}\right|\left|\frac{}{}\right|
$$

$$
\left|\frac{Vs\ Kac}{(Na - H2)\ (H2 + Kac)} - \frac{Vs\ Kac}{(Na - H1)\ (H1 + Kac)}\right|
$$

$$
\left|\frac{Vs\ Khco}{(Na - H4)\ (H4 + Khco)} + \frac{Vs\ Khco}{(Na - H3)\ (H3 + Khco)}\right| +
$$

$$
\left|\frac{Vs\ Khco}{(Na - H2)\ (H2 + Khco)} + \frac{Vs\ Khco}{(Na - H1)\ (H1 + Khco)}\right|
$$

$$
\left|\frac{Vs\ Kac}{(Na - H4)\ (H4 + Kac)} + \frac{Vs\ Kac}{(Na - H3)\ (H3 + Kac)}\right|\left|\frac{}{}\right|
$$

For bicarbonate:

a1=

$$\left|\frac{\partial Vs\,Kac}{(Na - H4)\,(H4 + Kac)} + \frac{\partial Vs\,Kac}{(Na - H3)\,(H3 + Kac)}\right| \left|\frac{\partial Vs\,Kac}{(Na - H2)\,(H2 + Kac)} - \frac{\partial Vs\,Kac}{(Na - H1)\,(H1 + Kac)}\right| + \left|\frac{\partial Vs\,Khco}{(Na - H4)\,(H4 + Khco)} + \frac{\partial Vs\,Khco}{(Na - H3)\,(H3 + Khco)}\right| \left|\frac{\partial Vs\,Khco}{(Na - H2)\,(H2 + Khco)} + \frac{\partial Vs\,Kac}{(Na - H1)\,(H1 + Khco)}\right| \left|\frac{\partial Vs\,Kac}{(Na - H4)\,(H4 + Kac)} + \frac{\partial Vs\,Kac}{(Na - H3)\,(H3 + Kac)}\right|$$

b1=

$$\left|\frac{\partial Vs\,Kac}{(Na - H2)\,(H2 + Kac)} - \frac{\partial Vs\,Kac}{(Na - H1)\,(H1 + Kac)}\right| \left|\frac{\partial Vs\,Kac}{(Na - H2)\,(H2 + Kac)} - \frac{\partial Vs\,Kac}{(Na - H1)\,(H1 + Kac)}\right| + \left|\frac{\partial Vs\,Khco}{(Na - H4)\,(H4 + Khco)} + \frac{\partial Vs\,Khco}{(Na - H3)\,(H3 + Khco)}\right| \left|\frac{\partial Vs\,Khco}{(Na - H2)\,(H2 + Khco)} + \frac{\partial Vs\,Kac}{(Na - H1)\,(H1 + Khco)}\right| \left|\frac{\partial Vs\,Kac}{(Na - H4)\,(H4 + Kac)} + \frac{\partial Vs\,Kac}{(Na - H3)\,(H3 + Kac)}\right|$$

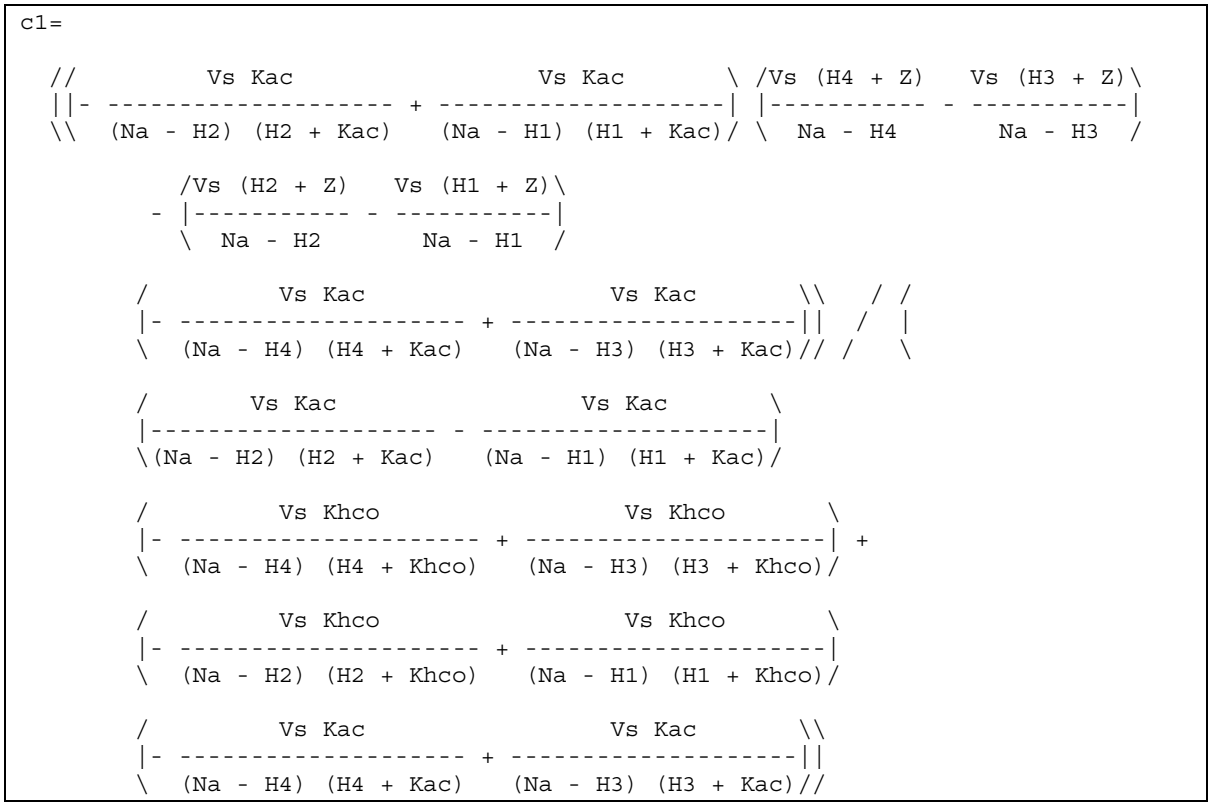
c1=
Vs Kac
(Na - H2) (H2 + Kac)
Vs Kac
(Na - H1) (H1 + Kac)
Vs (H4 + Z)
Na - H4
Vs (H3 + Z)
Na - H3
Vs (H2 + Z)
Na - H2
Vs (H1 + Z)
Na - H1
Vs Kac
(Na - H4) (H4 + Kac)
Vs Kac
(Na - H3) (H3 + Kac)
Vs Kac
(Na - H2) (H2 + Kac)
Vs Kac
(Na - H1) (H1 + Kac)
Vs Khco
(Na - H4) (H4 + Khco)
Vs Khco
(Na - H3) (H3 + Khco)
Vs Khco
(Na - H2) (H2 + Khco)
Vs Khco
(Na - H1) (H1 + Khco)
Vs Kac
(Na - H4) (H4 + Kac)
Vs Kac
(Na - H3) (H3 + Kac)

References

References

Ahn Y.H., Bae J.Y., Park S.M. and Min K.S. (2004) Anaerobic digestion elutriated phased treatment of piggery waste, Water Science and Technology, 49, 181-189.

Aiyuk S. and Verstraete W. (2004) Sedimentological evolution in an UASB treating SYNTHES, a new representative synthetic sewage, at low loading rates, Bioresource Technology, 93, 269-278.

Akcil A., Karahan A.G., Ciftci H. and Sagdic O. (2003) Biological treatment of cyanide by natural isolated bacteria (*Pseudomonas sp.*), Minerals Engineering, 16, 643-649.

Alcaraz-Gonzalez V., Harmand J., Rapaport A., Steyer J.P., Gonzalez-Alvarez V. and Pelayo-Ortiz C. (2002) Software sensors for highly uncertain WWTPs: a new approach based on interval observers, Water Research, 36, 2515-2524.

Almeida C.M.N.V., Lapa R.A.S. and Lima J.L.F.C. (2001) Automatic flow titrator based on a multicommutated unsegmented flow system for alkalinity monitoring in wastewaters. Analytica Chimica Acta, 438, 291-298.

American Society for Testing and Materials (1999) Standard Methods for Acidity or Alkalinity of Water, Copyright by American Public Health Association, American Water Works Association and Water Environment Federation.

Anderson G. H. and Yang G. (1992) Determination of bicarbonate and total volatile acid concentration in anaerobic digesters using a simple titration. Water Environment Research, 64, 53-59.

Annachhatre A.P. and Amornkaew A. (2001) Upflow anaerobic sludge blanket treatment of starch wastewater containing cyanide, Water Environment Research, 73, 622-632.

Atuanya E.I. and Aigbirior M. (2002) Mesophilic biomethanation and treatment of poultry waste-water using pilot scale UASB reactor, Environmental Monitoring and Assessment, 77, 139-147.

Banister S.S. and Pretorius W.A. (1998) Optimisation of primary sludge acidogenic fermentation for biological nutrient removal, Water SA, 24, 35-41.

Barber W.P. and Stuckey D.C. (1999) The use of the anaerobic baffled reactor (ABR) for wastewater treatment: a review, Water Research, 33, 1559-1578.

Bastin G. and Dochain D. (1990) On-line Estimation and Adaptive Control of Bioreactors, ELSEVIER, Amsterdam, The Netherlands, pp. 379.

Batstone D.J., Keller J., Angelidaki R.I., Kalyuzhnyi S.V., Pavlostathis S.G., Rozzi A., Sanders W.T.M., Siegrist H. and Vavilin V.A. (2002) Anaerobic Digestion Model no1, IWA publishing, London, UK, pp.77.

Batstone D.J., Keller J., Newell R.B. and Newland M. (2000[a]) Modelling anaerobic degradation of complex wastewater. I: Model development, Bioresource Technology, 75, 67-74.

Batstone D.J., Keller J., Newell R.B. and Newland M. (2000[b]) Modelling anaerobic degradation of complex wastewater. II: Parameter estimation and validation using slaughterhouse effluent, Bioresource Technology, 75, 75-85.

Benedetti L., Meirlaen J. and Vanrolleghem P. A. (2004) Model connectors for integrated simulations of urban wastewater systems. In: Sewer Networks and Processes within Urban Water Systems. J.-L. Bertrand-Krajewski, M. Almeida, J. Matos and S. Abdul-Talib (eds.), Water Environment Management Series (WEMS), IWA Publishing, London, UK, 13-21.

Bernard O. (2002) Design of models for normal working conditions, Technical report, TELEMAC IST 2000-28156, "Telemonitoring and Advanced Telecontrol of High-Yield Wastewater Treatment", Deliverable D3.1a.

Bernard O., Chachuat B., Hélias A., Le Dantec B., Sialve B., Steyer J.-P., Lardon L., Neveu P., Lambert S., Ratini P., Frattesi S., Lema J., Roca E., Ruiz G., Rodriguez J., Franco A., Vanrolleghem P., Zaher U., De Pauw D.J.W., De Neve K., Lievens K., Dochain D., Schoefs O., Fibrianto H., Farina R., Alcaraz Gonzalez V., Gonzalez Alvarez V., Lemaire P., Martinez J.A., Duclaud O. and Lavigne J.F. (2005) TELEMAC: an integrated system to remote monitor and control anaerobic wastewater treatment plants through the internet, Water Science and Technology (in press).

Bernard O., Hadj-Sadok Z., Dochain D., Genovesi A. and Steyer J.P. (2001) Dynamical model development and parameter identification for an anaerobic wastewater treatment process, Biotechnology and Bioengineering, 75, 424-438.

Bernard O., Polit M., Hadj-Sadok Z., Pengov M., Dochain D., Estaben M. and Labat P. (2001) Advanced monitoring and control of anaerobic wastewater treatment plants: software sensors and controllers for an anaerobic digester, Water Science and Technology, 43, 175-182.

Björnsson L., Murto M., Jantsch T.G. and Mattiasson B. (2001) Evaluation of new methods for the monitoring of alkalinity, dissolved hydrogen and the microbial community in anaerobic digestion, Water Research, 35, 2833-2840.

Bogaert H., Vanderhasselt A., Gernaey K., Yuan Z., Thoeye C. and Verstraete W. (1997) New sensor based on pH effects of denitrification process. Journal of Environmental Engineering, 123, 884-891.

Bonastre N. and Paris J.M. (1989) Survey of laboratory, pilot and industrial anaerobic filter installation, Process Biochemistry, 24, 15-20.

Borja R., Sanchez E. and Weiland P. (1996) Influence of ammonia concentration on thermophilic anaerobic digestion of cattle manure in upflow anaerobic sludge blanket (UASB) reactors, Process Biochemistry, 31, 477-483.

Bouallagui H., Touhami Y., Ben Cheikh R. and Hamdi M. (2005) Bioreactor performance in anaerobic digestion of fruit and vegetable wastes, Process Biochemistry, 40, 989-995.

Bouvier J.C., Steyer J.P. and Delgenes J.P. (2002) On-line titrimetric sensor for the control of VFA and/or alkalinity in anaerobic digestion processes treating industrial vinasses, In: Proceedings of VII Latin American Workshop and Symposium on Anaerobic digestion, Merida, Mexico, October 23-25, 2001, 65-68.

Bozzi A., Guasaquillo I. and Kiwi J. (2004) Accelerated removal of cyanides from industrial effluents by supported TiO2 photo-catalysts, Applied Catalysis B: Environmental, 51, 203-211.

Brent R.P. (1973) Algorithms for minimization without derivatives, Prentice-Hall, Englewood Cliffs, New Jersey, pp. 195.

Buchauer K (1998) A comparison of two simple titration procedures to determine volatile fatty acids in influents to waste-water and sludge treatment processes, Water SA, 24, 49-56.

Buswell E.G. and Neave S.L. (1930) Laboratory studies of sludge digestion, State of Illinois, Division of State Water Survey, Bulletin No. 30.

Butler D. and Schütze M. (2005) Integrating simulation models with a view to optimal control of urban wastewater systems, Environmental Modelling & Software, 20(4), 15-426.

Castillo E. D. (2002) Statistical Process Adjustment for Quality Control, Wiley Publishers, pp. 357.

Chachuat B. and Bernard O. (2004) Design of probabilistic observers for mass-balance based bioprocess models, In: 9th International Symposium on Computer Applications in Biotechnology (CAB9), Nancy, France, March 28-31, 2004.

Chiang L.H. and Braatz R.D. (2003) Process monitoring using causal map and multivariate statistics: fault detection and identification, Chemometrics and Intelligent Laboratory Systems, 65, 159-178.

Cho J.-H., Lee J.-M., Wook Choi S., Lee D. and Lee I.-B. (2005) Fault identification for process monitoring using kernel principal component analysis, Chemical Engineering Science, 60, 279-288.

Choi S.W. and Lee I.-B. (2004) Nonlinear dynamic process monitoring based on dynamic kernel PCA, Chemical Engineering Science, 59, 5897-5908.

Choi S.W., Lee C., Lee J.-M., Park J.H. and Lee I.-B. (2005) Fault detection and identification of nonlinear processes based on kernel PCA, Chemometrics and Intelligent Laboratory Systems, 75, 55-67.

Chu L.-B., Yang F.-L. and Zhang X.-W. (2005) Anaerobic treatment of domestic wastewater in a membrane-coupled expended granular sludge bed (EGSB) reactor under moderate to low temperature, Process Biochemistry, 40, 1063-1070.

Cinar S., Onay T.T. and Erdincler A. (2004) Co-disposal alternatives of various municipal wastewater treatment-plant sludges with refuse, Advances in Environmental Research, 8, 477-482.

Copp J. (ed) (2002) The COST Simulation Benchmark – Description and Simulator Manual, Office for Official Publications of the European Communities, Luxembourg.

Copp J., Jeppsson U. and Rosen C. (2003) Towards an ASM1-ADM1 state variable interface for plant-wide wastewater treatment modelling. In: Proceedings 76th Annual WEF Conference and Exposition, Los Angeles, USA, October 11-15, 2003. (on CD-ROM).

Costello D.J., Greenfield P.F. and Lee P.L. (1991) Dynamic modelling of a single-stage high-rate anaerobic reactor. II. Model verification, Water Research, 25, 859-871.

Cuzin N. and Labat M. (1992) Reduction of cyanide levels during anaerobic digestion of cassava, International Journal of Food Science and Technology, 27, 329-336.

Dague R.R., Banik G.C., and Ellis T.G. (1997) ASBR treatment of dilute wastewater at psychrophilic temperatures, Water Environment Research, 70, 155-160.

De Gracia M., Sancho L., García-Heras J.L., Vanrolleghem P.A. and Ayesa E. (2004) Mass and charge conservation check in dynamic models: Application to the new ADM1 model. In: Proceedings of the 6th IWA International Symposium on Systems Analysis & Integrated Assessment (Watermatex 2004). Beijing, China, November 3-5, 2004, 2, 335-345.

De Neve K. and Lievens K. (2004). On-line analyser solves monitoring problem in bio-digester. Water & Wastewater International, 19, 28.

De Neve K., Lievens K., Steyer J.-P. and Vanrolleghem P.A. (2004) Development of an on-line titrimetric analyser for the determination of volatile fatty acids, bicarbonate, and alkalinity. In: Proceedings of the 10th World Congress on Anaerobic Digestion (AD10), Montreal, Canada, August 29 - September 2, 2004, 3, 1316-1318.

De Pauw D.J.W. and Vanrolleghem P.A. (2003) Practical aspects of sensitivity analysis for dynamic models. In: Proceedings IMACS 4th MATHMOD Conference, Vienna, Austria, February 5-7, 2003.

Deutsche Einheitsverfahren (1971) Deutsche Einheitsverfahren zur Wasser, Abwasser und Schlammuntersuchung. DEV H21, Bestimmung der mit Wasserdampf flüchtigen organischen Säuren,1-2.

Devisscher M., Bogaert H., Gernaey K. and Verstraete W. (1998) Use of bubbleless aeration to improve the performance of titrimetric sensors for the study of denitrification processes. In: Proceedings Conference on New Advances in Biological Nitrogen and Phosphorus Removal Plants for Municipal or (Agro)Industrial Wastewaters, Narbonne, France, October 12-14, 215-222.

Di Pinto A., Limoni N., Pasión R., Rozzi A. and Tomei M. (1990) Anaerobic process control by automated bicarbonate monitoring, In: Instrumentation, Control and Automation of Water and Wastewater Treatment and Transport Systems (Advances in Water Pollution Control 10). Briggs R. (ed.), Pergamon Press, London, UK, pp. 51-58.

Dochain D. (2003) State and parameter estimation in chemical and biochemical processes: a tutorial, Journal of Process Control, 13, 801-818.

Dochain D. and Vanrolleghem P.A. (2001) Dynamical Modelling and Estimation in Wastewater Treatment Processes. IWA Publishing, London, UK, pp. 342.

Ehlinger F., Escoffier Y., Couderc J.P., Leyris J.P. and Moletta R. (1994) Development of an automatic control system for monitoring an anaerobic fluidized-bed, Water Science and Technology, 29, 289–295.

Ergon R. (2004) Informative PLS score-loading plots for process understanding and monitoring, Journal of Process Control, 14, 889-897.

Fallon R.D. (1992) Evidence of a Hydrolytic route for anaerobic cyanide degradation, Applied and Environmental Microbiology, 58, 3163-3164.

Fallon R.D., Cooper D.A., Speece R. and Henson M. (1991) Anaerobic biodegradation of cyanide under methanogenic conditions, Applied and Environmental Microbiology, 57, 1656-1662.

Fang H.H.P. and Zhang T. (2004) Microbial Characteristics of a Methanogenic Phenol-Degrading Sludge. In: Proceedings of the 10th World Congress on Anaerobic Digestion (AD10), Montreal, Canada, August 29 - September 2, 2004, 1, 161-166.

Feitkenhauer H., von Sachs J. and Meyer U. (2002) On-line titration of volatile fatty acids for the process control of anaerobic digestion plants, Water Research, 36, 212-218.

Fernandez J.M., Mendez R. and Lema J.M. (1995) Anaerobic treatment of eucalyptus fibreboard manufacturing wastewater by a hybrid USBF lab-scale reactor, Environmental Technology, 16, 677-684.

Ficara E., Rocco A. and Rozzi A. (2000) Determination of nitrification kinetics by the ANITA-DOstat biosensor. Water Science and Technology, 41(12), 121-128.

Garcia-Encina P.A. and Hidalgo M.D. (2005) Influence of substrate feed patterns on biofilm development in anaerobic fluidized bed reactors (AFBR), Process Biochemistry, 40(7), 2509-2516.

Gernaey K., Bogaert H., Vanrolleghem P.A., Massone A., Rozzi A. and Verstraete W. (1998) A titration technique for on-line nitrification monitoring in activated sludge. Water Science and Technology, 37(12), 103-110.

Gernaey K., Petersen B., Ottoy J.-P. and Vanrolleghem P.A. (2001) Activated sludge monitoring with combined respirometric-titrimetric measurements. Water Research, 35, 1280-1294.

Gijzen H.J., Bernal E. and Ferrer H. (2000) Cyanide toxicity and cyanide degradation in anaerobic wastewater treatment, Water Research, 34, 2447-2454.

Guiot S.R., Arcand Y. and Chavarie C. (1992) Advantages of fluidization on granule size and activity development in upflow anaerobic sludge bed reactors, Water Science and Technology, 26, 897–906.

Gujer W., Henze M., Mino T. and van Loosdrecht M.C.M. (1999) Activated Sludge Model No. 3, Water Science and Technology, 39, 183-193.

Guwy A., Hawkes D., Hawkes F. and Rozzi A. (1994) Characterization of a prototype industrial on-line analyzer for bicarbonate/carbonate monitoring, Biotechnology and Bioengineering, 44, 1325-1330.

Hamming R.W. (1983) Digital filters, 2nd ed., Englewood Cliffs, NJ: Prentice-Hall, pp. 257.

Hawkes F., Guwy A., Hawkes D. and Rozzi A. (1994) On-line monitoring of anaerobic digestion: application of a device for continuous measurement of bicarbonate alkalinity, Water Science and Technology, 30, 1-10.

Hawkes F., Guwy A., Rozzi A. and Hawkes D. (1993) A new instrument for on-line measurement of bicarbonate alkalinity, Water Research, 27, 167-170.

Heijnen J.J., Mulder A., Enger W. and Hoeks F. (1989) Review on the application of anaerobic fluidized bed reactors in wastewater treatment, the Chemical Engineering Journal, 41(3), B37-B50.

Hellinga C., van Loosdrecht M.C.M. and Heijnen J.J. (1999) Model based design of a novel process for nitrogen removal from concentrated flows. Mathematical and Computer Modelling of Dynamical Systems, 5, 351-371.

Henze M., Grady Jr C.P.L., Gujer W., Marais G.v.R. and Matsuo T. (1987) Activated Sludge Model No.1. IAWQ Scientific and Technical Report no. 1, IWA Publishing, London, UK.

Henze M., Gujer W., Mino T., and van Loosdrecht M.C.M (2000) Activated Sludge Models: ASM1, ASM2, ASM2d and ASM3. Scientific and Technical Report No:9, IWA Publishing, London, UK.

Hickey R.F., Vanderwielen J. and Switzenbaum M.S. (1989) The effect of heavy metals on methane production and hydrogen and carbon monoxide levels during batch anaerobic sludge digestion, Water Research, 23, 207-218.

Hidalgo M.D. and Garcia-Encina P.A. (2002) Biofilm development and bed segregation in a methanogenic fluidized bed reactor, Water Research, 36, 3083-3091.

Hoh C.Y. and Cord-Ruwisch R. (1996) A practical kinetic model that considers end product inhibition in anaerobic digestion processes by including the equilibrium constant, Biotechnology and Bioengineering, 51, 597-604.

Hulshoff Pol. L. (2002) Waste characteristics and factors affecting reactor performance. In: van Der Steen, P. (ed.) International Course on Anaerobic Treatment of Industrial Wastewater, Wageningen Agriculture University and IHE-Delft, Delft and Wageningen, The Netherlands, June 10-21, 2002.

Ince O., Anderson G.K. and Kasapgil B. (1997) Composition of the microbial population in a membrane anaerobic reactor system during start-up, Water Research, 31, 1-10.

Isa Z., Grusenmeyer S. and Verstraete W. (1986) Sulfate reduction relative to methane production in high-rate anaerobic digestion: Technical aspects, Applied and Environmental Microbiology, 51, 572-579.

Isik M. (2004) Efficiency of simulated textile wastewater decolorization process based on the methanogenic activity of upflow anaerobic sludge blanket reactor in salt inhibition condition, Enzyme and Microbial Technology, 35, 399-404.

Jawed M. and Tare V. (1999) Microbial composition assessment of anaerobic biomass through methanogenic activity tests, Water SA, 25, 345-350.

Jeppsson U., Rosen C., Alex J., Copp J., Gernaey K.V., Pons M.-N. and Vanrolleghem P.A. (2004) Towards a benchmark simulation model for plant-wide control strategy performance evaluation of WWTPs, In: Proceedings of the 6th IWA International Symposium on Systems Analysis & Integrated Assessment (Watermatex 2004), Beijing, China, November 3-5, 2004, 1, 285-293.

Jetten M.S.M., Strous M., Schoonen K.T., Schalk J., van Dongen L.G.J.M., van De Graaf, A.A., Logemann S., Muyzer G., van Loosdrecht M.C.M. and Kuenen J.G. (1999) The anaerobic oxidation of ammonium. FEMS Microbiology Reviews, 22, 421-437.

Jordening H.-J. and Winter J. (2004) Environmental Biotechnology: Concepts and Applications, Wiley Publishers, ISBN 3-527-30585-8.

Kalyuzhnyi, S. and Fedorovich, V. (1998) Mathematical modelling of competition between sulphate reduction and methanogenesis in anaerobic reactors, Bioresource Technology, 65, 227–242.

Kapp H. (1984) Schlammfaulung mit hohem Feststoffgehalt. Stuttgarter Berichte zur Siedlungswasserwirtschaft, Band86, OldenbourgVerlag, München, pp. 300.

Kapp H. (1992) On-line messung der organischen saüren, Korrespondenz Abwasser, 39(7), 999-1004.

Kennedy K.J. and Droste R.L. (1991) Anaerobic treatment in downflow stationary fixed film reactors, Water Science and Technology, 24(8), 157-177.

Khoa L.V. (1998) Industrial Environmental Management: A Case of the Tapioca Starch Industry in Vietnam, MSc. Thesis, UNESCO-IHE, Delft, The Netherlands.

Knezevic Z., Mavinic D.S. and Anderson B.C. (1995) Pilot scale evaluation of anaerobic codigestion of primary and pretreated waste activated sludge, Water Environment Research, 67, 835-841.

Koster I.W. and Lettinga G. (1988) Anaerobic digestion at extreme ammonia concentrations, Biological Wastes, 25, 51-59.

Koster I.W., Rinzema A., de Vegt A.L. and Lettinga G. (1986) Sulfide inhibition of the methanogenic activity of granular sludge at various pH-levels, Water Research, 20, 1561-1567.

Kugelman I.J. and Mc Carty P.L. (1965) Cation toxicity and stimulation in anaerobic waste treatment, Water Pollution Control, 37, 97-116.

Lahav O. and Loewenthal R.E. (2000) Measurement of VFA in anaerobic Digestion: The five-point titration method revisited, Water SA, 26 , 389-392.

Lahav O., Shlafman E., Morgan B.E., Loewenthal R.E. and Tarre S. (2002) Accurate on-site volatile fatty acids (VFA) measurement in anaerobic digestion – varification of new titrative method, In: proceeding of VII Latin American Workshop and Symposium on Anaerobic Digestion, Merida, Mexico, October 23-25, 2001, 118-125.

Lalman J.A. and Bagley D.M. (2000) Anaerobic degradation and inhibitory effects of linoleic acid, Water Research, 34, 4220-4228.

Lalman J.A. and Bagley D.M. (2001) Anaerobic degradation and methanogenic inhibitory effects of oleic and stearic acids, Water Research, 35, 2975-2983.

Lalman J.A. and Bagley D.M. (2002) Effects of C18 long chain fatty acids on glucose, butyrate and hydrogen degradation, Water Research, 36, 3307-3313.

Lardon L. and Steyer J.P. (2003) Using evidence theory for diagnosis of sensors networks: application to a wastewater treatment process. In: 18th International Joint Conference on Artificial Intelligence (IJCAI'2003) and Workshop on Environmental Decision Support Systems (EDSS'03), Acapulco, Mexico, August 9-15, 2003.

Lardon L., Punal A. and Steyer J.-P. (2004) On-line diagnosis and uncertainty management using evidence theory-experimental illustration to anaerobic digestion processes, Journal of Process Control, 14, 747-763.

Lee C.k., Choi S.W. and Lee I.-B. (2004) Sensor fault identification based on time-lagged PCA in dynamic processes, Chemometrics and Intelligent Laboratory Systems, 70, 165-178.

Lee D.S., Park J.M. and Vanrolleghem P.A. (2005) Adaptive multiscale principal component analysis for on-line monitoring of a sequencing batch reactor, Journal of Biotechnology, 116, 195-210.

Lee J.-M., Yoo C.K. and Lee I.-B. (2004) Fault detection of batch processes using multiway kernel principal component analysis, Computers & Chemical Engineering, 28, 1837-1847.

Lee J.-M., Yoo C.K., Choi S.W., Vanrolleghem P.A. and Lee I.-B. (2004) Nonlinear process monitoring using kernel principal component analysis, Chemical Engineering Science, 59, 223-234.

Lettinga G., van Velsen A.F.M., Hobma S.W., De Zeeuw W. and Klapwijk A. (1980) Use of the upflow blanket (UASB) reactor concept for biological wastewater treatment, specially for anaerobic treatment, Biotechnology and Bioengineering, 22, 699-734.

Lin C.-Y. (1993) Effect of heavy metals on acidogenesis in anaerobic digestion, Water Research, 27, 147-152.

Lin C.-Y. and Chen C.-C. (1999) Effect of heavy metals on the methanogenic UASB granule, Water Research, 33, 409-416.

Lin J.-G., Chang C.-N. and Chang S.-C. (1997) Enhancement of anaerobic digestion of waste activated sludge by alkaline solubilization, Bioresource Technology, 62, 85-90.

Ljung L. (1999) System Identification: Theory for the User, 2nd edition, Prentice Hall, Englewood Cliffs, New Jersey, pp. 519.

Lomas J.M., Urbano C. and Camarero L.M. (1999) Evaluation of a pilot scale downflow stationary fixed film anaerobic reactor treating piggery slurry in the mesophilic range, Biomass and Bioenergy, 17, 49-58.

Lomas J.M., Urbano C. and Camarero L.M. (2000) Influence of recirculation flow in a pilot scale downflow stationary fixed film anaerobic reactor treating piggery slurry, Biomass and Bioenergy, 18, 421-430.

Lubberding H. J. (2002) International Course on Organic Chemistry, IHE-Delft, Delft, The Netherlands.

Mailleret L., Bernard O. and Steyer J.-P. (2003) Robust regulation of anaerobic digestion processes, Water Science and Technology, 48(6), 87-94.

Mailleret L., Bernard O. and Steyer J.-P. (2004) Robust nonlinear adaptive control for bioreactors with unknown kinetics, Automatica, 40(8), 365-383.

Masse L. and Masse D.I. (2005) Effect of soluble organic, particulate organic, and hydraulic shock loads on anaerobic sequencing batch reactors treating slaughterhouse wastewater at 20 °C, Process Biochemistry, 40, 1225-1232.

Masse L., Kennedy K.J. and Chou S. (2001) Testing of alkaline and enzymatic hydrolysis pretreatments for fat particles in slaughterhouse wastewater, Bioresource Technology, 77, 145-155.

Massone A., Gernaey K., Bogaert H., Vanderhasselt A., Rozzi A. and Verstraete W. (1996[a]), Biosensors for nitrogen control in wastewaters. Water Science and Technology, 34, 213 –220.

Massone A., Antonelli M and Rozzi A. (1996[b]) The Denicon: A novel biosensor to control denitrification in biological wastewater treatment plants. Med. Fac. Landbouww. Univ. Gent, 61, 1709 – 1714.

Mathews C.K., van Holde K.E. and Ahern K.G. (2000) Biochemistry, 3rd Edition, (Benjamin Cummings), Oregon State Univ., Corvallis, Oregon, USA. ISBN 0-8053-3066-6.

McGhee T.J. (1968) A method for approximation of the volatile acid concentrations in anaerobic digesters, Water & Sewage Works, 115, 162-166.

Mehra R.K. (1974) Optimal input signal for parameter estimation in dynamic systems - survey and new results, IEEE Transactions on Automatic Control, 19, 753-768.

Meirlaen J., Huyghebaert B., Sforzi F., Benedetti L. and Vanrolleghem P.A. (2001) Fast simultaneous simulation of the integrated urban wastewater system using mechanistic surrogate models, Water Science and Technology, 43, 301-310.

Misra M., Yue H.H., Qin S.J. and Ling C. (2002) Multivariate process monitoring and fault diagnosis by multi-scale PCA, Computers & Chemical Engineering, 26, 1281-1293.

Montgomery H., Dymock J.f. and Thom N.S. (1962) The rapid colorimetric determination of organic acids and their salts in sewage sludge liquor, The Analyst, 87, 947-952.

Moosbrugger R.E., Wentzel M.C., Loewenthal R.E., Ekama G.E. and Marais G.v.R. (1993) Alkalinity measurement: Part 3 - a 5 pH point titration method to determine the carbonate and SCFA weak acid/bases in aqueous solution containing also known concentrations of other weak acid/bases, Water SA, 19, 29-40.

Moosbrugger R.E., Wentzel M.C., Loewenthal R.E., Ekama G.E. and Marais G.v.R. (1992) Simple Titration Procedures To Determine H_2CO_3 Alkalinity And Short-chain Fatty Acids In Aqueous Solutions Containing Known Concentrations Of Ammonium, Phosphate And Sulphide Weak Acid/Bases. WRC Report No. TT 57/92, UCT Research Report W 74.

Mosey F.E. (1983) Mathematical modelling of the anaerobic digestion process: Regulatory mechanisms for the formation of short-chain volatile acids from glucose, Water Science and Technology, 15, 209-232.

Nelder J.A. and Mead R. (1965) A simplex method for function minimization, Computer Journal, 7, 308-313.

Noike T., Endo G., Chang J.E., Yaguchi J.-I and. Matsumoto J.-I. (1985) Characteristics of carbohydrate degradation and the rate-limiting step in anaerobic digestion, Biotechnology and Bioengineering, 27(10), 1482-1489.

Novaes R.F.V. (1986) Microbiology of anaerobic digestion, Water Science and Technology, 18, 1-14.

Olsson G. and Newell B. (1999) Wastewater Treatment Systems - Modelling, Diagnosis and Control, IWA Publishing, pp 742.

Orfanidis S.J. (1996) Introduction to Signal Processing, Chapter 8, Sec 8.2, pp. 355-383, Prentice-Hall, Englewood Cliffs, NJ.

Petersen B., Gernaey K. and Vanrolleghem P.A. (2000) Improved theoretical identifiability of model parameters by combined respirometric - titrimetric measurements, a generalization of results. In: Proceedings IMACS 3rd Symposium on Mathematical Modeling, Vienna University of Technology, Austria, February 2-4, 2000, 2, 639 – 642.

Petersen B., Gernaey K. and Vanrolleghem P.A. (2001) Practical identifiability of model parameters by combined respirometric - titrimetric measurements, Water Science and Technology, 43, 347-356.

Petersen B., Gernaey K. and Vanrolleghem P.A. (2002) Anoxic activated sludge monitoring with combined nitrate and titrimetric measurements. Water Science and Technology, 45, 181-190.

Petzold L. (1983) A description of DASSL: A differential/algebraic system solver. In: Stepleman, R.E., (ed), Scientific Computing, IMACS / North-Holland, Amsterdam, 65-68.

Pind P.F., Angelidaki I. and Ahring B.K. (2001) A novel in-situ sampling and VFA sensor technique for anaerobic systems. In: Proceedings 9th World Conference on Anaerobic Digestion, AD 2001, Antwerpen, Belgium, September 2-6, 2001, 315-320.

Puñal A., Palazzotto L., Bouvier J.C., Conte T. and Steyer J.P. (2002) Automatic control of VFA in anaerobic digestion using a fuzzy logic based approach. In: Proceedings 7th Latin American Workshop and Symposium on Anaerobic Digestion, Merida, Mexico, October 22-25, 2002. 1, 126-133.

Puñal A., Palazzotto L., Bouvier J.C., Conte T., Steyer J.-P. and Delgenes J.-P. (2003) Automatic control of VFA in anaerobic digestion using a fuzzy logic based approach, Water Science and Technology, 48, 103-110.

Punal A., Roca E. and Lema J.M. (2002) An expert system for monitoring and diagnosis of anaerobic wastewater treatment plants, Water Research, 36, 2656-2666.

Rabitz H., Kramer M. and Dacol D. (1983), Sensitivity analysis in chemical kinetics, Annual Review of Physical Chemistry, 34, 419-461.

Rajan R.V., Lin J.G. and Ray B.T. (1989) Low-level chemical pretreatment for enhanced sludge solubilization, Research Journal of the Water Pollution Control Federation, 61, 1678-1683.

Rajeshwari K.V., Balakrishnan M., Kansal A., Lata K. and Kishore V.V.N. (2000) State-of-the-art of anaerobic digestion technology for industrial wastewater treatment, Renewable and Sustainable Energy Reviews, 4, 135-156.

Ramadori R., Rozzi A. and Tandoi V. (1980) An automated system for monitoring the kinetics of Biological oxidation of ammonia, Water Research., 14, 1555–1557.

Ramsay I.R. (1997) Modelling and control of high-rate anaerobic wastewater treatment systems, Ph.D. Thesis, Department of Chemical Engineering, The University of Queensland, Brisbane, Australia.

Raybuck S.A. (1992) Microbes and microbial enzymes for cyanide degradation, Biodegradation, 3, 3-18.

Reichert P., Borchardt D., Henze M., Rauch W., Shanahan P., Somlyódy L. and Vanrolleghem P.A. (2001) River Water Quality Model No.1, Scientific and Technical Report No. 12, IWA Publishing, London, UK.

Ripley L.E., Boyle J.C. and Converce J.C. (1986) Improved alkalimetric monitoring for anaerobic digestion of high-strength wastes, Journal of the Water Pollution Control Federation, 58, 406-411.

Romli M. (1993) Modelling and verification of a two-stage high-rate anaerobic wastewater treatment system, Ph.D. Thesis, Department of Chemical Engineering, The University of Queensland, Brisbane, Australia.

Rosen C. and Jeppsson U. (2002), Anaerobic COST benchmark model description, Technical Report, European Cooperation in the field of Scientific and Technical Research, COST-624 on Optimal Management of Wastewater Systems, pp. 14.

Rozzi A., Buffière P., Steyer J-Ph. and Massone A. (1998) Monitoring readily biodegradable COD load in winery wastewater and distillery slops by a titration biosensor, In: proceedings of 2nd International Specialized Conference on Winery Wastewaters, Bordeaux, France, May 5-7, 1998.

Rozzi A., Ficara E. , Cellamare C. M. and Bortone G. (1999) Characterization of textile wastewater and other industrial wastewaters by respirometric and titration biosensors, Water Science and Technology, 40, 161-168.

Rozzi A., Massone A. and Antonelli M. (1997) A VFA measuring biosensor based on nitrate reduction, Water Science and Technology, 36, 183-189.

Rozzi A., Remigi E. and Buckley C. (2001) Methanogenic activity measurements by the MAIA biosensor: instructions guide, Water Science and Technology, 44, 287-294.

Sawyer C.N., McCarty P.L. and Parkin G.F. (1994) Chemistry for environmental engineering, 4th ed., McGraw-Hill, Inc., pp 658.

Savitzky A. and Golay M.J.E. (1964) Smoothing and differentiation of data by simplified least squares procedures, Analytical Chemistry, 36, 1627–1639.

Seghezzo L., Zeeman G., van Lier J.B., Hamelers H.V.M. and Lettinga G. (1998) A review: the anaerobic treatment of sewage in UASB and EGSB reactors, Bioresource Technology, 65, 175-190.

Shizas I. and Bagley D.M. (2002) Improving anaerobic sequencing batch reactor performance by modifying operational parameters, Water Research, 36, 363-367.

Siegrist H., Renggli D. and Gujer W. (1990) Mathematical modelling of the single and two stage sewage sludge treatment. In: l'Hermite, P. (ed.) Treatment and use of sewage sludge and liquid agricultural wastes, London, Elsevier Applied Science, 45-58.

Siegrist H., Renggli D. and Gujer W. (1993) Mathematical modelling of anaerobic mesophilic sewage sludge treatment, Water Science and Technology, 27, 25-36.

Siegrist H., Renggli D. and Gujer W. (1995) Mathematical modelling of anaerobic mesophilic processes in a digester, In: the International Meeting on Anaerobic Processes for Bioenergy and Environment, Copenhagen, January 25-27, 1995.

Siegrist H. and Batstone D. (2001) Free ammonia and pH inhibition of acetotrophic methanogenesis at mesophilic and thermophilic conditions. In 9th World Congress: Anaerobic Digestion, Antwerp, Belgium, September 2-6, 2001, 395-400.

Siegrist H., Vogt D., Garcia-Heras J.L. and Gujer W. (2002) Mathematical model for meso- and thermophilic anaerobic sewage sludge digestion, Environmental Science & Technology, 36,1113-1123.

Siller H. and Winter J. (1998) Treatment of cyanide-containing wastewater from the food industry in a laboratory-scale fixed-bed methanogenic reactor, Applied Microbiology and Biotechnology, 49, 215-220.

Sin G. and Vanrolleghem P.A. (2004) A nitrate biosensor-based methodology for monitoring anoxic activated sludge activity. In: 2nd IWA conference in Automation in Water Quality Monitoring (AutMoNet 2004), Vienna, Austria, April 19-20, 2004, 61-68.

Skougstad M.W., Fishman M.J., Friedman L.C., Erdman D.E. and Duncan S.S. (1979) Methods for determination of inorganic substances in water and fluvial sediments. In: Techniques of Water-Resources Investigation of the United States Geological Survey, Book 5, Chapter A1, Washington, D.C.

Smith M.R., Lequerica J.L. and Hart M.R. (1985) Inhibition of methanogenesis and carbon metabolism in *Methanosarcina sp.* by cyanide, Journal of Bacteriology, 162, 67-71.

Spanjers H., Vanrolleghem P.A., Nguyen K., Vanhooren H. and Patry G.G. (1998) Towards a simulation-benchmark for evaluating respirometry-based control strategies, Water Science and Technology, 37(12), 219-226.

Stamatelatou K., Skiadas I.V. and Lyberatos G. (2004) On the behavior of the periodic anaerobic baffled reactor (PABR) during the transition from carbohydrate to protein-based feedings, Bioresource Technology, 92, 321-326.

Steyer J.P., Bouvier J.C., Conte T., Gras P., Harmand J. and Delgenes J.P. (2001) On-line measurements of COD, TOC, VFA, total and partial alkalinity in anaerobic digestion processes using infrared spectrometry. In: Proceedings 9th World Conference on Anaerobic Digestion, AD 2001, Antwerpen, Belgium, September 2-6, 2001, 305-310.

Steyer J-P., Bouvier J-C., Conte T., Gras P. and Sousbie P. (2002) Evaluation of a four year experience with a fully instrumented anaerobic digestion process, Water Science and Technology, 45, 495-502.

Stumm W. and Morgan J.J. (1996) Aquatic Chemistry, Chemical Equilibria and Rates in Natural Waters, 3rd ed. John Wiley & Sons, Inc., New York, pp 1022.

Theilliol D., Ponsart J.-C., Harmand J., Join C. and Gras P. (2003) On-line estimation of unmeasured inputs for anaerobic wastewater treatment processes, Control Engineering Practice, 11, 1007-1019.

Turanyi T. (1990) Sensitivity analysis of complex kinetic systems, tools and applications, Journal of Mathematical Chemistry, 5, 203-248.

Uyanik S., Sallis P.J. and Anderson G.K. (2002[a]) The effect of polymer addition on granulation in an anaerobic baffled reactor (ABR). Part I: process performance, Water Research, 36, 933-943.

Uyanik S., Sallis P.J. and Anderson G.K. (2002[b]) The effect of polymer addition on granulation in an anaerobic baffled reactor (ABR). Part II: compartmentalization of bacterial populations, Water Research, 36, 944-955.

van de Graaf A.A., De Bruijn P., Robertson L.A., Jetten M.S.M. and Kuenen J.G. (1996) Autotrophic growth of anaerobic ammonium-oxidizing microorganisms in a fluidized bed reactor, Microbiology, 142, 2187-2196.

Van de Steene M., Van Vooren L. Ottoy J.P. and Vanrolleghem P.A (2002) Automatic buffer capacity model building for advanced interpretation of titration curves, Environmental Science and Technology, 36, 715-723.

van Der Steen P. (ed.) (2002) International Course on Anaerobic Treatment of Industrial Wastewater, Wageningen Agriculture University and IHE-Delft, Delft and Wageningen, The Netherlands, June 10-21, 2002.

van Dongen U., Jetten M.S.M. and van Loosdrecht M.C.M. (2001) The SHARON-Anammox process for treatment of ammonium rich waste water, Water Science and Technology, 44, 153-160.

Van Haandel A.C. and Lettinga G. (1994) Anaerobic sewage treatment, a practical guide for regions with a hot climate, John Wiley & Sons, Chichester, pp. 226.

Van Hulle, S.W.H., Van Den Broeck S., Maertens J., Villez K., Schelstraete G., Volcke E.I.P. and Vanrolleghem P.A. (2003) Practical experiences with start-up and operation of a continuously aerated lab-scale SHARON reactor, In: Communications in Applied Biological Sciences, Proceedings FAB Symposium, Gent, Belgium, September 18-19, 2003, 68, 77-84.

Van Hulle, S.W.H. (2005) Modelling, simulation and optimization of autotrophic nitrogen removal processes, PhD. Thesis, Faculty of Bioscience Engineering, Ghent University, pp. 228.

Van Impe J.F., Vanrolleghem P.A. and Iserentant D. (1998) Advanced Instrumentation, Data Interpretation and Control of Biotechnological Processes, Kluwer Academic Publishers, Dordrecht, The Netherlands, pp. 464.

Van Lier J.B., Boersma F., Debets M.M.W.H. and Lettinga G. (1994) High rate thermophilic anaerobic wastewater treatment in compartmentalized upflow reactors, Water Science and Technology, 30, 251–261.

van Rensburg P., Musvoto E.V., Wentzel M.C. and Ekama G.A. (2003) Modelling multiple mineral precipitation in anaerobic digester liquor, Water Research, 37, 3087-3097.

Van Vooren L. (2000) Buffer capacity based multipurpose hard- and software sensor for environmental applications, PhD. Thesis, Faculty of Agricultural and Applied Biological Sciences, Ghent University, pp. 338.

Van Vooren L., Lessard P., Ottoy J.-P. and Vanrolleghem P.A. (1999) pH buffer capacity based monitoring of algal wastewater treatment, Environmental Technology, 20, 547-561.

Van Vooren L., Van De Steene M., Ottoy J.-P. and Vanrolleghem P.A. (2001) Automatic buffer capacity model building for the purpose of water quality monitoring, Water Science and Technology, 43, 105-113.

Van Vooren L., Willems P., Ottoy J.P., Vansteenkiste G.C. and Verstraete W. (1996) Automatic buffer capacity based sensor for effluent quality monitoring, Water Science and Technology, 33, 81–87.

Vangheluwe Hans (2000) Multi-formalism modelling and simulation, PhD. Thesis, Faculty of Sciences, Ghent University, pp. 301.

Vanhooren H., Meirlaen J., Amerlinck Y., Claeys F., Vangheluwe H. and Vanrolleghem P.A. (2003) WEST: Modelling biological wastewater treatment, Hydroinformatics, 5, 27-50.

Vanrolleghem P.A. (1995) Sensors for anaerobic digestion: An overview, In: Proceedings of Workshop Monitoring and Control of Anaerobic Digesters, Narbonne, France, December 6-7, 1995.

Vanrolleghem P.A. and Lee D.S. (2003) On-line monitoring equipment for wastewater treatment processes: State of the art, Water Science and Technology, 47(2), 1-34.

Vanrolleghem P.A., Rosen C., Zaher U., Copp J., Benedetti L., Ayesa, E. and Jeppsson U. (2005) Continuity-based interfacing of models for wastewater systems described by Petersen matrices, Water Science and Technology (in press).

Volcke E.I.P., Hellinga C., Van Den Broeck S., van Loosdrecht M.C.M. and Vanrolleghem P.A. (2002) Modelling the SHARON process in view of coupling with Anammox. In: Proceedings 1st IFAC International Scientific and Technical Conference on Technology, Automation and Control of Wastewater and Drinking Water Systems (TiASWiK'02). Gdansk-Sobieszewo, Poland, June 19-21, 2002, 65-72.

Volcke E.I.P., Van Hulle S.W.H., van Loosdrecht M.C.M. and Vanrolleghem P.A. (2003) Generation of Anammox-optimal nitrite:ammonium ratio with SHARON process: Usefulness of process control, In: Proceedings 9th IWA Specialised Conference on Design, Operation and Economics of Large Wastewater Treatment Plants. Prague, Czech Republik, September 1-4, 2003, 55-58.

Walter E. and Pronzato, L. (1997) Identifcation of Parametric Models From Experimental Data, Springer- Verlag GmbH, ISBN 3-540-76119-5, pp. 413.

Wang J., Huang Y. and Zhao X. (2004) Performance and characteristics of an anaerobic baffled reactor, Bioresource Technology, 93, 205-208.

Wang Z. and Banks C.J. (2003) Evaluation of a two stage anaerobic digester for the treatment of mixed abattoir wastes, Process Biochemistry, 38, 1267-1273.

Widyatmika I.N. (2004) Anaerobic Treatment of Cyanide Contained Cassava Wastewater, MSc. Thesis, UNESCO-IHE, Delft, The Netherlands.

Wild D., Kisliakova A. and Siegrist H. (1997) Prediction of recycle phosphorous loads from anaerobic digestion, Water Research, 31, 2300-2308.

Winter J.A. and Midgett M.R. (1969) FWPCA Method Study 1: Mineral and Physical Analyses, In: Federal Water Pollution Control Administration, Washington, D.C, Prentice-Hall, Englewood Cliffs New Jersey.

Wyffels S. (2004) Feasibility of combined autotrophic nitrogen removal processes for the treatment of high strength nitrogen wastewaters, PhD thesis, Ghent University, Faculty of Applied Biological Sciences, pp 135.

Yang Y., Tsukahara K., Yagishita T. and Sawayama S. (2004) Performance of a fixed-bed reactor packed with carbon felt during anaerobic digestion of cellulose, Bioresource Technology, 94, 197-201.

Yoo C.K., Lee D.S. and Vanrolleghem P.A. (2004) Application of multiway ICA for on-line process monitoring of a sequencing batch reactor, Water Research, 38, 1715-1732.

Yoo C.K., Lee J.-M., Vanrolleghem P.A. and Lee I.-B. (2004) On-line monitoring of batch processes using multiway independent component analysis, Chemometrics and Intelligent Laboratory Systems, 71, 151-163.

Yoo C.K., Vanrolleghem P.A. and Lee I.-B. (2003) Nonlinear modeling and adaptive monitoring with fuzzy and multivariate statistical methods in biological wastewater treatment plants, Journal of Biotechnology, 105, 135-163.

Young J.C. and McCarty P.L. (1969) The anaerobic filter for waste treatment, Journal of the Water Pollution Control Federation, 41, 160-173.

Zumbusch P.V., Meyer-Jens T., Brunner G. and Märkl H. (1994) On-line monitoring of organic substances with high-pressure liquid chromatography (HPLC) during the anaerobic fermentation of wastewater Applied Microbiology and Biotechnology , 42, 140-146.

Summary

This PhD research aimed at the optimisation and the smooth operation of anaerobic digestion and wastewater treatment. The research objectives were threefold. The first one is to implement and validate anaerobic digestion models as tools to pursue the above aim. Second, anaerobic digestion models should be integrated in plant-wide modelling. The third research objective is to develop, automate, apply and validate on-line titrimetric monitoring of anaerobic digestion and wastewater treatment processes.

A general review defined the links among modelling, monitoring and different data categories in an optimisation scheme for design and operation of anaerobic digestion. The review also guides the data collection activity that is dependent on anaerobic reactor types and wastewater characteristics. Therefore, it leads to a better definition of the anaerobic model and the monitoring system.

In achievement of the first objective, the IWA ADM1 model is implemented in the WEST simulation platform where different reactor configurations can be easily defined. For a successful standard ADM1 implementation, key updates were necessary to the model compared to the descriptions in the IWA ADM1 model report. Simpler modelling approaches for anaerobic digestion are introduced by the Siegrist (1995 version) and the AM2 models. A general procedure for pH calculation was developed to improve the simulation speed when using simple DE solvers. The general procedure can be applied with any model and was extended to calculate cation concentrations and to implement a Titrimetric Analyser Simulator, TAS, in WEST. The ADM1 implementation was validated using three different simulators: WEST, AQUASIM and SIMULINK. In one of the first world-wide endeavours, the ADM1 was validated with an experiment with very rapid dynamics. Excellent agreement between the measurements and simulation results from the three implementations was achieved. A conceptual approach was developed to achieve a detailed characterisation of the wastewater according the ADM1 state vector without laborious measurements of the influent wastewater. An update to the model was introduced to describe the effect of hydrodynamics on the solids retention and to make the modelling of highrate reactors simple and possible. The ADM1 was also extended to study and simulate the effect of irreversible toxicity on the anaerobic digestion process. A complete pathway for cyanide degradation and a procedure to model acclimatisation of the anaerobic digestion process to toxicants were developed. The model extension was validated using 3 lab-scale Upflow Anaerobic Sludge Bed (UASB) reactors with three different feedings of cyanide. Although the model was calibrated with data from only one reactor, agreement between measurements and simulation results was achieved in the three reactors. The AM2 control model implementation was validated for anaerobic digestion of vinasses. A general protocol was designed to use the Optimal Experimental Design (OED) procedure to set up

the monitoring system and the sensor network at an anaerobic digestion plant. The protocol was validated using a virtual case study that implements ADM1 as data generator and AM2 as the control model. The OED application showed the value of on-line monitoring of pH, alkalinity, VFA and biogas measurements.

In achievement of the second objective, a flexible approach of using model transformers is presented for integration of anaerobic digestion models in a plant-wide model. The approach is illustrated by connecting the Siegrist (1995 version) anaerobic digestion model with the standard Activated Sludge Model (ASM1). The example extends the standard benchmark model of activated sludge systems by a thickener, an anaerobic digestion unit and a centrifuge to simulate the practice of sludge treatment and drying. Overflows from the thickener and the centrifuge are recycled to the activated sludge plant inlet. The transformers allow flexibility to connect other flows than sludge to the digester and the digester to other post-treatment processes. The expected digester output and the impact of the recycled flows on the activated sludge plant were correctly simulated. The same designed plant was then applied to compare two interfacing methods to connect ASM1 and ADM1. The first method (CBIM) is designed to interface two models according their Petersen matrix definitions. The second method (MCN) was specifically developed to connect ASM1 and ADM1. This work is the first systematic application of the (CBIM) method and to present the results of both methods. Both methods have the same plant-wide output, i.e. effluent water quality, produced biogas and produced sludge. However, the CBIM method provides flexibility that helps in a better simulation of the digester dynamics in allowing better parameter estimation, control design and implementation of advanced treatment processes, e.g. for highrate nitrogen removal.

In achievement of the third objective, monitoring equipment and titrimetric applications were first reviewed. Three titrimetric analysers that were used throughout this research are described. Two of them were developed in previous research but were not commercially available. A third one was developed in parallel to and with support of this research and is now commercially available for on-line implementation methods. The titrimetric methods are reviewed and classified according their mathematical interpretation. The Buffer Capacity Software (BCS) was developed for robust off- and on-line determination of unknown buffer mixtures without human input or interaction. An automatic initialisation procedure has been developed as an extension to the Buffer capacity Optimal Model Builder (BOMB) software sensor. The initialisation procedure automatically determines from a titration curve which buffers are in the titrated sample and estimates lower and upper bounds of their concentrations. This information is required to run the BOMB optimisation. The extension has been integrated as a software layer around BOMB and the

result is BCS. The Titrimetric Analyser Simulator (TAS) is used to test the BCS's reliability to measure buffer systems in an anaerobic digester that is operated under strong dynamics and with very fast transitions between different buffer combinations. The BCS has been tested and is now working with off- and on-line titrimetric analysers. BCS was applied in three different case studies of titrimetric monitoring and compared with other titrimetric and standard methods. The three titrimetric analysers described in this research were also tested via these applications. In the first case study the BCS was applied for titrimetric monitoring of digester overload conditions, measuring bicarbonate, VFA and lactate. In the second case study, the BCS and titrimetric methods were challenged by complicating factors. An experiment was performed at an industrial scale digester in the presence of external doses of di- and tri-protic cations (calcium and iron ions). Also a complex mixture of buffer components was dosed to the anaerobic digester effluent. Titration was performed on-line using the titrimetric on-line analyzer AnaSense®. On-line measurements of VFA, bicarbonate, ammonia, phosphorus and lactic acid were compared with standard measurements. Results from the second case study were highly influenced by buffer interferences and precipitation dynamics. However, the results correlated nicely with the standard measurements and are suitable for control applications. The approximate titrimetric methods were robust in determining the bicarbonate and VFA concentrations. In the third case study, the BCS was tested for the titrimetric monitoring of highrate nitrogen removal processes that are used to treat digester liquors, i.e. using combined SHARON-Anammox processes. The BCS accurately measured total ammonia and total nitrite, both variables that are useful for process control. Also, from the same titration experiment the BCS measured phosphorus that is considered toxic to the Anammox biomass.

Finally, the three objectives of this research are achieved to large extent and, therefore, the developed tools can support future research and applications to optimise anaerobic digestion and wastewater treatment systems.

Dit doctoraatsonderzoek streefde de optimalisatie en robuuste bedrijfsvoering van anaërobe slibvergisting en afvalwaterzuivering na. De onderzoeksobjectieven waren drieledig. Het eerste objectief beoogde de implementatie en validatie van slibvergistingsmodellen als middel om het eerder vermelde algemene doel te bereiken. Een tweede luik omvatte de integratie van dergelijke modellen in een globaal model van een RWZI. Een derde en laatste objectief was de ontwikkeling, automatisatie, toepassing en validatie van de on-line titrimetrische opvolging van anaërobe slibvergisting en waterzuiveringsprocessen.

In een algemeen literatuuroverzicht werd het verband gelegd tussen de modelbouw van anaërobe vergisters, het opvolgen ervan en de verschillende types data die beschikbaar zijn. Dit overzicht werd gemaakt in het kader van een optimalisatieschema voor het ontwerp en de bedrijfsvoering van anaërobe slibvergisting. Het overzicht beschrijft ook de verzameling van data die afhankelijk is van het reactortype en de afvalwaterkarakteristieken. Deze analyse leidt aldus tot een betere definitie van het anaërobe model en het opvolgingssysteem.

Met het oog op het bereiken van het eerste objectief werd het IWA ADM1 model geïmplementeerd in het WEST simulatieplatform, waarin verschillende reactorconfiguraties op een eenvoudige wijze kunnen worden gedefinieerd. Voor een succesvolle ADM1-implementatie waren enkele belangrijke aanpassingen aan het in het IWA ADM1-rapport beschreven model noodzakelijk. Vereenvoudigde modelbenaderingen werden voorgesteld met de eerder ontwikkelde Siegrist en AM2 modellen. Een algemene procedure voor pH-berekening werd ontwikkeld ter verbetering van de simulatiesnelheid. Ze maakt gebruik van eenvoudige numerieke oplossingsmethoden voor sets van algebraïsche vergelijkingen. Deze algemene procedure kan voor elk model worden toegepast en werd ook uitgebreid om kationconcentraties te berekenen en om de Titrimetric Analyser Simulator, TAS, te implementeren in WEST. De ADM1-implementatie werd gevalideerd met drie verschillende simulatoren: WEST, AQUASIM en SIMULINK. Wereldwijd werd hiermee ook ADM1 voor de eerste gevalideerd met experimentele data waarin een snelle dynamica waargenomen wordt. Een zeer goede overeenkomst tussen de metingen en de simulaties werd gevonden. Een conceptuele aanpak zonder arbeidsintensieve metingen van het influent werd ontwikkeld om een gedetailleerde karakterisatie van het afvalwater overeenkomstig de ADM1 toestandsvector te bekomen. Een aanpassing van het model voor het beschrijven van hydrodynamische effecten op de slibverblijftijd en ter vereenvoudiging van het modelleren van hoogbelaste reactoren werd voorgesteld. ADM1 werd ook uitgebreid voor het onderzoeken en simuleren van irreversiebele toxiciteit op het slibvergistingsproces. Een volledige

cyanidedegradatieroute en een procedure voor het modelleren van acclimatisatie van het anaërobe slibvergistingsproces met betrekking tot toxische stoffen werd ontwikkeld. De modelextensie werd gevalideerd met 3 laboschaal Upflow Anaerobic Sludge Bed (UASB) reactoren met drie verschillende cyanidevoedingen. Hoewel het model gecalibreerd werd met data van slechts één van de reactoren, werd een goede overeenkomst tussen de metingen en de simulatieresultaten gevonden voor elk van de drie reactoren. De AM2-implementatie werd gevalideerd voor anaërobe slibvergisting van wijnafvalwater. Een algemeen protocol werd ontworpen voor het toepassen van een Optimaal Experimenteel Ontwerp (OEO) procedure voor het opzetten van een opvolgsysteem en het sensornetwerk op een anaërobe slibvergistingsite. Het protocol werd gevalideerd met behulp van een virtuele studie die gebruik maakte van ADM1 als datagenerator en AM2 als controle model. De OEO-toepassing zette het nut van on-line metingen van pH, alkaliniteit, vluchtige vetzuren en biogas in de verf.

In het kader van het tweede objectief werd een flexibele aanpak voor de integratie van anaërobe slibvergistingsmodellen in een globaal RWZI-model met behulp van modelinterfaces voorgesteld. De aanpak werd geïllustreerd door het verbinden van het anaërobe slibvergistingsmodel van Siegrist met het standaard ASM1 model. Het voorbeeld breidde de standaard benchmark van actief slibmodellen uit met een slibindikker, een slibvergistingseenheid en een centrifuge om de praktijk van slibbehandeling en –droging te simuleren. De overloop van de indikker en de centrifuge werden teruggekoppeld naar de ingang van de RWZI. De interfaces bieden de flexibiliteit om andere stromen dan slib naar de vergister en van de vergister naar andere nabehandelingsprocessen te verbinden. De verwachte effluenten van de vergister en de impact van de terugkoppelingsstromen op de RWZI werden correct gesimuleerd. Hetzelfde RWZI-ontwerp werd vervolgens gebruikt voor de vergelijking van 2 methoden voor het verbinden van ASM1 en ADM1. De eerste methode (CBIM) is ontworpen voor het koppelen van 2 modellen op basis van hun Petersen matrix definities. Een tweede methode (MCN) werd specifiek ontworpen voor het koppelen van ASM1 en ADM1. Dit werk is de eerste systematische toepassing van de CBIM-methode en stelt de resultaten van beide methodes voor. Beide methodes resulteren in dezelfde globale RWZI-outputs, i.e. effluentkwaliteit, biogasproductie en slibproductie. De CBIM-methode is echter meer flexibel waardoor een betere simulatie van de vergistingsdynamica mogelijk wordt en aldus betere parametervoorspellingen, ontwerpen van controlestrategieën en implementaties van geavanceerde behandelingsprocessen (vb. voor snelle stikstofverwijdering) mogelijk worden.

Voor het bereiken van het derde objectief werden eerst bestaande meettoestellen en titrimetrische toepassingen geëvalueerd. Drie titrimetrische analysetoestellen die binnen dit

onderzoek werden gebruikt, werden beschreven. Twee van deze toestellen werden in vorig onderzoek ontwikkeld en zijn niet commercieel beschikbaar. Een derde werd in nauwe samenwerking parallel met dit onderzoek ontwikkeld en is nu commercieel beschikbaar voor on-line implementatie. De methoden werden bekeken en geklasseerd volgens hun mathematische interpretatie. De Buffer Capacity Software (BCS) werd ontwikkeld voor robuuste off- en on-line bepaling van ongekende buffermengsels zonder interactie met de gebruiker. Een automatische initialisatieprocedure werd ontwikkeld als uitbreiding van de Buffer capacity Optimal Model Builder (BOMB) software sensor. De initialisatieprocedure bepaalt automatisch op basis van een titratiecurve welke buffers zich in het getitreerde staal bevinden en voorspelt onder- en bovengrenzen van hun respectievelijke concentraties. Deze informatie is noodzakelijk voor het betrouwbaar uitvoeren van een BOMB-optimalisatie. De extensie werd geïntegreerd als een softwarelaag rond BOMB, resulterend in BCS. De Titrimetric Analyser Simulator (TAS) werd gebruikt voor het testen van de betrouwbaarheid van BCS bij het meten van buffersystemen in een anaërobe slibvergister die wordt bedreven onder sterke dynamische omstandigheden en met snelle transities tussen verschillende buffercombinaties. BCS werd getest en bleek zowel met off-line als on-line titrimetrische meettoestellen te werken. BCS werd toegepast in drie verschillende studies van titrimetrische opvolging en werd vergeleken met andere titrimetrische en standaardmethodes. De drie titrimetrische toestellen beschreven in dit werk werden ook getest gedurende deze 3 studies. In een eerste studie werd BCS toegepast voor titrimetrische opvolging van een overbelaste vergister voor het meten van bicarbonaat, vluchtige vetzuren en lactaat. In de tweede studie werden de BCS en titrimetrische methodes op de proef gesteld door complicerende factoren. Eén behelsde een experiment op een vergister op industriële schaal waarin externe dosissen van twee- en driewaardige kationen (calcium en ijzer) toegevoegd waren. Bovendien werd een complex mengsel van bufferende componenten aan het vergistingseffluent toegevoegd. De titratie werd on-line uitgevoerd door het titrimetrische on-line analysetoestel AnaSense®. On-line metingen van vluchtige vetzuren, bicarbonaat, ammonium, fosfor en melkzuur werden vergeleken met standaard metingen. De resultaten van deze tweede studie werden sterk beïnvloed door bufferinterferenties en neerslagvorming. Desondanks werd een goede correlatie gevonden met de reële concentraties en is de techniek aldus geschikt voor controletoepassingen. De benaderende titrimetrische methodes waren robuust in het bepalen van de concentraties aan bicarbonaat en vluchtige vetzuren. In een derde studie werd BCS getest voor titrimetrische opvolging van hoge snelheid stikstofverwijderingsprocessen die worden gebruikt voor het verwerken van vergistingseffluenten, i.e. het gecombineerde SHARON-Anammox proces. De BCS kon de totale ammoniakale stikstof en het totale nitrietgehalte, beiden interessante

variabelen voor controle, accuraat meten. Hetzelfde titratie-experiment leverde ook metingen van het fosforgehalte dat toxisch is voor de Anammox-biomassa.

De drie objectieven van dit onderzoek werden grotendeels bereikt en de ontwikkelde technieken kunnen aldus gebruikt worden ter ondersteuning van verder onderzoek en toepassingen ter optimalisatie van anaërobe slibvergisting en RWZI's in het algemeen.

Curriculum Vitae and List of Publications

NAME : Usama Elsayed Zaher (usama.zaher@biomath.ugent.be)

DATE OF BIRTH : 16 October 1968

NATIONALITY : Egyptian

MARITAL STATUS: married

LANGUAGES :
ARABIC (Mother Tongue)
ENGLISH (Excellent)
FRENCH (Good)
SPANISH (Good)

EDUCATION:

PhD, Applied Biological sciences: Environmental Technology,
Department of Applied Mathematics, Biometrics and Process Control,
Faculty of Bioscience Engineering,
Ghent University, Belgium, June 2005.
Thesis title: "Modelling and Monitoring of anaerobic digestion process in view of optimisation and smooth operation of WWTPs "

M.Eng., Pollution Prevention & Control,
Specialised: "sanitary engineering - Sector Utility Management,
International Hydraulics institute, IHE-Delft, Netherlands, 2001.

M.Sc. Environmental & Sanitary Engineering,
Faculty of Engineering,
Cairo University, Egypt 2000.
Thesis Title: "*Dynamic Modelling of the Return Activated Sludge Process forReal Time Monitoring and Control*"

B.Sc. in civil engineering,
Zagazig university- faculty of engineering, 1991,
structure modelling and design.

EMPLOYMENT RECORD:

Time	Position	Organization
2001-2005	Researcher	Department of Applied Mathematics, Biometrics and Process Control, Ghent University, Belgium.
1994 - 2000	Project Engineer	Cairo Wastewater project Organization (CWO) - Design and planing department
1992 - 1994	Contract engineer	Cairo Wastewater project Organization (CWO) Gabal Al Asfar treatment plant
1991 - 1992	Site engineer	"Egyptian Contractors Co." construction of high elevated tanks using modern slip form technologies

COMMUNITY SERVICES AND JOBS OF HONOUR:

2000-2001	Students Association general secretary	International Hydraulics institute, IHE-Delft, Netherlands
1991 **to** 2000	design Engineer	Environment and sanitary engineering consultation for community service, several agencies.
1990-1991	Computer system supervisor	5th Africa games – Ministry of youth and sports, Cairo, Egypt

LECTURES, COURSES, SEMINARS and RESEARCH:

Subjects: Hydraulics and process; modelling and design, Instrumentation technology, Process monitoring and control, Simulation software, Management skills,

Belgium: 2001-2005

Department of Applied Mathematics, Biometrics and Process Control,
Ghent University, Belgium.

TRAINING:

- Wastewater treatment design courses (30 Aug to 11 Dec 1997), U.K. in Strathclyde University – West of Scotland Water – WTI training group, As follows:

EP2 – Process Design of Sewage Treatment	WTI
EP3 – Hydraulic Design of Sewage Treatment System	WTI
EP4 – Advances in Sewage and Sludge Treatment	WTI
EM20 – Design of Pumping Installation	WTI
Control and Instrumentation Technology for Wastewater treatment plants.	Strathclyde University
PD1- Introduction to STOAT software - Analysis Interpretation	WOSW
PD2- Advanced Application of STOAT (wastewater treatment plants simulation package)	WOSW
PD3 – Design Parameter of Wastewater Sewage Treatment	WOSW
PD4- Novel Activated Sludge Processes	WOSW
PD5- Sludge Treatment and Disposal Management	WOSW
PD6- Optimization of Wastewater Treatment Processes	WOSW
Trade Effluent Control	WOSW

- Wastewater treatment workshop (1994) " American university - Cairo "
- Project management : (1989 - 1990)

On tunnels construction program in :
PROJECT : "Caretira Rounda De Malaga (high way around Malaga - pain)"
OWNER : " Puplica De Carieteras - Spain "
CONTRACTOR : " EL FOMENTO - SPAIN "

- International law for administrative contracting, Faculty of law, Cairo University, Egypt.

- Courses of instruction on process and hydraulic design for wastewater treatment: British Overseas Development Administration (ODA), UK.

COMPUTER SOFTWARE :

- ***PROGRAMMING:***

***LANGUAGES* : Very Good**
C++ , Fortran, Visual Basic, Quick Basic.
***PACKAGES:* Very Good**
MATLAB® , SIMULINK® , LabView® Instrumentation Programming, Model Specification Language (MSL) WEST®

- ***ENGINEERING APPLICATIONS :*** **Very Good**
  Wastewater and water treatment: WEST®, STOAT ®, AQUASIM ®
  Hydraulic design: CHAT®
  Project management: Primavira®
  Structure analysis: SAP®
  Engineering drawing: Autocad®

- ***MICROSOFT GENERAL APPLICATIONS:*** **Excellent**
  OFFICE XP professional and its APPLICATIONS

MEMBERSHIP OF PROFESSIONAL ORGANISATIONS:
- International water association (IWA)
- Egyptian syndicate of civil engineering.

YEARS OF EXPERIENCE:
PROFICIENAL EXPERIENCE **: 14 YEARS**
COMPUTER SOFTWARE **: 19 YEARS**

INTERNATIONAL CONFERENCES AND SYMPOSIA:
10th World Congress: Anaerobic Digestion 2004 "Anaerobic Conversion for Sustainability", Montreal, Canada , 29 August – 02 September, 2004.

IWA Conference on Environmental Biotechnology, "Advancement on Water and Wastewater Application in the Tropics", Kuala Lumpur , Malaysia, 09-10 December, 2003.

4th PhD symposium of the Faculty of Applied Sciences, Belgium , Ghent, 3 December, 2003.

9th IWA Specialised Conference on Design, Operation and Economics of Large Wastewater Treatment Plants, Prague, Czech Republik, 01-04 September, 2003.

3rd PhD symposium of the Faculty of Applied Sciences, Belgium , Ghent, 11 December, 2002.

VII Latin American Workshop and Symposium on Anaerobic Digestion, Merida , Mexico, 22-25 October, 2002.

9th World Congress: Anaerobic Digestion 2001 "Anaerobic Conversion for Sustainability", Antwerpen , Belgium, 02-06September, 2001.

MAJOR EXPERIENCES IN INTERNATIONAL PROJECTS:

Project	Place	International Partners Luckily I have worked with
TELEMAC Telemonitoring and advanced telecontrol of high yield wastewater treatment plants 2001-2004	European community Research and Development Project	**France:** INRIA - French National Institute for Research in Information Technology and Automation. **France:** GEIE-ERCIM - European Research Consortium for Informatics and Mathemetics Administrative **France:** INRA, French National Institute in Agronomic Research Laboratoire de Biotechnologie de l'Environnement, Narbonne Analyse des systèmes et biométrie, Montpellier **Belgium:** AppliTek, a SME specialized in R&D and production of on-line sensors for use in wastewater treatment and industrial processes. **Belgium:** Ghent University Department of Applied Mathematics, Biometrics and Process Control (BIOMATH) **Belgium:** University of Louvain Centre for Systems Engineering and Applied Mechanics (CESAME) **UK:** CCLRC Central Laboratory of the Research Councils, Rutherford Appleton Laboratory **Italy:** SPES, a company specialized in consultancy in electronics and

Project	Place	International Partners Luckily I have worked with
		information technology **Spain:** University of Santiago de Compostela Dep. of Chemical Engineering - Institute of Technology **Italy** ENEA, National Agency for New Technologies, Energy and the Environment Waste water treatment and water cycle **Spain**: AGRALCO, a co-operative producing vinic alcohol and calcium tartrate. **France:** Pierre Lemaire, a private company designing anaerobic digesters **Mexico:** Tequila SAUZA S.A.de C.V., producer of tequila spirits. **Mexico:** University of Guadalajara Department of Chemical Engineering **UK:** Allied Domecq Spirits & Wine Ltd, spirits company **Brazil**: Allied Domecq Brasil Distillery Principal contractor
Gabal Alasfar Wastewater treatment plant - 2nd stage 1996-1999	Cairo – East bank of Nile river	- Funding agencies: • EIB • French Government • National bank of Egypt - Designer: • French consultant SOGREAH INGENERIE - Engineer: • Canadian consultant AXOR GROUP. - contractor: • French contractor DEGRAMOUNT with Arab contractors - Egypt -Water Technology International corporation - Ontario – Canada, In association with Egyptian consultant CEWWE – Egypt
Contract 13 Maadi Rocktunnel 3.2km length 1996-1998	Cairo – East bank of Nile river	- Funding agencies: • Kwait Fund • National bank of Egypt - Designer: • Taylor Binnee & partiners (U.K.) - Engineer: • CH2MHILL – USA - contractor: • ZUBLIN (GERMANY)
Contract 14 Boulac branch tunnels 8 km length (inSoft-clays) 1994-1996	Cairo – East bank of Nile river	- Funding agencies: • EIB • National bank of Egypt Designer: • GKW–CONSULT (Germany) - Engineer: • American British Consultants AMBRIC - contractor: • British companies consortium CWC
Gabal Elasfar treatment plant 1st stage 1,000,000 m3/day 1992-1994	Cairo East Bank	- Funding agencies: • EIB • Italian government • National bank of Egypt - Designer and Engineer: • American British Consultants AMBRIC - contractor: • Italian Companies consortium ANSCO

PUBLICATIONS:

International journals:

Zaher U., Widyatmika I.N., Moussa M.S., van der Steen P., Gijzen H.J. and Vanrolleghem P.A. (2005) Update of the IWA ADM1 for modelling anaerobic digestion of cyanide-contaminated wastewater, Bioresource Technology. (Submitted)

Zaher U., Grau P., Benedetti L., Ayesa E. and Vanrolleghem P.A. (2005) Transformers for interfacing anaerobic digestion models to pre- and post-treatment processes, Environmental Modelling & Software. (Submitted)

Zaher U. and Vanrolleghem P. A. (2005) Automatic initialisation of buffer composition estimation for on-line analysis of unknown buffer solutions, Analytical and Bioanalytical Chemistry .(Submitted)

Vanrolleghem P.A., Rosen C., **Zaher U.**, Copp J., Benedetti L., Ayesa, E. and Jeppsson U. (2005) Continuity- Based Interfacing of Models for Wastewater Systems Described by Petersen Matrices. Water Science and Technology. (in press)

Bernard O., Le Dantec B., Chahuat B., Steyer J.-P., Lardon L., Lambert S., Ratini P., Lema J., Ruiz G., Rodriguez J., Vanrolleghem P.A., **Zaher U.**, De Pauw D., De Neve K., Lievens K., Dochain D., Schoefs O., Farina R., Alcaraz Gonzalez V., Lemaire P., Martinez J.A., Duclaud O., Lavigne J.F. (2005) TELEMAC : An integrated system to remote monitor and control anaerobic wastewater treatment plants through the Internet. Water Science and Technology. (in press)

Abdel-Halim H.S., Abdalla K.Z., **Zaher U.** and Vanrolleghem P.A. (2004) Dynamic modeling of the activated sludge process for real time monitoring and control. Water Intelligence On-line,
http://www.iwaponline.com/wio/2004/08/default001.htm

Zaher U., Rodríguez J., Franco A. and Vanrolleghem P.A. (2004) Conceptual approach for ADM1 application. WEMS, ISBN 1 84339 503 7, pp 249-258.

International conferences:

Zaher U., Moussa M.S., Widyatmika I.N., van der Steen P., Gijzen H.J. and Vanrolleghem P.A. (2005) Modelling anaerobic digestion acclimatisation to a biodegradable toxicant: Application to cyanide, The 1st International Workshop on the IWA Anaerobic Digestion Model No. 1, Lyngby, Copenhagen, September 4-6, 2005. (accepted)

Van Hulle S.W.H., **Zaher U.**, Vanrolleghem P.A. (2005) Monitoring of a lab-scale SHARON-Anammox process using titrimetric data, The 2nd IWA Conference on Instrumentation, Control and Automation, Busan, Korea / May 29 - June 2, 2005. (accepted)

Ruiz, G., Molina, F., Steyer J.-P, Vanrolleghem, P.A., **Zaher U.**, Roca, E. and Lema, J.M. (2005). Industrial scale validation of a new titrimetric sensor for on line monitoring of VFA and bicarbonate in anaerobic digestion: comparison of methodologies, The 2nd IWA Conference on Instrumentation, Control and Automation, Busan, Korea / May 29 - June 2, 2005. (accepted)

Zaher U., Bouvier J.C., Steyer J.-P. and Vanrolleghem P.A. (2004) Titrimetric monitoring of anaerobic digestion: VFA, alkalinities and more. In: Proceedings 10th World Congress on Anaerobic Digestion (AD10). Montreal, Canada, August 29 - September 2 2004, Vol. 1, 330-336.

De Pauw D.J.W., **Zaher U.** and Vanrolleghem P.A. (2004) Protocol and optimal experimental design to set up a monitoring and control system at an anaerobic digester. In: Proceedings 10th World Congress on Anaerobic Digestion (AD10). Montreal, Canada, August 29 - September 2 2004. Vol. 3, 1319-1324.

Abdel-Halim H.S., Abdalla K.Z., **Zaher U.** and Vanrolleghem P.A. (2003) Dynamic modeling of the activated sludge process for real time monitoring and control. In: Proceedings 9th IWA Specialised Conference on Design, Operation and Economics of Large Wastewater Treatment Plants. Prague, Czech Republik, September 1-4 2003. 87-90.

Zaher U., Rodríguez J., Franco A. and Vanrolleghem P.A. (2003) Application of the IWA ADM1 model to simulate anaerobic digester dynamics using a concise set of practical measurements. In: Proceedings IWA Conference on Environmental Biotechnology. Advancement on Water and Wastewater Applications in the Tropics. Kuala Lumpur, Malaysia, December 9-10 2003. (on CD-ROM).

Zaher U., de Gracia M. and Vanrolleghem P.A. (2002) Implementation of anaerobic digestion models for plant wide modelling and performance benchmarking. In: Proceedings 7th Latin American Workshop and Symposium on Anaerobic Digestion. Merida, Mexico, October 22-25 2002. Vol. 2, 73-76.

ISBN 90-5989-070-1